



Durham E-Theses

Coastal changes in Hong Kong and Southern China

Englefield, Gregory J. H.

How to cite:

Englefield, Gregory J. H. (1992) *Coastal changes in Hong Kong and Southern China*, Durham theses, Durham University. Available at Durham E-Theses Online: <http://etheses.dur.ac.uk/6000/>

Use policy

The full-text may be used and/or reproduced, and given to third parties in any format or medium, without prior permission or charge, for personal research or study, educational, or not-for-profit purposes provided that:

- a full bibliographic reference is made to the original source
- a [link](#) is made to the metadata record in Durham E-Theses
- the full-text is not changed in any way

The full-text must not be sold in any format or medium without the formal permission of the copyright holders.

Please consult the [full Durham E-Theses policy](#) for further details.

Coastal changes in Hong Kong and Southern China

Volume one

Gregory J. H. Englefield

thesis submitted for the degree of
Master of Philosophy

University of Durham

Department of Geography

1992

The copyright of this thesis rests with the author.
No quotation from it should be published without
his prior written consent and information derived
from it should be acknowledged.

The first of two volumes



30 JUN 1994

Coastal changes in Hong Kong and southern China

Abstract

This research examines past coastal changes and the possible impacts of future changes in southern China and Hong Kong. It aims to both assess coastal changes at a number of defined sites, and to examine more general trends in sea-level during the Holocene. This provides a context within which impacts of future sea-level changes and marine flooding are examined.

The methods used in this work may be divided into two broad categories. Sedimentary analysis, together with an examination of fossil diatom remains has revealed changes in the sedimentary history of three coastal lowland sites, and has highlighted significant changes in the palaeogeography of these sites. Evidence of former sea-levels lower than present mean sea-level has been found. The methods for this work are based on research carried out along many coasts around the world, but particularly in northwest Europe. This detailed stratigraphic analysis has not been applied to sites in southern China before. This study suggests that it could be used very successfully in the future.

A Geographical Information System has been used to integrate a wide range of data on coastal lowlands to assess the possible risks and impacts of sea-level changes and marine flooding in southern China. This builds on the work on past sea-level changes. The method of analysis using the Geographical Information System was developed for this study.

An analysis of coastal changes at three sites has been carried out, and the results of this are evaluated and discussed. A database of radiocarbon dated sea-level index points from southern China has been created from information derived from many published and unpublished sources. These data suggest that sea-levels rose rapidly from between 8000 and 5000 years B.P., and have then fluctuated around present mean sea-level. It is still unclear whether sea-levels have risen significantly above present levels for any prolonged period of time during the late Holocene. The analysis of possible impacts of future sea-level rise has shown that a large part of the Zhujiang delta is already at risk from any rise in sea-level of more than a few centimetres. A small part of the eastern part of the Zhujiang delta has been analysed in detail. This has demonstrated the potential for using a Geographical Information System to examine larger coastal areas.

This study highlights the deficiencies in the data currently available, particularly from China, and shows the potential for future work in this field. Sea-level have changed dramatically over a variety of timescales in the past, and the risks and impacts of any future rise in sea-level are considerable.

List of Figures

List of Tables

Declaration

Statement of Copyright

Important note

Acknowledgements

1	Introduction	15
1.1	Aims	16
1.2	Past sea level and coastal changes	17
1.3	Impacts of future sea level changes	19
1.4	The south China coast	22
1.4.1	The Zhujiang delta	
1.5	Past research on sea level changes - Hong Kong and southern China	29
1.5.1	Past sea level changes around Hong Kong	30
1.5.1.1	Late Pleistocene sea- level changes	31
1.5.1.2	Holocene sea-level changes	41
1.5.2	Past sea level changes off the coast of South China	48
1.6	Conclusions	53
2	Aims	54
2.1	Sediment analysis	54
2.1.1	Stratigraphic analysis	54
2.1.2	Methods of sampling	55
2.1.3	Particle size analysis	60
2.2	Levelling	61
2.3	Micropaleontological analysis	62
2.3.1	Diatom analysis	63
2.3.1.1	Halobean classification	65
2.3.1.2	Counting and identification	66



2.4	Geographical Information Systems	67
2.5	Conclusions	69
3	Sedimentary analyses	71
3.1	Introduction	71
3.2	Selection of sites	72
3.3	Shajing	74
3.3.1	Introduction	74
3.3.2	Shajing Lagoon	75
	3.3.2.1 Sediment stratigraphy	76
	3.3.2.2 Particle size analysis	81
	3.3.2.3 Diatom analysis	84
	3.3.2.4 Discussion	89
	3.3.2.5 Coastal changes	91
3.4	Sham Wan	94
3.4.1	Introduction	94
3.4.2	Tung O	96
	3.4.2.1 Stratigraphy	96
	3.4.2.2 Particle size analysis	98
	3.4.2.3 Diatom analysis	100
	3.4.2.4 Discussion	104
	3.4.2.5 Coastal changes	106
3.5	Tin Shui Wai	109
3.5.1	Introduction	109
3.5.2	General stratigraphy	110
3.5.3	Field sites	111
3.5.4	Site TSW/A	113
	3.5.4.1 Stratigraphy	113
	3.5.4.2 Particle size analysis	115
	3.5.4.3 Diatom analysis	116
3.5.5	Transect TSW/B	116
	3.5.5.1 Stratigraphy	117
3.5.6	Coastal changes	118

3.6	Conclusions	120
3.6.1	Methods	120
3.6.2	Coastal changes	121
4	Holocene sea-level changes	123
4.1	Introduction	123
4.2	Sources of Data	124
4.3	Defining sea level change curves	125
4.3.1	Methods	125
4.3.2	Errors	128
	4.3.2.1 Age determination errors	128
	4.3.2.2 Altitudinal errors	130
4.4	South Chinese sea level indicators	134
4.4.1	Time altitude diagrams	134
	4.4.1.1 Hong Kong	136
	4.4.1.2 Shenzhen	137
	4.4.1.3 Zhujiang Delta	138
	4.4.1.4 Hanjiang Delta	139
	4.4.1.5 Xisha Islands	141
	4.4.1.6 Hainan Island	142
	4.4.1.7 Western Guangdong	143
	4.4.1.8 Fujian coast	144
4.4.2	Analysis of the data sets	144
	4.4.2.1 Reduction of the database	145
	4.4.2.2 Analysis of regional sea-level change envelopes	147
4.5	Final conclusions	152
5	Possible impacts of future sea-level changes	155
5.1	Introduction	155
5.2	Risks of flooding	155
	5.2.1 Altitudinal factors	156
	5.2.2 Social and economic factors	158
	5.2.3 Other factors	159
5.3	Impacts of flooding	159
	5.3.1 Past research	159

5.3.2	The study area	161
5.4	Aims of the study	161
5.5	Methods	162
5.6	The study area	164
5.6.1	Study area definition	165
5.6.2	Administrative divisions in China	166
5.6.3	Data availability	168
5.6.4	Size of the study area	168
5.7	Data used in the study	169
5.7.1	Altitude	169
5.7.2	Land use data	170
5.7.3	Land resources	171
5.7.4	Population data	172
5.7.5	Communications	172
5.7.6	Settlements	173
5.7.7	Tidal data	173
5.7.7.1	The Zhujiang Delta	173
5.7.7.2	Hong Kong	174
5.7.7.3	Trends in mean sea level	175
5.8	Techniques	176
5.9	Risks of marine flooding	178
5.9.1	Past sea level	179
5.9.2	Altitudinal data	182
5.9.3	Definition of the Flood Risk Zone	184
5.10	Impacts of future marine flooding	186
5.10.1	Population	187
5.10.2	Land use	188
5.10.3	Land resources	191
5.10.4	Communications	191
5.11	Future changes in flood risks and impacts	193
5.11.1	Changes in sea levels	193
5.11.2	Changes in land altitudes	196
5.11.3	Other factors	197
5.12	Conclusions	200
6	Conclusions	202
6.1	The sedimentary analysis	202
6.2	The methodology	203

6.3	Past changes in sea-level	205
6.4	The impacts of future sea-level changes	207
6.5	Future work	208
Appendix 1	Stratigraphic descriptions of boreholes from three sites.	211
Appendix 2	Bacillariophyta (diatoms) identified in the study and diatom floras used during diatom analysis.	261
Appendix 3	Key to the stratigraphic symbols.	264
Appendix 4	Sources of radiocarbon dated sea-level index points from Hong Kong and the south coast of China.	265
Appendix 5	Radiocarbon dated sea-level indicators.	268
Appendix 6	Changes in sea-levels and sedimentation during the Quaternary	273
Bibliography		275

List of Figures

- 1.1 The south coast of China and the location of the study area
- 1.2 Tentative Quaternary stratigraphy from Hong Kong (after Yim et al 1988)
- 3.1 Location of sites studied
- 3.2 The site at Shajing
- 3.3 The location of bore holes at Shajing Lagoon
- 3.4 Stratigraphy at Shajing Lagoon "A"
- 3.6 Stratigraphy of bore holes SJA1 - SJA5
- 3.7 Diatom diagram SJA8
- 3.8 Diatom diagram SJA19
- 3.9 The location of the Sham Wan site bore holes, Tung O, Lamma Island
- 3.10 Stratigraphy at Sham Wan (Tung O)
- 3.11 Diatom diagram SW4
- 3.11a Photograph of Sham Wan sediment core SWA4/4i
- 3.12 The location of the bore holes and sediment sections at Tin Shui Wai
- 3.13 Interpreted stratigraphy of "Dutch" bore holes transect A (see figure 3.12)
- 3.14 Interpreted stratigraphy of "Dutch" bore holes transect B (see figure 3.12)
- 3.15 Interpreted stratigraphy of "Dutch" bore holes transect C (see figure 3.12)
- 3.16 Sketch of the TSW/A section
- 3.17 Stratigraphic diagram of section TSW/A
- 3.18 Stratigraphy at Tin Shui Wai, eastern culvert - TSW/B
- 4.1 Map of south China, and location of sites
- 4.2 Time-altitude graph of 217 sea level index points
- 4.3 Hong Kong sea level index point time-altitude plots
- 4.4 Shenzhen sea level index point time-altitude plots

- 4.5 Zhujiang Delta sea level index point time-altitude plots
- 4.6 Hanjiang sea level index point time-altitude plots
- 4.7 Xisha Islands sea level index point time-altitude plots
- 4.8 Hainan Islands sea level index point time-altitude plots
- 4.9 West Guangdong sea level index point time-altitude plots
- 4.10 Fujian coast sea level index point time-altitude plots
- 4.11 Combined sea-level change envelopes from all parts of the south China coast
- 4.12 South China coast sea-level index points. Fixed and relational indicators. (Total of 98 data points).
- 4.13 South China coast sea-level index points (not including Hainan Island and western Guangdong data). Fixed and relational indicators. (Total of 48 data points).
- 4.14 Sea-level indicators from the Zhujiang delta including Shenzhen.
- 4.15 Sea-level indicators from Hong Kong.
- 4.16 Sea-level indicators from Hainan Island.
- 4.17 Sea-level indicators from the coast of western Guangdong.
- 4.18 Sea-level indicators found on the Xisha Islands.
- 4.19 Sea-level indicators found in the Hanjiang delta.
- 4.20 Sea-level indicators from the coast of Fujian province.
- 5.1 The structure of a G.I.S. to analyze the impacts of coastal change
- 5.2 The Zhujiang Delta, and the location of tide gauge stations
- 5.3 The location of the study area
- 5.4 The structure of local government administration in the study area
- 5.5 Levelled transect across the study area, 2 km south of Shajing (see Figures 5.3 and 5.10 for location)
- 5.6 Recorded sea levels during three storms at the tide gauges in the Zhujiang Delta (all altitudes in metres Y.S.D.)
- 5.7 The tide gauge network in Hong Kong
- 5.8 Ground settlement of the North Point tide gauge 1954-1976
- 5.9 Altitudinal data for the study area

- 5.10 Reproduction of the 1:10,000 map of part of the study area
- 5.11 Relative altitudes of sea levels and land in the Zhujiang Delta
- 5.12 Population and altitude maps of the study area
- 5.13 Communication routes in the study area
- 5.14 Estimates of future sea level rise
- 5.15 Estimates of future sea level rise added to the highest recorded sea level at Shanbanzhou
- 5.16 Sea level rise scenarios for the Zhujiang Delta, according to Hoffman et al (1986)
- 5.17 Sea level rise scenarios for Shanbanzhou, combined with an estimate of subsidence of 2 mm/year
- 5.18 Sea-level rise scenarios for the Zhujiang Delta, combined with an estimate of land subsidence of 2mm/year
- 5.19 Possible increase in population for the Zhujiang Delta (10 counties) 1983-2100
- 5.20 Possible increase in population for the Zhujiang Delta (19 counties) 1983-2100
- 5.21 Possible increase in population of the Flood Risk Zone, Bao'an County, 1983-2100

List of Tables

- 1.1 Sea level change methodology
- 1.2 Offshore Quaternary stratigraphy of Hong Kong
- 1.3 Radiocarbon dated former sea level indicators
- 1.4 Sedimentation rates in the Zhujiang Delta
- 3.1 Particle size analysis, Shajing Lagoon - SJA5, SJA6, SJA8, SJA19
- 3.2 Particle size analysis, Sham Wan SW4
- 3.3 Particle size analysis, Tin Shui Wai - TSW/A
- 3.4 Stratigraphy at Sham Wan as described by Frost (1978)
- 4.1 Information collected for each dated sea level index point from southern China
- 4.2 Types of organic material dated using radiocarbon dating in the database of sea level index points
- 5.1 Mean tidal measurements from tide gauge stations in the Zhujiang Delta
- 5.2 Recorded altitude of tide gauge at North Point
- 5.3 List of topologies generated by the Geographical Information System
- 5.4 Annual recorded maximum sea levels, Hong Kong
- 5.5 Magnitude of storm surges and maximum sea levels in Hong Kong during three tropical cyclones
- 5.6 Sea altitudes recorded in Hong Kong during three tropical cyclones - mean monthly maxima
- 5.8 Percentage of work force employed in different economic activities in the study area in 1983
- 5.9 Income *per capita* in the study area in 1983
- 5.10 Percentage of gross income of each district in the study area derived from different economic activities
- 5.11 Land use data for the study area related to altitude
- 5.12 Land resource data for the study area related to altitude
- 5.13 Estimates of future mean sea level change
- 5.14 Possible effects of future sea level change scenarios in the Zhujiang Delta

- 5.15 Medium and high sea level rise estimates added to highest recorded sea levels
- 5.16 The effects of scenarios of future sea level change combined with estimates of subsidence in the Zhujiang Delta of 2 mm per year
- 5.17 Projected population growth in 10 counties in the Zhujiang Delta 1983-2100

Declaration

No material contained in this thesis has been submitted previously for any degree.

Statement of Copyright

The copyright of this thesis rests with the author. No quotation from this should be published without his prior written consent and information derived from it should be acknowledged.

Important Note

Some of the maps and data contained in this thesis are of a sensitive nature. None of the diagrams contained in chapters 3 and 5 should be reproduced without the written permission of the author.

Acknowledgements

I am delighted to acknowledge the help, advice and encouragement of my supervisor Dr Michael Tooley. I would also like to thank Dr Ian Shennan for his help. Many other colleagues at the Department of Geography have helped me during this project, and I would especially like to thank Derek Coates and Brian Priestley for their great technical help and for always being in a good mood! Dave Bedlington, Jim Innes, Antony Long, Andy Plater, and Ian Sproxton gave much generous advice, liquid company and put up with tales of China. My thanks go to Professors John Dewdney and Ian Simmons for allowing me to use the facilities at the Department of Geography in Durham and to all the staff of the department who helped me.

I would like to thank Dr Wyss Yim at the Department of Geography and Geology of the University of Hong Kong who gave me great help over a period of two years in Hong Kong. Professor Cheung generously allowed me to use facilities at the department. Mrs Wu gave me very useful advice on the diatoms of southern China. Dr Raynor Shaw at the Geological Control Office, Hong Kong, gave his time, advice, practical help and sediment samples, and I am very grateful to him and his colleagues at the GCO.

Many colleagues in China gave generous help and great happiness. I would like to thank all of them, and I hope that this work will encourage cooperation in the future between scientists in Britain and China. This research was interrupted by the tragic events in Beijing in June 1989, and the rigorous political control after this. I hope that the environment for research will improve in the future.

Yongqiang Zong gave me enormous help throughout this project, and I am delighted to have had such a great colleague as well as to have made a close friend. Yongqiang's family have shown me wonderful hospitality whenever I have visited them.

My family have been a great support throughout my life. Their help over the years was more important than they know.

Henrietta Cotterell has put up with this work and high train and telephone bills for far too long. In an effort to get rid of a persistent suitor she helped me with long hours of typing. I hope it will all be worth it.

The research described in this thesis was funded by a grant from **Darchem Ltd, Darlington**. I would like to thank the company for the generous support given, and in particular the former chairman Darchem ~~Dr~~ C Grant. Additional funds for fieldwork were provided by the Royal Institute of Chartered Surveyors Education Trust/AUTOCARTO fund, the British Council and the University of Durham Council.

Chapter 1: Introduction

1.0 Introduction

In this study the evidence for past sea-level and coastal changes along the coasts of southern China and Hong Kong will be examined, and the likely impacts of future marine flooding in coastal lowlands in southern China will be considered. It is therefore a study using a wide variety of techniques, and aims to present new evidence as well as synthesising a large amount of published and unpublished data from various sources. As well as examining the empirical evidence for coastal changes, the study also tests the applicability of certain techniques in southern China.

The work is confined principally to the Zhujiang (Pearl River) Delta and the islands of Hong Kong (22° N 113° E, 21° 20'N 114° 30'E) (Figure 1.1). However, evidence from a number of Chinese studies from the South China coast between Hainan Island and Fujian Province (see Figure 1.1) is also examined to provide a wider spatial context for past sea-level changes. The work on past sea level changes concentrates on the last 10,000 years, during which time sea-levels along the coasts of southern China are estimated to have risen by up to 40 m (Pirazzoli, 1991).

An assessment of the impacts of future sea-level rise on the coastal lowlands of this subtropical coastline, and the risks of marine flooding, has also been carried out. This is confined to a small area (about 270 square kilometres) on the eastern side of the Zhujiang Delta (see Figure 1.1). The methodology used in the assessment of impacts of marine flooding involves the application of a Geographical Information System to the problem. The application of the methodology to a larger section of coastline is discussed.

Chapter 1: Introduction

1.1 Aims

The study has four major aims:

1. To examine the sedimentary changes that have occurred at a series of small coastal embayments and infilled lagoons in the study area.

2. To apply methods of detailed sedimentary and micropalaeontological analysis to a tropical coastline, developing on work carried out in temperate areas (Tooley 1981, 1987) and a tropical coastal lowland in Brazil (Ireland 1988). This detailed methodology has not been applied to the coastal environment of China before.

3. To build a database of radiocarbon dated samples from coastal sites in Hong Kong and southern China, and to identify sea-level index points from these data. An analysis of the data and the possible changes in sea-level along the south China coast over the past 10,000 years has been attempted.

4. To examine the possible impacts of future short and long term sea-level changes on the coastal lowlands of southern China using a Geographical Information System (G.I.S.). This involves both an assessment of the risks of future sea-level rises (both short and long term) along the coast, and the development of a methodology for assessing the impacts of flooding.

Chapter 1: Introduction

1.2 Past sea-level and coastal changes

The methodology used to examine past coastal sedimentary changes uses stratigraphic and micropalaeontological analysis, levelling and radiocarbon dating of carefully selected organic samples which have been related to a former sea-level and therefore are defined as sea-level index points. It has been largely developed in Europe, and has been applied extensively to temperate coastlines, especially in north west Europe (see for example Jelgersma 1961, Tooley 1978, 1981, Shennan 1981, Shennan et al 1983, Tooley and Shennan 1987). Some of these techniques have also been used in studies of subtropical coastlines, particularly in Australia (Chappell 1987 provides a good overview). However along tropical coastlines the studies have generally not undertaken very detailed analyses of coastal sediment stratigraphy.

The analysis of intercalated organic and inorganic sediment deposits and their altitudinal relation to tidal levels is fundamental to this research. Detailed analysis of sediments, and in particular microfossils preserved within them, allows past coastal changes to be estimated. Past changes in sea-level can also be inferred from sedimentary changes, and coastal vegetation changes inferred from microfossil analysis.

The main unit of study is the site. Site selection is very important since all data are collected from the site, and choice of site will therefore have a direct bearing on the quality of the study. A site should be a coastal lowland where sediments have accumulated under uniform low-energy conditions, and have not been disturbed since deposition. Post-depositional disturbance, for example by coastal erosion, or by land subsidence caused by the lowering of the watertable or

Chapter 1: Introduction

neotectonic crustal movements, can be a major problem. Alteration of the sediments after the sea-level and coastal conditions under which they were initially deposited have changed, may introduce significant errors.

A series of boreholes is put down across a site to determine the stratigraphic relationships of the unconsolidated sediments. These are described and classified according to the system proposed and developed by Troels-Smith (1955). It is a descriptive systems and does not involve any interpretation of the origin of sediments. Levelling techniques are used to establish the altitude of sediment samples and stratigraphic units relative to a defined datum. Sediment cores are collected, taking care to minimise the disturbance of the samples during their recovery. In the laboratory these samples are examined for microfossils (in particular diatoms and pollen). After careful analysis, sea-level index points can be defined and tendencies of sea-level change can be determined (Shennan et al 1983). Sites can then be compared to identify significant sea-level changes over a larger area. This methodology is summarised in table 1.1. This detailed methodology, with a strong emphasis on stratigraphic and micropalaeontological analysis of sediments, has not been applied before to the coasts of southern China, or indeed to many tropical and subtropical coasts.

Along the south China coast a number of studies of past sea-level changes ^{have} ~~has~~ been ^{under taken} done. These have concentrated on collecting single sediment samples identified as sea-level indicators, and dating them in order to establish a generalised graph of sea-level index points plotting their radiocarbon dates against their altitudes (see for example Huang et al 1986, Yim 1984a and Pirazzoli, 1991). Some diatom and pollen analyses have been carried out on individual sediment cores, but at a very coarse

Chapter 1: Introduction

resolution (Shaw et al 1986, Huang et al 1982, 1983, 1987). No detailed stratigraphic surveys of small sites have been carried out previously. In terms of the methodological sequence described in table 1.1, there has been a marked tendency to concentrate on the later aspects of the methodology without a detailed examination of the stratigraphic context of the samples.

This study will show the results of detailed analyses of three sites along the eastern side of the Zhujiang (Pearl River) Delta and in Hong Kong. It was not possible to date samples identified as possible sea-level index points for financial reasons, however a number of sediment sequences have been defined as sea-level index points, and could be dated. The criteria used for selecting the sites in southern China and Hong Kong are discussed in chapter 3.

1.3 Impacts of future sea-level changes

Past coastal and sea-level changes provide a context for examining possible future changes, and the risks of flooding to coastal areas. An understanding of the extent of marine influence in the past is important when assessing the risks of future marine flooding. However, a clear assessment of the present geography of coastal regions is also needed for an analysis of the risks and possible impacts of future flooding. The second part of this study, therefore, concentrates on developing and applying methods of assessing the risks and impacts of coastal changes on a small area of the eastern Zhujiang delta.

As economic and population growth continues throughout south east Asia, the pressure to develop coastal land, and the dependence of large populations on these areas, will increase. Yong (1989) has estimated that between 60% and 75% of the 300 million people

Chapter 1: Introduction

in the member states of the Association of South East Asian Nations (ASEAN) live on or very close to the coast. In southern China large populations are concentrated in lowlying coastal deltas, in particular the Zhujiang and Hanjiang Deltas. Chen (1988) has estimated that 15 million people live in the Zhujiang Delta. The coastal deltas of China are the *foci* for major economic growth - the Zhujiang, Hanjiang and Shanghai deltas have all had major increases in investment and population growth. Coastal flooding is a serious hazard, and this will increase as the socio-economic importance of the delta areas grows.

If predictions of future short and long term sea-level rise, together with coastal development, prove to be correct, the risks and hazards of coastal flooding will increase. It is important to estimate and understand the nature of the impacts of this hazard, in order that suitable precautions can be taken to avoid unnecessary costs. The analysis can be divided into three sections.

1. Identification of the hazard involves an analysis of past recorded sea-levels, and identification of past sea-level maxima, rates of sea-level change and areas that have experienced coastal flooding in the past.
2. The risk can then be estimated by assessing the probability of future sea-level rise and the geography of the coastal lowland being studied and thus assessing the degree and nature of the hazard.
3. Finally an evaluation of the impacts of flooding can be made. This involves an estimate of the costs of a sustained hazard (a flood) set against the costs of measures to reduce the hazard and the consequences, whether social,

Chapter 1: Introduction

economic, psychological, physical or other on a population or area affected by flooding.

Coastal areas can be zoned into various risk levels based on an assessment of the risks and costs of flooding. This has been attempted in the United States by the Federal Emergency Management Agency (F.E.M.A.) and Federal Insurance Administration (F.I.A.). Flood Insurance Studies for flood-prone communities have been carried out as part of the National Flood Insurance Program. Coastal High Hazard Areas (V zones) have been defined by estimating wave elevations associated with 100-year floods. V zones can be mapped on the Flood Insurance Rate Maps which provide base flood elevations and divides land into flood hazard zones that are used to establish actuarial insurance rates (F.E.M.A. 1988).

Along tropical coasts systematic work on the risks of coastal flooding and future sea-level changes has been limited. Milleman et al 1989 have examined the consequences of marine flooding in Bangladesh. This has been done at a very general scale however.

The aim of this study is to show the potential for applying a G.I.S. to help assess the risks and likely impacts of future marine flooding in a small defined lowland area of approximately 270 square kilometres. The technique is applicable at a wide variety of spatial scales. Since data for the Chinese coast are limited in certain areas, (particularly sea-level and tidal data), the full potential of the methodology has not been realised in this study. However, future work in this field is discussed in chapter 6.

Chapter 1: Introduction

1.4 The south China coastline

The South China Sea is a warm tropical and subtropical sea, enclosed by the southern coast of the China - Vietnam land mass and the islands of Borneo, the Philippine archipelago and Taiwan. The area is seismically active, particularly to the east.

The coast of southern China is made up of a series of blocks divided by major fault systems. This has had a major influence on the geological and geomorphological development of the region, as well as on the hydrological system. The coastal area is dominated by a fault system running in a south-west to north-east direction (the Neocathaysian system - Zhang 1982). A secondary fault system, running in a south-east to north-west direction, has created a series of faulted blocks (see figure 1.1).

The basement rock, made up of granites and volcanic basalts was consolidated during the Mesozoic (230-65 million years ago). Granitic intrusions and the major north-east trending fault system are thought to have developed during the Cretaceous, followed by volcanic activity. The region experienced severe seismic pressures during the middle and late Tertiary, especially as a result of the uplift of the Himalayan range, and it is thought that the major fault lines in the region were activated during the middle Tertiary (Zuang 1982) causing uplift and subsidence of blocks along the present coastal region of southern China. Tertiary sandstones in western Guangdong province were deposited in subsiding areas, notably the northern part of the Zhujiang delta, and the northern part of Hainan Island and the Leizhou peninsula (see figure 1.1).

During the late Pleistocene the block fault system along the coast is thought to have been reactivated, leading to subsidence

Chapter 1: Introduction

and uplift of different sections along the coast. Areas of subsidence on the coast have been the focus for sediment deposition and delta formation during the Pleistocene and Quaternary. Examples of such areas include the Zhujiang and Hanjiang deltas.

The southern China coast currently experiences vertical tectonic movement related to the fault system. Repeated levelling since 1954 has revealed rates of vertical movement between +3.8 mm/year and -2.27 mm/year (Huang et al 1986). The main deltas (the Zhujiang, Hanjiang and Minjiang) have been generally subsiding over the past 35 years (see figure 1.1), with uplift of other areas of the coast. However this process is not regular as noted by Huang et al (1986). This issue is discussed further in chapter 4.

The coastline of much of southern China is made up of steep slopes and cliffs, with few protected embayments for undisturbed sediment accumulation. The tropical lagoon systems that have been studied by Ireland (1988) in Brazil, and by various authorities in Australia (see examples in Hopley 1978, Chappell 1987) are generally absent from this coast, except in the major deltaic areas where land subsidence has led to sediment accumulation during the late Pleistocene and the Quaternary. The Zhujiang Delta has a few examples of active and relic lagoon systems. These may be divided into two major types:

Lagoons may be formed between a series of sand barriers built up parallel to a coastline, such as those south of Shajing town, in Bao'an County in the eastern part of the Zhujiang delta, close to the village of Dawan (see figure 3.3).

Chapter 1: Introduction

Beach barrier lagoons are formed where a sand beach has developed across the mouth of an embayment, leading to the ponding up of water and the deposition of lagoonal sediments landward of the beach deposits. Examples of these include the Tung O and Sham Wan basins on Lamma Island (discussed in chapter 3 and illustrated in figure 3.9), and at Pui O on Lantau Island, Hong Kong and at Dameisha on the northern side of Mirs Bay. These lagoons vary considerably in their exposure to the open sea, and in the size of both the sand barrier and the lagoon.

It is unclear what processes operated to form these barriers, however it appears from the work at Sham Wan (reported in Meacham 1978), and in the Zhujiang delta (Huang et al 1982) that a variety of processes acted along different coastlines, including longshore drift and tropical storm deposition. The altitude of these barriers varies. At Daman the relic sand barriers and sand dunes have been surveyed up to an altitude of +7.6 m Y.S.D. (see map F-49-48-(53) scale 1:10,000, Chinese National Survey reproduced in figure 5.10). At Sham Wan the sand barrier reaches an altitude of up to +7 m P.D. (7.85 m Y.S.D.)¹. It is possible that higher sediments were deposited during tropical storms, and Morton (1978) argues that this is the likely process by which the sand barriers at Sham Wan were built up.

¹ Altitudes in China are measured relative to two datums, Yellow Sea Datum (Y.S.D.) and Zhujiang Datum. In this study all altitudes of features in China are described relative to Y.S.D. In Hong Kong all features are levelled relative to Principal Datum (P.D.). An explanation of these systems and their relationship is given in chapter 2, section 2.2.

Chapter 1: Introduction

1.4.1 The Zhujiang Delta:

The Zhujiang delta covers an area of approximately 8000 square kilometres. It is surrounded to the west, north and east by heavily weathered mountains and hills of granite and basalts. It is an area that is subsiding, and is divided from adjacent parts of the coast by fault lines as described above. The delta is therefore one of the series of blocks lying along this coast.

Three major rivers flow into the delta, the West river, North river and East river (see figure 1.1). The North and East rivers flow along major fault lines, and drain a relatively small area of eastern and northern Guangdong province. The West river drains much of Guangxi Province, west of the Zhujiang Delta, cutting across the major fault sequence. This has led to a series of gorges and minor rapids along the west river, in particular between Wuzhou and Guangzhou. These three main rivers flowing into the Zhujiang delta have a combined mean annual discharge of 2902.8 billion cubic metres according to figures presented by Huang et al (1982)². The West river has the highest discharge, making up over 75% of the total. The amount of sediment brought into the Zhujiang delta by the rivers is considerable. Data presented by Huang et al (1982) suggest that a mean annual total of 81.1 million tonnes of sediment is discharged into the Zhujiang from all rivers entering the delta³. The West river makes up 89.4% of this discharge. These are mean figures which are likely to vary significantly between years.

² Note: Huang et al (1982) give no details about the way these data were collected, and a number of calculating errors have been found in this work.

³ If a mean density for sediments of 2.65 tonnes m³ is assumed, this would mean that approximately 30.6 million cubic metres of sediment is discharged each year into the Zhujiang delta.

Chapter 1: Introduction

The delta region is geologically heterogenous. It is surrounded by upland areas made up of Mesozoic granites and basalts, and lower tertiary sandstones. Older sandstones and metamorphic outcrops are found at various points across the delta, particularly in the eastern part of the delta (Huang et al 1982). The main upland regions within the delta are made up of mesozoic granite. Hong Kong is similarly composed of granites and basalts.

During the late Pleistocene and Holocene the Zhujiang delta basin was filled with a large amount of sediment up to 80 metres in depth. Huang et al 1982 have summarised the sediment layers by analysing over 1700 borehole records from throughout the Zhujiang delta. It is unclear how accurate the borehole records are, both with regard to altitudinal control, and sediment classification. They have identified six depositional phases in the delta (see appendix 6 and table 1.4).

Phase Q3²⁻¹ during the late Pleistocene comprises a basal gravel and coarse sand with occasional wood fragments. This is considered to be a terrestrial deposit. Above this, Q3²⁻² is a grey silt and clay with marine fossil diatom and occasional *Ostrea* shell remains. Huang and his colleagues suggest that this may represent an early marine transgressive event, perhaps during the last interstadial at the end of the Pleistocene. Q3³/Q4¹ has been defined as the boundary between the Holocene and late Pleistocene. It is defined as a terrestrial deposit. Mottled clays, silts, sands and gravels are found together with wood fragments. The sediments show evidence of exposure to air, with iron oxide nodules and concretions. Huang et al (1982) maintain that these sediments, found throughout the Zhujiang delta basin at depths of between 10 m and 30 m, represent the pre-Holocene land surface.

Chapter 1: Introduction

Three major Holocene sediment layers have been identified in the delta lying above the transition layer $Q3^3/Q4^1$. The layers consist of alternating marine and terrestrial deposits. A lower marine clay and silt with *Ostrea* shell remains and marine and brackish fossil diatom valves ($Q4^{2-1}$) has been dated as early-middle Holocene, and represents the major marine transgression across the delta during this period. A weathered clay and silt layer with coarser sediment fractions and freshwater diatom assemblages ($Q4^{2-2}$) is found above this. Huang and his colleagues describe this phase as a period of land emergence, during which the delta grew due to sediment deposition whilst sea-levels remained relatively stable. An upper marine clay and silt with shell and fossil marine diatom assemblages ($Q4^3$) lies above this, representing a marine transgressive event.

These sediment sequences are very generalised. The Zhujiang delta is an enormous sedimentary system, and the strong flow of the major rivers in the delta has led to considerable mixing of sediments both during and after deposition. The boreholes that have been put down across the delta can be used to identify these major changes. However this study concentrates on detailed sedimentary changes at protected coastal sites at the margins of the delta.

The coastline in the Zhujiang delta and around Hong Kong has been altered very significantly by Man. Large areas of land have been reclaimed from the sea, both in the delta and around Hong Kong. Lagoonal and salt marsh environments have generally been destroyed during land development, for example at Shajing, and along most of the west coast of Bao'an County (see chapter 3) and in the Tin Shui Wai basin in the Hong Kong New Territories (see chapter 3). As a result Holocene coastal deposits have often been disturbed by construction work, or by agricultural development,

Chapter 1: Introduction

and the "natural" intertidal vegetation sequences have been destroyed along most of the coast. The construction of fish ponds has led to the disturbance of Holocene sediments in rural areas close to the coast.

The coastal vegetation consists of mangrove swamps and other salt marsh communities, where these have not been destroyed by development. Mangrove refers to plants from various plant families living under intertidal conditions. In the Zhujiang delta and around the Hong Kong islands cool winter temperatures restrict the growth of mangrove plants to a maximum height of about 5 metres. Species include *Kandelia candel*, *Avicennia marina*, *Aegiceras corniculatum* and *Acanthus ilicifolius*. Though large areas of mangrove marsh have disappeared over the past 100 years because of land reclamation (Irving and Morton 1988) the Mai Po marshes in the Hong Kong New Territories still have examples of mangrove communities. *Avicennia marina*, and *Aegiceras corniculatum* occupy the most seaward positions, and colonise open mud flat. Other coastal species growing along the coast, particularly along coastlines of reclaimed land, include *Phragmites communis*. This thrives along the banks of coastal creeks, as well as at the edge of mangrove stands (Zhou 1985).

Chapter 1: Introduction

1.5 Previous research on sea-level changes in Hong Kong and southern China:

Research into sea-level changes along the southern coast of China has developed rapidly over the past decade, even though much of the work may be considered very general (see chapter 4). However research into coastal changes, and the evidence for past sea-level changes has been done since the early part of the twentieth century, notably in Hong Kong.

In Hong Kong initial research was based on the examination of morphological features above present sea level, and was largely a by-product of other work, particularly archaeological studies of near-shore Mesolithic and Neolithic sites. More recently however, the availability of borehole records of Quaternary unconsolidated sediments, has led to research specifically on past sea-level changes as registered in sediment sequences. Research has however been based on rather coarse sampling intervals, and has not involved much detailed work, either stratigraphic or micropalaeontological.

In southern China research into sea-level change has been particularly concentrated in coastal deltas, notably the Zhujiang and Hanjiang deltas (Huang et al 1982, 1983, 1987, Zong 1992). Sea level curves have been drawn using stratigraphic evidence from large numbers of sediment cores, and limited microfossil evidence (Huang et al 1982). A generalised Quaternary sea-level change history for these deltas has been developed.

This section outlines the literature on sea-level change in Hong Kong and southern China, and tries to identify particular geographical areas, and problems, which have been identified as needing research. This review has been divided into two sections

Chapter 1: Introduction

(Hong Kong and southern China) in part because the work has rarely been coordinated between the two areas, and because the history and quality of the work varies considerably.

1.5.1 Past sea-level changes around Hong Kong:

Over the past twenty years a considerable amount of work has been carried out on the Quaternary sedimentary stratigraphy of Hong Kong. Site investigations by engineering firms, as well as academic studies, particularly related to near-shore archaeological remains, have revealed a large amount of data on changes in sedimentation as well as past sea-level and other environment changes. A number of generalised patterns are beginning to emerge from the data collected around Hong Kong (Bennett 1984, Yim 1984a, 1986a, Yim et al 1988).

Yim et al (1988) have suggested a general model for late Quaternary sedimentation (and hence environmental changes) around Hong Kong. Summarising evidence from sixteen borehole sites in Hong Kong (of which nine have been studied in detail) they have developed a model of late Quaternary sedimentation based on the earlier work of Bennett 1984, Yim 1984a, and Shaw et al 1986.

Yim et al (1988) identify six sedimentary layers illustrated in figure 1.2 and described in appendix 6. In two bore holes they tentatively identify a Lower Marine and Lower Terrestrial layer, both of which are undated, but are assumed to pre-date the last global interglacial, that is to say before 40,000 years ago. Yim and Yu (in press) have identified this Lower Marine sediment layer using diatom and pollen analysis, and suggest that this layer may represent a marine transgression over 200,000 years B.P. Above this four main sediment layers have been identified clearly at a number of sites and have been dated. The middle

Chapter 1: Introduction

terrestrial layer (Yim et al 1988) is dated before 40,000 B.P. Above this a middle marine layer has been dated between 30,560 B.P. and 36,230 B.P. (Yim 1986). Yim et al (1988) claim that this represents a relatively high sea-level during the last global interstadial. Yim (1986a) suggests that mean sea-level may have risen to -9 m P.D. at this time. Pollen of two mangrove species found in this sediment (*Sonneratia caseolaris* and *Sonneratia alba*) suggest a warm climate. These species are not found in Hong Kong, and are now confined to the coasts of Hainan Island where the mean annual temperature is 2°C warmer than in Hong Kong (Yim et al 1988).

An upper terrestrial layer has been dated between $8,520 \pm 270$ B.P. and less than 30,000 years B.P. (Yim et al 1988) and coincides with lower global sea-levels during the last pre-Holocene glaciation, and the early Holocene. Above this is an upper marine layer, corresponding to a general rise in sea-levels during the Holocene. This is a soft grey clay and silt layer.

The two upper sedimentary divisions have been given formational status (Strange and Shaw 1986, Shaw and Arthurton 1988). The older predominantly alluvial deposits are termed the Chep Lap Kok formations after a continuously sampled borehole (B13/B13A) at Chep Lap Kok off the north shore of Lantau Island. The overlying marine deposits have been named the Hang Hau Formation after a continuously sampled borehole (JBS1/JBS1A) near Hang Hau Town in Junk Bay.

1.5.1.1 Late Pleistocene sea-level changes:

Early work on past sea level changes in Hong Kong concentrated on the study of erosional surfaces and raised beaches. These

Chapter 1: Introduction

studies suggested that past sea level has been relatively higher than it is at present, but that during the late Pleistocene glacial periods, sea level was lower than at present, and rose during the Holocene.

Kingsmill (1862) discussed higher sea levels around Hong Kong. He described a light coloured deposit with fossil marine shells on Hong Kong Island approximately 100 feet above present sea level (summarised in Berry 1961). However the site has since been destroyed by various building projects (Berry 1961).

Brock and Schofield (1926) further developed the idea of previously higher sea levels. They suggested that rock terraces at 145 m, 108 m, 61 m, 30 m and 19 m above present mean sea-level are evidence of past higher relative sea levels. Davis (1952) agreed with Brock and Schofield (1926) and noted "wave cut platforms", terraces, and old beaches at 60 feet, 40 feet and 30 feet (18 m, 12 m, and approximately 9 m) above present mean sea level. Davis (1952) suggested two complete oscillations of sea level during the late Pleistocene, followed by a recent relative rise during the Holocene, up to present sea level. However, speculation regarding these oscillations is not supported by other evidence, and is not related to any stated datum.

Berry (1961) followed Davis's (1952) conclusions, describing early Pleistocene sea levels at +70 m P.D., +54 m P.D., +40 m P.D., +21 m P.D., +13 m P.D., and +3-4 m P.D. Berry (1959) considered the +13 m P.D. and +3-4 m P.D. sea levels in some detail. He suggested that a +13 m P.D. raised beach exists around Castle Peak and Deep Bay. The Yuen Long Basin must then have been

Chapter 1: Introduction

inundated by sea water. Indeed Davis (1952) mentioned fossil marine shells found in clay workings at Sheung Shui, but provided no possible age for them. Berry (1959) also discussed sand bars and "raised beaches" at an altitude of +3-4 m P.D. which he claimed represent a higher than present mid-Holocene relative sea level.

Evidence for past relative sea-level being lower than present is given by Berry (1961). He summarised the findings from 943 boreholes taken in Victoria Harbour, Hong Kong. These boreholes penetrated Holocene and late Pleistocene sediments. A recognisable old terrestrial surface between -10 m P.D. and -13 m P.D. was identified in 309 borehole records. Berry (1961) suggested that a former sea-level, lower than -12 m P.D., must have existed, and that this may well represent lower sea-level during the last glaciation (though Berry provided no dated samples of this palaeo-terrestrial layer).

Examination of the late Pleistocene and Holocene sediments in Hong Kong was initiated by Berry (1959, 1960) Berry and Ruxton (1960) and Holt (1962). They, and many subsequent workers, studied past sea-level changes around Hong Kong by examining the sedimentary record, and this led to the development of Yim's (1984a) model of coastal sedimentation during the late Quaternary.

A general sequence of unconsolidated sediments identified offshore in Hong Kong was described by Berry and Ruxton (1960) and Holt (1962). They identified three major stratigraphic units, summarised in Shaw et al (1986) (see table 1.2). This sequence has been substantiated by Kendall (1975), Whiteside (1984) and Willis and Shirlaw (1984). Although they appear to contradict

Chapter 1: Introduction

Yim's (1984a) model, Yim has accommodated these studies within his own model (see below).

At the West Dam site, High Island, Kendall (1975) examined sediments from below present sea level. He identified a marine layer of clay and silt with shells and organic fragments (of Holocene age), overlying an alluvial layer of sands and gravels, (local volcanic rhyolites), apparently laid down by a fast flowing stream. Macrofossil evidence from this alluvial layer suggests that oak (*Quercus*) forest and evergreen laurel (*Lauraceae*) flourished. This corresponds well to the microfossil evidence produced by Shaw et al (1986) for this pre-Holocene layer. Radiocarbon dating of wood fragments from this alluvium layer, at altitudes of between -20.0 m P.D. and -20.15 m P.D. all gave infinite ages (>36,600 years B.P. and >40,000 years B.P.). This alluvial layer must have been laid down when sea-levels were considerably lower than at present, perhaps either during the last global glaciation or the last interstadial, that is to say pre-Holocene. Kendall (1975) found no "lower marine" layer below the alluvial sediments, as reported by Yim (1984a,b).

Whiteside (1984) identified a similar sequence of late Quaternary sediments at Sha Tin (see figure 4). Beneath a thick marine sediment layer, the base of which occurred between -10 and -12 m P.D. he found an alluvial layer divided into three units. The highest unit (unit 1) consisted of a grey silty sand. A sample of wood from this layer was radiocarbon dated to $23,270 \pm 720$ years B.P. (corresponding in age to the upper terrestrial of Yim (1984a)). Below this Whiteside identified unit 2, an orange brown (weathered) sand. There was an apparent disconformity between the grey sand (unit 1) and this weathered sand layer (unit 2). The interface occurred between -14 and -16 m P.D. A localised third alluvial layer (unit 3) occurred below approximately -19 m P.D.;

Chapter 1: Introduction

this was a white, silty, plastic layer with some wood remains. Though no "lower marine" zone was found, Whiteside (1984) suggests that the radiocarbon dated wood remains in alluvial unit 1 may correspond to "upper terrestrial" and unit 2 to "lower terrestrial" of Yim (1984a); the disconformity between these two units "hiding" the intermediate "lower marine" of Yim (1984a). Whiteside (1984) draws obvious comparisons between his evidence at Sha Tin and the sequence found by Kendall (1975) at High Island.

At Victoria Park, Causeway Bay, on Hong Kong Island, Willis and Shirlaw (1984) have investigated marine clays and silts overlying alluvial deposits. A series of boreholes were drilled, and Standard Penetration Tests, combined with visual observation of sediment samples, allowed a general stratigraphy to be estimated. This appears to show a pattern similar to that found by Kendall (1975) and Whiteside (1984). Willis and Shirlaw (1984), using macrofossil evidence, suggest that a transitional "backswamp" sediment may exist between the marine clays and the underlying alluvial deposits. A piece of wood taken from this transitional layer was radiocarbon dated to $20,410 \pm 610$ years B.P. (Willis and Shirlaw 1984). This would correspond to the last Wurm glaciation in Northern Europe, when sea level would have been lower, i.e. Yim's (1984a) "upper terrestrial".

Willis and Shirlaw (1984) recognise that their stratigraphy (like that of Kendall (1975) and Whiteside (1984)) does not identify a lower marine layer (see Yim 1984). Willis and Shirlaw (1984) suggest that alluvial deposits in one borehole between -23 m P.D. and -30 m P.D. exhibit a single fining-upward sequence above which is a disconformity separating more alluvial deposits. This might possibly represent a "low alluvial" layer, with the "upper terrestrial" directly above it.

Chapter 1: Introduction

Yim(1984b) has identified four major sedimentary units at High Island (upper marine, upper terrestrial, lower marine, lower terrestrial) to correspond with his generalised model of environmental and sedimentation changes during the late Quaternary. The upper marine layer consists of coarser material near the top of the layer, corresponding to the present high energy marine environment, and finer material near the base. Mollusc remains of the species *Saccostrea cucullata* and *Crassostrea gigas* suggest a former low energy environment, perhaps when sea level was lower, and the High Island inlet was a very shallow lagoonal/open water environment. A charred piece of wood found at -12 m P.D. has been dated at 5980 ± 180 years B.P. The upper terrestrial, of variable thickness, is made up of sands, gravels and cobbles, of weathered volcanics. Below this the "lower marine" is a dark grey, thinly laminated clay/silt with plant remains, suggesting a coastal marsh or swamp. This is found between -18 m P.D. and -24 m P.D. Shell fragments were found. Coarser sediment towards the base of this layer may represent a higher energy marine environment. Below this is a "lower terrestrial" layer consisting of pebbles and cobbles with yellow clay and silt and low organic matter, suggesting oxidising conditions. This sequence corresponds well with those found at Lei Yue Mun Bay, Chai Wan (Yim 1984a, Wang and Yim 1985), Chep Lap Kok (Yim 1984a, Shaw et al 1986) and Junk Bay (GCO, 1986).

Yim (1984a) discusses the variation between the sequences described by Kendall (1975), Whiteside (1984), Willis and Shirlaw (1984) and others, and his model as suggested by the evidence from East High Island. He shows that the lower marine deposits may not exist in some sedimentary records because of subsequent erosion producing a disconformity between now adjacent upper terrestrial and lower terrestrial layers. Whiteside (1984) and Willis and Shirlaw (1984) both agree with this, and suggest that

Chapter 1: Introduction

such disconformities do exist in the deposits they studied. Kendall (1975) indeed agrees that there was considerable scouring prior to deposition of plant remains dated by him to exceed 36,600 years B.P. This scouring may represent the erosion of a former layer of late Pleistocene marine sediments. However Yim (1984a) admits that considerable "follow-up work by pollen analysis and investigation of marine microfossils such as foraminifera and ostracods" is necessary.

Shaw et al (1986) have undertaken a limited palaeontological study of Chep Lap Kok borehole B13/B13a, which appears to correspond to Yim's (1984a) model for late Pleistocene and Holocene sea level and environmental changes. This borehole consists of 29 m of Quaternary deposits. Dark grey mud with shell fragments overlies late Pleistocene oxidised mottled clays and silts. Below this is an alternating sequence of laminated grey organic muds and mottled clays and silts. By macrofossil analysis, Shaw et al (1986) suggest that there is little doubt that the upper muds are of Holocene age. However, micropalaeontological analysis of the lower sequences was carried out to examine the origin of the lower sediment layers. Successful foraminifera and pollen and spore analysis was undertaken using seven samples from the core. Shaw et al (1986) suggest that the lower mottled and laminated clay/silt layers (-26.54 m P.D. to -29.74 m P.D.) were deposited in a supralittoral environment (corresponding to Yim's (1984a) lower terrestrial sediment layer). No marine taxa were recorded, and 73.2% of the assemblage consisted of woody plant pollen. Shaw et al (1986) suggest deposition of pollen may have taken place in a temporary pool situated in a lowland area. Low diversity of pollen suggests little fluvial input. The upper laminated grey organic mud (-14.2 m P.D. to -16.79 m P.D.) has abundant *Sonneratia* pollen (mangrove) and may represent a littoral depositional environment

Chapter 1: Introduction

and hence a transgressive overlap, corresponding to Yim's (1984a) "lower marine".

The decline of mangroves and the high proportion of fern pollen (*Pteris*, *Polypodiaceae*) and woody plants (*Quercus*, *Castanopsis* and *Pinus*) in the mottled oxidised clay silts above (-9.80 to -12.50 m P.D.) suggests a regressive overlap comparable to the "upper terrestrial" of Yim (1984a) at High Island. Radiocarbon dates from adjacent boreholes at Chep Lap Kok relating to this mottled clay layer range from 16,420 ± 660 years B.P. to 36,480 ± 830 years B.P., suggesting that this layer does indeed represent subaerial deposition, during the last global glacial. Finally the structureless grey muds, with shell fragments, at the top of the sequence were laid down in a slowly deepening sublittoral environment, not deeper than 30 m, as shown by foraminifera evidence (Shaw et al 1986).

Howat (1986) has argued that the lower marine (laminated) clays described by Shaw et al (1986) are the result of slumps and cold mud flows, and suggested, based on data from boreholes adjacent to B13/B13a, that these marine deposits only sporadically contain marine debris, and that these clays are poorly sorted. Shaw (1986) has however confirmed that these laminated clays were probably deposited under shallow marine conditions as shown by the abundance of mangrove pollen, and that the sedimentological evidence from core B13/B13a closely resembles that of eleven other continuously sampled boreholes taken from Hong Kong coastal waters.

The existence of a marine transgressive event before the Holocene is strongly supported by the evidence given by Yim (1984b), and Shaw et al (1986). However, dating this lower marine layer, and producing a late Quaternary chronology for environmental, and

Chapter 1: Introduction

particularly sea-level change, is difficult since the main method of dating used (radiocarbon) is not very accurate for dates over 25,000 years in age (Olsson 1986, Mook and Van de Plassche 1986). Kendall (1975) has dated wood deposits from alluvium which may correspond to Yim's lower terrestrial layer (Yim 1984a) just below the lower marine. These samples between -20.0 and -20.15 m P.D. were dated as >36,600 years B.P. and >40,000 years B.P. RMP Econ (1982) reported dated samples from the lower alluvial terrestrial at Chep Lap Kok (Yim 1984a, Shaw 1986). Samples of wood in this layer were dated at 33,440 ± 1740 years B.P. (-26.5 m P.D.), 36,480 ± 830 years B.P. (-36.5 m P.D.) and >35,230 years B.P. (-23.3 m P.D.). This fits in well with a subsequent rise in sea level, due to the last interstadial rise in temperature.

Yim (1986c) has provided a list and analysis of a large number of radiocarbon dates taken from Holocene and late Pleistocene deposits in Hong Kong. Two of the samples had a high proportion of shells of the oyster *Crassostrea gigas*, and were radiocarbon dated as 30,560 ± 580 years B.P. and 36,230 ± 680 years B.P. These samples were found at altitudes of -18 m P.D., and -17 m P.D. respectively at Sheung Wan, Hong Kong Island. A third sample reported by Yim (1986c) had a radiocarbon age of 31,450 ± 610 years B.P. and was found at an altitude of -15.5 m P.D. Yim (1986a,b) suggests that sea level may have reached as high as -9 m P.D. between 30,000 and 36,000 years B.P., which compares favourably with findings of Milliman and Emery (1968).

Yim and Nau (1984) report a marine transgression in the Pearl River Delta discussed in Huang et al (1982) dating from 23,170 ± 980 years B.P. to 30,440 ± 2300 years B.P. (both samples are mud, found at elevations of -31.3 m and -23.4 m from mean sea level). Although these dates suggest a later marine transgression than that dated by Yim et al (1987), Howat (1985) notes that this

Chapter 1: Introduction

still falls within the margin of error found by Milliman and Emery (1968). It would appear then, that a marine transgression occurred in the region between about 36,000 years B.P. and 23,000 years B.P., although in Hong Kong the evidence suggests an earlier transgressive overlap within this broad period between 36,000 and 30,000 years B.P. (Yim 1986b).

Radiocarbon dates from upper terrestrial deposits at Chep Lap Kok range between $16,420 \pm 660$ years and $27,660 \pm 590$ years B.P. (the older date providing possible evidence for the date when a marine regression occurred, perhaps caused by a cooling of the global climate, followed by regression). This upper terrestrial layer probably corresponds to this cooler period. Yim (1984) suggests that sea level may have fallen to an altitude of as low as -120 m P.D., (and at least to -60 m P.D. (Berry 1959)), probably about 15,000 years B.P. (Emery et al 1970, quoted in Yim 1986). This could have caused the change to alluvial sedimentation over the lower marine layer, or indeed have led to erosion of lower marine and intertidal deposits, and subsequent deposition of alluvial material, as suggested by the evidence of Kendall (1975), Whiteside (1984), Willis and Shirlaw (1984), Shaw et al (1986) and evidence from Kwai Chung, (Shaw pers. comm. 1987).

Willis and Shirlaw (1984) give a date of $20,410 \pm 610$ years B.P. for a piece of wood taken from the upper part of the alluvial sediment layer (unit 1 in Willis and Shirlaw 1984). They suggest that this corresponds with the upper terrestrial of Yim (1984). Willis and Shirlaw (1984) suggest that this sediment layer is of lagoonal or backswamp origin, though they give little evidence for this conclusion. Whiteside (1984) reports a radiocarbon date of $23,270 \pm 720$ years for wood found at -11 m P.D. in an alluvial deposit, below recent marine sediments. Radiocarbon dates, combined with stratigraphic evidence, suggest that sea level fell

Chapter 1: Introduction

after 29,000 years B.P., leading to alluvial sedimentation either overlying older marine deposits (Yim 1984a), or lying disconformitably upon older terrestrial deposits, which pre-date the last interstadial, and cannot be dated by radiocarbon methods.

1.5.1.2 Holocene sea-level changes:

Evidence for a general rise in sea-level along the coasts of Hong Kong during the early Holocene, between about 10,000 and 5,000 years ago, is considerable. A large number of dated samples have been collected, allowing an estimation of the altitudinal change in mean sea level during the Holocene and its rate. The quality of much of the data appears to be good (see chapter 4).

Meacham (1975) has tried to summarise the Holocene changes in sea level around Hong Kong, using evidence from sediments below sea level, exposed during tunnelling operations at Lai Chi Kok, and from the work described by Kendall (1975) and Bard (1975). At Lai Chi Kok, Meacham (1975) found a large tree trunk at an altitude of -14.1 m P.D. in alluvial clay, just below marine clay. This was radiocarbon dated as 8785 ± 125 years B.P. It was not clear whether the tree was *in situ* or had been transported to the site. Meacham (1975) concluded that a marine transgression over -14.1 m P.D. must have occurred sometime after 8700 years B.P. Evidence from High Island, East Dam, collected by Kendall (1975), suggests that sea level may have risen above -17.4 m P.D. by 7900 years B.P., -17.03 m P.D. by 7830 ± 140 m B.P., and -16.13 m P.D. between 7790 ± 90 years B.P. and 6640 ± 100 years B.P. Kendall (1975) dated organic samples from the upper marine layer at High Island, just above the interface between this layer and the alluvial layer beneath.

Chapter 1: Introduction

Bard (1976) gives evidence for a subsequent rapid rise in sea level. He examined a raised beach at Chung Hom Wan. Although his work was largely archaeological, he provided a geomorphological interpretation of his evidence, suggesting that sea level was below +1.65 m P.D at least until 5500 years B.P., but that sea level rose above this level soon after 5500 years B.P.

Meacham (1975) summarises all these results in a Holocene sea level change curve. He suggests that mean sea-level rose after about 12,000 years B.P. but that there may have been a temporary relative fall in mean sea-levels between about 8700 years B.P. and 7900 years B.P. After this sea level rose rapidly up to its present level.

Meacham (1979, 1980) gives more evidence for the mid Holocene rise in sea level. He reports several radiocarbon dates for Holocene material. Marine samples collected from three construction sites (Admiralty, Argyle and Prince Edward Mass Transit Railway stations) were dated by him and are given in table 1.3. These suggest a relative rise in sea level from -11 m P.D. to -7.3 m P.D. between 7000 and 6500 years B.P. Meacham (1978, 1980) reports radiocarbon dates for marine shells at Sham Wan, at altitudes of -1.0 to -2.6 m. P.D. and +0.6 to +1.4 m. P.D. These shells are dated as 5520 ± 110 years B.P. and 3870 ± 80 years B.P. respectively.

This generalised picture of a sea level rise commencing between 9000 and 8000 years B.P., with a possible regressive overlap between 8700 and 7800 years B.P. (Meacham 1975), and a rapid sea level rise between 6700 and 5500 years B.P., followed by possibly fluctuating levels above and below present sea level, needs careful attention.

Chapter 1: Introduction

Frost (1975) gives further evidence for a high mid-Holocene relative sea level. Raised beach sands above a cobble colluvium, dipping at a slope of 1:8 (similar to the angle of beach material) was found on Sha Chow Island at a height of +3.6 m P.D. This material was not dated by Frost, but may well represent a high mid Holocene marine stand.

Fontaine and Delibraïis (1973) agree with Bard (1975) regarding a higher mid-Holocene sea-level than present, suggesting sea-level around Vietnam reached +4 m P.D. about 6000 years B.P. Shells found in sediments between +2 and +3 metres above present sea-level have been dated between 4800 and 5600 years B.P. (compared to Bard 1975).

Yim (1986) has summarised the evidence for sea-level change during the Holocene given by radiocarbon dated samples. He suggests that sea-level, having risen from -20 to 0 m P.D. between 8000 and 6000 years B.P. (an average rate of "about 1 cm/year" (Yim 1986)), has remained "essentially unchanged up to the present day". Several arguments are put forward against a higher mid Holocene sea-level stand by Meacham and Yim (1983), giving evidence from Pui O on Lantau Island. Although Berry (1959) argues that the sand bar deposits at Pui O are Neolithic raised beaches similar to others at Shek Pik and So Kun Wat, and Bard (1975), Fontaine and Delibraïis (1973) and Frost (1975) suggest a mid-Holocene sea-level higher than present, Meacham and Yim (1983) argue quite convincingly against this. By dating artifacts, particularly pottery, they have concluded that the sand deposit is of Tang Dynasty age (A.D. 618-907), and is therefore not evidence for higher Neolithic sea level. Yim (1986) argues that the "raised beaches" in Hong Kong identified by Berry (1959), Bard (1975), Frost (1975) and Meacham et al (1978) are in fact merely bay barriers, built up from the large amounts of

Chapter 1: Introduction

sediment delivered to coastal areas around Hong Kong, possibly by storm events.

Yim (1986) shows that during short extreme periods, such as cyclones, sea level may rise by up to 6.1 m. Such temporary higher sea levels could account for the build up of these sand bars.

Morton (1978) gives some consideration to the nature of formation of these sand bars, and hence to mid and late Holocene sea-level changes. By analysing molluscan evidence from Sham Wan, Lamma Island, and particularly the changes in species from a core taken from Sham Wan, he has developed a model for sea level and coastal changes at the site. This suggests a build up of two sand bars at Sham Wan as sea-level has risen during the Holocene and a resulting increase in brackish water conditions between these bars. Morton goes on to examine the following four hypotheses to explain the build up and altitude of these sand bars which now reach +10.0 m P.D.

- 1) The raised beaches were formed by a higher stand of sea-level at between +6.0 and +10.0 m P.D., and in subsequent stages of regression to the present.
- 2) The raised beaches were formed during the gradual rise or fluctuation of sea-level, eventually reaching +6 to +10 m P.D. (or by comparable uplift of land).
- 3) The raised beaches are in fact sand banks thrown up in single or multiple storm events, in the latter case involving erosion and reworking of the beach materials.

Chapter 1: Introduction

4) The raised beaches result from gradual accumulation of sand behind the beach, in a second storm beach or sand dune.

Hypothesis 1 is rejected as cultural remains are found within the deposits. Hypothesis 3 is rejected (although Morton notes that it was discussed in early pre-war literature), since many cultural deposits have survived intact in stratigraphic sequence since the middle Neolithic times, with no evidence of massive reworking of sediment.

The second hypothesis may seem possible from the evidence at Sham Wan, where the earliest (middle Neolithic) cultural deposits are at +5.9, +6.6 and +6.8 m P.D., late Bronze Age remains are at +7.5 m and early historical above \pm 7.8 m P.D. However, Morton notes that evidence from other sites yields cultural deposits at lower altitudes. From the Middle Neolithic to the present, occupation of sites down to a base level of +3.5 m P.D. has occurred. Although there is some evidence for storm flooding, and temporary rises in sea-level (sand layers), it appears that these sand bars formed with a mean sea level not exceeding +2.2 m P.D. (one metre above present mean sea level). Further Bronze Age carvings as low as +4.8 m P.D. at Po Toi and Kau Sai suggest that effective wave (storm) range was below +4.8 m P.D. and mean sea level below +2.8 m P.D. during the Bronze Age, and has not exceeded this limit since then (Morton 1978). Sand deposition took place at +7.4 m P.D. in the Middle Neolithic (Sham Wan site), at +9.2 m P.D. during the Bronze Age (Tai Long) and at +9.4 m P.D. in early historical times (Tai Long). Morton discusses the possible processes for this. Storm action is one possibility. Morton (1978) indicate that waves of six to eight metres may impact on exposed points on the coastline. The passage of typhoon Rose in 1971 left a debris line at

Chapter 1: Introduction

approximately +4.5 m P.D. at Sham Wan (Morton 1978). Another agent is wind. Sand movement, particularly during the winter monsoon, could explain the build up of sand barriers. Morton (1978) suggests that these "sand bars" might instead be termed "stabilised sand dunes". He shows that between two and three metres of sand has accumulated over the last 2000 years at an altitude of between +7 and +10 m P.D., further evidence that their accumulation is probably due to stormwave or wind action.

The Yuen Long area in the North West Territories may provide evidence of higher sea-levels during the mid-Holocene but this issue has not been resolved as yet. The basin consists of a large embayment, effectively a landward extension of Deep Bay, in the north west of the New Territories. Regionally metamorphosed sedimentary rocks (the Lok Ma Chow formation) underlie the central and northern part of the basin. Volcanic tuffs of the Repulse Bay formation, which are younger, occur to the southeast and east, and younger coarse-grained granite forms higher ground to the south and west of the Yuen Long basin. The Tuen Muen and Kam Tin valleys form extensions of the basin towards the south west and south east respectively.

Beggs and Tonks (1985) have briefly described the unconsolidated sediments within the basin. They identify a grey silty clay with occasional sand lenses and shell fragments, overlying a transitional clay silt and then alluvial silt, sand and gravel. They suggest that this represents a single Holocene transgressive overlap. They give a map showing the limit of the marine sediments, and have found marine sediments at +4 m P.D. suggesting a higher recent sea level than discussed by Morton (1978) and Meacham and Yim (1983). Resolving the change in sea level close to present levels during the Holocene remains an important question. The samples collected by Beggs and Tonks

Chapter 1: Introduction

(1985) have not been intensively analyzed and close investigation may well give clues as to small scale variations in sea level and sedimentation.

A large number of boreholes has been drilled and the sediments recorded in Yuen Long, particularly in the Tin Shui Wai district, on the western side of the basin where a large new town is being built. Boreholes have been drilled using Delft samplers, large diameter U100 cores and hand augers. The "Delft" boreholes,

show records of the sediment

layers found in Tin Shui Wai. These generally correspond to Beggs and Tonks (1985) general summary of sediment layers, however there are some interesting details. In core D8, a lens of black fibrous peat with "marine" silty clay below and above, at an altitude of +2.20 m P.D. suggests possible regressive and transgressive overlaps. Lenses of laminated clayey gravelly sand throughout the marine clay layer may represent storm events. Alternatively these layers may represent changes in the course of stream channels in a marsh or intertidal flat environment. Microfossil analysis of the sediments described by Beggs and Tonks (1985) as "marine silty clay" would help in more accurately defining their origin. Borehole D18 suggests a possible reduction in marine influence, perhaps due to sedimentation of the basin. A grey silty clay with numerous shell fragments is overlain by a slightly organic marine clay with abundant plant remains and occasional sand pockets.

On the eastern side of the Yuen Long Basin, a series of cores have been taken along the road from Yuen Long to Mai Po. Although the logging of the sediments is very simplistic, the cores show the sediment sequences close to the boundary of the "marine silty clay" identified by Beggs and Tonks (1985). Cores D501 - D516 suggest that two "tongues" of soft dark grey silty

Chapter 1: Introduction

clay ("marine deposit") project eastwards, perhaps representing two small embayments. These "marine deposits" reach a maximum altitude of +1.73 m P.D. (borehole D509), well within the altitude of present high tide.

Brimicombe (1986) discusses evidence found in the Yuen Long Basin for a higher than present sea-level during the mid Holocene. He describes various features which might indicate a former high sea level; a palaeo-delta at the mouth of the Tam Mei Valley, on the eastern side of the Yuen Long Basin, a strand line identified as a 3 to 5 m terrace and marine deposits throughout the Yuen Long Basin . Brimicombe qualifies this initial idea of sea level being higher than present between 6000 and 4000 years B.P. The apparent regressive overlap above the marine sediments may be due to increased sedimentation from surrounding upland areas, caused by climatic changes or by human impact, rather than by an actual fall in sea level. Brimicombe (1986) leaves the question of mid Holocene sea level around Hong Kong largely unanswered, but the questions he poses are still valid.

1.5.2 Past sea-level changes off the coast of southern China:

Research into sea-level changes along the south coast of China has increased over the past ten years, however work remains relatively simplistic in terms of the detail of analysis. A number of large projects involving stratigraphic and micropalaeontological work have been undertaken. These have generally concentrated on analysing the geomorphological history of deltaic areas, for example Zhujiang delta (Huang et al 1982) and the Hanjiang delta (Zong 1992). As in Hong Kong, relatively little very detailed stratigraphic work has been done, but this

Chapter 1: Introduction

is partly because the high rates of sedimentation within the deltas mean that Quaternary sedimentary sequences are very thick (up to 63.6m (Huang et al 1987a)). Chinese workers have managed to draw together models of relative Holocene sea level changes. There are a number of interesting discrepancies between these models, and those produced by workers in Hong Kong (eg. Yim 1984).

Huang et al (1982) drew together a summary of Pleistocene and Holocene tectonic, stratigraphic, and sea level changes for the Zhujiang delta. This system divides the Quaternary into eight periods (Q1 - Q4³) which correspond to eight evolutionary stages of the Zhujiang delta. This classification system has been used in many other studies of sea-level change (eg. Huang et al 1986, 1987a, Zong 1992).

Huang et al (1986) have attempted to summarise data related to late Pleistocene and Holocene sea level changes, from a large number of sites along this coast. 126 radiocarbon dated samples of eleven kinds of palaeo sea level indicator have been used by Huang et al (1986). The altitudes of these indicators have been adjusted to take into account tectonic movements, and thereby enable a eustatic, rather than merely a relative, sea level curve to be generated for the last 40,000 years. Tectonic movement during the Holocene has been estimated by extrapolating the vertical movement measured between 1957 and 1974. Extrapolating across the whole of the Holocene from a sample covering 27 years is obviously fraught with problems, and could well be considered impossible. The Zhujiang Delta has undergone subsidence at a rate of -2 mm per year between 1957 and 1974 whereas the area just north of Guangzhou has been uplifted at between +2.0 mm and +3.5 mm per year. Huang et al (1986) acknowledge the problems associated with extrapolation, and show for example that in

Chapter 1: Introduction

Putian (South Fujian) between 1957 and 1972 there was subsidence at a rate of -1.0 mm per year, but this was followed by uplift (+4.4 mm per year) between 1972 and 1974. This part of the south China coast is close to the tectonically active region of the western Pacific. Huang et al (1986) suggest nine major phases of sea level change. They agree with Yim (1986) that sea level rose sometime between 40,000 and 35,000 years B.P., and suggest a maximum rise to -15.2 m below present sea level. This was followed by a rapid marine regression to a minimum level of -100 m, as identified by a submerged ancient delta and submarine terraces in the northern South China Sea studied by Feng et al (1982). Huang and his colleagues then give a detailed analysis of the Holocene marine transgression. 91 radiocarbon dates between $10,230 \pm 320$ years B.P. and the present have been used. The results of this work are shown in fig. 15. They suggest that sea level rose rapidly to above present level by 6000 years B.P., possibly as high as +4 m, and since then has fluctuated, falling between 6000 and 3800 years B.P., rising between 3800 and 2200 years B.P., falling again until 1000 years B.P., and then rising since 1000 years B.P. Zong (pers. comm. 1987) has suggested that the sea-level maximum of +4 m around 6000 years B.P. is an overestimate, and that in fact sea level rose to just below present sea level before 6000 years B.P.

Zong and Li (. 1985 .) have examined Holocene beach rock along the East Guangdong coast. Fifteen samples of beach rock have been radiocarbon dated to between 4790 ± 120 years and 1990 ± 80 years. Taking tectonic vertical movements into account, Zong and Li (1985) calculated sea-level during the middle and late Holocene to have risen from -2.6 m to -2.45 m between 4700 and 3300 years B.P. and then up to present sea-level by 2000 years B.P. Comparing these values with samples collected from 14 drill holes along the coast of Guangdong, Zong and Li (1985) have

Chapter 1: Introduction

corrected their estimates of sea-level rise. They conclude that sea-level 4700 years B.P. was at an altitude of -2.3 m and then rose to -1.55 m by 3300 years B.P. and to +0.97 m by 2000 years B.P.

Huang et al (1987a) have produced a review of the geomorphological evolution of the Zhujiang Delta, and have related this to past sea level changes along the south coast of China. There is a marked discrepancy between the results of Yim (1984a) and Shaw et al (1986), and those of Huang et al (1987a) regarding the sea level and environmental conditions between 35,000 and 30,000 years B.P. This may be due to dating error, and certainly highlights the problems with identifying and dating sediments of this age. Huang et al (1987a) claim a sea-level high stand approximately 10,000 radiocarbon years after that proposed by Yim.

Huang et al (1987a) have tried to calculate sedimentation rates in the Zhujiang delta by measuring sediment thickness of various layers, related to radiocarbon dates, and trying to take into account rates and amounts of compaction (see table 1.4). They show that sedimentation has increased dramatically during the Holocene and suggest that human impact is a major cause. Increasing sedimentation may be caused by deforestation, land cultivation, joining dykes and construction of sluices. Huang et al (1987b) focus on Holocene ^{and late Pleistocene} sea level changes. They identify three buried forest beds at depths of -2 to -4 metres, -9 to -13 metres and -20 metres. These are radiocarbon dated as 2000 years B.P., 6000 years B.P., and 20-30,000 years B.P. Each forest is overlain by dark grey clay silt with fossil Ostrea shells and marine diatoms, suggesting three transgressive overlaps. They conclude that the burial of these forests is a function of sea level rise and subsidence. Like Huang et al (1982, 1986, 1987a),

Chapter 1: Introduction

Zong (1992) and, Huang et al (1987b) show that sea level has fluctuated since about 6000 years B.P. Huang et al (1987b) show that there was a marine transgression (transgressive overlap) between 1850 and 1250 years B.P. (compared with Huang et al (1982) who suggest a transgression between 2350 and 1260 years B.P.

The evidence from China suggests that relative sea-level changes have been broadly similar along the southern coast of China. A late Pleistocene high sea-level corresponding to the last interstadial was followed by a relative fall in sea-level. Huang et al (1986) do however suggest a temporary secondary rise in sea level between about 26,000 and 24,000 years B.P. and Li et al (undated) suggest that sea level was still at between -10.0m and -25.0 m approximately 19,000 years B.P. This general fall in relative sea level was probably a result of the onset of the Wurm glaciation. By 10,000 years B.P. relative sea-level was beginning to rise, and rose rapidly until approximately 6000 years B.P., after which relative sea-level fluctuated around its present value.

Zong (1992) has attempted to summarise the evidence for past sea-level and coastal changes in the Hanjiang delta, and along the south-east coast of China in eastern Guangdong Province and Fujian Province. Zong identified three major transgressive events between 12,310 and 6320 years B.P., 5380 and 3590 years B.P. and 2630 and 1840 years B.P. by ambitiously applying the approach adopted by Shennan et al (1983) to sea-level index points identified along the coast of south-east China. The model of fluctuating sea-levels between about 5000 years B.P. and the present is very tentative however, and Zong emphasises that the data may not be sufficiently robust to allow detailed analysis using this rather more sophisticated technique.

1.6 Conclusions:

The patterns of past sea-level change from southern China vary somewhat from the evidence found in Hong Kong. The late Pleistocene high sea-level, dated by Huang et al (1986) as finishing 23,000 years B.P. and by Li et al (in press) as continuing until at least 19,000 years B.P., is much later than that dated by Yim (1984a, 1986b), and other workers in Hong Kong.

The evidence from China suggests that sea level fluctuated above and below present sea-level between 6000 years B.P. and present (Huang et al 1982, 1986, 1987a, Li et al in press), or perhaps not until about 5000 B.P. according to Zong (1992). In this context however, note should be made of the evidence provided by Zong and Li (1985), who suggest that sea-level was not significantly higher than present between 4700 years B.P. and the present. In Hong Kong, Meacham and Yim (1983) and Morton (1978) have argued strongly against a mid Holocene sea-level higher than present. Yim and Nau (1984) maintain that "no evidence has so far been found in Hong Kong to support the identification of the marine transgression of Huang et al. (1982) during 1,260 to 2,350 years B.P.". They therefore go on to conclude that this discrepancy between data from the Zhujiang Delta and Hong Kong is due to "a regional downrifting event" in the Zhujiang Delta, causing a transgressive overlap to develop there, during this period, but not in Hong Kong. Considering the evidence of Beggs and Tonks (1985) who found marine sediments at up to +4 m P.D., much more detailed stratigraphic analysis of late Holocene deposits in Hong Kong and the Zhujiang Delta is required before a strong conclusion can be drawn regarding mid and late Holocene sea-level changes. In terms of prediction of near-future sea-level changes, this work would be of great value.

2.0 Aims

The aim of this chapter is to discuss the methods used in this study. Though the methods of sedimentary and micropalaeontological analysis are commonly applied to studies of coastal changes in north-west Europe, they have not been applied rigorously to the coasts of southern China. The application of the geographical information system (G.I.S.) used in this study to the analysis of the risks and impacts of coastal flooding in southern China has not been done before.

2.1 Sediment analysis

Two techniques have been applied to the analysis of sediments at three sites: stratigraphic analysis and particle size analysis.

2.1.1 Stratigraphic analysis

Stratigraphic analysis of sediments is of fundamental importance to this kind of study. It provides the framework within which all other associated sedimentary evidence is placed, and the interpretation of environmental changes can only be as good as the initial field data (Tooley 1981).

Interpretation of micropalaeontological and sediment data must be done within the context of the accurately recorded stratigraphy. This then allows conclusions to be made about the nature of individual stratigraphic units. As a second stage, interpretations and generalisations of environmental changes at

Chapter 2: Techniques

different spatial and temporal scales can be made, as shown by changes in the stratigraphy of a site or series of sites.

2.1.2 Methods of sampling

The equipment used to sample the unconsolidated sediments in Shajing Lagoon consisted of a gouge sampler and a "Dachnowski" piston sampler, together with associated rods and other equipment (Tooley 1981). The gouge sampler and rods were made by Eijelkamp, a Dutch company, and the "Dachnowski" piston sampler was made at the University of Durham.

The gouge sampler consists of a one metre long tube (22mm inside diameter), split longitudinally and sharpened at the base. The tube has a 30 cm rod at the top so that the sampler can be attached to extension rods. The extension rods are one metre in length, and can be linked together by metal cylinder sleeves. The "Dachnowski" piston sampler is made up of a metal cylinder (25 mm inside diameter and 25 cm long). It was designed to be compatible with the rods used with the Eijelkamp gouge sampler. Eight extension rods were taken, allowing sampling to be done to a maximum depth of 9.3 metres.

Both samplers can be used to sample adequately layers of organic and inorganic unconsolidated sediments. Although sampling of organic silts and clays and fine sands proved successful, a number of problems was encountered. Sampling of coarse sands with both the gouge or the piston sampler proved difficult. Passage of the samplers through medium sands can be made easier by fast vertical agitation of the sampler which results in the spontaneous liquefaction of the sediment (Tooley 1981). However very coarse sands and gravel, and stiff, tenacious clays and silts were difficult to penetrate both with the gouge and the

Chapter 2: Techniques

piston sampler. Extrusion of coarse sediment out of the "Dachnowski" piston sampler was hampered by the sediment jamming the mechanism. Coarse and very stiff sediments were found at all three sites examined in this study. At Shajing and Tin Shui Wai there were problems sampling coarse sands with the "Dachnowski" piston sampler.

Retrieval of very wet sediments, particularly medium to coarse sands was difficult. The sediments often tended to fall out of the bottom of the gouge sampler as it was being raised to the ground surface after sampling. The sediment core was often compressed and damaged during the sampling process. This was particularly a problem at Sham Wan. On a number of occasions sediments escaped from the gouge sampler before they could be extracted from the borehole and studied.

Contamination of sediment cores is a problem especially when using the gouge sampler since it does not have an isolated chamber within which the sediment sample can be retrieved. The open tube of the gouge is contaminated with sediment as it is lowered down to the sampling depth, and the outside of the sediment core will be effected as it is raised through the upper, previously sampled, sediment layers. The collapse of upper sediment into a bore hole which is not cased can cause the gouge chamber to fill up partially with sediment before it reaches the sampling depth. This problem is exacerbated if the sediments being sampled are very wet causing slumping of sediment from upper levels down into the hole left by the borer. This problem can be reduced by cleaning out the bore hole with the gouge sampler before a fresh layer of sediment is sampled. The gouge sampler tube has a spoon shaped upper end which allows most unwanted sediment to escape past the top of the tube as it is being lowered, but very stiff sediments may clog up the chamber

Chapter 2: Techniques

before it reaches the level at which sampling is planned. These problems are reduced when using the "Dachnowski" piston borer as it has an enclosed sampling chamber which reduces contamination of the chamber as it is lowered, and protects the sampled sediment as it is raised to the surface.

Compaction, and other damage to the sediment core during sampling, extrusion into the plastic storage tubes, and transport to the laboratory is a problem with all sampling methods. The "Dachnowski" sampler is only 25 cm long and the sediment must be extruded from the sampling chamber by applying pressure from the closed end of the sampler, pushing the sediment out of the bottom of the sampler. This pressure can lead to compaction of the sediment core and damage to the sediment structures. The narrow diameter of both the gouge and the piston sampler meant that the sediment cores were very delicate, and needed careful handling so as to avoid breaking up the samples. Sediments were transported to the laboratory in Durham in rigid plastic tubes 30 centimetres long. This seemed to work well, with little apparent sediment core deterioration during transport.

A network of sampling points was set out across the sites, and the gouge sampler was used to examine the sediment stratigraphy at each point. Sediment depth was measured from the top of the bore hole, marked by a metal nail, using a tape measure. The metal nail was then levelled. This was done satisfactorily in southern China and Hong Kong, though the wet conditions and long grasses found at Sham Wan, Lamma Island, made levelling in of the top of boreholes difficult (see chapter 3, section 3.4).

The scheme of sediment classification devised by Troels-Smith (1955) was used in the field. Troels-Smith includes a component in the sediment classification scheme referred to as Limus. The

Chapter 2: Techniques

inclusion of this component has provoked discussion in the literature. Limus is made up of small (sometimes microscopic) organic and inorganic particles deposited in lakes and coastal lagoons, which are the product of both organic productivity in the basin, and material washed in from the surrounding drainage basin. Shennan (1980) has argued that the term Substantia humosa, used by Troels-Smith (1955) to describe organic material with a homogeneous microscopic structure, should be used to describe all unidentifiable organic material. Shennan argues that the term Limus infers something about the origin of the deposit, contrary to the overall aims of the Troels-Smith classification scheme. Ireland (1987, 1988) supports Shennan's (1980) view. Tooley (1981) has defended the use of the term Limus and its subdivisions, and has explained how it can be identified in the field without inference being made to its origin. In this study the term Sustantia humosa has been generally applied to organic material that cannot be classified as Turfa or Detritus. However the term Limus ferrugineus has been used to identify 'rusty' particles, as defined by Troels Smith (1955). In this study it was very difficult to define clearly certain highly organic sediments, which were generally not peats but were very organic-rich clays.

The division of the components into quartiles can be difficult, particularly if a large number of different components exist. Care should be taken not to overestimate components which might have large individual units, such as shell particles, or pieces of well preserved organic material, but which in fact comprise a small proportion of the total sediment sample. Various methods of distinguishing between components in the field without the use of complicated analytical equipment have been devised and are discussed by Tooley (1981, pages 10-14). The division of organic sediments into quartile components often proved particularly

difficult. The great variety of sediments found at the sites in southern China made classification difficult and time consuming. Changes in the sediments were often very minor, with no clear boundary between layers. The clear distinction between organic and inorganic sediment layers that is described in many studies of coastal sediments in north west Europe was not found in the sediments examined in this study except at Shajing, where a clear organic rich layer was observed across a small embayment (see chapter 3). The division of sediments was a problem at Tin Shui Wai. This was particularly so in the inorganic sediment sequences where changes in sediment type often occurred gradually through the sediment core. The division between primarily organic and inorganic sediment sequences was rarely clearly defined. As detailed a description of the sediments as possible was made.

The accurate assessment of the types and quantities of different inorganic sediment types often proved difficult to estimate. The distinction between silt and clay deposits was often uncertain. Laboratory particle size analysis was used after the field investigation to provide a more accurate analysis of the quality of different sediment layers.

Altitudinal errors associated with the sampling of sediments also exist. Although this was not a major problem when sampling sediments along open exposures at Tin Shui Wai (see chapter 3), errors may have been introduced when using hand borers. Shennan (1982) and Ireland (1988) have discussed different altitude errors associated with sedimentary sampling techniques. No comprehensive assessment of the altitude errors was carried out as part of this study, however at Sham Wan three boreholes were put down within two metres of each other (Bore SW4, SW4i and SW4ii). The variation in the recorded depth of the division between the major organic layer and the lower inorganic sediment

Chapter 2: Techniques

varied between 0.08 m and 0.06 m. At this location a full record of the sediments was only made for borehole SW4.

2.1.3 Particle Size Analysis

The descriptions of sediment made in the field using the Troels-Smith system described above provides a large amount of information on the particle size of sediments. However this is only a generalised description of the sediments analyzed. By using methods described in the British Standards Institute particle size classification (BS 1377, 1967) and in Ministry of Agriculture Fisheries and Food (1981) a more detailed classification of the particle size distribution of sediment layers can be obtained. The method of analysis is described in detail in British Standards Institute (1967).

Sediments were analyzed using the pipette method (test 7(c) BS 1377, 1967) using a specific gravity of 2.65. The British Standards Institute grain size classification is shown in table 2.1, together with the relationship with the Troels-Smith (1955) sediment classification system as shown by Ireland (1988). No problems were experienced with this method. Each sample was more than 20 grammes dry-weight. Each sample was taken from within a sediment layer as described in the field. The sample thickness was 2 cm. No sediment stratum analyzed was less than 2 mm in thickness.

2.2 Levelling

In China sample sites and published data for tidal levels, land altitudes and sample altitudes are given relative to the Yellow Sea Datum (Y.S.D.). The Y.S.D. is the national datum of China and is derived from the mean sea-level measured at Qingdao on the Yellow Sea coast of eastern China. Zero metres Y.S.D. is defined as mean sea-level measured at Qingdao and was established in 1956 (Li 1988).

In Hong Kong engineering projects are levelled relative to Principal Datum (P.D.). This is 1.15 m. below mean sea-level at North Point. Chart Datum (C.D.) is 1.30 m. below the mean sea-level (Yim 1988). In this study all altitudes from Hong Kong and the New Territories are given relative to Principal Datum.

The relationship between Y.S.D. and P.D. has not been established accurately. However discussion with the Hong Kong Government Highways Department has established that the difference between the two data is 0.87 metres (personal communication, Fung 1989). In this study the difference is assumed to be 0.87 m. and the following relationship has been used:

$$+1.00 \text{ m. Y.S.D.} = +0.13 \text{ m. P.D.}$$

When comparisons have been made, the Hong Kong altitudes have been converted relative to Y.S.D.

In both Hong Kong and China there are systems of bench marks which are periodically relevelled to check for vertical movements. In China one bench mark was used south of Shajing. This was bench mark C32, which has an altitude of +3.226 m. Y.S.D. and is located close to the Shajing lagoon site (see

Figure 3.3). The bench mark is a small concrete post, driven into the ground. It appeared to be undamaged. All boreholes in Shajing Lagoon (SJA1-2, and SJA6-24 were levelled directly to this benchmark, without moving the level.

In Hong Kong a network of bench marks has been laid out throughout the colony. At Tin Shui Wai a temporary bench mark was used which had been accurately surveyed in 1988 by the engineering contractors preparing the site for the construction of the Tin Shui Wai new town. This bench mark, station point "F", with a Hong Kong grid location of 35068.688 North, 17799.081 East, had an altitude of +6.595 m. P.D. The altitude of sediments taken from Sham Wan was levelled to a bench mark at Tung O (see figure 3.9).

2.3 Micropalaeontological analysis

The environmental changes that have occurred at particular sites can be assessed by detailed analysis of the various microfossils found within the sediment layers. In temperate areas this has generally involved pollen analysis and diatom analysis, with occasional examination of other microfossils such as foraminifera.

Pollen analysis is used to assess the vegetational changes and therefore the water-level and climatic changes at a site. Some pollen analysis has been done both in Hong Kong and China. However detailed analysis of the natural coastal vegetation succession, and the regional pollen assemblage changes consequent upon climatic changes in the area, has not been carried out. It is thus unclear what vegetation successions occur if sea level changes. Shaw et al (1986) have analyzed fossil pollen changes

Chapter 2: Techniques

from sediments north of Lantau Island, and have suggested very coarse resolution changes in sea-level. However the detailed assessment of pollen changes from a single site has not been carried out. In China a number of pollen diagrams have been produced, assessing fossil pollen changes from various coastal sites (e.g. Huang et al 1982). However the resolution is coarse, and little assessment of present coastal vegetational successions has been made.

The problems in using pollen analysis in southern China are very similar to those found by Ireland (1987, 1988) in Brazil. As in Brazil, one particular problem is that the "natural" coastline and its vegetation succession has almost all been destroyed, or has been altered by human intervention. Mai Po marshes in the New Territories, Hong Kong, is an area of mangrove salt marsh partially corresponding to a previous "natural" salt marsh coastline; however even this nature reserve is enclosed with embankments and large areas of the old salt marsh have been reclaimed and developed.

Diatom analysis has proved very useful for assessing past changes in coastal environments, in particular water salinity and marine influence. The identification of diatom species has not proved a major problem. Diatoms along the south coast of China have been well studied, and have been used in a small number of studies (e.g. Huang et al 1982, 1987). Diatom analysis has not been applied extensively to coastal sediments in Hong Kong before.

2.3.1. Diatom Analysis

Diatoms are microscopic unicellular algae that live in wet environments, under natural light conditions. The diatom cells

Chapter 2: Techniques

may be free floating in water (planktonic) or attached to a substratum (sessile) which may be either organic such as a plant, or inorganic particles - sand, silt or boulders. The diatom cells surround themselves with hydrated silica shells known as the frustule. This is made up of two valves, one slightly smaller than the other, which join together encasing the diatom cell. The valves of an individual taxon have an unique shape and decoration. The shapes of diatom frustules may be divided into "pennate" (elongated) or "centric" types. The decoration is often very delicate and intricate, consisting of lines and points (*striae* and *punctae*) (Hendey 1964). Analysis by transmitted light microscope of diatom frustules generally allows the identification of diatom valves and frustules to species level, and this allows the species composition of diatom assemblages from different levels in a stratigraphic sequence to be quantitatively or qualitatively measured.

Many species have strong ecological preferences regarding for example water salinity, tidal regimes, water depth, flooding frequency and water pH. Diatom assemblages from different levels of a stratigraphic sequence can be compared, and variations in the absolute number and proportion of different diatom species can be used to infer changes in the local aquatic environment, and by secondary inference, changes in the wider coastal environment. Changes in relative sea-level, coastal geometry, sediment stores and movements, and fluvial systems may all influence the diatom communities living at a particular site, and these changes will be registered in the fossil diatom assemblage record.

Diatoms have been studied for some two hundred years (Batterbee 1986) and since the start of the 19th century a large body of literature related to the classification of diatoms according to

their ecological sensitivities has been built up. This literature covers diatom species in a wide range of areas throughout the globe. In China a number of studies on the diatom flora of both freshwater and marine environments have been published (Jin et al 1965; Jin et al 1982). These include large numbers of illustrations (plates and line drawings) which allow identification of well preserved fossil diatom frustules.

Samples were taken from sediments retrieved from boreholes at Shajing and Sham Wan and an open section at Tin Shui Wai (see chapter 3). Samples were 7 mm in thickness, and were taken from all the major sediment layers at each site. The sediment samples were placed in glass beakers and covered in a volume of 30% hydrogen peroxide. The samples were left overnight. The beakers were agitated and the sediments sampled using a glass pipette. A small amount of sediment was placed on a glass coverslip which was then dried slowly on a hot plate. The coverslip was then mounted on a glass plate using a diatom mounting agent (naphrax).

2.3.1.1 Halobean classification

Most sub-fossil diatoms that are found in Holocene sedimentary deposits are extant, and so the modern habitat of these diatom species can be taken as an analogue of the palaeoenvironment in which the sub-fossil diatom lived. The allocation of diatom species to different salinity classes is fundamental to the interpretation of fossil diatom assemblages, since it allows a detailed analysis of the water salinity, and hence the marine influence, at a particular site. A large number of classification systems has been drawn up, based on field investigations of modern diatom communities and laboratory analyses of diatom species.

Ireland (1988) has provided a synopsis of some of these schemes. The variations between these schemes are partly a result of variations between study areas. However he has compared the salinity classification of several species commonly found along the coast of Rio de Janeiro State, Brazil, and has shown that considerable differences can occur between classification systems. Ireland (1988) has shown that the use of several classification systems is useful in determining the probable salinity environment and changes shown by variations in fossil diatom assemblages.

In this study the classification system used was that of van der Werff and Huls (1957 - 1974). This was done because it subdivides the classification system used by Hustedt (1953) and is the classification system used by Jin et al (1965, 1982) in their flora of diatoms from southern China. This has allowed summary diagrams to be drawn up, and comparison with other Chinese studies which use a similar classification system (for example Huang 1982, Zong in press).

2.3.1.2 Counting and identification

Each diatom slide was examined using a Zeiss transmitted light microscope with a magnification of up to x1000. Initially a general assessment was made of the quality and quantity of fossil diatom frustules on each slide. This was done by scanning the slide. No counting was done at this stage.

Diatoms were counted using the relative counting method discussed by Battarbee (1986). A series of transects across the slide was made. The transects were divided by one full field of view. For each slide a minimum of 200 diatom valves was counted except where diatom frustules were very scarce when at least 150 valves

Chapter 2: Techniques

were counted. The whole slide was analyzed so that both central and peripheral parts of the slide were examined, so that any variation in the distribution of different sized diatom frustules across the slide would not skew the results of the diatom counts.

The extensive published diatom flora available during this study both from work carried out in Europe and in China allowed almost all valves to be identified, however where positive identification was not possible valves were counted as "unidentified". The diatom flora used in this study are listed in appendix 2. Of particular value were those produced by Jin et al (1965 and 1983).

If diatom valves had been broken into fragments only whole valves or unique parts of a valve (such as the centre) were counted. This proved a particular problem with larger diatom species such as *Nitzchia navicularis*, *Nitzchia scalaris* and *Coscinodiscus subtilis*. Identification of discrete individuals was difficult because of the uniformity of the markings across the valves. Some particles identified using the microscope needed very close scrutiny to confirm that they were or were not diatom valves.

2.4 Geographical Information Systems

As well as examining evidence for past coastal changes at a number of sites, this study was designed to consider the possible impacts of future changes in the coastal environment. An understanding of past coastal changes is important when considering the possible risks and impacts of future changes along any coast. By integrating information on the coastal topography, estimates of possible future sea-levels, and the

Chapter 2: Techniques

extent of previous marine influence, estimates of the risks of flooding can be developed. A clear understanding of the relationships between flood risk areas, population distributions, land use and other aspects of a coastal lowland's geography allow assessments of the possible impacts of flooding. A Geographical Information System (G.I.S.) has been used in this study to integrate information on a study area in the eastern part of the Zhujiang delta and to assess the possible risks and impacts of future coastal changes in the region. Evidence from the work on past coastal changes has been used to identify areas that may be at risk of marine flooding.

A G.I.S is a computer database used to store, manipulate, integrate, analyze and display spatial data in digital form. Data about spatial features and their attributes can be analyzed using a G.I.S., and the interrelationships between different features can be examined (Maguire et al 1991). A particular area can be simplified into a series of landscape elements: for example topography, population distribution, administrative areas, land uses, geology and hydrological networks. Within a G.I.S. information about landscape elements, in the form of spatial features (point locations, lines and areas), and attributes of those features, is stored. The G.I.S. can then be used to manipulate these data to examine relationships between the features and their attributes by integrating different combinations of carefully defined landscape elements.

The initial definitions of the various landscape features and their attributes is fundamental to the subsequent work done with the G.I.S. The resolution of the representation of the landscape elements in the G.I.S. will affect the sophistication, accuracy and worth of the conclusions from the G.I.S.

Chapter 2: Techniques

A Geographical Information System (G.I.S.) is a useful tool with which to assess the likely impacts of marine flooding on an area, and try to measure the risks of flooding. A G.I.S. provides a means of storing data about spatial features and their attributes, manipulating these data to examine relationships, and portraying these relationships in the form of maps and reports.

All G.I.S. work was carried out using pc ARC/INFO software, and some data analysis using a spreadsheet package (VPPlanner Plus; compatible with LOTUS 1-2-3). A database package, dBASE III+, was also used to analyze some of the data. All packages were compatible, allowing easy data transfer.

Feature coverages were digitised using the pcARC/INFO Arc Digitising System (A.D.S.) and a Summagraphics *Summagrid* 36"x48" digitising board. The A.D.S. is a vector based system. Areas are defined as polygons bounded by lines linking defined points. Feature attributes were added to the pcARC/INFO attribute database using a file management programme called TABLES. These are all programmes supplied with the pcARC/INFO system. A fuller discussion of the methods used is provided in chapter 5.

2.5 Conclusions

The techniques discussed in this chapter were selected to address the problems outlined in chapter 1, section 1.1. The various techniques used to analyse sediments are commonly used to analyse past coastal changes in north west Europe. The main problem was the selection of suitable field sites. Because of the reclamation of land along the coasts of the Zhujiang delta and the Hong Kong islands, many coastal sediments had been disturbed, notably at Tin Shui Wai (see chapter 3, section 3.5). The use of a G.I.S.

Chapter 2: Techniques

to examine the risks and possible impacts of future coastal changes proved successful. None of these techniques had been used previously to study in detail coastal lowlands in the Zhujiang delta.

COASTAL SITES ANALYZED

3.1 Introduction

The aim of this chapter is to describe and discuss the evidence for past coastal changes at three sites in Hong Kong and the Zhujiang delta. The suitability of using detailed sedimentary and micropalaeontological analyses, as described in chapter 2, in this subtropical coastal environment will also be discussed in this chapter and the concluding one.

Previous work examining past coastal and sea-level changes in southern China and Hong Kong has not used detailed field investigation methods (see chapter 1). The work presented here attempts to examine the sedimentary and micropalaeontological evidence for changes in three coastal embayments at Shajing (Bao'an County, Guangdong Province), Tin Shui Wai (New Territories, Hong Kong), and Sham Wan (Lamma Island, Hong Kong) (see figure 3.1). Because of difficulties both in finding suitable sites to study, and in carrying out field investigations, the work is rather more limited than was originally hoped. However this work provides a detailed description of two small coastal lowlands at Shajing and Sham Wan, and part of the much larger lowland area of Tin Shui Wai. The coastal sediment stratigraphy at Tin Shui Wai has been destroyed completely by construction work since the field work for this study was carried out in 1988.

3.2 Selection of sites:

The availability of sites in southern China, suitable for the study of past coastal changes, was found to be very limited. Logistics constrained possible fieldwork to the Zhujiang Delta and Hong Kong. In China, because of the conspicuous nature of the fieldwork involved in this study, cooperation of the local government authorities was needed. The Institute of Geography, Guangzhou, provided valuable support in 1988, however a major programme of fieldwork in China planned for 1990 was not possible because of travelling constraints imposed by authorities in Guangzhou.

A series of coastal lowland sites was required, which had not experienced intense human interference, and which provided a sheltered environment for the accumulation of coastal sediments by natural means. The coastlines of both the Zhujiang Delta and the Hong Kong archipelago have long been the *foci* of great human activity. Land reclamation in particular has occurred at most lowland sites. This has led to the destruction of naturally deposited sediment sequences at lowlying coastal sites because of the construction of buildings, and the excavation of numerous fishponds. The latter are up to 3 m deep. This was a problem particularly at Tin Shui Wai, in the New territories of Hong Kong.

Initially a search of the coastline of Hong Kong and the Zhujiang estuary was carried out using 1:50,000 maps of the Zhujiang delta (provided by the Institute of Geography, Guangzhou), and of Hong Kong published by the Directorate of Overseas Survey, Southampton.

Chapter 3: Sedimentary analyses

The Tin Shui Wai lowlands were identified as a possible area for investigation after careful examination of the maps of Hong Kong. Tin Shui Wai was a former large embayment in which coastal sediments have accumulated. The area has been reclaimed over the past 100 years (Irving and Morton 1988) but since 1988 the sediment sequences have been largely destroyed by construction work. The description and analysis of this site covering over 430 hectares (Dutton, 1985), which offered potential for understanding the coastal history of the region, had to be carried out extremely quickly. At one point the author was working next to mechanical excavators which dug up the sediments as they were being recorded. All the field work was completed a few hours before the sediment sequences that were recorded were destroyed.

A literature search highlighted the work carried out by the Hong Kong Archaeological Society at Sham Wan (Meacham, 1978) (see figure 3.1). The work carried out by the Society concentrated on the raised beach deposits to the east and west of the sediment basin that is examined in this study. Little work had been done on the sediment sequences between these two sand bars, although Frost (1978) and Morton (1978) did do some preliminary excavation work. Sham Wan was chosen as a site for investigation, both because of the previous work that had been carried out, and because detailed stratigraphic and micropalaeontological analysis of the sediment basins had not been undertaken.

A one week reconnaissance investigation throughout the Zhujiang Delta was carried out in September 1987, and a three day field investigation of various parts of the eastern part of the Zhujiang Delta and the northern coast of Mirs Bay was completed in April 1988 with the cooperation of the Institute of Geography, Guangzhou. During this period Shajing Lagoon was identified as

a site where lagoonal deposits had apparently accumulated, protected from the post-depositional reworking by tidal currents in the Zhujiang estuary and strong wind and wave action by a series of sand dune deposits (see figure 3.2 and 3.3). Although the area had experienced large scale land reclamation during the 1960s (Huang et al 1982) the sediment sequences landward of the sand dune system appeared not to have been disturbed by direct human interference.

Shajing Lagoon proved to be the only small embayment along the eastern part of the Zhujiang Delta where protective sand barriers existed. Another possible site was identified to the south of Shajing, close to Bao'an town. However access to this area was not granted in 1990 when fieldwork was scheduled. No other sites were examined in detail, and the reconnaissance work revealed very few other potential sites within the eastern part of the Zhujiang delta.

3.3 Shajing

The Shajing Lagoon site is on the eastern side of the mouth of the Zhujiang estuary, just to the south (and therefore downstream) of a point where the estuary widens (known as the Boca Tigris). The coastline at this point runs in a north - south direction (see figure 3.1).

3.3.1 Introduction:

The coastal zone at Shajing consists of a coastal plain which is between two and four kilometres in width and has an altitude of between about 0.5 and 2.0 metres Y.S.D. This coastal plain

Chapter 3: Sedimentary analyses

extends seaward from a series of headlands and hills which rise to altitudes of between 20 and 40 metres. The hills are heavily weathered Palaeozoic quartzite and granite of undefined age, and are covered by trees.

The coastal plain is intensively cultivated with rice paddy, brackish and freshwater fishponds and other irrigated and non-irrigated agriculture. A number of towns and villages has been built at the edge of the low lying coastal plain, at the foot of these hills such as Shajing, Fuyong and Xixiang.

Initially two sites were identified (see figure 3.2). To the north "Shajing Lagoon" consists of a series of relic sand dunes running parallel to the coastline, and between the sand dunes lagoonal sediment deposits have accumulated. About two kilometres to the south of this site two headlands project out into the coastal plain at right angles to the coast. Between these headlands a small embayment exists within which it was initially thought coastal sediments might have accumulated in a protected environment. It was thought that reworking of sediments by the action of tidal currents and waves in the main part of the delta would be limited in this embayment. Some exploratory boreholes were sunk at this site, however the sediments appeared to have been reworked and the site was not studied further.

3.3.2 Shajing Lagoon:

The Shajing Lagoon site consists of a series of sand barriers which are parallel to the line of the coast and the headlands, (a north-south direction). These sand barriers are divided by small lowlying basins filled with fine grained and organic sediments. This sand barrier and sediment basin system is located

about three kilometres from the present coastline (figure 3.2), and covers an area of about 1 km² (see figure 3.3).

The sand barrier system was first identified on 1:50,000 published maps of the Zhujiang Delta (Chinese map sheet F49-48-r). Examination of the 1:10,000 published map of the site (Chinese map sheet F-49-48-(53)) showed that the system consisted of three main sand barriers and three basins, each about 100 metres wide. Between the outer sand barrier and the coastline the ground varied in altitude between 0.6 m Y.S.D. and 1.1 m Y.S.D. Field investigation showed that the sand barriers had been partially destroyed as the sand was being used for house construction. Rice and vegetables were cultivated throughout the coastal plain, and a large number of fishponds had been excavated. Here the coastal sediment sequences had obviously been disturbed by both the digging of fishponds and the construction of embankments surrounding the fishponds.

3.3.2.1 Sediment stratigraphy:

The locations of the boreholes which were put down at Shajing Lagoon are shown in figure 3.3. The borings were put down over a period of five days. Closely spaced bore holes were put down in the sedimentary basins between the sand barriers and the line of coastal hills. More widely spaced bore holes were put down across the coastal plain (SWA3 - SWA5). This was in part because of the depth and lack of great variation in the sediments between the coastline and the outer sand barrier.

Initially five bore holes were put down running at right angles to the line of the coast (SWA1, SWA2, SWA3, SWA4 and SWA5). This revealed that the sediment basins between the sand barriers were

Chapter 3: Sedimentary analyses

between two and three metres deep, and that the unconsolidated sediments became much deeper between the sand barriers and the coast (see figure 3.6). Systematic sampling was not carried out within one kilometre of the present coast because the unconsolidated sediments were greater than eight metres in depth and appeared to consist of mixed grey esturine silts deposited in the Zhujiang estuary, and no clear differentiation of the stratigraphy could be discerned. Within the sediment basins already described the sampling was more intensive. Seventeen boreholes were put down within these basins (see figures 3.3 and 3.4). The sedimentary sequences of the basins between the sand barriers will be described first, and then the sediments between the coast and the sand barriers.

All the borings in the sedimentary basins (SJA1 - SJA2 and SJA6-SJA23) identified the base of the sediment sequences to be a mottled yellow and white silt and sand, often with red streaks and small iron concretions. This mottled base layer varies in altitude, being lowest in the centre of the two sediment basins, and rising towards the edges. The sediments are very hard and stiff and it was difficult to penetrate this basal layer to any appreciable depth. The lowest sampled altitude was -1.20 m Y.S.D. at borehole SJA11. The base layer is overlaid by a layer of sand and silt, generally grey in colour, often with organic material. At bore SJA12 the yellow/grey mottled sand and silt is overlaid by a grey sand and silt with organic material in a 30 cm horizon. This horizon does vary in character. At bore SJA8 some well preserved organic material was found at an altitude of -0.4 m Y.S.D. in a silt matrix. The high concentration of organic material included reeds (possibly *Phragmites communis*). The sediment layer covering the mottled base deposits is found throughout the basins between the sand barriers. The organic layer found at bore SJA8 does not extend throughout the basins.

Chapter 3: Sedimentary analyses

This may be in part because this was one of the deepest sediment layers and the basal deposits generally rose above this altitude around bore SJA8.

Above the organic sand and silt layer was a finer silt stratum, also with organic material. Coarse sand lenses were found in many sediment cores. Generally darker than the sediments below, this layer of silt also appeared to have a clay component when examined in the field. This layer extended up to an altitude of approximately +1.4 m Y.S.D. with the organic content apparently increasing towards the top of the sediment layer.

Above this stratum a very organic silt and clay layer with well preserved woody detritus extends across the sediment basin. This material was not a peat (see appendix 3, for example core SJA8 depths 79-96 cm, and core SJA11 depths 79-132 cm). Organic material was found within a matrix of dark brown clay and silt with individual sand particles. The top of this organic layer is found at an altitude of between +1.88 m Y.S.D. and +2.64 m Y.S.D. There appeared to be little variation in sediment type between samples found in different sediment cores. Only one bore hole registered no dark organic layer. This was at SJA7 which was very close to the small stream that runs through the site (see figure 3.3). This bore hole registered a grey sand with small fragments of organic material, between +1.5 m Y.S.D. and +1.9 m Y.S.D. It may be that past lateral movements in the location of this stream have resulted in the reworking of the sediment layers sampled in this bore. The thickness of the organic layer where it was recorded varied throughout the site between 11 cm and 46 cm.

It was noteworthy that the dark organic layer varied in altitude across the site (see figure 3.4). South of borehole SJA19 the organic layer occurred between +1.33 m Y.S.D. and +1.88 m Y.S.D.

Chapter 3: Sedimentary analyses

To the north of the basin (at boreholes SJA18, SJA20-SJA23) the organic layer was found at altitudes of between +2.17 m Y.S.D. and +2.64 m Y.S.D. There was a clear difference in altitude between sediment layers found in boreholes SJA19 and SJA18 (see figures 3.3 and 3.4). This variation in altitude of apparently related sediment sequences may be due to land drainage for agricultural purposes after the deposition of the sediments. The pattern of sediments suggests that drainage has caused the sediments to consolidate, and since the unconsolidated sediments are thickest in the southern part of the basin, the various stratigraphic layers are found at lower altitudes in this part of the basin than to the north where the unconsolidated sediments are shallower. This makes it very difficult to estimate the altitude of the sediments when deposited. However it seems likely to have been higher than the present altitude of the different sediment horizons.

Above this organic layer a light grey silt was found. As with the organic layer, this silt layer extended throughout the site though its altitude varied as with the highly organic layer (see previous paragraph). This layer had some sand lenses and organic material; generally small woody detritus. At SJA14 this layer is 0.35 m deep with a higher sand content towards the top of the layer. At SJA11 this pattern is repeated, though the sand content is rather greater. Individual sand particles were found within a fairly even silt matrix. The whole area is overlaid by a weathered sand and silt which is brown and grey, has strong ironstaining and has been disturbed at the ground surface to a depth of between 0.3 m and 0.5 m. No shell fragments were found in any of the sediment layers samples in the sediment basin.

The sediments between the coast and the sand barriers were sampled using a series of bore holes running out at right angles

to the coast. Bore holes SJA3-SJA5 were put down over a distance of 2 km (see figure 3.6). Bore holes were located in fields that were used for vegetable or rice cultivation, and were not close to areas that had been disturbed by the construction of fishponds. The sediment layers recorded in the bore holes were heterogeneous, and no detailed stratigraphic pattern was identified similar to that found in the sediment basin described above. A basal coarse sand and silt deposit was recorded at altitudes lower than -3.0 m Y.S.D. This deposit was very wet and appeared to be quite heterogenous with sand, silt and occasional shell fragments. The depth of this basal deposit appears to increase as one moves away from the outer sand barrier towards the coastline. Above this layer the sand and silt contained a higher concentration of shell fragments and larger particles identified in the field as *Ostrea spp.* This layer was up to two or three metres thick. At bore hole SJA5 a 1.46 m thick layer was recorded which had a "large number of shells (*Ostrea spp.*)" and "a large number of shell fragments" (see appendix 1) between depths of 2.90 m and 4.36 m (altitudes of -2.64 m Y.S.D. and -4.10 m Y.S.D. respectively). These sediment layers were very difficult to sample because of the coarse nature of the sand and the relatively high water content of the sediments compared to those found in the sediment basins behind the sand barriers. A grey and brown silt layer between 1.5 and 2 metres thick was found above the shell rich sediment layer.

The sediments appeared to have none of the quite delicate structures of the sediments found within the sand barrier system. Exploratory bore holes between SJA5 and the present coastline suggested that this area had been strongly influenced by erosive and depositional forces at the margins of the Zhujiang river mouth, and that accurate sampling of these sediments was not justified.

3.3.2.2 Particle size analysis

Sediment samples from four cores taken from Shajing Lagoon were analyzed for the particle size distribution using the technique discussed in section 2.1.3. The samples were from cores SJA6, SJA8, SJA19 and SJA5. The aim of this work was to examine the range of sediment types within the various sediment layers in the lagoon, and to assess the stratigraphic analysis carried out in the field.

SJA8

Ten samples were collected from core SJA8, and the results of this analysis are shown in table 3.1. Samples were collected from the upper sand level, and the organic clay silt between a depth of 0.7 m and 1.1 m, and from the lower coarser grey sand and silt between a depth of 2.08 m and 2.94 m.

The upper sand and silt, sampled between a depth of 65 and 78 cm in bore SJA8 is made up of coarse and medium sand together with a high clay content (30.6%). This suggests either post depositional mixing of this sediment layer, or a very varied depositional environment; possibly near still-water conditions combined with regular injections of coarser sands. The dark brown sediment below this was sampled at depths of 0.81 m and 0.91 m. The sand content is lower than the sediment above, and the clay and silt content is higher. Examination of the sediment sample in the field revealed large numbers of individual sand particles within a matrix of finer sediments with some organic material. This suggests again a depositional environment conducive to the build up of organic materials and fine clays, but with significant amounts of sand being deposited either by water

Chapter 3: Sedimentary analyses

action, or by wind action, possibly from sand dunes seaward of the depositional basin. A thin lens of coarser material was identified in the field between a depth of 0.97 m and 0.99 m, and this was confirmed by analysis of a sediment sample which gave particle size distribution of high coarse and medium sand content with clay. As with the samples from the sediment layers above, this suggests an injection of coarser material, from either maritime or land sources.

Below this organic material, a thick layer of grey silt with sand and occasional organic woody material exists. Three samples were taken from the upper part of this layer which appeared to be fairly homogenous. The results of the particle size analysis suggest a dramatic increase in the silt content of the sediment, with a corresponding decline in sand. The clay content also declines. Samples from depths of 0.99-1.00 m, 1.02-1.05 m and 1.08-1.10 m were analyzed. This grey silt was identified in the field as extending to a depth of 2.19 m.

SJA6

Three samples were analyzed from this bore hole, which was put down approximately 30 metres east of bore SJA8 (see figure 3.3). These samples were from depths between 1.48 m and 1.67 m (see table 3.1), and from a sediment layer which corresponds in depth and general appearance with the lower grey silt layer found in bore SJA8 described above. The sediment layer in bore SJA6 was classified in the field as being a grey sandy silt with wood particles. The three samples analyzed for particle size appeared to confirm this, with high silt content, and a higher sand content than the sample taken from a depth of 1.08-1.10 m from SJA8. The sample from 1.65-1.67 m depth in SJA6 is coarser than the samples taken from depths of 1.48-1.50 m and 1.55-1.58 m.

Chapter 3: Sedimentary analyses

This confirms the pattern of coarsening sediments between depths of 1.43 m and 2.60 m, found in bore SJA6.

SJA19

Five samples from core SJA19 were analyzed (see table 3.1). These samples were from a thick grey silt layer with organic material. This sediment layer occurs below the dark organic clay/silt found throughout the Shajing Lagoon basin, and is at a similar depth to the organic grey silt found in boreholes SJA8 and SJA6 between depths of 1.00-2.19 m respectively.

The five samples from bore SJA19 were found to consist primarily of medium sand and silt with a low clay content. There was a variation in sand content through the sediment layer, with sudden rises found between depths of 1.76-1.90 m and below 1.98 m. The sediments are coarser than those found at SJA6 between depths of 1.48-1.67 m (see above).

SJA5

Two sediment samples were retrieved from core SJA5, located seaward of the relic sand dunes dividing Shajing Lagoon from the sea (see table 3.1). These samples were from depths of between 5.10-5.22 m. The sediments found at SJA5 consisted of alternating grey and brown sands and silts, with a large number of shell particles. There appeared to be no dark organic material preserved similar to that found within Shajing Lagoon. The samples analyzed were found to consist of clay and fine-medium silt. The upper sample, found at a depth of 5.10-5.12 m also had a high fine sand content. The samples were taken from either side of a division between a higher grey sediment with a high shell content, and a lower brown silt which itself lay on top of

a mottled sand. This mottled sand which has evidence of iron staining and heavy aerial weathering, appears to be an old land surface, and is found at a depth of 5.82 m (an altitude of (-4.90 m Y.S.D.)). The lower sample, taken from the brown silt, at a depth of 5.18-5.22 m, had a very high clay content of 51.5%, suggesting a former very low energy water environment.

3.3.2.3 Diatom analysis:

Diatom analysis of sediment samples from two boreholes in Shajing Lagoon was undertaken in order to assess the nature of the depositional environment in which the various sediment layers were laid down. The causes of the changes in sedimentation might then be inferred. A secondary aim of the work was to assess the feasibility of using diatom analysis in conjunction with detailed stratigraphic analysis of sediment samples. This kind of detailed work has not been attempted at sites in southern China, though diatom analysis has been applied to individual sediment samples collected from the area. Samples were retrieved using the "Dachnowski" sampler, and were analyzed in Durham using the technique discussed in chapter 2.

At this stage no chronology can be fitted to the environmental changes identified, since no sediment samples have been dated scientifically.

The diatom sequences at all sampled layers within Shajing Lagoon are dominated by the brackish planktonic species *Cyclotella striata*, though a large number of other species were identified. Two diagrams have been produced to show the distribution of the diatom species at different depths in the boreholes sampled (see figures 3.7 and 3.8).

Bore SJA8:

Twenty five samples were analyzed for diatoms from borehole SJA8, located close to the centre of the inner Shajing Lagoon (see figures 3.3 and 3.7). The samples were taken from the depths of between 1.43 m (+1.09 m Y.S.D.) and 0.75 m (+1.77 m Y.S.D.). The sediment sequence was thus made up of a lower grey silt with clay and sand particles and some organic particles lying beneath the highly organic layer found throughout the basin (see descriptions of sediment layers in appendix 1 and in section 3.3.2.1). Above this organic layer was an upper silt with sand from which two samples were taken at depths of 0.755 m and 0.78 m.

Figure 3.7 shows the proportions of different individual diatom species at the various sampled depths, and the relative proportions of different salinity groups (see discussion of diatom techniques in section 2.3.1).

Within the lower grey silt and sand, between depths of 1.43 m (+1.09 m Y.S.D.) and 1.09 m (+1.43 m Y.S.D.) the diatom sequence is dominated by brackish and marine diatom species, in particular *Cyclotella striata*, *Nitzchia punctata*, *Grammatophora oceanica*, *Nitzchia cocconeiformis*, *Coscinodiscus blandus* and *Diploneis smithii*. The proportion of brackish species appears to increase slightly up the sediment sequence, though this is almost completely due to an increase in the proportion of one species, *Cyclotella striata*. Many other marine, marine-brackish and brackish-marine species have been found within this sediment layer. The proportion of brackish diatom species varies between 26% and 61%, showing a general increase up the sediment sequence. No freshwater, fresh-brackish or brackish-fresh diatom species were found below a depth of 1.03 m (+1.49 m Y.S.D.).

Chapter 3: Sedimentary analyses

The grey silt layer identified by the stratigraphic analysis between depths of 0.99 m and 1.19 m appears to be a transition layer between the lower grey silt below and the dark organic silt above. Freshwater and brackish-fresh diatom species were identified in this layer above a depth of 1.03 m. The first group of these species that appear includes *Nitzchia scalaris*. There is a transition from marine and brackish diatom species to primarily fresh and brackish diatoms found within the dark organic silt. Freshwater and brackish diatom species are dominated by *Nitzchia scalaris*, *Pinnularia major* and *Pinnularia microstauron*. A number of species of the genus *Eunotia* were also found within this dark silt. The highest proportion of freshwater diatoms was found in a sample taken from a depth of 0.89 m (+1.63 m Y.S.D.).

The proportion of marine and brackish species increased again in the silt and sand sediment found above the dark organic silt, above a depth of 0.89 m. The two shallowest sediment samples from depths of 0.755 m and 0.78 m contained a high proportion of *Nitzchia cocconeiformis*, *Diploneis Smithii* and *Cyclotella striata*. Valves of the species *Diploneis bombus* were found in these two upper samples, reappearing after a complete absence in samples taken from the dark organic silt. The number of species and individual frustules of fresh and fresh-brackish diatom species found in the samples from the upper silt and sand sediments was much lower.

Three major diatom assemblage zones have been tentatively identified by eye, examining the diatom distribution diagram (see figure 3.7). No statistical tests have been applied to the data. The boundaries in the assemblage zones have been defined by identifying samples where either marine or freshwater diatom species appear or disappear. Zone SJA8/I, below a depth of 1.03

Chapter 3: Sedimentary analyses

m (+1.48 m Y.S.D.) has no brackish-fresh, fresh-brackish or fresh diatom species. The assemblage is dominated by brackish species, in particular *Cyclotella striata*, and the proportion of this species rises up the sediment sequence. The proportion of marine and marine-brackish species falls gradually. Dominant species identified were *Nitzchia cocconeiformis*, *Coscinodiscus blandus*, *Diploneis Smithii*, *Grammatophora oceanica*, and *Nitzchia punctata*.

The boundary between zone SJA8/I and SJA8/II is marked by the appearance of freshwater diatom species, together with fresh-brackish and brackish-fresh. The sample found at a depth of 1.03 m (+1.48 m Y.S.D.) was the deepest level at which freshwater diatom taxa were identified. The rise in freshwater species is initially slow, but then increases rapidly above a depth of 1.00 m (+1.52 m Y.S.D.). Dominant freshwater taxa include *Pinnularia* spp. and *Eunotia* spp. This rise in the proportion of freshwater species is combined with a fall in the proportion and total number of brackish and marine diatoms found in the sediment samples. The proportion of *Cyclotella striata* diatom valves found falls immediately above 1.03 m depth (+1.49 m Y.S.D.). The proportion of marine diatom frustules declines up to a depth of 0.855 m (+1.665 m Y.S.D.).

The proportion of marine and marine brackish taxa begins to rise above a depth of 0.855 m, and this has been defined as the lower boundary of zone SJA8/III. This zone extends up to the top of the sampled core, a depth of 0.755 m (+1.77 m Y.S.D.). Zone SJA8/III is distinguished by a fall in the proportion of freshwater taxa and a corresponding rise in the proportion of both brackish and marine water diatoms. Freshwater diatom taxa include *Pinnularia* spp. and *Eunotia diodon*. Marine and brackish taxa are dominated by *Nitzchia cocconeiformis*, *Diploneis smithii*, *Diploneis bombus*, and the apparently omnipresent *Cyclotella striata*.

Bore SJA19

Fourteen sediment samples from borehole SJA19 were analyzed for diatoms. The samples were all taken from the lower grey silt and sand layer lying beneath a dark organic silt. Both sediment layers were found throughout the basin (see figures 3.4 and 3.8, and appendix 1) The lower samples from borehole SJA8 (below a depth of 1.10 m) were taken from this sediment layer. This allowed both a comparison to be made between samples from the two boreholes, and a more detailed analysis of the diatom sequences within this sediment layer which extends across the Shajing Lagoon basin. The samples analyzed for diatoms from borehole SJA19 were taken from depths ranging between 1.40 m (+1.16 m Y.S.D.) and 2.02 m (+0.54 m Y.S.D.).

The upper samples from SJA19 correspond in altitude and sediment type to the lower samples taken from bore SJA8. These samples both suggest a rise in maritime and brackish diatom species, dominated by *Cyclotella striata*. The samples taken from SJA19 are dominated by brackish and marine diatom species, with very occasional small numbers of freshwater diatom species found.

The lowest four samples from SJA19 taken at depths of between 2.02 m (+0.54 m Y.S.D. and 1.90 (+0.66 m Y.S.D.) show a strong but slightly declining brackish influence and corresponding increase in the proportion of marine diatom species such as *Actinocyclus ehrenbergii*, *Cocconeis pseudomarginata* and *Grammatophora oceana*. The brackish diatoms make up 68.2% of the count at a depth of 2.02 m, dominated by *Cyclotella striata*. The marine influence appears to reach a climax at a depth of 1.61 m (+0.95 m Y.S.D.) when the total number of marine and marine-brackish diatom valves make up 65.1% of the total diatom count

identified. This sediment layer is dominated by *Actinocyclus ehrenbergii*, *Cocconeis pseudomarginata*, *Coscinodiscus subtilis*, *Diploneis smithii* and *Nitzchia cocconeiformis*. Brackish diatom frustules (*Cyclotella striata*) make up 25.7% of the total count.

Above this depth the proportion of brackish diatoms increases. Occasional freshwater diatom species were found at various depths, however no consistent trend of freshwater influence was found, suggesting periodic but erratic injections of freshwater may have occurred in the lagoon. The upper sediment layer samples between depths of 1.48 m (+1.08 m Y.S.D.) and 1.40 m (+1.16 m Y.S.D.) had a brackish diatom frustule count of between 32.8% and 46.2%, rising with altitude. This was dominated by *Cyclotella striata*, but there was also a rise in *Navicula elegans*, *Nitzchia navicularis* and *Terpinosoe americana*. This appears to correspond well with the diatom counts for samples collected at similar altitudes from bore SJA8, though the proportion of brackish diatoms appears to be slightly higher in samples from bore SJA19.

Diatom assemblage zone definition has not been attempted on the data from this core. The diatoms found in the samples taken from bore SJA19 are similar to those found at similar depths in bore SJA8, in diatom assemblage zone SJA8/I.

3.3.2.4 DISCUSSION:

The diatom analysis of sediment samples from bores SJA8 and SJ19 appears to show clear changes in the water quality of the sedimentary environment of Shajing Lagoon, which correspond well with the major changes in sediment quality found both by stratigraphic analysis in the field and by laboratory particle size analysis of samples.

Chapter 3: Sedimentary analyses

The lower grey silt and sand deposit found throughout the Shajing Lagoon basin appears to have been deposited in a brackish water environment with a strong marine influence. The particle size analysis for samples from bore SJ19 suggests that the rise in the proportion of marine and marine-brackish diatoms is accompanied by a coarsening of material deposited at these levels. The lagoon at this stage therefore was probably an intertidal mud flat, with a constant opening to the sea, but was a relatively low energy environment. Thus marine and marine-brackish diatom species existed such as *Actinocyclus ehrenbergii*, *Cocconeis pseudomarginata*, *Coscinodiscus subtilis*, *Diploneis smithii* and *Nitzchia cocconeiformis*, together with brackish species dominated by *Cyclotella striata*.

The change from this grey silt and sand to the dark organic silt layer above represents a rapid reduction in the marine and brackish influence, and a rise in the freshwater influence in the lagoon, accompanied by an increase in the clay content of the inorganic material (see particle size analysis for bore SJA8). However, there is also an increase in the sand content of the dark organic sediments. This may have been caused by wind action, rather than by marine water deposition. Examination of the dark sediments in the field revealed that the coarser sand particles were deposited individually within a much finer clay and fine silt matrix. The darker organic samples are dominated by freshwater and brackishwater diatom taxa, as represented in diatom assemblage zone SJA8/II. Zone SJA8/IIb identified by one sample found at a depth of 0.915 m (+1.605 m Y.S.D.) provides some evidence for varying conditions, with injections of brackishwater into a predominantly freshwater environment.

The lighter silt and sand above the dark organic layer appears to represent a return to more brackish conditions, and a fall in

freshwater influence in the lagoon. The particle size of sediments increases slightly, and the proportion of brackish diatom valves rises. This rise is however predominantly due to a rise in the number of *Cyclotella striata* valves.

3.3.2.5 COASTAL CHANGES:

The various analyses carried out on the sediments found at Shajing Lagoon suggest that the site has experienced very different conditions in the past to those existing at the present. Shajing Lagoon is now located 4 km from the coast, behind a series of sea-embankments and fishponds. The altitude of the lowest surveyed land surface found landward of the outer sand dunes at Shajing Lagoon was +2.45 m Y.S.D. (Borehole SJA14), compared with a present day high astronomical tide level of approximately 2.2 m Y.S.D. (Huang et al 1982). In the past the marine influence was much stronger during at least two periods. Between these times the lagoon experienced freshwater conditions. These were induced either by a change in the sea-level or by changes in the morphology of the coastline causing a reduction in the marine influence, such as a build up of a protective sand dune barrier. Since it was not possible to bore down through the relic sand dunes at Shajing Lagoon, it has not been possible to determine the relative ages of the relic sand dune complex and the various sediment layers in Shajing Lagoon. However it appears that the changes in the nature of the sedimentary environment in the lagoon, combined with the diatom evidence for freshwater influence at Shajing Lagoon, together suggest that the lagoon was temporarily sealed off from marine influence. There is also strong evidence for a freshwater dominated environment at an altitude of about +1.60 m Y.S.D. (diatom assemblage zone SJA8/IIc). This must have been due to either a much lower sea-

level than at present, or a large barrier such as a sand dune cutting the site off from marine influence.

This may have been followed by a breach in the sand dune system, allowing an increase in the marine influence, causing the upper silt and sand above the dark organic layer to be deposited. The coarser material in this upper inorganic layer, compared to the organic layer beneath, suggests an increase in the energy of the depositional environment, combined with an increase in the proportion of marine and marine brackish diatom species.

This sedimentary evidence may be combined with historical evidence. Navigation charts of the Zhujiang estuary produced by Captain E Belcher in 1843, M Rocquemaurel in 1857 and F Callsen in 1907⁴ suggest that the coastline close to Shajing during the 1840s and 1850s followed a line very close to the headlands to the south of Shajing Lagoon, and the outer sand dunes at Shajing. The sand dunes at Shajing Lagoon may therefore have been active at this time, and only divided from the sea by later land reclamation at the end of the nineteenth century and during the twentieth century. Rapid land reclamation in the region during

⁴ These charts can be viewed at the Hydrographic Department of the Royal Navy in Taunton, U.K. The references for the charts are as follows: Charts L3083, L3087, L3084 and L3085 produced by Captain E Belcher aboard the ship *HMS Sulphur* in 1841, and published in January 1846 cover the Zhujiang estuary.

Chart D2859 published in 1857 by the French Maritime and Colonial Department, and originally surveyed by M Rocquemaurel aboard the ship *La Capricieuse*.

Chart C2301 produced between 1906 and 1907 by a team led by Acting Captain F Callsen for HM Customs Service. This chart covers the western coast of Bao'an County, and shows a similar coastline to that depicted in the chart produced by Rocquemaurel in 1857.

the late 1950s and 1960s is reported by Huang et al (1982). The main sea embankment 2.5 km seaward of Shajing Lagoon was built in 1961 and 1962 (Huang et al 1982). When exactly the sedimentary changes recorded at Shajing occurred cannot be estimated, however it may have been during the past few hundred years. What can be stated is that a strong marine water influence has been recorded at altitudes of up to +1.77 m Y.S.D. (borehole SJA8 sample depth 0.75 m) at Shajing Lagoon, four kilometres inland of the present coastline, and that this *may* have occurred during the past 100-150 years. It is known that High Astronomical Tide is approximately +2.2 m Y.S.D. along this coast (Huang et al 1982). This has important implications for the analysis of the possible impacts of future marine flooding discussed in chapter 5.

3.4 SHAM WAN:

3.4.1 Introduction:

Lamma Island is located about 10 km south west of Hong Kong Island (see figures 3.1 and 3.9). The island geology is made up almost entirely of granite (Chiu, 1978). The granite is heavily weathered giving a pale brown or white sandy silt. This is the material that makes up the sand bars at either end of the site (Meacham 1978). Quartz veins occur throughout the island, and in particular to the north of the site studied.

Much previous archaeological work has been done at the south west end of the site, at Sham Wan (see figure 3.9). Meacham (1978) discusses the site and the archaeological remains found in the sand bar deposits which suggest human occupation at the site since about 3000 years B.P. Morton (1978) discusses various theories for changes in the configuration of the coastline during the Holocene at Sham Wan, but also points out that a detailed survey of the basin deposits at Tung O are necessary in order to gain an understanding of the likely sedimentary changes at this site. This detailed survey had not been done before, though Catt (1978), Frost (1978) and Lau (1978) do discuss the results of a rather crude series of boreholes put down to the south west of Tung O in the Sham Wan basin (see figure 3.9). Catt (1978) undertook some pollen analysis of samples from one of these boreholes (borehole "B"), but this was not very successful. Few pollen grains were preserved. Frost (1978) discussed the stratigraphy of unconsolidated sediments in the valley that crosses Lamma Island at Sham Wan. The sediments consist of a lower light grey clay with sand and shells, above which the sediments become darker grey, finer, and have a higher organic content. A coarser upper layer of silt and clay with some sand

Chapter 3: Sedimentary analyses

covers the basin. The stratigraphy as recorded by Frost (1978) is shown in table 3.4.

An attempt was made to recover sediment samples from the valley where Frost examined the sediments, however on three occasions in the spring of 1988 and 1990 the valley was waterlogged, and it was not possible to recover samples with the equipment available. This problem was also encountered by Frost and his colleagues in 1977.

The site is situated at the southern end of the island. The eastern promontory projecting south is divided from the main part of the island by a lowlying marshy channel (see figure 3.9). This lowlying area is divided from the sea on either side of the promontory by two sand barriers that rise to altitudes of about +9.0 m P.D. on the south west end of the site and +6.0 m at the north east (close to the village of Tung O). These sand bars rise steeply from both the coast and the area of marsh ground that divides them. Figure 3.9 illustrates the topography of the site, and the location of boreholes that were put down during two periods of fieldwork at the Sham Wan site. The marsh ground surface is at between +3.2 m and +4.0 m P.D. The weathered granite slopes to the north and south of the site rise steeply. The site is divided into two parts by a ridge of rock on which part of the village of Tung O is built. A small lowlying sediment basin is situated directly between Tung O and the eastern sand barrier which is about 100 m x 100 m. This will be referred to as the "Tung O basin".

3.4.2 Tung O basin:

Eight boreholes were put down in the Tung O basin running in a north - south direction across the basin, and one borehole at right angles to this main axis (see figure 3.9). A detailed picture of the sediment sequences within the basin has been developed with boreholes spaced approximately every 10-15 metres across the site. The sediment stratigraphy of the site is shown on figure 3.10.

3.4.2.1 Stratigraphy

The sedimentary stratigraphy of the basin is illustrated in figure 3.10. This shows that the unconsolidated sediments reach a depth of about 4 metres, but are apparently confined by the solid rock geology to the north, west and south and by the coastal sand barrier to the east (see figure 3.9). Boreholes SW1 and SW8 at the margins of the basin only reach depths of 30 cm and 63 cm respectively. It appeared that the borer was stopped by very hard coarse sands and gravels in both cases.

At each borehole other than these two marginal locations a very coarse grey sand and gravel was found at the base of the sedimentary sequences. This was found at altitudes of between approximately -1.5 and -0.5 m P.D. Good sediment samples of this basal layer were not retrieved from all boreholes because the sediments were very coarse and wet, and occasionally fell out of the sampling auger as it was being withdrawn from the boreholes (SW2, SW3, SW5) as shown by the unshaded areas in the stratigraphic diagram (figure 3.10). The basal gravel and sand was a blue-grey colour and could not be penetrated by the gouge sampler. The texture of the sediment varied from sand and fine

Chapter 3: Sedimentary analyses

gravel, to finer sand with silt and clay. Samples with the higher silt and clay content were retrieved with the augur more successfully.

Above the basal sand and gravel, a darker silt with fine sand extended across the basin. This dark grey sand/silt displayed no evidence of layering. Above this layer a darker more organic silt and clay has been deposited, with small well-preserved twigs and branches. At borehole SW2, a large piece of wood was found at a depth of 3.83 m. (-0.45 m P.D.). Similar well-preserved organic matter was found across the basin at this altitude. This organic silt and clay varies with depth. Occasional sand lenses are intercalated. These sands generally have little organic material and are a lighter shade of brown to the dark organic rich silts and clays. At boreholes SW2 and SW4 a brown sand lens was found at depths of 1.95 - 2.10 m (+1.43 m P.D. to +1.28 m P.D.) and 2.00 - 2.09 m (+1.29 m P.D. to +1.20 m P.D.) respectively. At SW3, no sample was retrieved between depths of 2.11 and 2.20 m, though there appeared to be evidence of coarser sand at this depth in the sampling auger. Above this varied layer of organic silts with sand lenses, a dark, well-preserved peat with clay and silt was found. This layer contained well-preserved rootlets or reedlike plants, that appeared to be phragmites. The clay content of the sediment matrix around the organic material was high, but a few individual sand particles were found in this sediment. The sediment was a very dark brown colour. Although this layer was clearly identified across the Tung O basin in all boreholes except the two peripheral borings SW1 and SW8, the organic content of the samples varied with the highest concentration of well-preserved organic material towards the centre of the basin (in boreholes SW3 and SW4).

Chapter 3: Sedimentary analyses

The sediments above the peat and silt sediment layer were much lighter grey brown sand and silt with clay. This layer was also found across most of the basin and was approximately 0.5 m deep. It was a fairly homogenous inorganic layer with no layered structure. The sediment was darker and coarser above a depth of about 1.0 m. This top sediment layer varied in texture, with coarse sands concentrated towards the top of the layer. The sediments within about 0.5 m of the surface appeared to have been disturbed by modern plant growth.

Sediment samples taken from borehole SW4/4i are shown in figure 3.11. This photograph of the sediment core that was retrieved from the site was taken in Durham about one month after the sediments were extracted at the site. It shows clearly the variation in sediment colour, and highlights the layer of lighter silts and clays between 1.15 m and 1.50 m depth (+2.14 m P.D. to +1.79 m P.D.), and the dark peat with clay between 1.80 m and 2.25 m depth (+1.49 m P.D. to +1.04 m P.D.). The grey sand and fine gravel at the bottom of the core can also be distinguished as a lighter layer.

3.4.2.2 Particle Size Analysis:

Samples were taken from core SW4i for particle size analysis (P.S.A.). The methodology used is summarised in appendix 1 and section 2.1.3. Samples varied in dry-weight between 7.24 and 31.9 g, though the majority of samples is over 15.0 g in dry-weight. The results of the P.S.A. are shown in table 3.2. The basal deposit is made up of coarse sand and gravel, but with a high clay content. Between depths of 3.41 m and 3.87 m (-0.12 m P.D. to -0.58 m P.D.) the gravel content was calculated to be between 25.4% and 36% in the three samples tested. The clay content was

Chapter 3: Sedimentary analyses

much higher than the proportion of silt at these depths. This clay content increases farther up the core, in the organic rich silt and clay, and the sand and gravel content falls dramatically. The silt and clay layers with the highest concentration of organic material also appear to have the finest material with clay and medium or fine silt concentrations of over 60%. The lighter clay and silt is also a fine sediment. Medium and fine silt and clay make up 75.8% of the sample by weight at a depth of between 1.06 and 1.09 m (+2.23 m P.D. to +2.20 m P.D.), and 72.9% by weight at a depth of between 1.22 and 1.24 m (+2.07 m P.D. to +2.05 m P.D.).

The particle size analysis suggests that the deepest sampled sediments were deposited in a variable energy environment. Periods of low energy allowed some clay and silt deposition, but this was dominated by periods of relatively high energy which led to the dominance of gravel and coarse sand. These two coarser sediment categories made up over 55% of the sediments below a depth of 3.41 m (-0.12 m P.D.). There then appears to have been a change in energy environment. Sediments sampled at a depth of between 3.33 and 3.36 m (-0.04 m P.D. and -0.07 m P.D.) have a gravel and coarse sand content of only 10.0%, but a clay content of 34.6% and a combined medium and fine silt content of 32.8%. This low energy sediment deposition environment appears to continue up through the sediment layers until a depth of approximately 0.87 m (+2.42 m P.D.). There appears to be relatively little change in the particle size distribution between depths of 3.36 m and 0.96 m (-0.07 m P.D. and +2.33 m P.D.). This is confirmed by the field evidence (see appendix 1).

Above a depth of 0.96 m (+2.33 m P.D.) the proportion of gravel, and coarse and medium sand increases. The proportion of these three coarse sediment categories was calculated to be 6.8% at a

Chapter 3: Sedimentary analyses

depth of between 0.96 and 0.99 m, and 56.8% between 0.67 and 0.70 m. The proportion of fine sediment fell at corresponding depths. This upper sediment layer was deposited in a high energy environment.

3.4.2.3 Diatom analysis:

Diatom analysis was carried out on 28 samples from bore SW4 at Sham Wan other samples were examined which had no diatom remains and represented a diatom impoverished zone (see below). The methods used were the same as those carried out on the sediments taken from Shajing Lagoon. The proportion of different diatom taxa found in the samples analyzed and salinity classes are shown in figure 3.11.

From the bottom of the sediment core (a depth of 3.87 m; altitude -0.58 m P.D.) to a depth of 3.40 m (-0.10 m P.D.) there is an impoverished zone, and no diatom frustules were found in quantities that could be counted. The sediments found at this depth were primarily coarse sands and gravels, providing a poor environment for frustule preservation. The sample found at a depth of 3.39 m has a high proportion of freshwater-loving diatom taxa, dominated by *Pinnularia alpina* and *Amphora mexicana*. The proportion of freshwater diatom frustules is calculated to be 81.6%, because of the dominance of these two species. There is evidence of a marine influence in this sample. Over 10% of the diatom valves counted at this level were *Actinocyclus ehrenbergii*, a marine planktonic diatom species.

The eleven samples analyzed between depths of 3.20 m and 2.40 m (+0.09 m P.D. and +0.89 m P.D.) all show a fairly constant freshwater influence. The proportion of freshwater valves counted

Chapter 3: Sedimentary analyses

varied between 92.9% and 72.4%, with all assemblages dominated by two diatom species; *Pinnularia alpina* and *Amphora mexicana*. The marine diatom assemblage at these sampled depths was dominated by *Actinocyclus ehrenbergii*. The number of valves of the brackish-freshwater species *Nitzschia scalaris* was observed to increase up the sediment sequence, though brackish diatom valves (brackish-marine, brackish, and brackish-fresh) never made up more than 13% of the total number of identified diatom valves counted. The diatom valves were well preserved in high concentrations.

Above a depth of 2.40 m (+0.89 m P.D.), there appears to be a transitional zone. The proportion of freshwater diatoms counted declines rapidly, and the proportion of marine and marine-brackish valves increases. Between depths of 2.40 m and 2.20 m (+1.09 m P.D.) the proportion of total identified valves of the species *Pinnularia alpina* declined from 55% to 2.2%. No examples of this freshwater species were observed in samples from above a sediment core depth of 2.20 m. A similar pattern was observed for frustules of the species *Amphora mexicana*. This may be compared with the dramatic rise in the proportion of marine and marine-brackish diatom species, in particular *Coscinodiscus rothii* and *Diploneis fusca*. The apparent peak of marine influence found in the sample taken at a depth of 2.30 m (+0.99 m P.D.) is intriguing, as this pattern is due to a rise in the numbers of observed valves of one species *Diploneis fusca*, and was observed in just one sample. However the number of individual diatom valves of this species counted was considerable (61 out of a total count of 207).

The seven samples analyzed from depths of between 2.20 m (+1.09 m P.D.) and 1.80 m (+1.49 m P.D.) were all dominated by marine-brackish diatoms species; particularly *Coscinodiscus rothii*. The



Chapter 3: Sedimentary analyses

proportion of brackish diatom valves between depths of 1.95 m (+1.34 m P.D.) and 1.85 m (+1.44 m P.D.) was also higher than that found in samples from depths lower than 2.00 m (+1.29 m P.D.), reaching a maximum measured concentration at a depth of 1.90 m (+1.39 m P.D.). It should be noted that the freshwater influence is relatively low in these samples. The proportion of freshwater species valves at a depth of 2.10 m (+1.19 m P.D.) was 13.8%, declining to 3.2% at a depth of 1.85 m (+1.44 m P.D.).

Above a depth of 1.80 m (+1.49 m P.D.) the proportion of marine and brackish diatom frustules declines dramatically, with a corresponding rise in fresh-brackish species, particularly *Pinnularia major*. The diatom assemblage observed in the sediment sample from a depth of 1.55 m (+1.74 m P.D.) is dominated by *Pinnularia alpina* (136 valves observed out of a total of 204).

Between depths of 1.55 m and 1.05 m (+2.24 m P.D.) there is an impoverished zone, where diatom preservation is very poor. Two samples from depths of 1.26 m and 1.20 m were found to have sufficient diatom frustules that could be counted. These two samples suggest that the high concentration of fresh and fresh-brackish diatom species observed at depths of 1.55 m (+1.74 m P.D.) may continue above this level. The diatom assemblages at these two depths were dominated by *Pinnularia major*, *Synedra ulna* and various examples of the *Eunotia* species. However all other samples taken from sediments found between depths of 1.55 m and 1.05 m had very few broken fragments of diatom frustules preserved.

Above a depth of 1.05 m (+2.24 m P.D.) diatom preservation was good, up to a depth of 0.86 m (+2.43 m P.D.). The diatom assemblages between these two depths were dominated by fresh and fresh-brackish diatom species, particularly *Eunotia* spp.,

Chapter 3: Sedimentary analyses

Pinnularia major, *Stauroneis anceps*, *Pinnularia interrupta* and *Pinnularia microstauron*. The marine and brackish water influence appears to have been minimal, with minor counts of diatom species of these salinity groups.

Three broad diatom assemblage zones may be suggested, based on the evidence from the diatom analysis carried out. Zone SW4a between depths of 3.39 m (-0.10 m P.D.) and 2.40 m (+0.89 m P.D.) is dominated by freshwater diatom species, particularly *Pinnularia alpina* and *Amphora mexicana*. It has been defined as all samples with freshwater loving diatom valves making up more than 60% of the assemblage. There do not appear to be any significant changes in the diatom assemblages at different depths within this zone. Marine diatom valves make up no more than 10% of the total number of valves in any of the assemblages in this zone.

Zone SW4b is a transition zone which is represented by one sample at a depth of 2.30 m (+0.99 m P.D.). The assemblage is dominated by *Diploneis fusca* (marine) and *Pinnularia alpina* (freshwater). This minor peak in marine diatom species is limited to this transitional zone. Marine diatom valves make up almost 35% of the assemblage, and freshwater species make up 37.7% of the total number of valves counted.

Zone SW4c, between depths of 2.20 m (+1.09 m P.D.) and 1.80 m (+1.49 m P.D.) is dominated by marine-brackish diatom species. In all samples more than 40% of the diatom valves observed were of the species *Coscinodiscus rothii*. This species was not found outside this zone. There is an almost total absence of *Pinnularia alpina* and *Amphora mexicana* valves, and freshwater diatom valves make up less than 14% of the total number of valves counted in all samples. Zone 4d is divided into three subzones, due to the

Chapter 3: Sedimentary analyses

impoverished diatom zones between depths of 1.50 m (+1.79 m P.D.) and 1.05 m (+2.24 m P.D.). Zone SW4d is dominated by freshwater and fresh-brackish diatom species. Subzone SW4di (illustrated by two samples at depths of 1.75 m (+1.54 m P.D.) and 1.55 m (1.74 m P.D.) is dominated by examples of *Pinnularia alpina* which makes up over 60% of the diatom assemblage at a depth of 1.55 m. Subzone SW4dii (two samples at depths of 1.26 m (+2.03 m P.D.) and 1.20 m (+2.09 m P.D.) is also dominated by *Pinnularia alpina*, but diatom preservation is poor, the erosion and damage to individual valves is considerable, and the range of species is limited (see figure 3.11). Subzone SW4diii, the upper diatom assemblage zone, has a lower proportion of valves of the species *Pinnularia alpina*, and a far wider range of species than either subzone SW4di or SW4dii.

3.4.2.4 Discussion:

The lower "freshwater dominated" assemblages, between depths of 3.39 m (-0.10 m P.D.) and 2.40 m (+0.89 m P.D.) correspond to the lower organic rich grey and dark brown clays and silts. The particle size analysis of these samples shows that the inorganic sediments are made up primarily of clay and silt. Analysis of the sediments in the field and in the laboratory also suggests a low energy depositional environment with a large quantity of organic material. A well preserved piece of wood was found at a depth of 3.02 m (+0.27 m P.D.) in this sedimentary layer. Although it was not identified, and no rootlets were attached, this material was deposited within a strongly organic sediment.

Beneath this organic "freshwater" dominated layer is a coarser grey sand and silt layer, below a depth of about 3.40 m (-0.11 m P.D.). No preserved diatoms were found in any of the samples

Chapter 3: Sedimentary analyses

taken from below a depth of 3.39 m (-0.10 m P.D.), but the coarse nature of the material (see table 3.2 and discussion about particle size analysis) suggests that this layer was deposited in a higher energy environment to the organic layer above it, and may have been built up in an open coastal environment. The material was a grey/blue coarse sand with little organic material.

Above a depth of 2.40 m (+0.89 m P.D.) the diatom assemblage becomes dominated by marine and marine-brackish diatom species. There does not appear to be any major change in the sediment quality at this depth however. The sediment is dark and quite highly organic, similar to that below a depth of 2.40 m, though the sediments do get progressively lighter above a depth of about 1.70 m (+1.59 m P.D.). The diatom assemblage is dominated by *Coscinodiscus rothii*, a marine-brackish species. From the field analysis of the sediments, and the diatom analysis it appears that these sediments were laid in a relatively low energy environment, but one which had reasonably open access to marine conditions, thus allowing the planktonic diatom species to colonise the basin in what must have been a saline lagoon.

This low energy marine-brackish environment appears to have changed quickly at some point, since the diatom assemblages found in samples at depths of 1.80 m (+1.49 m P.D.) and 1.75 m (+1.54 m P.D.) are very different. The former, lower sample is dominated by marine-brackish diatom valves; the latter, higher sample is dominated by fresh-brackish and brackish-fresh species. This rapid change in the diatom assemblages is not coincident with a dramatic change in sediment quality. However the sediments above this do become progressively lighter in colour, and rather coarser.

Chapter 3: Sedimentary analyses

The lighter sediments found between depths of approximately 1.50 m (+1.79 m P.D.) and 1.10 m (+2.19 m P.D.) correspond to the diatom impoverished zone shown in figure 3.11 and discussed above. Though diatom remains were found at depths of 1.26 m (+2.03m P.D.) and 1.20 m (+2.09 m P.D.) that suggest the sediments were laid down under primarily freshwater and fresh-brackish conditions, this is a very tentative conclusion, because of the paucity of diatom evidence.

Above a depth of 1.10 m (+2.19 m P.D.) the sediments become darker, and are made up primarily of clay and silt fractions (see table 3.2). The diatom assemblage is dominated by a wide range of fresh and fresh-brackish water diatom species. It appears that the basin experienced quiet water conditions, separated from any strong marine or brackish water influences. Above a depth of 0.86 m (+2.43 m P.D.) no diatom remains were found, and the sediments appear to become much coarser. At a depth of between 0.67 m (+2.62 m P.D.) and 0.70 m (+2.59 m P.D.) the sediments consist primarily of sand and gravel (see table 3.2).

3.4.2.5 Coastal changes:

The diatom and sediment analysis of core SW4i suggests at least three major environmental changes, with both strong marine and freshwater influences as well as variations in the energy of the depositional environment at the Sham Wan basin.

The lower coarser sediments found below a depth of about 3.40 m in bore hole SW4 (-0.11 m P.D.) appear to have been deposited under high energy conditions which may well have been an open coast. The sediments are very coarse sands and gravels suggesting a coastal beach environment. However the area may have been

Chapter 3: Sedimentary analyses

slightly protected from open coastal conditions as clays were deposited as well as coarser sands.

The basin then became a low energy freshwater environment - apparently an enclosed lagoon. A large amount of organic matter was deposited at this time. Some reed deposits were found in the basin in this sediment layer (possibly *Phragmites* fragments). Conditions during this period of fresh and brackish water influence may have been quite varied. The range of sediments is considerable, and the variation between sediments across the basin found in the different boreholes is great. There is no very clear highly organic layer extending across the whole of the basin, however the general trends in sedimentary changes were found throughout the site. The diatom assemblages are dominated by well preserved pennate freshwater species, suggesting that the lagoon was protected from the open coast.

This freshwater environment appears to have been interrupted with an increase in marine influence, however this does not appear to have been accompanied by a significant rise in deposition energy. The saline-water loving diatoms deposited above a depth of 2.20 m (+1.09 m P.D.) are dominated by the planktonic species *Coscinodiscus rothii* (diatom assemblage SW4c). This apparent strong marine influence but low energy environment suggests that a coastal protective barrier that is likely to have existed seaward of the Tung O basin was breached but not destroyed. This change in water quality appears to have occurred over a considerable time since the sediments included in diatom assemblage zone SW4c are approximately 0.6 m thick.

The sediments above a depth of 1.75 m (+1.54 m P.D.) were deposited under primarily fresh water and low energy conditions. It is not clear what the cause of the change in sediment quality

in this sediment sequence was. The sediments change from a dark brown to light brown/grey colour at a depth of 1.50 m (+1.74 m P.D.), and a dark brown at a depth of 1.05 m (+2.24 m P.D.), however there is no significant change in particle size.

It is not clear what the relationship between the present sand barrier which protects the basin from the coast and the organic sediments found in the basin is. Borehole SW8 was put down close to the present sand barrier, however the sand deposits were not penetrated, and it is not known whether the sand barrier lies on top of an extension of the fine organic deposits and therefore postdates these deposits. It is also not clear whether the changes in the sediments and environmental quality are primarily due to changes in a sand barrier seaward of the basin influencing the impact of marine conditions, or due to past changes in sea-level. It should be noted that freshwater diatoms and organic deposits have now been found down to an altitude of approximately -0.1 m P.D., when present marine conditions may extend regularly up to an altitude of about +2.7 m P.D. (Yim 1988). These lower organic sediments with fresh water diatom assemblages may therefore represent a period of lower sea-levels. No age estimate has been made on these deposits.

3.5 Tin Shui Wai

3.5.1 Introduction:

Tin Shui Wai is an area of former marshland in the northwest New Territories in Hong Kong at the southern edge of Deep Bay. It makes up the western part of the Yuen Long Basin (see figure 3.12). The history of the area over the past 100 years has been discussed by Irving and Morton (1988). The general sedimentary stratigraphy of the area has been described by Beggs and Tonks (1985) based on a large number of engineering boreholes. The stratigraphy they describe is quite generalised, consisting of a grey marine clay/silt overlying a mottled alluvial terrestrial deposit. The "grey marine clay/silt" is not described in detail, but is described as a "marine" sediment. This may be interpreted as a coastal sediment.

Binnie and Partners (1981) have produced an internal document with details of borehole logs from the Yuen Long Basin made from cores taken with a Dutch mechanical borer. This document is not available for general inspection because of legal action taking place over construction work carried out at Tin Shui Wai. However notes on some borehole logs from the Tin Shui Wai basin have been obtained, and the general stratigraphy of the unconsolidated sediments found in Tin Shui Wai is shown in figures 3.13, 3.14 and 3.15. These show details from 16 boreholes along two main transects across the Tin Shui Wai basin. The large number of shells found together with coarser sediments and highly organic peat deposits suggests that the area has experienced periodic coastal environmental changes. The boreholes suggest that the unconsolidated grey sediments in Tin Shui Wai are coastal marsh deposits.

In this chapter the detailed stratigraphy recorded in the field during this project will be described, followed by a general analysis including reference to the general stratigraphy described in the boreholes obtained from the work by Binnie and Partners.

3.5.2 General stratigraphy:

The borehole logs drawn up by Binnie and Partners provide a stratigraphic context within which the detailed stratigraphic analysis of this study may be placed. The borehole logs have been divided into three transects. These are illustrated in figure 3.12.

Transect AA' (figure 3.13) extends out from the northern edge of the basin, in a south-east direction. The sediments consist of grey clays and silts, with an organic content at altitudes of between about +0.30 m P.D. and +3.00 m P.D. Shell fragments were found in boreholes TSWD46 and TSWD39 just above and below +0.00 m P.D. This is near the centre of the Tin Shui Wai basin, where the sediments are deepest. Thin highly organic layers were found in bore holes TSWD47 and TSWD39 between depths of +1.90 and +1.76 m P.D. and +2.05 and +1.85 m P.D. respectively.

Transect BB' (figure 3.14) runs north-west from the southern part of the Tin Shui Wai basin. The sediments found in the boreholes along this transect are similar to those found in transect A. The upper silts and clays have a high organic content, and some shell fragments were found below this in the two bore holes near the centre of the Tin Shui Wai basin (TSWD17 and TSWD18).

Transect CC' (figure 3.15) extends from the south-east corner of the Tin Shui Wai basin north and north-east. The sediments get deeper towards the centre of the Yuen Long basin. Organic sediments are concentrated in the shallowest cores to the south, with the deeper sediments closer to Deep Bay in the north consisting of silts and sands with shell fragments. Coarser sediment lenses also exist within the various sequences. In bore TSWB174 a fine silt and clay organic deposit was found below an altitude of -8.2 m P.D., lying beneath inorganic silts and sands.

The sediments in Tin Shui Wai basin appear to have been deposited under varying coastal conditions. Towards the present coastline to the north of the basin the sediments are primarily inorganic sand and silts with shell fragments, suggesting a stronger marine influence, and higher energy coastal environment. The sediments found close to the southern and northern margins of the basin in all three transects consist of finer inorganic material and poorly preserved organic material. Occasional thin layers of very organic detrital material and coarser inorganic sediment lenses suggest an often changing intertidal environment. Along Transect CC' this variation of coastal deposits appears to be concentrated in sediments above an altitude of -1.0 m P.D.

3.5.3 Field sites:

Two sites have been examined within the Tin Shui Wai basin, and the stratigraphic data have been compared with unpublished data from various engineering geology site studies produced by Binnie and Partners (1981). From these various sources a general model of Holocene sediment deposition within the basin has been developed. Diatom analysis of sediment samples was attempted,

Chapter 3: Sedimentary analyses

however very few diatom frustules were found in any samples analyzed, and this analysis was abandoned.

During the periods in which fieldwork was carried out at this site (October 1987, April 1988 and April 1990) the site was being excavated and built on during the first stages of land preparation for a New Town site. The sediments discussed have now been completely destroyed as a result of this engineering work. This study therefore provides a record of some of the sediments of this former coastal marsh, as well as providing rich evidence of past changes in the coastal environment.

To the west, at site Tin Shui Wai A (TSW/A) a 37 m section and two boreholes (TSW/A1 - TSW/A2) were examined. These were located within an area of former fishponds which had been drained. Mechanical diggers had excavated large parts of the surface clays and silts to a depth of approximately four metres, as deep as a mottled red-brown sand and gravel. The 37 metre section was excavated during April 1988, and this was recorded over three days just after the excavation.

To the east of the basin, about 1 km from the TSW/A, a long sediment section was examined over a distance of about 800 metres. The sequence of sediments was not recorded because access to this site was difficult (it was a construction site), and parts of the section had been damaged. However various sediments were identified, and their altitudes were measured using a theodolite. This has allowed some altitudinal comparisons to be made between the two sites within the Tin Shui Wai basin.

3.5.4 SITE TSW/A:

TSW/A is in an area of former fishponds about 200 m from the western edge of the Tin Shui Wai basin (see figure 3.12). The section that was recorded and sampled ran in a north - south direction and had been cut into the base of an old fishpond. The bottom of the fishpond (altitude about +1.3 m P.D.) was about one metre above the highest recorded sediments. No material above an altitude of +0.5 m P.D. was recorded.

3.5.4.1 Stratigraphy:

The section at TSW/A was about 37 m in length. A piece of string was stretched along the section and anchored to the sediment using nails placed in the sediment every three metres. One metre intervals were marked off on this string, and the sediment sequence directly above and below these marks was recorded according to the system described in chapter 2. Points along the string were levelled in to a benchmark (located about 100 metres from the section), and the depths of sediment layers were recorded relative to the level of the string at each "one metre" mark, allowing the altitude of the sediments to be calculated relative to principal datum. Figure 3.17 shows the sediments found in the section. The base of the section is defined by a yellow mottled sand and fine gravel layer. This dipped to the centre of the section, forming a channel feature. To the west of the section the sediments had been cleared over a distance of about 150 m. This fossil channel could be clearly identified, running at right angles to the line of the section, as it was filled with dark brown highly organic material that was the same as the sediment above the basal sands and gravels in the section (see figure 3.16).

The yellow and brown mottled sand was covered by a thin layer of coarse light grey sand which had a very low silt and clay component. It could be excavated easily and was very friable when rolled in the hand. This layer varied in thickness from 10 to 40 cm. The sand was quite homogeneous and had little structure, though occasional finer intercalated sand or silt layers appeared. The top of this grey sand layer was very well defined, with a clayey peat and was found at an altitude of between -1.9 m P.D. and -1.1 m P.D. This was the sharpest division between two sediment layers found anywhere in the Tin Shui Wai basin. Figure 3.16 represents the variation in the depth of the lower mottled basal sand and grey sand found below the organic peat layer.

The organic material found above the friable sand layer appeared to contain both well preserved rootlets and twigs and branches, with well preserved pieces of *Phragmites* reeds. The peat layer was about 30 - 40 cm in depth, though the upper boundary was very difficult to define, as the organic content of the sediment diminished very gradually. A dark organic silt and clay replaced the peat. This dark organic silt layer, which had no clear upper or lower boundaries, also varied in texture along the section, occasionally becoming coarser, for example between 10.50 m and 12.50 m from the southern end of the section. Towards the top of this layer very small shell fragments appear at an altitude of about -1.0 m P.D. The concentration and size of shell fragments increases dramatically in the dark grey silt deposit above, with occasional whole shells found in their living positions and identified as *Ostrea gigas*, commonly found along the present coast throughout the region in intertidal mud flats and salt marshes. The inorganic sediments are coarser at the top of the sequence, below the fishpond detritus which has been deposited above the sediments already described. There is then a gradual change from a highly organic peat to an inorganic coarse

silt/fine sand with well-preserved shells which is about 1.50 metres deep.

3.5.4.2 Particle Size Analysis

Nine sediment samples were taken from a monolith tin which had been placed in the section between -1.15 m P.D. and - 1.65 m P.D. (see figure 3.17). The grey sand layer, peat and lower clay and silt deposits were sampled using this monolith tin. The results of the particle size analysis are shown in table 3.3. This shows that the sediments are made up of a mixture of sands, silts and clays.

The basal grey friable coarse sand deposit which is overlain by highly organic material consists of coarse, medium and fine sand making up over 84% of the sediment. This sediment was described in the field as a light grey coarse sand. The organic sediment above this has a lower sand content and a higher clay content. A fall in the sand content from 84.8% to 44.1% and a rise in the clay content from 2.8% to 19.8% was measured between the samples found at altitudes of ~~-1.60 to -1.61 m P.D.~~ and ~~-1.63 to -1.65 m P.D.~~ . The peat and organic silt layer described above and shown in figure 3.17 is made up of fine sand and clay. Of interest is the relatively constant nature of the fine sand content within the samples varying between 33.0% and 50.6%. The fine and medium silt content was found to be constantly low, never reaching higher than 8.9% in either category.

3.5.4.3 Diatom analysis:

Twelve sediment samples were analyzed for fossil diatoms. The samples were taken from the sediments collected in the monolith tins between an altitude of -0.88 m P.D. and -1.60 m P.D. The sediments that were analyzed consist of the basal sand and silt, overlain by the highly organic silt and peat. Above this was an organic silt with sand, from which samples were not analyzed for diatoms. No diatom frustules were identified.

3.5.5 Transect TSW/B

A large trench was dug in the eastern part of the Tin Shui Wai basin in a north - south direction as part of the major construction works in the basin during March and April 1988 (see figure 3.12). The trench, 1200 metres in length and approximately three metres in depth, revealed the structure of surface sediments in the eastern part of the Tin Shui Wai basin. The detailed stratigraphy was not measured because of the length of the trench, and the building of a concrete culvert in the trench. The stratigraphic work that was carried out was done a few days before the sediments were permanently removed by the construction work or covered in reinforced concrete.

The trench cut across an area of former fishpond. The sediments were therefore a combination of sediments deposited before the area was reclaimed, and sediments deposited within the fishponds, and disturbed by the construction of the fishponds. No samples were collected for micropalaeontological or particle size analysis.

3.5.5.1 Stratigraphy:

Unconsolidated sediments covered heavily weathered bedrock and gravels which were clearly exposed along most of the culvert. The unconsolidated sediments consisted of grey sands and silts with a large number of shell fragments. The organic and sand content of the sediments varied along the transect. The upper sediments appeared to have a higher organic content. *Ostrea sp.* shells were found, often in their living positions and undamaged in the lower sediments above the basal bedrock and gravels. Above these sediments organic fishpond sediment layers were observed. The division between these fishpond deposits and the coastal deposits below was very gradual and difficult to define clearly. However the transect cut through a number of relic fishpond walls, under which the coastal deposits extended. This confirmed that there was a distinct difference between the deposits, and the lower organic sands and silts overlying the weathered bedrock were not just extensions of the fishpond deposits.

Figure 3.12 shows the location of the eastern culvert in the Tin Shui Wai basin, and the fishponds that used to cover the basin. A levelling exercise was carried out in order to calculate the altitude of sediments found at various points along the culvert. Figure 3.18 shows a summary of the sediments found. The top basal gravels and weathered bedrock vary considerably in altitude. The depth of the shell rich silts appeared to grow shallower as one moved further from the present coastline, and the altitude of the basal bedrock rose.

Silts with shell fragments were found up to an altitude of +0.53 m P.D. at the southern (landward) end of the transect, and down to a lowest altitude of -1.07 m P.D. Above the shell rich layer a dark organic silt and clay, similar to the organic layer found

in section TSW/A, was observed. This organic layer was found down to an altitude of approximately 0.0 m P.D. The boundary between the lower shell-rich layer and the organic sediment layer above was very defused.

3.5.6 Coastal changes

The sites studied in the Tin Shui Wai basin show that there has been considerable variation in the coastal environment throughout the basin. The lower coarse sand and gravel sediments found at transect TSW/A suggest a former high energy coastline, with beach deposits being laid down. This appears to have been overlain by fine clays and silts with organic remains suggesting a low energy salt marsh environment, possibly dominated by *Phragmites* and mangroves. This organic deposit was found down to an altitude of at least -1.80 m P.D. suggesting that it may be of considerable age, since contemporary mean sea-level is at approximately +1.15 m P.D. The transition layer from coarse sand to organic rich silt and clay is therefore almost three metres below present mean sea-level. The organic samples have not been dated.

A marine influence appears to have increased after the deposition of the organic layer found at TSW/A. The gradual increase in silts and sand is accompanied by an increase in shell fragments. It is very unfortunate that diatom analysis was not successful when applied to the sediment samples taken from this site. No clear pattern of salinity changes has been derived therefore.

The lack of detailed stratigraphic survey throughout the Tin Shui Wai basin makes it very difficult to relate the sedimentary stratigraphy found at TSW/A to that found in the various boreholes summarised in figures 3.13 - 3.15 and at TSW/B (see

Chapter 3: Sedimentary analyses

figure 3.18). However it should be noted that at TSW/B shell fragments were found down to an altitude of -1.07 m P.D. At TSW/A sediments with remains of *Ostrea spp.* shells were found down to a depth of -1.0 m P.D. (see figure 3.17). The organic sediments found at TSW/B above an altitude of 0.0 m P.D. were not found at TSW/A since sediments at this altitude were the result of recent deposition within fish ponds.

It appears therefore that the highly organic sediments found at TSW/A may represent a general sediment layer found over much of the Tin Shui Wai basin, and may be evidence of a former lower sea-level. After deposition this organic deposit was subsequently overlain by sands and silts deposited under higher energy conditions. Dating of the lower organic deposits has^{not} been done, however this deposit represents the lowest altitude at which organic coastal deposits have been found at any of the sites examined in this study.

A comparison of the sediments studied at TSW/A and TSW/B and the boreholes sunk by Binnie and Partners suggests that the organic sediments found at TSW/A are at a lower altitude than many other organic deposits in the basin. Neither transects A-A' or B-B' (figures 3.13 and 3.14 respectively) show significant organic deposits below 0.0 m P.D. Only in boreholes TSWD33 and TSWD72 were thin organic layers, described as "peat" found below 0.0 m P.D. In borehole TSWD33 this organic layer was recorded between depths of -1.10 m and -1.15 m P.D. In borehole TSWD72 an organic layer was recorded between -0.85 m and -0.95 m P.D., and between -3.3 m and -3.45 m P.D. Since these deposits were not analyzed it is not possible to conclude whether the organic sediments found between -0.85 m and -1.15 m in boreholes TSWD33 and TSWD72 are related in any way to the organic deposits found at TSW/A at a depth of between -1.9 m P.D. and -1.1 m P.D.).

Chapter 3: Sedimentary analyses

3.6 CONCLUSIONS

3.6.1 Methods:

The detailed analyses of sediment sequences described above have identified major environmental changes at three coastal sites, and have shown that changes in water quality and sedimentology have occurred. The chronology of these changes has not been calculated as no relative or absolute dating methods were applied to the samples collected from the various sites.

The detailed stratigraphic analysis of coastal sediments as discussed in chapter 2 worked very well at all sites in the Zhujiang Delta. The method allowed accurate models of the sediment sequences in three basins to be derived, and sediment samples to be retrieved for laboratory analysis.

Diatom analysis combined with detailed stratigraphic analysis have been used successfully to identify environmental changes at Shajing Lagoon and Sham Wan, however diatom analysis was not successful when examining samples from Tin Shui Wai. It is not clear why diatoms were not preserved in the samples taken from the Tin Shui Wai basin. The sediments did not appear to have been disturbed prior to sampling. The techniques do work within this environment although care needs to be taken with the selection of sites to study. Within the very dynamic environment of the Zhujiang Delta the sedimentary sequences are up to 50 m deep.

Previous work of this kind in the region has often used some of these techniques to identify environmental changes in the delta, but detailed stratigraphic survey have not been employed (see Huang et al 1982, 1986, 1987 for example). The present studies show that the variations in sediment types and diatom assemblages can

often be considerable over quite small altitudinal ranges. Very great care must be taken in the selection of sites for analysing Holocene sediments in order to identify environmental changes.

Unfortunately in the Zhujiang Delta and along the coasts of Hong Kong there are very few coastal sites at which the surface sediments down to four - five metres have not been radically changed by human interference particularly over the last 50 years. Tin Shui Wai basin provided great potential as a site for more detailed work. However this site has now been destroyed by construction work. A very small area of coastal lowland still remains as a nature reserve in the Hong Kong New Territories (Mai Po Marshes). It would be interesting to carry out similar stratigraphic and micropalaeontological analyses on sediments in this area.

Although no sediment samples were dated using radiocarbon dating or other techniques, samples which demonstrate changing marine influence at the coast have been identified. Sea-level index points could therefore be identified using the detailed stratigraphic and micropalaeontological methods described. Dating of these sea-level index points would allow a much more accurate assessment of the chronology and nature of coastal change to be made than is possible now with the existing proposed sea-level index points from sites in southern China (see chapter 4).

3.6.2 Coastal changes

The evidence from all three sites suggests that there have been major coastal changes in the Zhujiang delta and around Hong Kong during the Holocene. Although no timescale within the Holocene is available, at all three sites there is clear evidence of

former strong marine conditions prevailing inland from the present coastline. At Shajing Lagoon past marine conditions have been identified up to 4 km inland of the coast. Whether this is due to former higher sea-levels or changes in coastal morphology, and over what timescale this change has occurred is not clear.

At Tin Shui Wai and Sham Wan organic deposits have been found that may have been deposited when sea-levels were significantly lower than at present, since freshwater conditions were apparently prevailing at altitudes well below the present highest astronomical tide levels in basins close to the present coastline. Alternatively these organic and freshwater deposits may be more recent, but deposited in basins lying below contemporary highest sea-levels. At Tin Shui Wai organic deposits with remains of *Phragmites communis* were found at altitudes of between -1.9 m P.D. and -1.1 m P.D. (-1.03 m Y.S.D. and -0.23 m Y.S.D.). At Sham Wan organic deposits with fossil freshwater dominated diatom assemblages were found between -0.1 m P.D. (+0.77 m Y.S.D.) and +1.0 m P.D. (+1.87 m Y.S.D.). The organic deposits at both sites may represent a relative fall in marine influence at altitudes well below the current high astronomical tides. This has important implications for the debate on the formation of beach ridges and possible higher mid Holocene sea-levels discussed in chapter 1.

4.1 Introduction:

The analysis of the altitudes and ages of scientifically dated samples from coastal sites in order to develop chronologies of past sea-level changes has been carried out for many of the world's coastlines (Pirazzoli 1991). Stratigraphic and sedimentary analyses are carried out at defined coastal sites, after which clearly defined samples which have a known altitudinal relationship with mean sea-level at the time of their deposition may be dated by a variety of techniques. Radiocarbon dating of organic samples has been used by many workers to assess the chronology of sediment deposition, and then to infer the timing of coastal changes and in particular changes in altitude of mean sea-level relative to the coast. A sea-level index point refers to a sample of known age, altitude and vertical relationship with mean sea-level when it was first deposited.

The aim of this chapter is to study the radiocarbon dated samples from a number of sites along the southern coast of China. The data have been collected from a wide range of published and unpublished sources from China and Hong Kong. A series of stages to the work have been followed which are outlined below:

- 1 The quality of the data in terms of altitudinal and age control has been assessed with reference to the available information about each dated sample. Particular attention has been paid to the suitability of each sample to be used as a sea-level index point in terms of the accuracy of the dating of the age of the sample, and the altitudinal relationship of the sample to past sea-levels. Initially all known samples were included in a database. Later samples were screened, and those sea-level index points

considered suitable according to a set of defined criteria were included in a final sea-level index point database.

- 2 The chronology of sea-level movements as suggested by the data for each site has been examined, and comparisons between sites have been made.

- 3 An attempt has been made to build up a chronology of general sea-level changes along the southern coast of China during the past 10,000 - 12,000 years. Tentative conclusions about the various responses of different sections of the south China coast to coastal changes have been made.

It is stressed that this study represents a general assessment of the data. Because the information about the stratigraphic context of most samples was limited, the margins of error in the following analyses may be considerable.

4.2 Sources of data:

Previous studies of changes in sea-levels along the coasts of southern China over the last 15,000 years have concentrated on dating large numbers of organic sediment samples which have previously been defined as sea-level index points (see for example Huang *et al* 1982, 1986, Wu 1987, Zhang and Lui 1987). A large number of sample types has been dated using radiocarbon dating techniques and attempts have been made to produce chronologies of past changes in sea-level along particular coastlines. Although this work generated a large number of radiocarbon dated samples, relatively little attention has been paid to the stratigraphy of the parent material from which

samples were taken, and to the quality of the data. Little detailed micropalaeontological or macrofossil analyses have been carried out on the sediment samples.

The data that are available in the literature offer the possibility of building a generalised picture of past sea-level changes in southern China. This framework can then be used both to stimulate questions for further study, and to provide a context for more detailed local studies of sea-level and coastal changes.

The data have been collected together from a variety of sources (see appendix 4). They represent work in a number of areas of the south China coast between Hainan Island in the west, and Fujian Province in the east (see figure 4.1). Data have also been collected from the Xisha (Paracel) Islands in the South China Sea. Information about two hundred and seventeen radiocarbon dated samples has been entered into a computerized database. Thirteen separate data fields exist in the database, and these are summarised in table 4.1. Attributes of each of the sea-level index points (see table 4.1) were derived from the original published sources and from discussions with researchers working in the area (Dr W Yim of the University of Hong Kong, Professor Li, Professor Huang and Mr Y Zong of the Guangzhou Institute of Geography).

4.3 Defining sea-level change curves:

4.3.1 Methods:

Sea-level index points have been identified, and time-altitude plots of samples from a defined area have been made. The various

known and estimated errors in the data have been identified. Models of changes in the altitude of sea-level index points through time have been made, and so estimated changes in sea-level have been inferred. The detailed comparison of tendencies of sea-level changes between different coastal sites as described by Ireland (1988) for the tropical coast of southern Brazil has not been attempted because of the poor quality of the data set.

The problems of defining sea-level curves from dated sea-level index points have been discussed in considerable detail (Chappell 1987, Kidson 1982, van der Plaasche 1986, Tooley 1982, Shennan 1982, 1986, 1987). Errors in age determinations of samples, the altitudes of samples, and the inferred sea-levels at different times will exist. A clear understanding of the nature of the samples used to determine sea-level index points, the stratigraphic and geographical context within which these samples are found, and the probable relationship of the samples to former sea-levels are vital before conclusions about possible past sea-level changes can be made.

Chappell (1987) has shown the use of error bars for both the altitudinal and age errors of sea-level index points derived from data from sub-tropical coasts, and has discussed the use of sea-level change "envelopes" rather than sea-level "curves", taking into account the indicative meanings of different types of samples. Chappell (1987) emphasised that the radiocarbon dated data for Australia, and indeed for other tropical and subtropical coasts, are not as detailed as that collected along the coasts of north west Europe or North America. He argued that such detailed investigations may not be so applicable to tropical and subtropical coastlines. The evidence from China is certainly not of a detailed nature, with limited stratigraphic evidence and

altitudinal control. This study therefore builds on the methods proposed by Chappell (1987).

One major problem has been trying to assess the quality of the data. Little or no indication is given in the Chinese literature as to the altitudinal control of the dated sediment samples or the accuracy of the radiocarbon date assays. The intense debate as to what constitutes a suitable sea-level index point sample that has taken place in the literature of sites in north-west Europe has not been undertaken in the Chinese literature. Initially all samples defined as sea-level index points in the Chinese, Hong Kong and international scientific literature were entered into the database. The data were then assessed according to a series of criteria (see section 4.4.2), and the database of 219 sea-level indicators has been reduced down to 98.

Sea-level index points:

A range of organic deposits have been identified at various sites in southern China which give evidence of past coastal and sea-level changes. Chappell (1987) has divided sea-level indicators into two groups; those that form at a fixed elevation relative to a tidal datum (**fixed indicators**) and those that always form above or below tidal datum (**relational indicators**). Fixed indicators include samples whose deposition is defined by tide levels (for example mangroves and certain littoral organisms). Relational indicators can be divided into subtidal (estuarine sediments) and supratidal (sand dunes, storm surge deposits, beach rock). By assessing the age-altitude plots of a series of sea-level indicators, and including both age and altitude errors, a model of probable sea-level changes through time can be established.

Chapter 4: Holocene sea-level changes

In this study the sea-level index points were initially divided into fourteen types of material (see table 4.2). The suitability of many of the sample materials for use as sea-level index points must be questioned. Rootlets, peat deposits and certain undisturbed shell deposits are considered suitable for use as sea-level index points as post depositional disturbance and contamination are limited. However these represent a small proportion of the total number of samples. Beachrock, coral deposits and the various organic clay / mud deposits are difficult to define as sea-level index points. Radiocarbon dating of these materials is difficult, and the indicative meaning (the altitudinal relationship of the sample to sea-level at the time of deposition) is unclear. Dating organic muds is very difficult since the organic content of the samples is much lower than a fully developed peat or other well preserved organic deposit such as a shell or rootlet. Van der Plassche (1986) discusses the suitability of a number of materials for use as sea-level index points including corals and beachrock. Although these have been used in other studies, they are susceptible to contamination, particularly when found exposed at the ground surface.

4.3.2 Errors:

Errors in both age and altitude can be associated with all sea-level indicators.

4.3.2.1 Age determination errors:

Systematic age errors exist with all radiocarbon dated samples, and these are generally given as a \pm error, where the error term represents one standard deviation of the gaussian error distribution (Potlach, 1977).

Chapter 4: Holocene sea-level changes

Dates have been derived from a wide variety of radiocarbon dating laboratories. The possibility of inter-laboratory variation, and hence distortion of results is considerable (Potlach 1977 Olsson 1986 - see Berglund 1986). An added complication is that some of the samples from Chinese studies do not have laboratory codes, so the origin of some of the dates cannot be accurately assessed. These data have been included in the database.

Age errors caused by contamination of organic samples by external material which may be of a different age to the original sample is also a problem. This may be particularly acute in samples exposed to recent surface contamination (for example beachrock deposits) or to samples which have been retrieved from deep sediment cores and have been mixed with younger surface materials during the retrieval of the sediment core.

Because of these possible errors, one standard deviation of the age error distribution is given in the graphical representation of the data in figures 4.3 - 4.10. Sea-level change envelopes have been drawn in figures 4.3 - 4.10 around the plotted sea-level index points and the error bars. It should be noted that some of the organic material dated has been classified as either sub-tidal (for example marine clays) or supratidal (for example ridge beach rock deposits). The sea-level change envelope derived from this subset of the data therefore does not include the age-altitude of the actual sample. For a subtidal deposit, it is assumed that the sea-level change envelop is above the altitude of the deposit. For a supratidal deposit the reverse is assumed.

4.3.2.2 Altitudinal Errors:

Altitudinal errors may be divided into three groups.

The altitude of the sample which is used as a sea-level index point may not be accurately surveyed during the retrieval of the sample.

The sample may have experienced post depositional altitudinal change.

The relationship between the sample and the sea-level at the time of the sample's deposition may be incorrectly estimated.

Poor sampling may lead to altitudinal errors being introduced. Different methods of levelling and sample retrieval have been used. It is not known how accurate the sampling of many of the samples found in China was. Discussions with various scientists involved in the work suggest that many of the deeper samples may have a sampling altitudinal accuracy of $\pm 1-2$ metres, the errors being caused by the poor recovery of samples from boreholes. Little indication is given in the literature as to the degree of accuracy of these altitudes.

After deposition, a sample's altitude may change due to a number of processes which may be independent or partially independent of sea-level changes. Post-depositional compaction of sediments may cause a sample's altitude to change after deposition. Compaction can be a problem, particularly in thick unconsolidated Holocene sediments which have been deposited rapidly with high initial water content. In the large deltas of southern China (the Zhujiang and the Hanjiang Deltas for example) this may be a

particularly serious problem. In the Zhujiang Delta, Huang *et al* (1982) have shown that Holocene sediments are up to 70 metres thick. Eighty-eight of the 217 samples that have been dated are from these two deltas. However sediment compaction and variable vertical movement of a sediment layer may also be a problem in much shallower sediments. For example the sediments found at Shajing Lagoon (see chapter 3) have apparently experienced differential vertical movement. These sediments are only a few metres thick, and cover an area of less than one square kilometre.

Compaction caused by the pressure of the weight of sediment deposited above a sample may vary spatially and over time. It may be discontinuous if erosion produces unloading, and periods of rapid deposition may cause enhanced loading. Particle size and organic content of sediments will vary in coastal sediments, producing varying responses. Greensmith and Tucker (1986) have suggested that highly organic peat strata may be reduced to 10% of their initial thickness; clay mud to 11-25% and sands to 66-75%. Most of the sediment samples found in the Zhujiang and Hanjiang Deltas consist of silts and sands, sometimes found at considerable depths. The amount of altitude change caused by compaction of sediments has been difficult to assess given the data.

Vertical neotectonic movement of coastal areas may be caused by hydro-isostasy, sediment loading in large deltas or longer term tectonic movements associated with plate movements. Chappell (1987), Chappell *et al* (1982) and Hopley (1978) have discussed the influence of hydro-isostasy on the altitudes of sea-level index points. Hopley (1978) has also highlighted the effects of local sediment loading in the Burdekin Delta, Queensland, Australia, which caused the down-warping of earlier land surfaces and hence of dated sea-level index points.

Chapter 4: Holocene sea-level changes

Little work has been done on neotectonic movement during the Holocene along the south China coast. Huang et al (1986) have discussed the results of periodic levelling along the south coast of China over the past 30 years. This suggests areas of uplift and subsidence related to the patterns of fault lines along the coastal region. The areas of subsidence during the Pleistocene are thought to have led to the creation of the major deltas in the region - the Zhujiang and Hanjiang. North Hainan Island is identified as an area of contemporary uplift, compared with limited subsidence in south Hainan Island (Huang et al 1986). The existence of Quaternary volcanics on the island as well as contemporary earthquakes suggest that neotectonic activity is more likely.

Altitude errors may also be introduced when trying to estimate the altitudinal relationship between the dated sample and the mean sea-level when the sample was deposited. The indicative meaning of a sample is the relationship of the sample, and by inference the environment in which it accumulated, to a contemporary reference tide level. Altitude errors are due to uncertainties in a sample's indicative altitude. The indicative meaning of different sorts of samples must be estimated. Careful investigation of modern coastlines which have similar landform and vegetational successions, away from the sea, to those represented in the sedimentary record, can be useful. Shennan (1982) has discussed the indicative altitude of a range of organic materials commonly found along temperate coasts. Ireland (1988) has discussed the indicative meanings of peats and various mollusc species along the subtropical coasts of Brazil. He suggests that in situ *Ostrea* shells have a wide indicative range, and:

"may be found scattered at any height in the upper tidal zone".

(Ireland, 1988)

Chapter 4: Holocene sea-level changes

Laborel (1979) suggested that the use of *Ostrea* shells can lead to an overestimation of the altitude of former sea-levels.

Huang et al (1982) discussed the indicative meaning of a range of sea-level indicators, and these are summarised in table 4.3. This work has been based on extensive fieldwork, examining present day coastlines in southern China. Since the South China coast is a microtidal coastline (Bird 1986), the indicative range, and therefore altitudinal errors of some of the sea-level indicators, may be smaller than along macrotidal coasts. However the control on altitudinal error is considered limited. In this study a set of altitudinal errors have been applied to all sea-level index points (table 4.2). Samples of similar type have been given the same altitudinal error bands.

The determination of the indicative altitude of different samples has proved difficult. Few present-day analogues of the "natural" coastline exist in southern China, and the samples used for dating by Chinese researchers are often not clearly defined. For example, at a number of sites throughout southern China "intertidal organic clays" have been dated and defined as sea-level index points, though no accurate indicative altitude has been given for the sample in the literature, and sample descriptions do not allow a clearer relationship between the sample and the contemporary sea-level to be defined.

The altitudes of all the sea-level index points are quoted in metres, to the nearest 0.1 m relative to Yellow Sea Datum. In the present study the altitudes of the samples as quoted by individual researchers have been used.

4.4 South Chinese sea-level indicators

A database of 217 dated sea-level index points from the south coast of China and Hong Kong has been assembled. The area covered by these studies is from Fujian Province in the east to Hainan Island in the west, and includes dated samples from the Xisha Islands in the South China Sea (see figure 4.1). These sea-level index points comprise a range of organic materials: mangrove roots, wood, organic silts and clays, shells, oysters, beach rock and corals. The indicative meaning and the altitudinal and age reliability of the different samples varies considerably. The data are not as detailed, nor is the quality control as sophisticated as for some other databases of sea-level index points (see for example Shennan 1989). All dates have been included in the initial analysis even though information about the stratigraphic context, the contamination and the dating of many of the samples was not available. The relationship of the data to present variations in tidal regimes as discussed by Shennan 1989 has not been defined. The south coast of China is a microtidal coast (Bird and Schwartz 1985) with the main spring tidal range of no more than about 2 metres. This falls within the altitude error band of a large proportion of the samples, and detailed analysis of the likely tidal effects on the samples in different coastal compartments was not carried out. The quality and quantity of the data about each sea-level index point is also limited compared to studies in north-west Europe.

4.4.1 Time-Altitude Diagrams

The 217 sea-level index points reported for southern China and Hong Kong have been plotted in an age-altitude diagram (Figure 4.2). The samples are varied and comprise wood, shells, fragments

of *Ostrea* shells and whole individuals, beach rock, organic clays and silts and coral sands.

The data were initially entered into a database (table 4.1). An altitude correction factor and error band for each sample was then estimated, based on the indicative meaning and indicative range of each sample. The corrections and errors of the different sample types are listed in table 4.2. These corrections were applied to all the samples. Detailed field descriptions for each sample were rarely available, radiocarbon date laboratory code numbers were often omitted, and very limited information about the stratigraphic context within which the sample was found was given. Detailed information on the likely errors associated with each sample was often lacking.

Initially eight time-altitude plots for different geographical areas were produced (see figures 4.3 - 4.10). These groups of samples have been divided into discrete geographical areas. These areas are divided into those parts of the coastline that are known to be subsiding at present based on the levelling results presented by Huang *et al* (1986) (the Zhujiang and Hanjiang deltas and Shenzhen), those parts that are experiencing uplift at present (Fujian, western Guangdong, and the Xisha archipelago) and the data from Hong Kong and Hainan Island. The data from Hong Kong are considered separately because they represent a set of sea-level indicators which are found in a small well defined area, where a considerable amount of information is available about the accuracy of the data. At this stage no corrections are made for possible variations in vertical crustal movements between the eight geographical areas.

The eight time-altitude plots are considered separately. The altitudes of the dated samples have been altered by adding the

estimated indicative meaning altitude error as shown in table 4.2 to the original altitude. Vertical and horizontal error bars have been added to represent the probable margin of altitude and age errors (see Thom and Chappell 1978). The age error is one standard error of deviation, as given in the various studies from which the data are derived. The altitudinal errors are those estimated for the different sample types with reference to the work of Huang et al 1986, and shown in table 4.2.

Once all the data had been plotted (figures 4.3 - 4.10) lines were drawn around the extremes of the error bars to create a sea-level change "envelope". These are shown on the graphs.

4.4.1.1 Hong Kong (figure 4.3)

The data for Hong Kong includes various sea-level index points not previously considered with the earlier data for Hong Kong summarised in chapter 1. The index points consist of dates and altitudes measured for unidentified shells, shells of *Ostrea sp.*, wood and organic muds. Arthurton et al (1989) have reported twenty-three radiocarbon dates from the western New Territories, and five of these have been added to the database as potential sea-level index points. The remaining 18 dates were not derived from littoral material. The altitude plot of the samples includes error boxes showing one standard deviation of error for the age of the sample and the likely altitudinal errors for the different sample types as shown in table 4.2.

Figure 4.3 suggests that relative mean sea-level was at an altitude of approximately -18 m. P.D. c.8,500 B.P., rose rapidly between 7,500 B.P. and 5,500 B.P., and reached approximately -1 m. P.D. at about 5,500 B.P. A shell deposit found at Sham Wan,

at an altitude of -2 m. P.D. has been dated as $5,520 \pm 110$ B.P. (I 10059) by Meacham (1978). Arthurton et al (1989) report two dated rootlets in intertidal mudflat deposits (one autochthonous deposit). The ages are $5,475 \pm 155$ B.P. and $5,093 \pm 130$ B.P. and the altitudes are +0.4 and +0.3 m. P.D. respectively. No detailed stratigraphic context is given with these data. Between c.4,000 B.P. and c.3,000 B.P. sea-level appears to have been similar to, or possibly only slightly higher than present mean sea-level (+1.15 m. P.D. or +0.30 m. Y.S.D.). Two samples reported by Arthurton et al (1989) suggest a slightly higher sea-level. They report two dates ($3,220 \pm 95$ B.P. and $3,160 \pm 100$ B.P.) for organic muds found at +2.49 m. P.D. and +2.50 m. P.D. These are described as intertidal mud flat deposits. These conclusions are consistent with work carried out at Pui O, Lantau Island, where Yim and Meacham (1983) have provided strong archaeological evidence for sea-level not having risen above present levels over the past 4,000 years.

4.4.1.2 Shenzhen (figure 4.4)

Evidence of past sea-levels from the Shenzhen area consists of 25 dated samples: estuarine organic clays, beach rock, *Ostrea* shells, and autochthonous organic rootlets. Most of the samples dated are organic muds which are not considered to be good sea-level indicators, as both the age and altitude errors are likely to be great.

The time-altitude plots suggest that sea-level movements generally mirrored those in Hong Kong, with a rise in sea-level up to about 5000 years B.P., followed by oscillating sea-level to the present. Mangrove roots have been dated by Huang et al (1983, p.90-91). Found at an altitude of -6.9 m Y.S.D. in a

matrix of intertidal silts with brackish diatom remains, this sample was dated to 6120 \pm 160 years B.P. Although an accurate indicative altitude for this sample is difficult to estimate, it suggests a mean sea-level of perhaps between -7 and -6 m Y.S.D. about 6100 radiocarbon years ago. Wood and *Ostrea* shell samples found at Fisha at an altitude of -3.0 m Y.S.D. which have been dated 5090 \pm 160 years B.P. support the conclusion of a rising sea-level before 5000 radiocarbon years B.P. Diatom analysis of this sample confirms a strong marine influence above -3.0 m Y.S.D. after 5090 years B.P. (Huang et al 1983).

The pattern of sea-level movements after 5000 years B.P. along the coasts of Shenzhen is unclear because of the poor quality of the data. The samples dated younger than this are almost all organic intertidal or marine muds.

4.4.1.3 Zhujiang Delta (figure 4.5)

The data for the Zhujiang Delta are numerous but generally poor. Sampling techniques are not clearly defined. 17 of the 38 samples are organic clays or muds and nine of the samples consist of *Ostrea* shells which are considered poor sea-level indicators as discussed above (see Ireland 1988). The location of the sites where samples were collected for radiocarbon dating are shown in figure 4.1a. The geographical distribution of sites covers much of the delta. A time altitude plot for all the radiocarbon dated samples is shown in figure 4.5. The time-altitude plot, even when corrected for indicative meaning and range, is not very clear. A rise in sea-level before 6,000 years B.P. may be registered, but numerous outliers suggest either poor sampling, dating error, or noise caused by the dynamic nature of the depositional environment.

Chapter 4: Holocene sea-level changes

Figure 4.5 shows the distribution of data from the database, and the proposed error bands. Past changes in sea-level are very unclear, with a number of outliers both above and below the proposed "sea-level change envelope". The closely defined sea-level change curves proposed by Huang et al (1982, 1986) are considered too ambitious given the poor quality of the data. There are however a small number of sea-level index points that have been proposed that may be useful in determining past relative sea-level changes in the Zhujiang delta. An *Ostrea* shell sample found at Shunde, in the Zhujiang delta, at an altitude of -0.5 m Y.S.D. in an intertidal silt and clay and dated 5920 \pm 300 B.P. suggests a contemporary sea-level of perhaps between -1.5 and -0.5 m Y.S.D. Before this time the pattern of sea-level index points is very unclear. Between 5000 radiocarbon years and the present, the time altitude plot suggests a variable relative sea-level, between about -3 m Y.S.D. and +3 m Y.S.D. The data are not considered reliable enough to produce a more tightly defined sea-level change envelope.

4.4.1.4 Hanjiang Delta: (figure 4.6)

The Hanjiang (Han river delta) lies approximately 300 km to the east of the Zhujiang Delta, on the south east coast of China. The area of the delta is 915 km² (Zong 1988). The delta experiences frequent freshwater and marine flooding as a result of rapid runoff from the Han river catchment and tropical cyclones crossing the South China Sea. The annual silt discharge from the Han river is estimated to be 7.6 million tons (Huang et al 1987). Zong (1992) has reported a maximum recorded tidal range of 4.08 m during a tropical storm. This delta therefore is a geomorphologically very dynamic area, similar to the Zhujiang Delta, with high sediment inputs.

Chapter 4: Holocene sea-level changes

Forty one radiocarbon dated samples have been reported in the literature for the Hanjiang delta and eastern Guangdong province. A time altitude plot for these samples is shown in figure 4.6. and the locations of the sites where samples were collected are shown in figure 4.1c. The data suggest a rise in relative sea-levels up to approximately 5000 years B.P. The samples dated as being older than 5000 years B.P. are not considered very accurate as the materials dated are almost all organic clays and silts. One shell fragment was found at an altitude of -5.5 m Y.S.D. at Meilin Lake, and this was dated to 5440 \pm 100 years B.P. (CG-451). The indicative altitude of this sample is not clear.

Samples younger than 5000 years B.P. are primarily made up of beachrock and shell fragments of mollusc species allegedly (Huang *et al* 1987) associated with brackish water. It is not clear from the literature what the species of shell are, and the indicative altitude of these samples is unclear. A general pattern of sea-level rise before 5000 years B.P. appears from figure 4.6, followed possibly by fluctuating relative sea-levels. Zong (1992) has attempted to apply the methodology proposed by Shennan *et al* (1983) to these data, together with data from Fujian Province to the east. Although Zong claims to have identified three transgressive phases and three regressive phases during the Holocene, no clear evaluation of the errors in the data is given. At this stage a detailed analysis of the data following the techniques discussed by Shennan *et al* (1983) and Zong (1992) is not attempted. This issue will be discussed further at the end of this chapter, after the data are assessed (see section 4.4.2.2).

Chapter 4: Holocene sea-level changes

4.4.1.5 Xisha Islands: (figure 4.7)

The Xisha Islands are situated in the South China Sea, approximately 300 km south east of Hainan Island. The data are reported in appendix 5.

Ten samples have been collected from the Xisha Islands, defined in the Chinese literature as sea-level index points (Huang *et al* 1986) and have been radiocarbon dated. The dates range from 5030±200 B.P. to 910±120 B.P.. The samples come from four sites. The materials that have been dated are beachrock and coral reef deposits. Possible dating errors for these types of deposit are summarised by Hopley (1986). Altitude error bands have been added to figure according to the errors shown in table 4.2.

The time - altitude plot of these dates (figure 4.6) suggests a relative sea-level above 0.0 m Y.S.D. since about 5000 B.P. One apparent outlier exists - the sample collected at Shidao and dated 4850±200 B.P.. This sample is a coral reef deposit found at +5.0 m Y.S.D. The other samples dated suggest a fluctuating relative sea-level recorded between about 5000 B.P. and 1750 B.P., with a lower sea-level during the fourth millennium B.P.. As with other samples in this database the stratigraphic detail of each sample is limited, and so detailed analysis of the possible altitudinal errors is very difficult if not impossible, given the quality of the data.

The overall pattern of the data suggests a gently falling relative sea-level since about 5000 years B.P. from an altitude of +5.0 m Y.S.D. This compares with lower estimates of sea-level 5000 years ago from the other coastal sectors analyzed in this study. This variation may be due to vertical land movements. If the Xisha islands are being uplifted relative to other sites,

then the sea-level signal from the index points would register a general relative fall in sea-level. However the samples are primarily made up of beachrock, making the altitudinal and age determinations extremely difficult.

4.4.1.6 Hainan Island (figure 4.8):

Hainan Island is located to the west of the southern Chinese coast close to the border with Vietnam. Fifty radiocarbon dated samples have been reported from sites along the island's coastline. The age determinations for the samples range from 10,230 \pm 320 B.P. to 260 \pm 60 B.P.. The samples, age determinations and altitudes are listed in appendix 5.

It appears from figure 4.8 that sea-level around the Hainan coast rose between approximately 10,000 B.P. and 7,000 B.P. from an altitude of below -20 m Y.S.D. Only eight samples have been dated earlier than 6500 B.P. making it difficult to define clearly the sea-level rise envelope before this. Two outliers appear with radiocarbon dates of 8420 \pm 115 B.P. and 8235 \pm 105 B.P. and corrected altitudes of +3.0 m and +3.8 m Y.S.D. respectively. These samples are taken from exposed coral reefs. Although it cannot be categorically stated that these dates are in error because no detailed information is available about the samples dated, if they were correct it would suggest a very rapid and early rise in sea-level after 10,000 B.P. If the three younger dates in this first group of eight samples (6750 \pm 140 B.P., 7150 \pm 110 B.P. and 7280 \pm 140 B.P.) are good, then this would also suggest a rapid fall in sea-level between about 8000 B.P. and 7000 B.P. Such a fall is not registered anywhere else along the coast of southern China. The coastal peat sample collected at Shanya and dated 9480 \pm 290 B.P. suggests that sea-level may have

Chapter 4: Holocene sea-level changes

reached an altitude of about -10m metres Y.S.D. at this time. The peat has been found lying above a terrestrial sand and gravel deposit and below a marine clay, suggesting a marine transgressive event after the deposition of the peat.

Most of the samples with radiocarbon dates after 6500 B.P. are beachrock or coral sand deposits. Although these samples are difficult to date accurately, and many of the samples were exposed which may have contributed to dating error, a sea-level envelope has been drawn in figure 4.8 around the corrected time - altitude plots. From these plots it is suggested that sea-level has fluctuated above or below 0.0 metres Y.S.D. since about 6000 B.P. Remains of a mollusc species allegedly associated with brackish water was found at an altitude of 0.0 m Y.S.D. in an intertidal deposit at Wenchang. These were radiocarbon dated 2214 ± 156 B.P. However as with other samples the stratigraphic detail available is limited, and it is not known what species the shell was.

4.4.1.7 Western Guangdong (figure 4.9):

Nine radiocarbon dated samples have been identified along the coast of western Guangdong Province. The time-altitude plot of these data shown in figure 4.9 appears to confirm the general pattern of sea-level changes in the Holocene found along other parts of the south China coast. It appears that relative sea-levels rose before 6000 years B.P. and have fluctuated between approximately 0 m Y.S.D. and +4 m Y.S.D. since then. The four samples dated older than 5000 radiocarbon years B.P. are considered to be poor sea-level indicators, particularly the intertidal clays found at depths of -12.5 m Y.S.D. and -17.3 m Y.S.D.

4.4.1.8 Fujian coast (figure 4.10):

Eighteen samples have been identified along the coast of Fujian Province at the eastern end of the study area (see figures 4.10, 4.1 and appendix 5). The time-altitude plot of the samples (figure 4.10) shows a widely fluctuating sea-level change envelope, particularly during the middle and late Holocene (since about 6000 years B.P.). The sea-level change envelope appears to have reached a high altitude of above +5 m Y.S.D. about 5000 years B.P. however this conclusion is based on only one sea-level index point (a beachrock deposit found at Putian at an altitude of +9 m Y.S.D. and dated 4820 ± 120 years B.P.).

4.4.2 Analysis of the data sets:

The time altitude plots for the eight areas examined in this study show considerable variation. Figure 4.12 shows all the sea-level envelopes plotted on a single graph, and the sea-level change envelope generated from the data from Hong Kong. The combined pattern seems to confirm a rise in sea-level up to about 5000 years B.P.

There are clear differences in the sea-level change envelopes derived from the data from different parts of the coast of southern China (see figures 4.3 - 4.10). This may be in part due to the various sampling errors discussed above. However variations in the signal of the sea-level index points in the coastal sectors also may be due to variations in the relative movements of land and sea between these areas. This may be either due to different eustatic sea-level changes, or variations in the vertical movement of the land. Comparison of the relative sea-

level change envelopes of the two large deltas (Zhujiang and Hanjiang) and the more detailed data from Hong Kong, suggest a relative subsidence within the delta areas, assuming the eustatic sea-level rise signal were the same for all three areas. This conclusion is very tentative.

Reduction of the database:

Having plotted and assessed the time - altitude plots of all 217 radiocarbon dated samples that have been defined as sea-level index points in the Chinese and Hong Kong literature, the database was analyzed in order to delete indicators which were considered to involve very large error bands. A series of procedures was involved:

All data derived from primarily inorganic samples such as "marine" and "intertidal" muds, silts and clays were rejected from the database. This was done because the indicative range of these samples is very unclear, and both age and altitude errors were thought to be considerable. Discussions with people involved in the analysis of some of these samples (Professor Y Huang, Mr Y Zong and Professor Li) suggested that these sample types involved particularly large errors. The sediments were collected from open bucket samples, and the altitudinal control was especially limited.

Secondly, samples for which the relationship with contemporary sea-level is unclear were rejected. This group included two crocodile bone samples from the Zhujiang delta dated 3020 ± 80 years B.P. and 2540 ± 120 years B.P. which had been reported in the literature as sea-level index

points (Huang et al 1986) but which had no clear indicative meaning.

A third stage of analysis was then carried out in order to try and clarify the pattern of sea-level index points. Samples were classified into fixed and relational sea-level indicators following the analysis of Chappell (1987). Relational sea-level indicators were further subdivided into subtidal and supratidal. Supratidal relation indicators were defined as *beachrock* and *coral reef* deposits and *lagoonal peats*. *Intertidal shell* and *marine shell* fragments were defined as subtidal relational indicators. *Mangrove rootlets* were defined as fixed indicators. This is a crude definition of sea-level indicators, however the altitude and age errors associated with the data and discussed above, suggest that at this stage more sophisticated definitions of sea-level indicators are not warranted.

Figure 4.13 is a time-altitude plot of the 105 fixed and relational sea-level indicators from the screened database. Points marked "B" refer to subtidal relative sea-level indicators. Supratidal sea-level indicators are marked "P" and fixed indicators are marked "F". Of the 105 data points remaining in the screened database, 45 have been derived by dating beachrock samples, and 22 are derived from coral reef or "coral sand" deposits. Both these categories are not particularly reliable sample types (Hopley 1986). Both are susceptible to dating errors due to contamination of organic material in the deposit after deposition, and the indicative meaning is rarely very clear or possible to quantify accurately.

The screened data indicate that relative sea-levels along the south coast of China rose to about 0 m Y.S.D. before 5,000 years B.P. After 5,000 years B.P. there may have been a slight relative fall in sea-levels as there is a concentration of supratidal sea-level index points between altitudes of -1 m Y.S.D. and +3 m Y.S.D. dated between 5000 years B.P. and 3,800 years B.P. Sea-level indicators dated younger than 4,000 years B.P. suggest a possible rise in sea-levels between 4,000 and 3,000 years B.P. Figure 4.14 shows the data from the south eastern part of the South China coast (the Hanjiang delta, the coasts of Fujian and Eastern Guangdong, Hong Kong and the Zhujiang delta) that have passed through the screening process. This graph appears to confirm the conclusion of a fluctuating sea-level between 5,000 years B.P. and the present, with data points covering a wide altitudinal range of 7-8 metres over the past 5000 years.

The subtidal, supratidal and fixed indicators were then divided into seven geographical regions (Hainan Island, western Guangdong, Zhujiang delta and Shenzhen, Hong Kong, Hanjiang delta, Fujian province coast). These are the same areas as the previous analysis, but the Zhujiang delta and Shenzhen coast have been combined. This has been done because only three sea-level indicators from Shenzhen were left after the screening process, and the coast of Shenzhen is effectively part of the south east coast of the Zhujiang delta basin.

4.4.2.2 Analysis of regional sea-level change envelopes

The time-altitude plots of the sea-level indicators for the different sections of coast are shown in figures 4.15 to 4.21. The plot for the Zhujiang delta and Shenzhen (figure 4.15) appears to confirm a fluctuating sea level during the past 6000

years with sea levels at or just below 0.0 m Y.S.D. as suggested in the initial analysis of all the sea-level indicators. Sea levels appear to have risen to 0.0 m Y.S.D. initially at about 5,500 years B.P. The sea-level index points derived from this region are almost all *Ostrea* shells found in what appeared to be intertidal deposits with marine and brackish water diatom frustules (Huang *et al* 1982, 1986). The indicative meaning of *Ostrea* shells is unclear as has been discussed by Ireland (1988) (see section 4.3.2.2). At Shonggang a mangrove root was found at a depth of -6.9 m Y.S.D. and has been dated as 6120 \pm 160 years B.P. This has been defined as a fixed sea-level indicator from an intertidal environment.

The plot of indicators from Hong Kong (figure 4.16) suggests a rise in sea-level up to about 5500 years B.P. The two fixed indicators, dated 5475 \pm 155 B.P. and 5095 \pm 130 B.P., are both mangrove rootlets found at Lok Ma Chau. These intertidal plant remains suggest a mean sea-level of about 0.0 m P.D. (+0.85 m Y.S.D.) by about 5475 years B.P. This fits well with two other dated indicators found around Hong Kong. A piece of wood found at an altitude of +1.2 m P.D. (+2.05 m Y.S.D.), and considered to be a supratidal deposit was dated 5455 \pm 105 B.P. and a marine shell found in a deposit at Sham Wan, on Lamma island at an altitude of -2.0 m P.D. (-1.15 m Y.S.D.) was dated 5520 \pm 110 B.P. and interpreted as sub-tidal. The piece of wood found at Chung Hom Wan was a log of the Lauraceae family and had bark attached to it (Bard 1976). It was found within a coastal beach deposit. This suggests that the sample was either deposited very close to its point of growth, or had been a piece of drift wood for a very short period of time before deposition in a coastal environment. The sample is considered to be a supratidal deposit. These dated samples provide further evidence for a mean sea-level of about 0.0 m P.D. (+0.85 m Y.S.D.) at about 5500 years B.P.

Chapter 4: Holocene sea-level changes

The data derived from samples found on Hainan Island (figure 4.17) suggest a sea-level of about 0.0 m Y.S.D. since at least 6000 years B.P. This appears to confirm the earlier conclusions. However the two samples of "coral reef" found at Shanya at altitudes of 0.0 m Y.S.D. and +0.8 m Y.S.D. which were dated 8420 ± 115 B.P. and 8235 ± 105 B.P. remain in the database after the screening procedure. These two samples appeared to be outliers when the full data set from Hainan Island was examined (see section 4.4.1.6 and figure 4.8). However these two data points suggest that relative sea-level may have reached about 0.0 m Y.S.D. before 8000 years B.P. If this were true it would suggest a very different relative sea-level signal between that recorded around Hainan Island and that recorded in the Zhujiang delta and Hong Kong. However this is based on just two sea-level index points, and the nature of the coral reef and the accuracy of the dating is unclear. If real, the differences between the sea-level signal from Hainan Island and Zhujiang and Hong Kong might be due to variations in neotectonic vertical movements during the Holocene. Hainan Island may have experienced uplift relative to the Zhujiang delta and Hong Kong. However the data are not considered reliable enough to derive an accurate magnitude for this possible relative uplift.

The sea-level indicators found along the coast of western Guangdong and the Xisha islands have been plotted in figures 4.18 and 4.19 respectively. These appear to show similar patterns to those found in the screened data from Hainan Island, though the number of sea-level indicators is considerably less, and the time variation is much less. On the Xisha islands the oldest dated sample that was passed by the screening process was dated as 5030 ± 200 years B.P., and on the coast of western Guangdong 7120 ± 165 B.P. The pattern of sea-level indicators as shown in figures 4.18 and 4.19 suggests that relative sea-levels were at or above 0.0

Chapter 4: Holocene sea-level changes

m Y.S.D. from about 7000 B.P. along the coast of western Guangdong, thus mirroring the pattern found in the data from Hainan Island. The Xisha Island data suggests sea-levels above 0.0 m Y.S.D. from 5000 years B.P. until the present. Most of the data for these two areas are derived from breachrock and coral reef samples which are difficult to date accurately, and the indicative meaning of the samples is difficult to assess. As there are relatively few data points for both areas the conclusions are very tentative.

The data from Hanjiang delta have been severely reduced by the screening process, since many of the original data were derived from *intertidal organic clays* and *intertidal organic silts* which were rejected during the screening process. The data for the Hanjiang delta are plotted in figure 4.20. No very clear pattern emerges, though it appears relative sea-levels were above 0.0 m Y.S.D. during the past 5000 years. The data appear to show a higher possible sea-level envelope to that recorded in the Zhujiang delta. However this may be as much to do with differences in the sample types between the two deltas as real differences between regions. In the Hanjiang delta many of the samples were derived from beachrock found on relic storm ridges which has led to a sea-level signal at a higher altitude to that found in the Zhujiang delta.

The data from Fujian province (figure 4.21) suggest a relative sea-level above 0.0 m Y.S.D. since about 5000 years B.P. No sea-level indicators dated before 5300 years B.P. survived the screening process, though all those dated after this did. The time-altitude plot shows relative sea-level well above those recorded in the Zhujiang delta. The data set from Fujian province is small however, and the altitudinal variation is considerable.

After careful consideration of all the data, the detailed analysis of sea-level tendencies as demonstrated by workers in north-west Europe (after Shennan et al 1983) has not been attempted, since the quality of the data does not appear to justify this work (see comments by Chappell, 1987). This conclusion has been reached because of the lack of detailed stratigraphic information about many samples, the likely dating errors associated with the majority of samples, and the altitudinal errors and vague indicative meaning of samples. Many authorities in China have not reported the dated samples in full, omitting laboratory codes and stratigraphic details about the data. The technique demonstrated by Shennan et al (1983) and applied to a similar environment in Brazil by Ireland (1988) demands very high quality data, for which any likely errors are known with some confidence. If this is not achieved the analysis of the data is in danger of becoming a statistical exercise with little relation to what has actually happened in the region in the past. Ideally, sea-level indicators will have been derived using a common methodology from samples which represent a known tendency of sea-level movement. This has not been done in southern China, and though samples exist which appear to be good potential sea-level index points (see chapter 3) a database of reliable points has not been established yet.

Zong (1992) has attempted to use the techniques discussed by Shennan et al (1983) employing the data from Hanjiang Delta, Fujian province and eastern Guangdong assembled during this study. However it is argued here that such a method is not justified in this study. Nine of the dates used by Zong are derived from "organic silts and clays" apparently deposited under "intertidal conditions". These dates have been rejected in the screening process described in section 4.4.2.1. for the reasons given in that section. Another three samples are "subtidal flat -

organic silt/clay". A further nine samples are undefined shells found in intertidal and subtidal sands, beach sand or shell ridges. It is not clear what the true indicative meaning of many of these samples is. Of the 64 dated samples that Zong includes in the analysis (one of which has no known altitude) only 25 are included in the database after the screening process described in section 4.4.2.1, and 16 of these dates are derived from beachrock samples which are considered relatively unreliable as sea-level indicators (see Hopley, 1986).

4.5 Final conclusions

The time - altitude plots of all 217 dated samples in the database (figures 4.1, 4.3 - 4.10) suggest that sea-level rose rapidly before 5500 B.P., to approximately 0.0 m Y.S.D., and that since that point sea-levels have fluctuated. There is considerable variation in the altitude of similar dated sea-level index points between sites, particularly between 4000 and 2000 years B.P., and it seems unlikely that all of this altitudinal range is due to sample error. The variation may be due to differences in neotectonic vertical land movements along the coast over a long period during the Holocene, similar to the very short term changes measured over the past 40 years and reported by Huang et al (1986).

Analysis of the database that has been assembled suggests that the existing data can be used to produce generalised sea-level change envelopes. The classification of sea-level indicators into subtidal, supratidal and fixed indicators suggests that sea-level may not have risen much above present sea-levels between 5000 years B.P. and the present. However many dated samples have no

clear indicative meaning, and the altitudinal and age errors are likely to be considerable, though the magnitude is not certain.

Analysis of a screened subset of sea-level indicators suggests variations in the sea-level change signal between regions along the coast of southern China. Whether this may be due to variations in the eustatic sea-level curve during the Holocene along the coast of southern China, or variations in vertical land movements between different sections of coastline is not known. However differences in the sea-level change signal between the two delta areas (Zhujiang delta and Hanjiang delta) and Hainan Island, Xisha Islands and Fujian province, appear to be considerable. These differences have not been quantified since the margin of altitudinal errors for the data is not known.

Before clear relative sea-level change envelopes for this coast can be generated, and regional variations in the sea-level change signal can be identified, the sea-level index point database will have to be improved very significantly. Very few of the existing data are considered accurate enough for such an analysis. If the 67 data points derived from beachrock and coral deposits are removed from the screened database only 38 data points remain. Of these 10 are from the coasts of Hong Kong, seven are from sites in Fujian province, 14 are from the Zhujiang delta and Shenzhen, two are in western Guangdong, two are from the Hanjiang delta and three are from Hainan Island. The screened data from Hong Kong are considered reasonably accurate, particularly in terms of the altitudinal measurement of many of the dated samples. However the data from China, though of interest in developing a general picture of sea-level changes during the Holocene and identifying possible patterns of sea-level and land movement, are not considered to be suitable for more rigorous analysis. There is a clear need for coastal sediments that are

Chapter 4: Holocene sea-level changes

identified as sea-level index points using the methodology described in chapters 2 and 3 to be dated. Accurate surveying and careful sampling of sediments is vital.

5.1 INTRODUCTION:

The risk of marine flooding in a coastal area is a function of many factors: for example land altitudes; storm surge and tidal altitudes; the frequency of storm surge events; absolute and relative sea-level changes; the nature and history of sea defences both natural and artificial; the geomorphology of coastal compartments; land uses and demographic characteristics of the coastal area. An ability to analyze the relationships between these different factors, and to model changes through time and space, contributes to an understanding of both the risks of coastal flooding and the possible consequences of a flooding event.

This study will concentrate on the relationships between land and sea altitudes, and the social and economic development of a coastal zone within the Zhujiang delta, using a Geographical Information System and data collected in P.R. China. Although the specific risks and impacts of flooding in southern China will be discussed, this methodology could be applied to other coasts.

5.2 RISKS OF FLOODING

The response of countries to the risks of coastal flooding vary considerably. In the United Kingdom the National Rivers Authority is primarily responsible for sea defences. In the United States, the Federal Emergency Management Agency (FEMA) is responsible for assessing the risks of coastal flooding and for organising the National Flood Insurance Programme (NFIP). The aim of this programme is to encourage communities that are at risk from flooding to adopt a flood management scheme that will enable them to assess the risks of flooding and therefore the need for and cost of flood insurance.

Chapter 5: Possible impacts of future sea-level changes

In China no such elaborate system of flood risk mapping exists. All work on risk assessment and control is done by central and local government agencies. One of the most elaborate systems of flood risk assessment and management in China is that for the lower Yangtze river, developed by the Land Resources and Environmental Information System in Beijing.

5.2.1 Altitudinal factors influencing future marine flooding:

The altitudinal relationship between the land and sea along a coastline is fundamental to an understanding of the risks of marine flooding. Changes in this relationship may be due to three general causes: short term sea-level fluctuations; longer term sea-level changes; and changes in land altitude due to processes causing subsidence or uplift.

A coastal area may be susceptible to storm surges and the backing up of freshwater runoff. These are generally short term, high intensity events which may raise water levels substantially but temporarily. Commonly flooding occurs over a period of a few hours or days. Examples of coastal flooding of this nature are numerous. In Hong Kong in 1937 a storm surge affecting the Tai Po channel caused extensive flooding around Sha Tin and Tai Po Kha (Chan 1983). In 1953 a storm surge in the North Sea led to flooding in eastern England, the Netherlands and Germany. Bangladesh has experienced flooding both due to storm surges in the Bay of Bengal and the backing up of floodwaters from the Ganges and Brahmaputra river basins.

Over a longer time scale (50 - 100 years) the rise in atmospheric radiatively active gases and resulting global temperature changes may influence global sea-levels. Higher global temperatures are

Chapter 5: Possible impacts of future sea-level changes

likely to influence sea-levels in two main ways. Firstly, thermal expansion of the upper layers of the oceans may raise global sea-levels. Secondly, higher global temperatures, especially if increases are particularly great at higher latitudes, may lead to melting of high latitude and high altitude ice, and a transfer of water from land to sea. These possible changes in global sea-levels will not be uniform throughout the globe. Clarke and Primus (1987) have demonstrated that sea-levels at present vary by over 100 metres across the globe's surface relative to the shape of the geoid, and that any increase in sea-levels due to the melting of high latitude ice is not likely to be uniform. It should also be noted that longer term global temperature and sea-level changes may influence the nature of short term storm surges, possibly increasing the frequency and intensity of storm surges along particular coastlines. Rossiter (1962) has calculated that storm surges in the Irish Sea may increase in frequency by a factor of three if sea-levels rise by 0.15 metres.

Various estimates have been made of the effects on global sea-levels of the rise in atmospheric radiatively active gases and the resulting global temperature changes (table 5.13). Hoffman et al (1983, 1986) and Robin (1986) have predicted that mean sea-levels could rise by between 0.2 metres and 2.2 metres by the year AD 2100. A consensus appears to be developing that, by AD 2030, mean sea-levels are likely to have risen by at least 0.3 metres and by AD 2100 sea-levels may have risen by 0.6 metres. In 1990 the Intergovernmental Panel on Climatic Change (IPCC) produced a series of estimates of future possible sea-level rise (Tegart et al 1990). This study assumed sea-level could rise by between 0.3 and 0.5m by 2050 AD, and by 1.0m by 2100 AD. These are similar to the estimates for sea-level rise given by Hoffman et al (1983) which are used in this study (see table 5.13).

Chapter 5: Possible impacts of future sea-level changes

These estimates of future sea-level rise can be compared with measured rates of past sea-level rise over similar time periods. Gornitz and Lebedeff (1987) have estimated that global sea-levels have risen by about 0.1 metres in the past 100 years.

Land altitudes may change due to natural or anthropogenic factors. Regional or local land uplift or subsidence may be caused by isostatic pressures such as hydroisostacy and sediment loading of the earth's crust. Sediment loading may be particularly important in a large delta such as the Zhujiang where Holocene sediments may be up to 60 metres in thickness (Huang et al 1982). Land reclamation and drainage may also influence land altitudes. Extraction of ground water from an area can lead to a fall in ground altitudes (Milliman et al 1989).

5.2.2 Social and economic factors:

The risks of marine flooding may also be influenced by changes in the economic and social structure of a coastal area. Rapid development of a coastal area at risk from flooding because of physical factors will increase the impacts of marine flooding on the local population. Examples of this kind of development include investment in capital intensive activities such as industrial plants; increases in populations both natural and because of immigration; intensive use of coastal agricultural land; development of toxic waste facilities in low lying areas. These developments may increase the risks and impacts of flooding to the local population of a coastal zone even if the physical factors influencing flood risk do not change. A wider geographical area may be affected if the coastal zone has strong economic and social linkages with a large hinterland.

Chapter 5: Possible impacts of future sea-level changes

5.2.3 Other factors:

The nature of sea defences is an important consideration in analysing the risks of flooding. A limited amount of information about the altitude of artificial sea defences has been collected for the study area. No detailed plans of the construction of artificial sea defences have been obtained. However discussions with an individual involved in the construction of sea embankments in the Zhujiang Delta during the 1970s revealed that most are made simply of mud. Along almost all of the coastline of the Zhujiang delta the intertidal zone has been reclaimed, and artificial seawalls extend out to the low water mark. Natural sea defences have therefore been almost completely destroyed. The artificial seawalls built to defend the coastal lowlands in the study area are typical of those throughout the Zhujiang delta. They are built from mud dredged from the intertidal zone, and no concrete reinforcements were observed.

5.3 IMPACTS OF MARINE FLOODING:

5.3.1 Past research:

The nature and likelihood of future sea-level rise and its possible impacts have been examined by a number of researchers (e.g. Tooley 1971, Barth and Titus 1984, Henderson-Sellers and McGuffie 1986, Carter 1987, Titus 1987, Shennan and Tooley 1987, Milliman et al 1989, Shennan and Sproxton 1990). Hoffman et al (1983, 1986) have examined the possibilities of sea-levels rising in the future, and have developed a range of scenarios for mean global sea-level rise up to AD 2100.

Very detailed analyses of the impacts of marine flooding have generally concentrated on a smaller number of coastlines in developed countries (Barth and Titus 1984, Titus 1987, Shennan

Chapter 5: Possible impacts of future sea-level changes

and Sproxton 1990). Relatively little similar work has been done to assess either the possible impacts of marine flooding or a suitable methodology for examining the problem in heavily populated tropical coasts. Very little work has been done by Chinese researchers on the risks and impacts of future sea-level rise on the low lying coastal areas of China.

The most sophisticated studies of coastal flood impacts are those carried out in the United States. Flood Insurance Studies (FISs) are conducted for communities at risk of flooding. The Federal Insurance Administration (FIA) Office of Risk Assessment has drawn up a set of guidelines for preparing FISs. Coastal areas at risk from flooding (known as V zones) are defined using these guidelines, and Flood Insurance Rate Maps (FIRMs) are drawn, dividing areas into flood hazard zones. These maps define the V zones (defined as areas susceptible to wave elevations associated with the 100 year flood). The Federal Emergency Management Agency publishes FIRMs for flood prone areas throughout the United States. Mapping started in the early 1970s. Between 1975 and 1980, FIRMs with V zones were published for about 270 communities along the Atlantic and Gulf coasts of the United States. These maps may be combined with the results of Flood Insurance Studies in order to provide a full analysis of the possible impacts of flooding for use by local communities, government agencies, local businesses and insurance companies. The FEMA does not, however, take into account possible future sea-level rise scenarios when developing its FIRMs.

The detailed assessments of the impacts of flooding attempted by the Federal Emergency Management Agency are not common in other countries, particularly in poorer parts of the world. Longer term future sea-level rise is not an important aspect of calculations of the risk of marine flooding. In poorer parts of the world the

Chapter 5: Possible impacts of future sea-level changes

consequences of marine flooding are often reported in an anecdotal way, and few systematic studies have been done. Milliman et al (1989) have attempted to analyze the effects of future marine flooding and sea-level rise for the Nile Delta and Bangladesh.

Hoffman et al (1984) highlighted the need to assess the impact of sea-level changes on decision making, as well as the physical impacts. They identified four categories of decisions that sea-level rise will influence: location decisions, structural and site decisions, decisions about protective measures against floods and erosion and flood mitigation planning. This aspect of future sea-level change impact assessment is not considered in detail in this study.

5.3.2 The study area:

Little work on the impacts of sea-level rise has been carried out in southern China and Hong Kong. Li (1988) has attempted to summarise the likely impacts of sea-level rise in the Zhujiang Delta, however this is not a detailed analysis. No official analysis of flood risk in the Zhujiang Delta has been found. However, as Li is a member of the Institute of Geography at Guangzhou, a government research agency which carries out research on aspects of the Zhujiang Delta and the coasts of Guangdong Province, it appears that relatively little attention is paid to flood risk assessments for the whole delta.

5.4 AIMS OF THE STUDY:

The aim of this study is to assess the risks of flooding in a small part of the Zhujiang delta, and some of the likely

Chapter 5: Possible impacts of future sea-level changes

consequences of major flooding and coastal retreat. The study assesses the consequences of flooding by analysing a wide range of disparate data including tidal, ground altitude, land use, population and transport data. Although the acquisition of information from China is very difficult, it has been possible to derive conclusions through a Geographical Information System (G.I.S.), and thus to assess some of the likely costs of flooding to the study area. A possible methodology for larger scale and more sophisticated analysis has been developed and this is discussed at the end of this chapter. Although detailed data for the Chinese coastal lowland areas which would allow more sophisticated analyses to be carried out is known to exist and has been seen by the author, it was not possible to retrieve these data from China for this study. Detailed altitudinal data for a very small area of the Zhujiang delta (approximately 12 sq. km) have been obtained and these data are illustrated in figure 5.10.

5.5 METHODS:

A Geographical Information System (G.I.S.) is a useful tool with which to assess the likely impacts of marine flooding on an area, and to try to measure the risks of flooding. A G.I.S. provides a means of storing data about spatial features and their attributes, manipulating these data to examine the spatial and attribute relationships between them, and portraying these relationships in the form of maps and reports. The various relationships between geographical features of a landscape that may influence the risks and impacts of flooding can be analyzed; for example land altitudes, land uses, the distribution of populations (see sections 5.2 and 5.3).

Chapter 5: Possible impacts of future sea-level changes

A major problem when developing the methodology was deciding the scale of the study, and the resolution of the data. Shennan and Tooley (1987) and Shennan (1988) have collected generalised data for each census ward area in two regions of the United Kingdom threatened by future sea-level rise, and combined these data into a simple G.I.S. The major problem with the G.I.S. used in these studies is that the only features in the G.I.S. are the polygons representing ward boundaries. All the data collected for the two study areas have had to be generalised to attribute data related to these polygons. Therefore the resolution of the G.I.S. is generalised to ward level, and any variation within wards, which in the case of altitude data is often considerable, is lost. This immediately qualifies some of the conclusions drawn from the G.I.S. However Shennan (1987) has explained that the method is for use in planning at the national level, and would have to be re-evaluated for specific local requirements. A more sophisticated analysis has been attempted by Shennan and Sproxton (1990) for the Tees estuary in north east England, using the same software package as used in this study.

This study uses a G.I.S. which allows the input of both feature and attribute data. The G.I.S. package used is pcARC/INFO. The package has been run on an IBM AT and an IBM PS2 personal computer. A series of routines within the pcARC/INFO software allow various manipulations of the available data to be undertaken, interactive questioning of the data, and the production of graphical and statistical output. The great advantage of this system of analysis is that feature data can be digitised and combined very easily, allowing the G.I.S. to incorporate as much of the available data as possible rather than having to generalise it. Editing of data sets and addition of new data are very easy, allowing periodic correction and updating of analyses.

Chapter 5: Possible impacts of future sea-level changes

The overall structure of the G.I.S. used is summarised in figure 5.1. It allows the integration of spatial data of various coastal landscape attributes at different time periods. Perhaps most importantly modelling of future flood scenarios can be done given sufficient data on the present configuration of the coastal environment. Changes in particular coastal attributes at different times in the future could be examined. For example the impacts of different altitudes for the mean high water mark at a coastal location given a generalised rise in sea-levels through time can be assessed. Alternatively, variations in future populations, land uses or transport systems can be modelled to assess the variations in risks and costs associated with particular flooding scenarios. This study has not attempted to model future changes in land use.

5.6 THE STUDY AREA:

The Zhujiang Delta in southern China (figure 5.2) is an area of low altitudes, high population densities and intense economic activity. A number of important commercial centres lie within the delta area, including Guangzhou, Macao, the Shenzhen and Zhuhai Special Economic Zones (S.E.Z.) and Fushan. Hong Kong lies at the south east edge of the delta. The Zhujiang delta supports a thriving agricultural sector, as well as one of the economically fastest growing areas of mainland China. Almost 14 million people live in the delta according to Chen (1988) and a larger number of people are economically linked to this area.

It is probably the most economically developed part of southern China, and has attracted much foreign and domestic investment. The coastal zones of Bao'an County and Shenzhen S.E.Z. have been particular foci for rapid development since the mid 1980s. In 1992 a new airport will be opened, built on a low lying coastal

site west of Shenzhen City, just to the south of the area discussed in this study. Large factories have already been built on land reclaimed from the sea (Griffiths 1988).

A large proportion of the delta lies at very low altitudes, generally below the highest recorded tide levels mark, and even below the mean water level (see table 5.1). Huang et al (1982) and Li (1988) defined the delta as an area below the +10 metres Y.S.D. contour line that surrounds the main area of the delta (see figure 5.2), and have shown that almost 81% of the delta lies below +0.9 metres Y.S.D. (an area of 6,932 square kilometres (Huang et al 1982, table 2.2). Li (1988) estimates that almost 4,000 square kilometres (43.7% of the area of the Zhujiang Delta) is below +0.3 metres Y.S.D. Since mean sea-level in the delta is at present +0.4 metres Y.S.D. \pm 0.1 metre, and the highest recorded sea-levels at eleven tide gauge stations in the delta recorded between 1950 and 1980 were between +2.99 metres Y.S.D. and +2.38 metres Y.S.D. (see table 5.1), the threat of marine flooding is considerable. The locations of the tide gauge stations are shown in figure 5.2.

5.6.1 Study area definition:

Three general criteria were used to define the study area. Firstly, the aim of the G.I.S. was to analyze the likely impacts of marine flooding on various human and physical elements of the coastal lowlands of southern China, and to help future planning of the economic development of these coastal areas. The study area therefore had to be based on an area which was related to the local administrative and planning systems. Secondly, adequate data on the study area had to be available. Thirdly, the study area had to be small enough to allow adequate analysis of the data given the resources available.

Chapter 5: Possible impacts of future sea-level changes

If more data and resources had been available this study might have examined a much larger area, such as the whole of the Zhujiang Delta which is threatened by marine flooding (Li 1988). However this was not possible because data were not available after 1989, and so a smaller study area was chosen which could act as a test for the methodology, and would also provide interesting conclusions which could be related to other parts of the Zhujiang Delta.

The study area is shown in figure 5.3. Located on the eastern side of the Zhujiang delta, it is approximately 271 km² in area, and consists of four districts within Bao'an County (see following section on Chinese administrative divisions). The area is representative of much of the Zhujiang Delta. Altitudinal variation is similar to that in other parts of the delta. The population density and land use system corresponds to much of the Zhujiang delta, with a concentration of intensive agricultural land use and high population densities on the lowlying, very gently undulating coastal plain.

5.6.2 Administrative divisions in China:

The geographical structure of local government in China has been summarised in figure 5.4. **Township** areas can be compared to wards or enumeration districts in the United Kingdom. They are the smallest unit for administrative purposes, and are also the basis for the collection of population census data. Each township may have a number of villages within its boundaries. In this study the largest township has a population of just less than 4,000 people (Haoyie township in Shajing district). Townships combine to make up **districts** administered by the district government. This will be based at the district centre, generally the largest urban unit within the district. Districts are responsible to the

county government at the county centre, which is itself under the jurisdiction of a **city**. Cities are responsible to their provincial or autonomous region government. There are 30 **provinces, autonomous regions and municipalities** in the People's Republic of China.

This study concentrates on a small area of Bao'an County in the eastern part of the Zhujiang delta (figure 5.3). Bao'an County is one of nine counties in the delta region in Guangdong Province. Between 1979 and 1980 the southern part of Bao'an County, bordering Hong Kong, and centred on the small town of Shenzhen, was divided off from the rest of the county. Initially a "special export zone" was created in July 1979. In November 1979 Shenzhen was changed to a municipality directly controlled by the provincial government of Guangdong Province in Guangzhou. In 1980 this was changed to the Shenzhen Special Economic Zone (S.E.Z.), controlled by a municipal government in Shangbu responsible to the Guangdong provincial government. Bao'an County and Shenzhen S.E.Z. combine to make up Shenzhen City (figure 5.3). The Shenzhen S.E.Z. consists of five administrative districts, each controlling a series of administrative agencies. Bao'an County, however, falls into the standard pattern of Chinese local administrative units. It now consists of 16 districts controlled by the county government in Xin'an. Each district has a series of townships. This study is concerned with just four districts in the western part of Bao'an County: Songgang, Shajing, Fuyong and Xixiang. These four districts are made up of 51 townships. In 1983, the total population of these four districts, according to the census, was 64,182. This was 25% of the total population of Bao'an County.

5.6.3 Data availability:

The second criterion for choosing the study area was data availability. Fieldwork had been done in Shajing district in order to examine the sedimentary history of the coastal lowlands south of Shajing town (see chapter 3) and a detailed levelling exercise was carried out during this fieldwork period. Data on the population, land use and transport for the western part of Bao'an county were available from various sources in China, and these were collected during a visit to Guangdong province in 1988. General verification of the land use data was possible during the fieldwork period although no systematic checks were possible. Topographical and land use maps for a larger area of the Zhujiang Delta were examined in China, but it was not possible to take these maps or the topographical information out of China.

5.6.4 Size of the study area:

The constraints on the size of the study area were in part a function of the time available for data preparation, and also the amount of data made available. The main time expenditure involved preparing maps of the various data sets for digitising and the process of digitising data for use in the G.I.S. As this detailed work had not been carried out before for this area, no digital data were available. The size of this study area was considered large enough for interesting conclusions to be reached regarding the impacts of marine flooding on a coastal community, but also small enough to allow data to be entered into the G.I.S. within the time available. All data were prepared, digitised and analyzed by the author.

5.7 Data used in the study:

The data available for the study were from a variety of sources, and can be divided into six sections.

5.7.1 Altitude data:

These were derived from topographical maps published by the Chinese National Survey at a scale of 1:50,000. These maps show contours at a vertical interval of 10 metres (and include the +5 m Y.S.D. contour), and spot heights to an accuracy of 0.1 metre. The altitude data have been derived from a series of levelling exercises carried out over the past forty years by the Chinese National Survey. (Chen 1984, Huang *et al* 1986). The accuracy of these data has not been studied in detail. However a levelling exercise carried out in April 1988 in the coastal plain approximately two kilometres south of Shajing in western Bao'an County suggests that the spot height data are correct to within at least ± 0.2 metres (figure 5.5). The altitude data used in the G.I.S. are relatively crude compared to the very detailed altitude data that are presented on 1:10,000 scale maps, but which were not made generally available to this study. The +5 metre Y.S.D. contour and all spot heights below +5 m Y.S.D. in the study area marked on the 1:50,000 scale maps have been used.

Four digitised coverages with altitude data for the study site have been created. A line coverage of the +5 m Y.S.D. contour line, and three "point" feature coverages of spot heights below +2 m Y.S.D., between +2 and +2.5 m Y.S.D., and above +2.5 m Y.S.D. have been created, and attribute data about the spot height "points" has been added.

Chapter 5: Possible impacts of future sea-level changes

A 1:10,000 map of a small part of the study area was obtained and this is reproduced in figure 5.10. As the area covered by this map is only approximately 12 square kilometres, no major conclusions could be based on it. However, the 1:10,000 topographic map provides detailed altitudinal data. Contour lines at a one metre interval are drawn on these maps. Spot heights to an apparent accuracy of ± 0.1 m are also drawn on the maps. The total number of these spot heights on the coastal plain is 360. If a set of these maps had been obtained covering the whole study area, the altitude resolution would have been much higher, and a better assessment of the risks and impacts of flooding could have been made. This resolution of the data would have allowed useful modelling of different sea-level rise scenarios to be done, as described above and summarised in figure 5.1

5.7.2 Land-use data:

Data on the pattern of land use in the study area has been provided by the Institute of Geography in Guangzhou, and published by Wen et al (1985). The data were collected using remotely sensed images and fieldwork, and are accurate to the end of 1983. Wen et al (1985) emphasise that land use patterns are changing rapidly in Bao'an County and the Shenzhen Special Economic Zone, with increasing economic development. The western part of Shenzhen (the four districts in the study area) is used particularly intensively. The pattern of land use, and attributes of the various land use areas, have been entered into the G.I.S. Wen et al (1985) identify twenty land use types, including beaches, "exposed land" (undefined by Wen et al op. cit.) and four types of forest. Of these eleven have been used in the G.I.S. Forest areas have been generalised into one category, and beach areas have been removed by land reclamation in this part of Bao'an County. Industrial areas, harbours, tourist areas,

Chapter 5: Possible impacts of future sea-level changes

"exposed land" and reed marsh are identified by Wen et al as important land uses in Bao'an County, however of these land uses only reed marsh is identified within the study area, and this is not extensive.

A more up-to-date land use inventory was outside the scope of this study. Although remotely sensed data can be used to produce a land use survey, and high resolution SPOT images of the study area taken in October 1988 were examined at the Institute of Geography, Guangzhou in early 1990, this was not possible in this study. Future work on this problem would require a new systematic inventory of land use in the study area.

5.7.3 Land resources:

A land resource map for the whole study area has been generated, based on information given by Yu et al (1985). Five major categories of land resource are identified by Yu et al (1985): land suitable for rice cultivation, dry farming, forestry, pasture and lakes or fish ponds. A number of criteria for categorising different areas is given by Yu et al. The criteria are topography, water drainage, soil depth and soil type. Land suitable for rice cultivation, dry farming and forestry have been divided into three classes according to quality, although the method of classification is not defined by Yu et al (1985). Pasture areas have been divided into two classes. The classified land areas have been entered into the G.I.S.

5.7.4 Population data:

The P.R. China has conducted four population censuses in 1953, 1964, 1982 and 1990. This study uses data from the third national census. Data were collected between 1 - 20 July 1982, and have been summarised in Zhou (1985).

The total population for each township in the study area as measured in the 1981 and 1983 local censuses has been entered into the G.I.S. as attribute data for the digitised map of the township areas. The accuracy of the data is unknown. The total population for each township area was obtained from the Institute of Geography, Guangzhou. Population data for the counties in the Zhujiang Delta were also obtained and these are discussed in a later section of this chapter.

5.7.5 Communications:

Roads are the major form of communication in the area. Roads have been digitised as line features from the 1:50,000 scale published maps produced by the Chinese National Survey. Attribute data for each section of road has been taken from Zhong (1985). Roads are divided into three types: trunk, primary and secondary roads. The main road between Shenzhen and Guangzhou passes through the study area, and has been entered into the G.I.S. as a trunk road. A new road is being built through the study area which will link Hong Kong and Guangzhou, however its location has not been identified. No railways pass through the study area. Minor unsurfaced tracks which cross field systems have not been entered into the G.I.S., although these are of importance to local communications.

5.7.6 Settlements:

The locations of villages within the township areas have been digitised from the 1:50,000 scale maps of the study area. Villages are marked on these maps. Lines were traced around these village areas, and these lines were then digitised. The village areas are not related to accurately surveyed village boundaries, but are estimated generalisations from the 1:50,000 scale maps. The estimated geographical area of these villages derived from the G.I.S. has therefore been ignored. Since rapid building work is taking place throughout the study area, causing villages to expand in area, the accuracy of these data are limited.

5.7.7 Tidal data:

Two sets of data of measured altitudes of past sea-levels relevant to the present study have been examined. Both sets come from established tide gauges in the Zhujiang Delta and Hong Kong (see figure 5.2). It is unclear how accurate the Chinese data from the Zhujiang Delta are, however they have been corroborated by published data in Huang et al (1982), and discussions with various Chinese scientists suggests that measurements are reasonably accurate. The data from Hong Kong has been rigorously checked by the Royal Observatory in Hong Kong. Although the Chinese data from the Zhujiang Delta are of primary importance to this study, the data from Hong Kong are interesting in comparison.

5.7.7.1 The Zhujiang Delta:

Tidal measurements from eleven tide gauge stations in the Zhujiang delta are shown in table 5.1. These were the only data

available, and it was not possible to obtain a set of more detailed measurements. No published analysis of extreme sea-levels in the Zhujiang Delta was discovered, despite a thorough search in Guangzhou. The data show the maximum recorded sea-level at eleven tide gauge stations during periods of between 30 and six years recorded prior to 1980. The longest running record is for 30 years at Guangzhou between 1950 and 1980. It is not known what proportion of the sea-level rise registered by these data is due to tidal variations and storm surge effects, although this is discussed further in section 5.9.1 (see below). No detailed time series of tide data for the Zhujiang Delta is available.

5.7.7.2 Hong Kong:

The tide gauge network in Hong Kong consists of nine tide gauges (see figure 5.7). The data from Hong Kong appear to be accurate and have been rigorously checked for any recording errors by the Royal Observatory, Hong Kong. The longest tidal record in Hong Kong is that for North Point, Hong Kong Island. The equipment was installed in 1950 and provides a record of sea-levels until 1986 when the tide gauge was moved to Quarry Bay, about 0.5 km east of North Point. Checking for ground settlement of tide gauges is not done regularly. The altitude of the gauge at North Point was measured between 1954 and 1976 by the Port Works Division of the Hong Kong Government, using precise levelling techniques. The gauge was levelled at regular intervals using a benchmark at 323 Java Road. The recorded levels at North Point are presented in table 5.2 and figure 5.8.

The mean rate of settlement between 1954 and 1976 has been calculated as 5.04 mm/year. It appears from figure 5.7 that settlement is unlikely to have stopped suddenly after 1976, although settlement rates are likely to decline over time. At

Chapter 5: Possible impacts of future sea-level changes

Quarry Bay the mean settlement rate at the new tide gauge station is 6.1 mm/year. Levelling of three reference points at the tide gauge station has been carried out since 1984.

Statistics on extreme sea-levels measured at various tide gauges in Hong Kong have been analyzed by Chan (1983) and by Yim (1988) and other data provided by the Royal Observatory, Hong Kong, are presented here. Chan provides detailed data on extreme sea-levels between 1906 and October 1982. Many of these extreme sea-levels are due to tropical cyclones. Chan also gives detailed data on the calculated magnitude of storm surges measured at three tide gauge stations: North Point, Tai Po and Chi Ma Wan. All the tidal data from Hong Kong have been corrected for ground settlement, by subtracting the amount of ground settlement that occurred between the time that the tide gauge station was established and the time of the measurement of sea-level using a rate of 5.04 mm/year.

5.7.7.3 Trends in mean sea level

Yim (1988) first drew attention to the use of tide gauge data to examine trends in mean sea-level around Hong Kong over a period of a few years during the recent past. Tidal records collected between 1962 and 1987 from North Point were analyzed. An apparent trend of rising sea-level was found, although Yim emphasised that subsidence at the gauge was likely to have been responsible for most of this apparent rise. When mean annual sea-level at North Point is corrected for ground settlement, sea-level appears to have fallen very slightly over the past 30 years in Hong Kong (Yim 1988). This conflicts with the trend of global sea-levels measured over the past 100 years and reported by Gornitz and Lebedeff (1987). However Yim (1988) suggests that this pattern in Hong Kong may be in part due to land subsidence around the

Chapter 5: Possible impacts of future sea-level changes

tide gauge at North Point leading to a distortion of the recorded sea-level altitudes.

5.8 TECHNIQUES:

This study tries to use a variety of data sets to assess the likely impacts of maritime flooding on an area of coastal lowland, and to identify a methodology for doing this in different study areas. The use of a G.I.S. involves a series of methods and stages of analysis. After the study area was defined, a series of data sets was collected for the study area. These included cartographic data as well as numerical information on extreme sea-levels within and around the study area.

The cartographic data had to be converted to a standard base map. For the G.I.S. study the data were traced onto a copy of a 1:50,000 topographical map of the study area published by the Chinese National Survey in 1966. This was the most up-to-date map at a suitably large scale which was made available to this study. Copies were made onto sheets of transparent acetate. The land use, land resource, transport and population data were taken from published sources or were provided by the Institute of Geography, Guangzhou, and were copied onto the base map.

Land altitude, land use, land resource, village area and transport maps were then digitised using a Summagraphics digitising table and the pcARC/INFO Arc Digitising System (ADS) software. All these digitised coverages had a common outer boundary, and control points (termed "TIC" points in pcARC/INFO) were common for all the digitised maps. There were therefore no major problems in overlaying the different coverages later in the analysis. Great care was taken in digitising the coastline and external administrative boundaries of the coverage as these

Chapter 5: Possible impacts of future sea-level changes

defined the extent of the study area. This initial "external boundaries" coverage of the study area was used as a base for all other coverages. The coastline was digitised from the 1966 1:50,000 scale map used. Comparison with field notes taken in 1988 showed that the coastline has been extended seawards since 1966. However, as no accurate data were available to show the extent of this land reclamation along the whole of the coastline of the study area, no editing of the 1966 cartographic data could be undertaken.

The "external boundaries" coverage was used as a base for the other coverages of land use, land resource, population, altitude and transport data. These were each digitised and checked against the original data before topologies were generated using the CLEAN and BUILD commands within pcARC/INFO (see pcARC/INFO manuals for details, ESRI 1987,1988). Table 5.3 shows the topologies generated for different coverages. Once all coverages had been digitised, they were transformed to the coordinate system used on the Chinese published 1:50,000 maps which was the source of the data used in the digitising process. When each transformation procedure was carried out, the Residual Mean Square error was calculated (table 5.3). This represents the accuracy of the control points of the digitised coverage as compared to the coordinate system on the published maps to which the digitised coverage was converted. The relationships between the digitised coordinates are compared with the relationships between the corresponding points on the map coordinate system. The lower the RMS error the better the match between the digitised coverage and the original map data. A RMS error of below 0.003 was achieved on all but three of the coverages. The highest RMS error was 0.005 which was considered acceptable, since the sources of the land use and land resource data were 1:200,000 maps, and data loss had occurred during the transfer

Chapter 5: Possible impacts of future sea-level changes

of the data from the source map to the 1:50,000 tracing used for digitising.

The accuracy of the data is limited by the small scale of the original maps from which the data were taken (generally 1:200,000), and the number of stages of data transfer. Ideally, larger scale original maps would have been made available. These do exist and have been seen at the Institute of Geography, Guangzhou.

Once the coverages had been generated, and attribute data had been added, analysis of the data was carried out using the various OVERLAY routines within pcARC/INFO (ESRI 1988). The results of these are discussed below (section 5.9).

Output of data was done by two methods. Attribute data were copied from the pcARC/INFO database files to a spreadsheet file, and analyzed. Feature data was analyzed and presented using the pcARC/INFO ARCPLOT module. Tidal data were analyzed using the spreadsheet package.

5.9 THE RISK OF MARINE FLOODING:

The initial aim of the study was to identify parts of the study area most at risk from marine flooding, and to analyze the nature of that risk. Once this had been done an analysis of the possible impacts of flooding could be carried out. A large number of factors affect the threat of marine flooding on an area. Primarily these are the relative altitudes of coastal lowlands, sea defences and sea-levels, the latter obviously varying over different time periods. Other factors include the strength of sea defences; the incidence and nature of storms, and in particular storm surges; and the nature of the intertidal zone.

Chapter 5: Possible impacts of future sea-level changes

In this study an analysis of the relationships between sea-levels, sea defences and coastal land altitudes was carried out, in order to define a Flood Risk Zone. Once this was done, the possible impacts of flooding within this zone were analyzed. The secondary stage of analysis was carried out in order to account for factors other than altitude which may influence the extent of the Flood Risk Zone (such as the nature of sea defences along the coast).

5.9.1 Past sea-levels

Records of past sea-levels have been collected at a series of tide gauge stations throughout the Zhujiang Delta and Hong Kong over the past 30 years (Huang *et al* 1982, Yim 1988). Published and unpublished data from these gauges provide a record showing the highest measured altitudes of the sea at these points during these periods, as well as measurements of mean sea-levels.

The Zhujiang Delta is an area of small tidal range. The difference between Mean High Water and Mean Low Water, as measured at the Chinese tide gauge stations, varies between 1.70 m and 1.28 m (see table 5.1). Within the Zhujiang Delta the length of the tidal record varies between 30 and 6 years. The maximum recorded high water altitude was at Guangzhou, on 22 July 1974, was measured as reaching +2.99 m Y.S.D. The other highest recorded sea-levels range between +2.38 m Y.S.D. and +2.88 m Y.S.D. The dates on which these sea-levels occurred were 22 July 1974, 29 July 1969 and 28 May 1964.

In Hong Kong, the Royal Observatory records show that all three of the dates given above coincided with tropical cyclone storms in the area. On 28 May 1964, tropical cyclone Viola passed within 55 nautical miles west of Hong Kong in a north westerly

direction, producing maximum gusts in Hong Kong of 82 knots. On 29 July 1969, a second cyclone named Viola passed within 54 nautical miles east of Hong Kong. Maximum recorded gusts in Hong Kong reached 67 knots. On 22 July 1974, tropical cyclone Ivy passed within 130 nautical miles west of Hong Kong, producing maximum gusts of 61 knots. It would appear that the highest recorded sea-levels in the Zhujiang delta were, at least in part, due to the progression of tropical storms recorded in Hong Kong. No data are available for recorded sea-levels in the Zhujiang Delta during the passage of other tropical cyclones.

The available data suggest that the highest sea-levels recorded in the eastern part of the delta, close to the study area, were between +2.38 m and +2.50 m Y.S.D. (see figure 5.2). One may assume from historical records that land below +2.50 m Y.S.D. is at risk from marine flooding unless defended by sea-walls or other defences. At this stage in the analysis scenarios of future sea-level rise, as discussed by Hoffman et al (1983, 1986) for example, are ignored.

The records of sea-levels from the Zhujiang Delta do not extend over a very long period. The earliest recorded maximum sea-level is 1950. Sea-level may have been much higher at some point in the past, due to storm surges for example. Li (1988) states that the highest ever recorded sea-level in the Zhujiang Delta was +3.95 m Y.S.D., measured in 1937 at Doumen in the southern part of the delta. No tide gauge data have been found for the Zhujiang Delta before 1950.

In Hong Kong, the record of past sea-levels is more comprehensive and covers a longer time period than that for the Zhujiang delta. Chan (1983) has discussed extreme sea-levels in Hong Kong, and gives detailed information regarding the meteorological

conditions influencing past sea-levels. The great majority of extreme sea-levels recorded in Hong Kong by the Royal Observatory between 1906 and 1982 coincided with the passage of tropical storms. Data for maximum sea-level recorded around Hong Kong between 1954 and 1988 are shown in table 5.4. These tropical storms both raised sea-levels and caused storm surges. The storm surge components measured at North Point, Hong Kong of the three tropical cyclones discussed above (which caused the highest recorded sea-levels in the Zhujiang Delta between 1950 and 1980) are shown in table 5.5.

Table 5.5 and figure 5.6 show two important processes. The first is the apparent importance of tropical cyclones in raising sea-levels. The second is the geographical variation in sea-levels within the Zhujiang Delta. There appears to be a funnelling effect, increasing sea-levels up the Zhujiang estuary. On 22 July 1974 the highest recorded sea-level at North Point was 1.64 m Y.S.D., and at Tai Po Kau it was 1.58 m Y.S.D. At Shanshakou it was 2.74 m Y.S.D. and at Guangzhou 2.99 m Y.S.D.

No "storm surge" residual values are available for the extreme sea-level data from the tide gauge stations in Zhujiang, as it is not known at what stage in the tidal cycle the highest sea-levels noted in table 5.1 were recorded. The difference in the altitude of recorded Mean High Water level and the maximum recorded sea-level, at the eleven tide gauge stations in the Zhujiang Delta for which data are available (see table 5.1), varies between 1.67 m and 1.37 m. During the "Ivy" cyclone, which produced the highest recorded sea-levels at six of the eleven tide gauge stations in the Zhujiang on 22 July 1974, the difference between maximum recorded sea-level at the North Point tide gauge stations on that date in Hong Kong, and altitude of

Chapter 5: Possible impacts of future sea-level changes

mean monthly maximum sea-level as given by Yim (1988), was 1.09 m (see table 5.6).

On 29 July 1969, when the difference between Mean High Water and the highest recorded sea-levels at Dasheng, Chewan and Shanbanzhou were 1.42 m 1.39 m and 1.52 m respectively, the difference between mean monthly maximum sea-level and highest recorded sea-level at North Point was 1.54 m (see tables 5.1 and 5.6). It may be assumed that the storm surge effect measured in Hong Kong on all three dates influenced sea-levels throughout the Zhujiang Delta, raising them. This may have been particularly the case on 22 July 1974 and 28 May 1964 when the centres of the tropical cyclone storms passed 130 nautical miles and 55 nautical miles west of Hong Kong Royal Observatory respectively, passing over the Zhujiang Delta.

The tidal data from both the Zhujiang delta and Hong Kong suggest that high sea-levels are generally caused by tropical storm surges and that within the Zhujiang Delta the sea may rise to between +2.50 m Y.S.D. and +3.00 m Y.S.D. It is not clear what the storm surge component of the highest recorded sea-levels in the Zhujiang Delta over the 30 year period between 1950 and 1980 was. However the highest recorded sea-levels all coincided with tropical cyclone storms, and with recorded sea-level maxima at Hong Kong tide gauge stations.

5.9.2 Altitudinal Data

The topography of the study area is representative of much of the Zhujiang Delta, and may be divided into two areas. A lowlying coastal plain with an altitudinal variation of no more than ± 1.0 metres extends from behind the sea-defence walls. Landward of this coastal plain there is an undulating area rising to

Chapter 5: Possible impacts of future sea-level changes

altitudes of over +150 m Y.S.D. The low-lying coastal plain extends over a distance of between four and ten kilometres within the study area.

The altitudinal data used in this study are summarised in section 5.7.1. The digitised 1:50,000 topographical map was used to estimate the total area below +5 m Y.S.D., adjacent to the coast using the BUILD subroutine within pcARC/INFO. This calculates the area of polygons digitised using ADS. The total estimated area was 118.4 km² (see figure 5.9). This represents 44.7% of the total study area.

The lowland area is all adjacent to the coast. Spot height data have been combined with contour data to analyze the distribution of lower altitudes within this coastal lowland area. The distribution of spot heights below +5 m Y.S.D. demonstrates that a large proportion of the land below the +5 m Y.S.D. contour line is in fact below +2.5 m Y.S.D. The distribution of spot heights below +2.5 m Y.S.D. extends away from the coast towards the +5 m contour line, particularly across the coastal plain just north of Shajing. A levelling exercise was carried out two kilometres south of Shajing in order to check the accuracy of the topographical maps used in the G.I.S. A transect was levelled across the coastal lowland area from the 5 m Y.S.D. contour to the coastline, a distance of about 4 kilometres (figure 5.5).

This transect shows very clearly how the lowland between this part of the coast and the +5 m Y.S.D. contour line descends to below +1.0 m Y.S.D. over a large area. This is confirmed by an analysis of the 1:10,000 topographical map published by the Chinese National Survey. This shows contour lines at an interval of 1.0 metres (see figure 5.10). The altitude of the highest sea embankment crossed by the levelling transect was +2.7 m Y.S.D.

The cartographic evidence, combined with levelling in the field, suggests that most of the area below the +5 m Y.S.D. contour line is in fact below +2.5 m Y.S.D. The levelling transect and the 1:10,000 map evidence suggest that the coastal lowland plain extends back from the coast below +1.0 m Y.S.D. for up to 3 kilometres, and then rises only gently until within a few hundred metres of the +5.0 m Y.S.D. contour line.

These data from the study area may be compared with data given by Li (1988) and Huang et al (1982), who have examined topographic maps covering the whole of the Zhujiang Delta. Li (1988) has estimated that 6,900 square kilometres of the Zhujiang Delta lies below +0.9 m Y.S.D. This represents 81% of the area of the delta, which Li (1988) defines as the area lying within the +10 m Y.S.D. contour line surrounding the delta area (an area of 8,700 square kilometres). Li estimates that 3,400 square kilometres lies below +0.3 m Y.S.D. The lowlying coastal plain in the study area is therefore at a relatively high altitude compared with most of the Zhujiang Delta, since the lowest spot height found on the 1:50,000 topographic map of the study area is +0.4 m Y.S.D. and the lowest altitude levelled along the transect south of Shajing was +0.9 m Y.S.D.

Figure 7.11 shows the altitudes of recorded sea-levels in the Zhujiang Delta and Hong Kong, and ground altitudes in the study area and the Zhujiang Delta.

5.9.3 Definition of the Flood Risk Zone

The records of sea-levels measured in the Zhujiang Delta and in Hong Kong, which have been summarised in section 5.8.1, show that, along the coast of the study area, sea-levels have risen to as high as 2.50 m Y.S.D. Analysis of the tide gauge

Chapter 5: Possible impacts of future sea-level changes

measurements from Hong Kong suggests that severe tropical storms could raise sea-levels to altitudes higher than those recorded during the three tropical cyclone storms which resulted in highest sea-levels between 1955 and 1980. It would appear from the historical evidence of past tide gauge stations that land in the study area below +2.50 m Y.S.D. is at risk from marine flooding. A future severe storm surge may raise sea-levels even further. The storm surge residuals, measured at North Point, caused by the three tropical cyclones, which raised sea-levels in the Zhujiang Delta to their highest levels between 1950 and 1980, have all been exceeded by storm surges recorded at Hong Kong.

The storm surge recorded on 28 May 1964 at North Point, Hong Kong, which was the largest of the three (see table 5.5) and raised sea-levels at North Point by 0.94 metres, has been exceeded by eighteen measured storm surges between 1906 and 1982. The largest storm surge recorded at North Point was on 1 September 1937 and was 1.98 metres in magnitude, raising sea-levels to 3.90 m PD (3.03 m Y.S.D.). Li (1988) claims that the sea-level at Doumen in 1937 rose to 3.37 m Y.S.D., but no detailed tidal or sea-level data are available for the Zhujiang delta for this period, and it is not clear from Li's work when this occurred in 1937.

The Flood Risk Zone has therefore been defined as *all ground lying below +2.50 m Y.S.D.*, based on the analysis of records of past sea-levels. However it should be noted that higher sea-levels have been recorded both in Hong Kong and the Zhujiang Delta during the twentieth century, and that this may therefore represent a *conservative* estimate of the extent of the flood risk zone. This estimate does not consider future sea-level rise. The evidence of the Hong Kong tide gauge data shows that sea-levels

Chapter 5: Possible impacts of future sea-level changes

above +3.00 m Y.S.D. have occurred along the coast of Hong Kong Territory for example in 1906 and 1937 (Chen 1983). Since sea-levels during tropical storms seem to be higher in the Zhujiang Delta compared to Hong Kong, there is no reason to suppose that sea-levels in the Zhujiang Delta would not have been higher than +3.0 m Y.S.D. during these period, and could rise to these levels in the future, irrespective of any long term global rise in sea-level.

Analysis of altitude data for the study area suggests that the low lying coastal plain, extending between the sea defence walls and the 5 m contour line, is generally below +2.0 m Y.S.D., and much of it is below +1.0 m Y.S.D. As no detailed altitudinal data for the whole of the study area are available which would allow contours at a 0.5 m interval to be accurately interpolated, it has been assumed that all ground adjacent to the coast which is below the +5.0 m Y.S.D. contour line can be defined as constituting the Flood Risk Zone. Refinements to this broad definition could be made given more accurate altitudinal data. However given the constraints of the existing altitudinal data no refinement of the Flood Risk Zone definition has been made at this stage for the whole study area.

5.10 THE IMPACTS OF FUTURE MARINE FLOODING:

Having defined a simple Flood Risk Zone, the G.I.S. can be used to examine the relationship between different landscape attributes and this zone. Impacts of future marine flooding can be modelled.

5.10.1 Population

The Chinese National Census held in 1983 provides population totals for village areas. These have been entered into the G.I.S. as attribute data to the digitised village area coverage. The total population of the four districts in the study area in 1983 was 64,182, according to the Chinese census records. The G.I.S. was used to calculate the population density of each village area according to the 1983 census data.

The population density map shows that the highest densities occur in village areas below +5 m Y.S.D., with the exception of Shajing town, which is located on land just above this level (see figure 5.10). The area above +5 m Y.S.D. is largely made up of townships with population densities of less than 199 people per square kilometre (see figure 5.12). Two of the largest areas above this level have population densities of less than 49 people per square kilometre and absolute populations of less than 999 people in 1983. This can be compared with townships lying wholly below +5 m Y.S.D. Four of these villages had population densities of more than 1,000 people per square kilometre. Three village areas in this category had populations of between 2,000 and 4,000 people per square kilometre.

An initial broad estimate of the number of people living below +5 m Y.S.D. in 1983 has been made by multiplying the areas of individual townships below +5 m Y.S.D. by their overall population density values. The results of this obviously assume that the distribution of people within individual townships is even. The total area below +5 m Y.S.D. is 118 square kilometres. The calculated number of people living below +5 m Y.S.D., according to the 1983 census data, is 39,002. This represents an

Chapter 5: Possible impacts of future sea-level changes

estimate of 62.3% of the total population of the study area living in 44.7% of the land area, all below +5 m Y.S.D.

When the coverage of the location of villages and the +5 m Y.S.D. contour line are combined, using the G.I.S. (figure 5.12), it becomes clear that the majority of villages are located below +5 m Y.S.D. Figure 5.12 shows clearly that the majority of villages are located along the coastline, extending back from the sea defence walls. In the area covered by the 1:10,000 topographic map coverage, villages by the coast extend over large areas below +1 m Y.S.D., and if coverages of spot height data and village locations are combined, this further confirms that villages situated along the coast are built on land below +2 m Y.S.D. The levelled cross section (figure 5.5) supports this conclusion.

This suggests that the initial assumption regarding the even distribution of population throughout village areas would lead to an underestimate of the number of people living in the Flood Risk Zone below +5 m Y.S.D. There is a concentration of domestic housing stock below +5 m Y.S.D., and much of it appears to be very near to the coastline (see figure 5.12). The calculated figure of 39,002 people living below +5 m Y.S.D. may therefore represent a minimum value.

5.10.2 Land use:

The local communities in the four districts covered in this study are heavily dependent on agriculture for employment. The largest source of employment is in the agricultural sector (table 5.8). Income per capita, largely derived from agriculture and aquaculture, is also high in these four districts compared to other parts of Bao'an County. In 1983 mean per capita income in Bao'an County was Y 407 (Deng 1985a). The four districts in this

Chapter 5: Possible impacts of future sea-level changes

study all had incomes greater than this value (table 5.9). Shajing and Xixiang districts achieved the highest per capita income within the whole of Bao'an County, and also higher than Nantou administrative district in Shenzhen S.E.Z. These four districts are therefore of considerable economic importance, and constitute some of the most economically productive areas within Shenzhen City outside of the S.E.Z. The source of this income is heavily concentrated within the agricultural and aquaculture economic sectors (table 5.10). Agriculture and aquaculture together accounted for well over half the income in each of the districts. In Shajing (the most prosperous district in Bao'an County as measured by per capita income) 66% of all income was generated by these activities. There is then a heavy dependence on these two functions both to generate employment and income with the four districts, and to contribute to the economy of Shenzhen City.

The nature of this agricultural and aquacultural production varies between districts. Songgang and Fuyong are predominantly areas of freshwater fishpond aquaculture. Shajing is a major centre for lucrative offshore oyster production. In 1983 approximately 40% of aquatic production by weight in Shajing district was made up of offshore oyster cultivation. 55% consisted of "freshwater farming" as defined by Deng (1985b). This is likely to include fresh water fish-pond production. The four districts, together with coastal areas in the S.E.Z. dominate aquaculture in Shenzhen City.

The land use coverage and the altitude data have been combined in the G.I.S., and their relationships have been summarised in table 5.11. The land use in the defined Flood Risk Zone is dominated by rice paddy, fresh and brackish water fish ponds, and some vegetable and built-up areas. Over 80% of built-up areas are

Chapter 5: Possible impacts of future sea-level changes

situated within the Flood Risk Zone, as are 66% of paddy fields. Fish ponds are almost exclusively within the Flood Risk Zone. The impact of marine flooding could therefore be devastating for paddy agriculture and aquaculture, the two major sources of income for the local population. Almost 50% of the land outside the Flood Risk Zone in the study area is made up of woodland, which provides very little direct income to the local population. Very little data is available about industrial and commercial land uses. However Xixiang and Shajing are both centres for light manufacturing. The whole of Xixiang is within the Flood Risk Zone, and spot height data suggests that much of this area is below +2.5 m Y.S.D., and is thus at risk from marine flooding.

The fish ponds are all surrounded by embankments. Although detailed altitude data for the top of these embankments are not available, the levelling exercise summarised in figure 5.5 did also measure the level of the top of fish ponds. The measured altitudes were between +2.5 m and +2.8 m Y.S.D. Fish ponds are concentrated close to the coast. Although the embankments of the fish ponds could provide a form of secondary defence behind the existing sea walls, the fish ponds do not provide a continuous line of defence along the length of the coast.

The impacts of marine flooding on the land use of the area, and therefore on the population could be considerable. As the majority of paddy and fish pond land use is located within the Flood Risk Zone, this important aspect of the local economy could be devastated by major flooding. According to Deng (1985), Songgang and Fuyong districts relied on agriculture to provide 49% and 54% of gross income respectively in 1983. 89% of the land area used for paddy, vegetable and non-irrigated arable land in Songgang is located within the Flood Risk Zone, and within Fuyong it is 93%. Employment within the four districts is heavily

Chapter 5: Possible impacts of future sea-level changes

dependent on the agricultural sector, particularly in labour intensive activities such as rice production, and the development of aquaculture. Xixiang is an centre for light industry, which provided 22% of the district's income in 1983. This industry is almost all concentrated in the Flood Risk Zone.

5.10.3 Land resources

The land resource data presented by Yu et al (1985) have been entered into the G.I.S. The proportion of land which either is used or could be used for different activities, and which might be affected by marine flooding within the Flood Risk Zone, has been calculated (see table 5.12). Of particular interest, when considering the economic effects of marine flooding, is the distribution of land that is used or could be suitable for rice cultivation. Rice production is still of great importance to local economies and populations. The majority of paddy is located below +5 m Y.S.D. Unlike fish ponds, rice paddy fields are not protected from possible marine flooding by surrounding embankments. The location of grade 1 paddy fields, considered the optimum land for rice production, is almost entirely below +5 m Y.S.D., and closer analysis of the spot height data suggests that much of this land is in fact below +2.5 m Y.S.D. The data shown on the 1:10,000 map shows that the minimum altitude for rice paddy fields (grade 1) in this part of the coast is +0.4 m Y.S.D. This is approximately 1.8 m below the Mean High Water Spring Tide Level.

5.10.4 Communications

By combining the altitude and communication network coverages in the G.I.S. it has been estimated that 65% of the road network in

the study area is within the Flood Risk Zone, including sections of the main road running the length of the study area. This is the main road link between Hong Kong, Shenzhen and Guangdong, and is therefore of vital strategic importance. Spot heights lower than +2.5 m Y.S.D. are located on either side of the existing road north of Shajing. About 50% of this main road in the four districts runs across ground below +5 m Y.S.D. Although it is to be replaced by a large trunk road, the proposed route of the new road may follow the course of the present link very closely (Zhong, 1985).

Roads are the core of the local communication network. In the event of marine flooding, roads would be the primary means of providing relief for the population affected by the flooding, and of evacuating people from the flood zone. In order to estimate the isolation settlements would experience in the event of a flood, the altitude, village and road coverages were combined. Villages below +5 m Y.S.D. and the parts of the road network lying above +5 m Y.S.D. were extracted from their respective coverages. A buffering routine within pcARC/INFO was used to identify all villages within the Flood Risk Zone which are more than one kilometre from a road above +5 m Y.S.D. Figure 5.13 shows those villages which may be cut off from roads outside the Flood Risk Zone. Shajing, which lies just above the Flood Risk Zone may be cut off from the higher hinterland, and from the main Shenzhen to Guangzhou road as the primary road linking the town with the main trunk road crosses the Flood Risk Zone.

Some roads are built on embankments. No accurate altitudinal data for different sections of the road network are available. However, it is clear that marine flooding could have severe, if temporary, consequences for transport both within the study area and over a larger scale around the study area.

5.11 Future changes in flood risk and impacts:

The risks and impacts of marine flooding will be influenced by future changes in the altitudes of sea-level and coastal areas. These changes may occur as a result of a rise in sea-levels or changes in the altitude of the coastal land areas due to subsidence or uplift, or changes in the human development of the coastal zone (for example changes in population concentrations and land use).

5.11.1 Changes in sea-levels

Various scenarios for future sea-level changes have been proposed (see figure 5.13). A rise in mean global temperatures due to increases in the concentration of radiatively active gases in the atmosphere has been suggested by a large number of researchers. Although no clear rise in temperatures has been recorded, a rise in various gases in the atmosphere (notably carbon dioxide) has been recorded over the past 100 - 200 years (Neftel *et al* 1985). Hansen and Lebedeff (1987) have collected data for surface air temperature changes recorded at stations throughout the globe between 1880 and 1987, and suggest global warming from 1880 to 1985 of between +0.5°C and +0.7°C. However the causes and permanence of this change are not clear.

Global sea-levels have also risen over the past century. Gornitz and Lebedeff (1987) have examined the evidence for global sea-level changes from 1880 to 1980 using a large database of tide gauge measurements, and data for longer term glacio-isostatic and neotectonic trends. The data were divided into eleven geographical regions, and the results were weighted according to their relative reliability. They estimated a mean eustatic sea-

Chapter 5: Possible impacts of future sea-level changes

level rise over the past 100 years of 10 cm \pm 1 cm (1mm per year). Barnett (1984), Hansen et al (1983), Meier (1984) and Robin (1986) have also examined recorded sea-level changes, and all confirm a rise in global sea-levels over the past 100 years.

Various estimates of future sea-level changes have been made. Hoffman et al (1983, 1986), Robin (1986) and Revelle (1983) have all suggested scenarios for a rise in sea-levels over the next century. Although arguments have been put forward for a fall in sea-level due to climatic changes over the next century (eg Sugden and Hulton 1991), it is important to assess the possible impacts of predictions of sea-level rise.

The estimates of future sea-level rise have been used to model the effects on sea-levels if the conditions resulting in the highest recorded sea-levels at the eleven tide gauge stations in the Zhujiang Delta were repeated. This model ignores the possible enhancement of any storm surge effects due to increases in the volume of water in the ocean basin. The estimates of Hoffman et al (1983 and 1986) have been added to the recorded highest sea-levels at each tide gauge station in the Zhujiang Delta. The low level estimate of Hoffman et al (1986) (see table 5.14) proposes that sea-level would rise by 0.205 metres by AD 2050. In Guangzhou this would result in the sea-level rising to +3.195 m Y.S.D. if the storm surge experienced on 22 July 1974 was repeated. This does not take into account the possible enhancement of the storm surge effect due to a rise in mean sea-level as suggested by Rossiter (1962).

Three sea-level rise scenarios have been assessed using the tidal data from Shanbanzhou, the tide gauge closest to the study area (see figure 5.2). The highest recorded sea-level was 2.68 m Y.S.D. recorded on 28 July 1969. The three lowest sea-level rise

Chapter 5: Possible impacts of future sea-level changes

scenarios proposed by Hoffman et al (1983, 1986) have been used to model the possible rise in extreme sea-levels. These are shown in figure 5.15. As can be seen from the graph, if the storm on 28 July 1969 was to be repeated in AD 2050, the model suggests that sea-level might rise to between 2.89 m Y.S.D. (Hoffman et al 1986, low estimate) and 3.20 m Y.S.D. (Hoffman et al 1983, mid-low estimate). The model suggests that by AD 2100 the extreme sea-level might rise to between 3.24 m Y.S.D. (Hoffman et al 1983, low estimate) and 4.12 m Y.S.D. (Hoffman et al 1983, mid-low estimate).

Figure 5.16 shows the result of combining Hoffman et al 1986 low sea-level rise scenario with the highest recorded sea-levels at six tide gauge stations in the Zhujiang Delta: Guangzhou, Chewan (just south of the study area), Nansha, Yuanqingsha, Hengmen and Shanbanzhou. The results show that if this low estimate is used extreme sea-levels within the Zhujiang delta may rise to between 3.58 m Y.S.D. (at Guangzhou) and 2.97 m Y.S.D. (at Chewan) by AD 2100. Hoffman et al (1986) consider this to be a minimum possible rise, and suggest that sea-levels may increase more rapidly.

If these results are compared with the land altitude and sea-defence altitude data summarised in section 5.6.1 and in figures 5.5 and 5.11, it appears that the risks of flooding will increase dramatically if even the lowest estimate of sea-level rise proposed is fulfilled. The highest sea-defence found within the study area was +2.9 m Y.S.D. in altitude. Extreme sea-levels at Shanbanzhou may reach this altitude by AD 2060, according to Hoffman et al (1986) low estimate.

5.11.2 Changing land altitudes

The risk of future coastal flooding may also be influenced by a change in ground altitudes. Land subsidence will increase the risks of marine inundation of a low-lying coastal area. The Zhujiang Delta appears to be an area of land subsidence caused in part by sediment compaction and possibly by neotectonic movements caused by sediment loading in the delta (see chapter 6).

If subsidence does occur in the delta, this will lower the altitude of both the land and sea defences relative to sea-levels. This factor must be added to any sea-level rise scenario in order to model the future relative altitudes of the sea and land. No detailed data are available for current subsidence levels. However estimates can be made. Huang et al (1982 and 1987) have provided data derived from repeated levelling exercises across the Zhujiang Delta between 1966 and 1973. They suggest that the Zhujiang Delta land altitudes are subsiding at a mean rate of 2mm/year, and a maximum rate of 4mm/year in Shunde county in the middle of the delta.

A rate of subsidence over the next 100 years of 2mm /year has been added to the model of future sea-levels to simulate the effect of land subsidence on the relative altitudes of sea-level and ground levels. An increase in sea-level of 2mm/year has been added to the various scenarios of sea-level change proposed by Hoffman et al (1983 and 1986) (see table 5.16). Figure 5.17 shows the results of this on the altitude of extreme sea-level at Shanbanzhou. By AD 2050 the model suggests that the risk of flooding would be the equivalent of raising sea-level to between +3.01 m Y.S.D. and +4.34 m Y.S.D. It must be emphasised that this is not an estimate of future sea-level, but of the effect of

Chapter 5: Possible impacts of future sea-level changes

adding a rate of increase of 2mm/year to the various scenarios of sea-level rise to simulate the effect of a similar rate of land subsidence. If land subsidence were 3mm/year the equivalent figures for AD 2050 would be +3.07 m Y.S.D. and +3.38 m Y.S.D. and for AD 2100, +3.60 m Y.S.D. and +4.45 m Y.S.D.

This is a very crude model of land subsidence and does not take into account geographical variations within the delta, or uneven temporal variations. Extrapolations of rates of subsidence measured over a short time period (between 1966 and 1973) are very difficult. However this does show that the risks of flooding will increase if these processes operate. From the data presented it appears that by the middle of the next century the sea defences of the Zhujiang Delta may be regularly overwhelmed by marine floodwaters. The calculated sea-level equivalent for six tide gauge stations is shown in figure 5.18.

5.11.3 Other factors

The nature of the land which may be flooded also influences the risks and impacts of flooding. If high capital investment or high levels of population growth occur within a coastal region at risk from flooding, the impacts of any flooding will increase.

Data have been obtained from the 1981 population census of China for Guangdong Province. These data are for county and city areas (see figure 5.4). There are nineteen counties and cities which either completely or partially lie within the Zhujiang Delta area. Ten of these counties and cities are wholly within the delta, and have land altitudes generally below +1 m Y.S.D. (see figure 5.2). The total population of these ten counties and cities in 1983 was 5,697,104 people (see table 5.17). The birth

Chapter 5: Possible impacts of future sea-level changes

and death rates calculated for the period 1981-82 are also shown in table 5.17. (figures published in Population Census Office 1987).

If the birth and death rates quoted are used to extrapolate population change for these ten counties between 1984 and 2100, the result is a huge growth in the population of the Zhujiang Delta. The ten counties and cities listed in table 5.17 would increase their populations to over 14 million by 2050 and 28 million by 2100. The total population of the nineteen counties covering the Zhujiang Delta in 1983 was just below 12 million (11,904,839). If the birth and death rates given in the 1983 census are used, the projected total population for this area would be 30 million by 2050 and almost 64 million by 2100.

If the growth rate of the population over the next century is reduced evenly from its present mean level for the ten counties listed in table 5.17 to a rate of zero by 2100, the estimates of the population of the Zhujiang Delta are less alarming. The mean growth rate of +1.44% in 1981 has been reduced by 116 equal increments between 1984 and 2100. This would lead to a growth in the population of the ten counties to 11.3 million in 2050 and 13.2 million in 2100. The nineteen counties would grow in population to almost 23.7 million in 2050 and 27.5 million in 2100. These calculated growths in the populations of the ten counties and cities wholly within the Zhujiang Delta and the nineteen areas covering the delta are shown in figures 5.19 and 5.20. It appears very unlikely that there will be a rapid reduction in population in the near future. Guangdong Province, and the Zhujiang Delta in particular, has been experiencing high rates of immigration, particularly in the past two to three years (1988 - 1990). This has been in part because of the high levels of investment and better economic prospects within the delta

Chapter 5: Possible impacts of future sea-level changes

area, as a result of the growth of the Hong Kong economy. The weakening of the Chinese economy, particularly in 1989 and 1990, as a result of the government's tighter control on spending, has encouraged large numbers of Chinese to migrate to this relatively prosperous part of China. These processes are likely to continue.

The effect of population growth on the study area can be assessed using a similar technique. The estimate of birth and death rates in Bao'an county in 1981 were 2.62% and 0.54% respectively, giving a net rate of increase of 1.08%. If this rate occurs within the population of the Flood Risk Zone defined in the study area, which had an estimated minimum population of 39,002 in 1983, the population in 2050 would be approximately 155,000, and by 2100 the area would have a population of about 434,000 (see figure 5.21). The mean population densities in the Flood Risk Zone, which has an area of 118 km² would be approximately 1,300 and 3,700 people/km² in 2050 and 2100 respectively. This assumes that people would not move out of the area. If the growth rate is reduced over the 116 year period between 1984 and 2100 to a rate of 0%, the growth in population within the flood risk zone would be to only 105,000 by 2050 and 131,000 by 2100.

Future changes in land use and economic development in the coastal regions are difficult to estimate. Development plans for the Shenzhen SEZ and the town of Xixiang have been produced, and these show potential for major investment in infrastructure, and especially in light industry in low lying coastal areas over the next 10 - 15 years. An airport is being built on land that was previously below +5 m Y.S.D. just south of the study area (close to Xixiang) which will service Shenzhen. Investment within the Zhujiang Delta is high by Chinese standards as a result of the proximity of Hong Kong, and the Special Economic Zones in the Delta. The impacts of flooding in terms of loss of fixed capital

Chapter 5: Possible impacts of future sea-level changes

assets is therefore likely to grow in the near future. This study does not attempt to quantify this.

5.12 CONCLUSIONS:

The analysis discussed in this chapter using a G.I.S. together with data on recorded sea-levels over the past forty years, suggests that the Zhujiang Delta is at serious risk of major marine flooding, and that if mean sea-levels rise in the next 100 years by even published conservative estimates, this risk may increase dramatically. An area of over 6000 km² may be permanently flooded if sea-levels rise by more than one metre, and may experience regular flooding if sea-levels rise by 50 cm. The threat of flooding now due to storm surges is serious as sea defences are generally weak and are rarely built higher than 50 cm above the highest recorded sea-level. In the Shajing area the sea defences are only between 30 and 50 cm above the highest astronomical tide level. A relatively minor storm surge could therefore lead to local flooding. As the population of the Zhujiang Delta and capital investment in the area increase so the impacts of any flooding will become more serious.

Within the study area the impacts of major flooding would be very serious. The area is dependant on lowlying coastal areas for much of its income and employment. The area within the Flood Risk Zone contains a large majority of the intensively used agricultural land in the four districts that make up the study area.

If more data were available a more sophisticated G.I.S. analysis could have been attempted. The model described in figure 5.1 allows for the synthesis of a large number of data sets, and for the modelling of future flooding scenarios. Of particular interest would be a systematic survey of sea defences and of

Chapter 5: Possible impacts of future sea-level changes

recorded sea levels along a series of coastal compartments, together with more detailed altitudinal data for both sea defences and the coastal lowlands. This would allow an assessment to be made of the sections of coastline most susceptible to flooding and therefore a more refined analysis of the impacts of flooding. Flood Risk Zones could be defined with greater sophistication and these areas could be analyzed to determine the impacts of flooding. The data exist in a published format in the P.R. China.

Ideally a model of a larger part of the south China coast can be built, and changes in sea and land altitudes and the social and economic development of the coast can be modelled. This would allow analysis at a variety of scales to be carried out, and related to various geographical regions based on administrative units or other criteria. This analysis in China may have to await a more accommodating political climate. However similar analyses could be attempted for other coastlines. Although much effort would be required for initial data input (data assembly, digitising of base maps), the resulting model would allow planning authorities to assess where threats of marine flooding existed, and decide the necessary action required.

6.0 CONCLUSIONS

6.1 The sedimentary analysis

The sedimentary stratigraphy of three lagoons in the Zhujiang delta and Lamma Island has been examined by using detailed surveying techniques. The sediments are believed to have been deposited during the middle and late Holocene under varying water conditions.

At Shajing Lagoon, organic and inorganic sediment layers have been deposited landward of a sand dune system. The site appears to have been open to the sea initially, but to have then been enclosed, leading to a freshening of the water quality, and deposition of dark organic rich sediments. A breach in the dune system, or a slight rise in sea-level, may have caused a subsequent increase in marine and brackish influence in the lagoon. No chronology is available for the development of this lagoon system, but cartographic evidence suggests that the dunes may have been active during the last century. The sediments may therefore be quite recent. Fossil diatom analysis has revealed a former strong marine and brackish water influence at an altitude of +1.8 metres Y.S.D. approximately 4 kilometres inland from the present coastline. Much of the land between the coast and this site is below +1.0 m Y.S.D.

At Sham Wan at least three environmental changes have been identified by analysing the sediments sampled from this site. A strong marine influence in the Tung O basin appears to have been replaced by freshwater and relatively low energy conditions. More saline water conditions then seem to have prevailed before the basin reached its present condition of landlocked marshy ground. No chronology is available for these changes, and it is not

Chapter 6: Conclusions

altogether clear whether these changes were due to changes in sea-level or the morphology of the coastline. More work is required to identify the detailed stratigraphic changes in the main Sham Wan basin, and to relate these both to changes in the Tung O basin, and the more general coastal changes around Lamma Island.

At Tin Shui Wai clear changes in past water quality and sediment deposition have been identified, and this site may provide strong evidence for a previously lower sea-level as distinct from just coastal morphological changes. At site TSW/A a rapid change from inorganic to highly organic sediments has been identified, and tentatively classified as a sea-level index point. The small rootlets and other organic material suggests an intertidal environment. The highly organic sediments were found at an altitude of -1.80 m P.D., almost three metres below present mean sea-level (+1.15 m P.D.). This suggests a former sea-level well below present levels. This sample has yet to be radiocarbon dated and no fossil diatom remains were found. Sea-levels then appear to have risen, as sediments above this organic layer show increasing marine influence. However it has been difficult to assess the quality of the depositional environment for these sediments as no diatom valves were found. The particle size analysis supports the conclusion of changes in depositional environment.

6.2 The methodology

The techniques of detailed field survey of sedimentary basins, and laboratory analysis of fossil diatoms and particle size distribution have been shown to be applicable to the coasts of southern China, and to reveal the complexity of the lagoonal

Chapter 6: Conclusions

sedimentary histories. All three exercises discussed in chapter 3 showed that the coastal environment has changed significantly in the past. Diatom analysis proved particularly useful for establishing the conditions under which sediment sequences were deposited in the lagoons. No major problems were encountered when trying to identify diatom valves, though unfortunately no diatom valves were found in samples taken from sediments found at Tin Shui Wai. Though pollen analysis was not attempted, it is thought that very similar problems to those highlighted by Ireland (1988) would be encountered if pollen analysis were used to study detailed coastal changes at particular sites.

The field survey techniques have allowed much more detailed stratigraphic analyses of coastal sediments to be made than have previously been done in China. The classification scheme devised by Troels-Smith (1955) was successfully applied to sediments at all sites analyzed. The hand borer proved very useful for analysing the stratigraphy of the sites chosen, though minor problems were encountered when trying to sample coarse sandy sediments. This was not specific to this study however.

Particle size analysis proved useful in providing detailed information on the quality of sediments deposited at different levels. Changes in sediment quality appear to correspond closely with changes in environmental quality suggested by the diatom analysis.

The major problem encountered in the stratigraphic analysis of coastal lowlands was finding suitable sites for fieldwork. There were considerable logistical problems doing fieldwork in China after 1989. Many lowlying coastal areas suitable for stratigraphic analysis are also the sites of major construction works. In the lowland area south of Shajing town, Bao'an County,

fishponds are being built, disturbing the coastal sediments. In Tin Shui Wai, Hong Kong, almost the whole of the lowland area has now been excavated and is being built on. Sites where no construction work is happening are generally very small, such as the Tung O basin on Lamma Island, or the small area of "Shajing Lagoon" landward of the sand dune complex. One area that might be suitable for future work is the Mai Po marsh, at the eastern end of Deep Bay, in the Northern Territories, Hong Kong.

6.3 Past changes in sea-level

The analysis of past sea-level changes along the southern coast of China has been hindered by the poor quality of the sea-level index point database. The deficiencies of the database have been discussed in chapter 4. However the analysis of the existing radiocarbon dated sea-level index points from various studies in southern China has revealed general patterns of sea-level change during the Holocene. Mean sea-level appears to have risen rapidly between 8,000 years B.P. and 5,000 years B.P., possibly reaching 0.0 m Y.S.D. (-0.85 m P.D.) just before 5,000 B.P. Between 4,500 B.P. and 2,000 B.P. relative sea-levels are thought to have fluctuated. Analysis of the existing sea-level index point data has not allowed a very detailed assessment of the movement of mean sea-level during this period. Detailed field surveys of sediment basins and dating of carefully selected sea-level index points are necessary.

There appear to be variations in the sea-level change signal recorded between different parts of the South China Sea coast, notably between the deltaic regions (the Hanjiang and Zhujiang) and other parts of the coast (Fujian Province, western Guangdong Province and Hainan Island). These differences may be due to variations in the vertical movement of different sections of the

Chapter 6: Conclusions

coastline. However before this can be quantified, more accurately dated and surveyed sea-level index points will need to be collected.

Chapter 6: Conclusions

6.4 The impacts of future sea-level changes

This study has demonstrated that the risks of future sea-level rise and coastal flooding in the Zhujiang delta are considerable. If conservative estimates of sea-level rise are realised, then the highest recorded sea-levels in the delta might overtop present sea defences in the eastern part of the delta by 2100 AD. If land subsidence is assumed to continue in the delta, high sea-levels may overtop seawalls in the middle of the next century. If a rather more radical scenario of sea-level rise (Hoffman et al 1983 *mid-low* estimate) is considered, high sea-levels may reach the level of the top of present sea-defences by 2025 AD. The sea-level rise scenarios used are similar to more recent estimates produced by Tegart et al (1990).

The number of people directly affected by future flooding could be considerable. The ten counties within the Zhujiang delta that are almost completely below the +5 m Y.S.D. contour line had a total population of over 5 million people in 1982. If population growth rates of the early 1980s are maintained, these counties would have a total population of almost 30 million people by 2100 AD. Within the Flood Risk Zone in Bao'an County analyzed in this study the number of people at risk from flooding in 1982 is estimated to have been about 39,000, and is now likely to be greater. By 2050 AD this population could be over 100,000. Many more people living close to the Flood Risk Zone are likely to be indirectly affected. As investment in the region increases, the risks of flooding will grow, and the impacts both in human and capital terms will rise.

Within the study area the majority of rice paddy and irrigated agriculture occurs within the ^(see section 5.9.3) FRZ. Much of this activity occurs below the mean high water mark. Villages and parts of the main

Chapter 6: Conclusions

road connecting Guangzhou and Hong Kong could be inundated in the event of a major coastal flood.

Although no detailed information has been collected about the altitudes and quality of sections of the sea-walls in the Zhujiang delta, those that were observed in the study area appear of a poor quality. The sea-walls are made of earth. Almost all the mangrove forest along the coastline of the study area, and across most of the Zhujiang delta has been destroyed due to land reclamation (Zhou 1985). The natural and artificial coastal defences are therefore considered to be of a poor quality. Measured altitudes of sea-defences show that highest recorded sea-levels have risen to within about 0.4 metres of the top of the main sea-wall defending a section of coast south of Shajing town in Bao'an County.

The construction of new fishponds that has occurred during the last 10 years within parts of the Zhujiang delta, including the study area, may help to reduce the impacts of coastal flooding. The large number of new embankments that have been constructed around fish ponds could be used as lines of defence against future floods. However these new embankments may also channel flood waters into low lying areas further from the coast, exacerbating the impacts of flooding in hinterland areas. The likely effects of fishpond development have not been examined.

6.5 Future work

There is a need for detailed surveys of sediment basins along the south coast of China in order to assess the evidence for sea-level changes during the middle Holocene, and in particular the apparent high sea-level stand that may have occurred between 4,500 years B.P. and 3,000 years B.P. The techniques described

Chapter 6: Conclusions

in this study could be used. The rapid development of coastal areas in China and Hong Kong however means that many potential sites for study may be disturbed. Suitable lowlying sites should be surveyed, and sediment samples should be collected after accurate stratigraphic analysis, before these sites are developed. Tin Shui Wai had enormous potential as a site, but it has already been destroyed. These studies should be integrated along the coast of southern China, with a standard methodology being applied so that comparisons of data can be made between sites.

A G.I.S. approach to studying the risks and likely impacts of coastal flooding has been shown to be useful, and could be applied to any type of coastline. If more detailed altitudinal data were available, together with detailed land use maps, a more sophisticated analysis of the risks and impacts could be made. These data exist for coastal areas of China. Of particular interest would be an assessment of the possible impacts on marine floodwaters of changing drainage networks in low lying coastal areas. An analysis of different sections of the coastline would enable priorities for flood defence construction to be developed. Most of the data for such an analysis exist in China. Surveys of the altitudes and quality of sea defences in the Zhujiang delta should be a priority, so that this can be integrated with the existing topographic, land use and demographic data for the region. Information from the 1991 Chinese national census could be used in such a study to give more up-to-date conclusions as to the impacts of future marine flooding.

These two rather different areas of study should complement each other. An assessment of past coastal changes, particularly the highest recorded sea-levels during the Holocene, could be added

Chapter 6: Conclusions

to a developing G.I.S. of the region along the lines of the model suggested at the beginning of chapter 5.

Appendices:

Appendix 1

Stratigraphic descriptions of boreholes from three sites.

Date borings made: April 6 19, 1988

Shajing Lagoon site (see figure 3.3).

Bore hole: SJA1

Depth (cm)	Description
0 - 31	Disturbed sediments SC4
31 - 78	Weathered iron stained sand with silt. Brown, yellow and red. Ga3, Ag1, Lf+ nig. 2, strat. 0, elas. 0, sicc. 3
78 - 106	Slightly mottled dark brown / grey silt with clay. Organic material. As2, Ag1, Sh ⁴ ₁ nig. 3+, strat. 0, elas. 0, sicc. 3
106 - 147	Grey silt clay with pieces of well humified organic material. As2, Ag1, D1 ² ₁ nig. 3, strat. 0, elas. 0, sicc. 3
147 - 153	Dark grey / brown organic detritus with silt and some organic material with rootlets. D1 ³ ₂ , Ag1+, Th ³ ₊ nig. 2, strat. 0, elas. 0, sicc. 2
153 - 163	Grey sand with silt. Ga3, Ag1 nig. 2, strat. 0, elas. 0, sicc. 2
163 - 183	Grey silt with small amounts of sand and organic material. Ag2+, Ga1-, As+, Sh+ nig. 2, strat. 0, elas. 0, sicc. 2
183 - 215	UNSAMPLED Appeared to be coarse sand.
215 - 245	Grey sand and silt. Sticky. Ga2+, Ag2 nig. 2, strat. 0, elas. 0, sicc. 2
245 - 305	UNSAMPLED Appeared to be sand.

Sampler stopped by hard object, possibly a rock at a depth of 305 cm.

Appendices:

Bore hole: SJA2

Depth (cm)	Description
0 - 25	Disturbed sediments (SC4)
25 - 49	Brown, yellow weathered sand with silt. Gs2, Ga1, Ag1 nig. 2, strat. 0, elas. 0, sicc. 2
49 - 57	Brown yellow weathered sand with evidence of iron staining. Ga3, Ag1, Lf+ nig. 2, strat. 0, elas. 0, sicc. 2
57 - 66	Dark brown organically rich silt with sand. Ga1, Ag3, Sh+ nig. 3+, strat. 0, elas. 0, sicc. 2
66 - 84	Grey brown silt with clay and some organic material. Ag3, As1, Sh+ nig. 2, strat. 0, elas. 0, sicc. 2
84 - 97	Light grey sand with silt. Ga2, Ag2 nig. 2, strat. 0, elas. 0, sicc. 2
97 - 128	Sand with some silt. Ga3, Ag1 nig. 2, strat. 0, elas. 0, sicc. 2
128 - 175	UNSAMPLED
175 - 235	Very wet sand and silt, grey in colour. Ga2, Ag2+ nig. 2, strat. 0, elas. 0, sicc. 1
235 - 270	UNSAMPLED
270 - 275	Hard sand with silt. Gg2, Ga1, Ag1 nig. 2, strat. 0, elas. 0, sicc. 2

Appendices:

Bore hole: SJA3

Depth (cm)	Description
0 - 50	Disturbed sediments. SC4
50 - 94	Weathered red, brown and grey silty clay. Some iron staining. Ag2, As2, Lf+ nig. 2, strat. 0, elas. 0, sicc. 2
94 - 118	Silty clay with black humified organic particles. As3, Ag1, Sh+ nig. 2, strat. 0, elas. 0, sicc. 2
118 - 152	As above but very slightly less organic material at base of unit.
152 - 285	UNSAMPLED Some shelly material brought up by sampler.
285 - 430	UNSAMPLED Sand and silt. Dried hard oxidised sand.
430 - 460	Grey sand and silt with shells. Ga3, Ag1, Test moll + nig. 2, strat. 0, elas. 0, sicc. 2
460 - 530	Sandy silt with very small amount of shell material as broken fragments. Ga2, Ag2+, Test moll + nig. 2, strat. 0, elas. 0, sicc. 2
530 - 610	UNSAMPLED. Becoming more sandy.

Sampler stopped by hard object (sand, rock or shell?) at a depth of 610 cm.

Appendices:

Bore hole: SJA4

Depth (cm)	Description
0 - 14	UNSAMPLED
14 - 104	Brown/grey silt with nodules of dried weathered silt. Ag3+, As1 nig. 2, strat. 0, elas. 0, sicc. 2
104 - 107	Brown/grey silt with very small amount of sand. Ag3, As+, Ga+ nig. 2, strat. 0, elas. 0, sicc. 2
107 - 128	Silt, even with no sign of ironstaining or weathering. Fragments of organic material, well humified. Ag3, As+, Sh ⁴⁺ nig. 2, strat. 0, elas. 0, sicc. 2
128 - 160	Sand and silt, brown/grey with numerous shell particles and whole shells. Ga1, Ag2+, Test moll ++ nig. 2, strat. 0, elas. 0, sicc. 2
160 - 170	Brown/grey sandy silt Ga2, Ag2 nig. 2, strat. 0, elas. 0, sicc. 2
170 - 210	UNSAMPLED
210 - 270	Wet sand with many fragments of shells. Ga3, Ag+, Test moll + nig. 2, strat. 0, elas. 0, sicc. 3
270 - 300	Sand with silt (sticky). Numerous shells. Larger shell pieces including example of Ostrea spp. Ga2, Ag1+, Test moll ++ nig. 2, strat. 0, elas. 0, sicc. 3
300 - 333	Silt with sand and numerous shell fragments. Ga1+, Ag2+, Test moll ++ nig. 2, strat. 0, elas. 0, sicc. 3
333 - 370	Sand with silt. Some shell fragments. Ga3, Ag1, Test moll + nig. 2, strat. 0, elas. 0, sicc. 2

Appendices:

370 - 406

Heavily weathered base rock. Iron staining.
Gg4, Lf+
nig. 2, strat. 0, elas. 0, sicc. 2

Appendices:

Bore hole: SJA5

Depth (cm)	Description
0 - 27	UNSAMPLED
27 - 145	Brown grey silt with nodules of dried weathered silt. Ag3+, As1 nig. 2, strat. 0, elas. 0, sicc. 2
145 - 205	Brown silt with clay. Very small amount of organic material. Ag3, As1, Sh+ nig. 2, strat. 0, elas. 0, sicc. 2
205 - 227	Brown silt with fine sand. Ag2, As1, Sh+ nig. 2, strat. 0, elas. 0, sicc. 2
227 - 289	UNSAMPLED (Sands)
289 - 371	Sand with little silt, and large number of shells (Ostrea spp.) Ga3, Test moll 1, Ag+ nig. 2, strat. 0, elas. 0, sicc. 2
371 - 389	UNSAMPLED
389 - 412	Sand with a large number of shell fragments (brackish species and Ostrea) Ga3, Ag+, Test moll ++ nig. 2, strat. 0, elas. 0, sicc. 2
412 - 436	Sandy silt with large number of shells. Ga1+, Ag2, Test moll ++ nig. 2, strat. 0, elas. 0, sicc. 2
436 - 465	Grey silt with small amount of sand and shells. Ga+, Ag 3+, Test moll + nig. 2, strat. 0, elas. 0, sicc. 2
465 - 496	Grey sand with small amount of silt. Ga3, Ag1, Test moll + nig. 2, strat. 0, elas. 0, sicc. 2
496 - 512	Grey silt with large amount of shell material - silvery blue. Test moll 1+, Ag2+, Ga+ nig. 2+, strat. 0, elas.0 , sicc.2

Appendices:

- 512 - 523 Brown sand with some shell material.
Ga3, Ag1-, Test moll +
nig. 2, strat. 0, elas. 0, sicc. 2
- 523 - 581 Brown/yellow (buff) silt with small amount
of shell material, declining towards the
base.
Ag3, Ga1, Test moll +
nig. 2, strat. 0, elas. 0, sicc. 2
- 581 - 589 Yellow/brown grey sand with silt. Iron
staining. Heavily weathered.
Ga2, Ag2, Lf+
nig. 2, strat. 0, elas. 0, sicc. 2

Appendices:

Bore hole: SJA6

Depth (cm)	Description
0 - 59	Disturbed sample. Sc4
59 - 78	Weathered mottled sand and silt. Ga3, Ag1 nig. 2, strat. 0, elas. 0, sicc. 2
78 - 98	Very dark brown silt with some sand particles. Ag2, Ga1, Sh++ nig. 3, strat. 0, elas. 0, sicc. 2
98 - 125	UNSAMPLED
125 - 129	Wet grey/brown sand. Ga3+, Ag+ nig. 2, strat. 0, elas. 0, sicc. 1
129 - 142	Sandy silt with organic material, quite well preserved. Some wood fragments. Ga1+, Ag2+, D1 ²⁺ , Dh ²⁺ nig. 2, strat. 0, elas. 0, sicc. 2
142 - 167	Sandy silt with woody organic material. Ga1-, Ag2+, D1 ²⁺ nig. 2, strat. 0, elas. 0, sicc. 2
167 - 205	UNSAMPLED
205 - 214	Grey sand with well preserved organic material. Ga2, Ag1+, D1 ³⁺⁺ nig. 2, strat. 0, elas. 0, sicc. 2
214 - 226	Grey sand with some poorly preserved organic material. Ga2+, Ag1, Sh+ nig. 2, strat. 0, elas. 0, sicc. 2
226 - 260	Grey sand with a little silt. Very wet. Ga3+, Ag+ nig. 2, strat. 0, elas. 0, sicc. 1
260 - 286	UNSAMPLED (Sediment appeared to be too waterlogged).

Appendices:

- 286 - 312 Wet brown/buff coloured sand
 Ga³⁺, Ag⁺
 nig. 2, strat. 0, elas. 0, sicc. 1
- 312 - 327 Wet dark grey sand; small amounts of very
 poorly preserved organic material.
 Ga³⁺, Ag⁺, Sh¹⁺
 nig. 3, strat. 0, elas. 0, sicc. 1

Sampling stopped at a depth of 327 cm.

Appendices:

Bore hole: SJA7

Depth (cm)	Description
0 - 60	Disturbed sediments Sc4
60 - 110	Brown mottled sand; heavily weathered. Ga3+, Ag+ nig. 2, strat. 0, elas. 0, sicc. 3
110 - 163	Grey silt with organic material. Ga+, Ag3, D1 ²⁺⁺ nig. 2, strat. 0, elas. 0, sicc. 2
163 - 178	Grey sand with some organic material. Ga2+, Ag1, Sh+ nig. 2, strat. 0, elas. 0, sicc. 1
178 - 202	Grey silt with sand (sometimes sand in lenses or "pockets"). Ga1, Ag2+, Sh+ nig. 2, strat. 0, elas. 0, sicc. 2
202 - 227	Sand with a little silt. Grey in colour. Ga3+, Ag1 nig. 2, strat. 0, elas. 0, sicc. 2
227 - 289	Grey sand with some silt. Very wet. Ga3+, Ag1 nig. 2, strat. 0, elas. 0, sicc. 1

Sampling stopped at a depth of 289 cm.

Appendices:

Bore hole: SJA8

Depth (cm)	Description
0 - 27	UNSAMPLED
27 - 64	Disturbed sediment (Weathered sand). Ga ³⁺ , Ag ⁺ nig. 2, strat. 0, elas. 0, sicc. 2
64 - 78	Brown sand with some silt. Ga ³ , Ag ¹ nig. 2, strat. 0, elas. 0, sicc. 2
78 - 96	Dark brown silt with sand particles. Some organic material. Some Ga ⁺ , Ag ² , Sh ¹⁺ nig. 3, strat. 0, elas. 0, sicc. 2
96 - 99	Organic sand layer. Ga ³ , Ag ¹ , Sh ⁺ nig. 3, strat. 0, elas. 0, sicc. 2
99 - 119	Detrital silt with a little sand. Grey buff colour. Ag ³ , D ¹⁺ , Ga ⁺ nig. 2, strat. 0, elas. 0, sicc. 2
119 - 219	Detrital woody material set within a grey silt. Ag ³ , Ga ⁺ , D ^{1²+} nig. 2, strat. 0, elas. 0, sicc. 2

Appendices:

Bore hole: SJA8a

Depth (cm)	Description
0 - 150	UNSAMPLED
150 - 170	Grey sand with silt, laminated, with some organic material. Ga2, Ag2, Sh+ nig. 2, strat. 0, elas. 0, sicc. 2
170 - 189	Large pieces of wood mixed with coarse sand, sand and silt. Gs2, Ga+, Ag+, D1 ³ nig. 2, strat. 0, elas. 0, sicc. 2
189 - 196	Grey silt and sand. Ga2, Ag2 nig. 2, strat. 0, elas. 0, sicc. 2
196 - 212	Grey silt and clay with well preserved branches and twigs. Ga1, Ag2, D1 ² nig. 2, strat. 0, elas. 0, sicc. 2
212 - 260	Grey sand with silt. Small amounts of well preserved twigs and branches. Ga2, Ag1+, D1 ²⁺ nig. 2, strat. 0, elas. 0, sicc. 2
260 - 276	Grey sand with some silt and occasional organic remains, usually woody. Ga3+, Ag+, Sh+ (possibly D1). nig. 2, strat. 0, elas. 0, sicc. 1
276 - 282	Light grey sand. Ga3+, Ag+ nig. 2, strat. 0, elas. 0, sicc. 2
282 - 287	Dark grey silt with organic reed like and woody material. Reeds have some rootlets. Possibly <i>phragmites</i> . Ag2, T11 (<i>phrag.</i> ?), D11 nig. 3, strat. 0, elas. 0, sicc. 2
287 - 295	Grey/blue sand with some silt. Very wet. Gs2, Ga1, Ag1 nig. 2, strat. 0, elas. 0, sicc. 1

Sampling stopped at a depth of 295 cm.

Appendices:

Bore hole: SJA9

Depth (cm)	Description
0 - 25	Disturbed sediments. Sc4
25 - 150	Weathered, mottled white and brown sand. Heavy iron staining. Ga ³⁺ , Ag ¹ , Lf ⁺ nig. 2, strat. 0, elas. 0, sicc. 2
150 - 160	Heavy weathered brown and red sand. Weathered bedrock. Gs4 nig. 3, strat. 0, elas. 0, sicc. 2

Sampling stopped at a depth of 160 cm.

Appendices:

Bore hole: SJA10

Depth (cm)	Description
0 - 25	Disturbed samples. Sc4
25 - 61	Yellow sand. Ga3+, Ag+ nig. 2, strat. 0, elas. 0, sicc. 2
61 - 82	Grey/white sand. Some yellow iron staining. Ga3+, Ag+, Lf+ nig. 1, strat. 0, elas. 0, sicc. 2
82 - 103	Yellow silt, with some iron staining. Ag3, As+, Ga1-, Lf+ nig. 1, strat. 0, elas. 0, sicc. 2
103 - 118	Yellow brown sand and silt. Ga2, Ag2 nig. 2, strat. 0, elas. 0, sicc. 2

Sampling stopped at a depth of 118 cm.

Appendices:

Bore hole: SJA11

Depth (cm)

0 - 13	Disturbed sediments Sc4
13 - 34	Brown sand with iron staining. Ga3, Ag1, Lf+ nig. 2, strat. 0, elas. 0, sicc. 3
34 - 48	Brown sand with little evidence of iron staining. Ga3, Ag1, Lf+ nig. 2, strat. 0, elas. 0, sicc. 3
48 - 64	Brown and grey sand and silt. Ga2, Ag2 nig. 2, strat. 0, elas. 0, sicc. 3
64 - 78	Dark brown silt with sand. Ag3, Ga1-, As+ nig. 3, strat. 0, elas. 0, sicc. 3
78 - 89	Very dark brown organic silt with sand particles. Ga+, Ag2+, As++, Sh++, nig. 3, strat. 0, elas. 0, sicc. 3
89 - 132	Dark brown organic silt, slightly less dark than the layer above. Ga+, Ag2+, As+, Sh++, nig. 3, strat. 0, elas. 0, sicc. 3
132 - 142	White grey silt with sand. Ga+, Ag3, As+, Sh+ nig. 1, strat. 0, elas. 0, sicc. 2
142 - 153	Grey silt with sand. Ga+, Ag3, As+, Sh+ nig. 2, strat. 0, elas. 0, sicc. 2
153 - 157	White silt with sand. Ga+, Ag3, As+, Sh+ nig. 1, strat. 0, elas. 0, sicc. 2
157 - 160	Grey silt with sand. Ga+, Ag3, As+, Sh+ nig. 2, strat. 0, elas. 0, sicc. 2

Appendices:

- 160 - 193 White silt and sand with considerable mottling and staining. Some organic material present.
Ga⁺, Ag³, As⁺, Sh⁺⁺
nig. 1, strat. 0, elas. 0, sicc. 2
- 193 - 210 White silt and sand. No organic matter.
Ga¹⁺, Ag²⁺
nig. 1, strat. 0, elas. 0, sicc. 2
- 210 - 298 Mottled grey/white and buff coloured silt with well preserved humified twigs.
Ag³⁺, Ga⁺, D¹²⁺⁺
nig. 2, strat. 0, elas. 0, sicc. 2
- 298 - 310 Yellow brown silt and clay.
Ag²⁺, As¹⁺
nig. 2, strat. 0, elas. 0, sicc. 2
- 310 - 327 Mottled yellow brown silt and clay with small pieces of detrital organic material.
Ag², As¹⁺, D¹⁺⁺
nig. 2, strat. 0, elas. 0, sicc. 2
- 327 - 339 Yellow brown silt and clay.
Ag²⁺, As¹⁺
nig. 2, strat. 0, elas. 0, sicc. 2
- 339 - 357 Grey clay and silt.
Ag², As²
nig. 2, strat. 0, elas. 0, sicc. 2
- 357 - 387 Yellow weathered silt with sand nodules.
Ag², Ga²
nig. 2, strat. 0, elas. 0, sicc. 2

Sampling stopped at a depth of 387 cm.

Appendices:

Bore hole: SJA12

Depth (cm)	Description
0 - 30	Disturbed sample. Sc4
30 - 93	Yellow/brown sand and silt. Ga3, Ag1 nig. 2, strat. 0, elas. 0, sicc. 2
93 - 109	Brown silt and sand. Ag3, Ga++, Sh+ nig. 3, strat. 0, elas. 0, sicc. 2
109 - 121	Black organic silt with some sand particles. It appears that sand may have been wind blown into deposit. Ag3, Ga+, Sh++ nig. 4, strat. 0, elas. 0, sicc. 2
121 - 127	UNSAMPLED
127 - 149	Wet grey silt with well preserved organic detritus material. Ag2, As1, Dl ²⁺⁺ nig. 2, strat. 0, elas. 0, sicc. 2
149 - 156	Very wet grey silty sand. Ga2, Ag2 nig. 2, strat. 0, elas. 0, sicc. 1
156 - 215	Grey silt and sand with organic material. A coarse sand lens found at a depth of 180 cm made up of quartz particles. Very wet. Ag2, Ga1, Dl ²⁺ , As+ (Gg at depth 180 cm.) nig. 2, strat. 0, elas. 0, sicc. 1
215 - 227	UNSAMPLED
227 - 243	Grey silt, very wet. Ga2, Ag2 nig. 2+, strat. 0, elas. 0, sicc. 1
243 - 273	Dark grey slightly organic sand. Ga3, Ag+, Sh+ nig. 3, strat. 0, elas. 0, sicc. 1
273 - 290	Sand (white granules) in a grey matrix of silt. Ga3+, Ag+ nig. 1, strat. 0, elas. 0, sicc. 1

Appendices:

290 - 310 Yellow/grey mottled sand and silt.
Weathered appearance.
Ag2, Ga2
nig. 2, strat. 0, elas. 0, sicc. 2

Sampling stopped at a depth of 310 cm.

Appendices:

Bore hole: SJA13

Depth (cm)	Description
0 - 20	UNSAMPLED
20 - 39	Disturbed sediment. Sc4
39 - 58	Yellow sand/silt. Ga3, Ag1 nig. 1+, strat. 0, elas. 0, sicc. 2
58 - 73	Heavy iron staining. Ga3, Ag, Lf+ nig. 2, strat. 0, elas. 0, sicc. 2
73 - 89	Dark grey silt with sand. Ag3, Ga1 nig. 2+, strat. 0, elas. 0, sicc. 2
89 - 102	Dark brown silt with sand particles. Ag3, Ga+, Sh++ nig. 3, strat. 0, elas. 0, sicc. 2
102 - 129	UNSAMPLED
129 - 229	Grey/brown sand with silt. Gravel (Gg min) occasionally (150 - 170 cm). Ga3, Ag1, Gg+ nig. 2+, strat. 0, elas. 0, sicc. 2

Sampling stopped at a depth of 229 cm.

Appendices:

Bore hole: SJA14

Depth (cm)

0 - 18	Disturbed sediment. Sc4
18 - 47	Iron staining. Sand. Ga3+, Ag+, Lf+ nig. 1+, strat. 0, elas. 0, sicc. 2
47 - 57	Iron staining. Sand/silt. Ga2+, Ag1+, Lf+ nig. 1+, strat. 0, elas. 0, sicc. 2
57 - 72	Blue grey. Getting siltier towards base. Ga2+, Ag1+ nig. 2+, strat. 0, elas. 0, sicc. 2
72 - 82	Dark grey silt with sand. Ag2+, Ga1 nig. 3, strat. 0, elas. 0, sicc. 2
82 - 94	Dark brown organic silt with some small rootlets, well preserved. Ag2+, Sh1, Tl ²⁺⁺ nig. 3+, strat. 0, elas. 0, sicc. 2
94 - 106	Grey organic silt/clay. Ag2+, As1+, Th ²⁺ , Sh+ nig. 2, strat. 0, elas. 0, sicc. 2
106 - 156	Grey silty clay with abundant humified woody detritus and rootlets. Dl ²¹ , Tl ²¹ , Ag1+, As++ nig. 2, strat. 0, elas. 0, sicc. 2
156 - 160	Sand layer, possibly stratified. Ga3+, Ag+ nig. 2, strat. 0, elas. 0, sicc. 2
160 - 163	Grey silt with rootlets. Ag3, Th1 nig. 2, strat. 0, elas. 0, sicc. 2
163 - 166	Sand with silt Ga3, Ag1 nig. 2, strat. 0, elas. 0, sicc. 2
166 - 170	Grey sand with silt. Twig. Ga2+, Dl ²¹ , Ag1 nig. 2, strat. 0, elas. 0, sicc. 2

Appendices:

170 - 173 Grey sand with silt.
 Ga3, Ag1
 nig. 2, strat. 0, elas. 0, sicc. 2

173 - 180 Silt with sand.
 Ag3, Ga1
 nig. 2, strat. 0, elas. 0, sicc. 2

180 - 190 UNSAMPLED

190 - 204 Grey silt with sand and some well preserved
 wood fragments.
 Ag2, D1²1, Ga1
 nig. 2, strat. 0, elas. 0, sicc. 2

204 - 224 Brown/grey sand.
 Ga3+, Ag+
 nig. 3, strat. 0, elas. 0, sicc. 2

224 - 228 Pale grey/yellow sand. Wet.
 Ga3+, Ag+
 nig. 1, strat. 0, elas. 0, sicc. 2

228 - 230 Yellow sand.
 Gs2, Ga2
 nig. 1, strat. 0, elas. 0, sicc. 2

230 - 272 Mottled sand with silt. Strong evidence of
 weathering below a depth of 250 cm.
 Ga3, Ag1
 nig. 2, strat. 0, elas. 0, sicc. 2

Sampling stopped at a depth of 272 cm.

Appendices:

Bore hole: SJA17

Depth (cm)	Description
0 - 25	Disturbed sediment. Sc4
25 - 57	Yellow and buff coloured sand. Ga3+, Ag+ nig. 2, strat. 0, elas. 0, sicc. 2
57 - 70	Buff sand with iron staining. Ga3+, Ag+, Lf+ nig. 3, strat. 0, elas. 0, sicc. 2
70 - 79	Buff sand with iron staining and silt. Ga2+, Ag1+, Lf+ nig. 2, strat. 0, elas. 0, sicc. 2
79 - 91	Brown silt with sand. Ag3, Ga1 nig. 2, strat. 0, elas. 0, sicc. 2
91 - 100	Yellow and red iron stained silt. Ag3, Ga1, Lf+ nig. 2, strat. 0, elas. 0, sicc. 2
100 - 124	Dark brown silt with some sand particles. Ag2+, Sh1, Ga+ nig. 3, strat. 0, elas. 0, sicc. 2
124 - 157	Grey silt with woody detritus. Ag2+, Dl ² 1, As1 nig. 2, strat. 0, elas. 0, sicc. 2
157 - 162	Well preserved woody twigs and rootlets with reeds (possibly <i>phragmites</i>). Dl ² 1+, Th ² 1 (<i>phrag?</i>), Ag1+, As+ nig. 2, strat. 0, elas. 0, sicc. 2
162 - 228	Weathered silt and sand. Grey, red and yellow, turning white towards the base of the unit. Weathered former surface material, possibly heavily weathered bedrock. Ag1, Ga2, Gg min+, Gg maj+ nig. 2, strat. 0, elas. 0, sicc. 2

Sampling stopped at a depth of 228 cm.

Appendices:

Bore hole: SJA18

Depth (cm)	Description
0 - 23	Disturbed sediments Sc4
23 - 27	Iron staining of coarse and medium sand. Pottery shard found. Ga1, Gs2, Ag+, Gg min+, Lf+ nig. 2, strat. 0, elas. 0, sicc. 2
27 - 40	Iron staining of coarse and medium sand, declining towards base. Ga1+, Gs2, Gg min+, Lf+
40 - 53	Organically stained sand. Ga1+, Gs2, Sh+ nig. 3, strat. 0, elas. 0, sicc. 2
53 - 65	Slightly iron stained silt and sand with gravel. Gs1, Ga1, Ag+, As1, Gg min/maj+, Lf+ nig. 2, strat. 0, elas. 0, sicc. 2
65 - 73	Heavy iron staining of silt and sand. As1, Ag+, Ga1+, Gs1, Gg min/maj+, Lf+ nig. 2, strat. 0, elas. 0, sicc. 2
73 - 80	White and grey coarse sand. Gs2, Ga+, Ag1+, As+ nig. 2, strat. 0, elas. 0, sicc. 2
80 - 110	Iron stained and white/grey and yellow mottled silt and fine sand. Distinct banding and changes in coarseness of material. Gg maj+, Ga+, Ag2, As1+, Lf+ nig. 2, strat. 0, elas. 1, sicc. 2
110 - 129	Yellow sand with evidence of iron staining. Ag2, Ga1, Gs1, Lf+ nig. 2, strat. 0, elas. 0, sicc. 2
129 - 178	White coarse sand and gravel. Iron staining and mottling. Variations in colour and iron staining throughout sediment layer. Gs2, Ag1+, Gg min/maj+, Lf+ nig. 1, strat. 0, elas. 0, sicc. 2

Sampling stopped at a depth of 178 cm.

Appendices:

Bore hole: SJA19

Depth (cm)	Description
0 - 33	Disturbed sediments Sc4
33 - 46	Buff coloured coarse and medium sand. Very hard sediment layer. Iron staining, reducing towards base of sediment layer. Gs3, Ga1, Ag+, Lf+ nig. 3, strat. 0, elas. 0, sicc. 2
46 - 50	UNSAMPLED
50 - 62	Slight iron staining, lessening near base of sediment unit. Brown colour. Ga3, Ga+, Ag++, Lf+ nig. 3, strat. 0, elas. 0, sicc. 2
62 - 75	Organic rich, brown sand and silt, increasing silt near base. Gs1+, Ga1+, Ag1, Sh+ nig. 3, strat. 0, elas. 0, sicc. 2
75 - 80	Brown silt and clay and slight iron staining. Ag2, As1, Ga+, Lf+ nig. 3, strat. 0, elas. 0, sicc. 2
80 - 108	Dark grey (mushroom) organic rich silt and clay with sand particles. Ga+, Ag2, As1, Sh+, Dl ⁴⁺ nig. 3, strat. 0, elas. 0, sicc. 2
108 - 135	Grey clay with silt. Detritus fragments with rootlets quite well preserved. Ag1, As2, Dh ²⁺ , Dl ²⁺ , Th ²⁺ nig. 2, strat. 0, elas. 0, sicc. 2
135 - 224	Battleship grey silt with detritus. Woody large pieces and fragments. Rootlets well preserved. Ag2, As1, Th ²⁺ , Dl ²⁺ nig. 2, strat. 0, elas. 0, sicc. 2
224 - 234	Grey silt with some small rootlets. Ag2, As1, Ga+, Th ²⁺ nig. 2, strat. 0, elas. 0, sicc. 2
234 - 241	Grey coarse and medium sand. Gs1, Ga2, Ag1 nig. 2, strat. 0, elas. 0, sicc. 2

Appendices:

241 - 249

Grey silt.
Ag₂⁺, As₁, Ga⁺
nig. 2, strat. 0, elas. 0, sicc. 2

249 - 280

Weathered white and yellow mottled coarse
sand and silt.
Gs₁, Ga₁, Ag₁⁺, As⁺
nig. 2, strat. 0, elas. 0, sicc. 2

Appendices:

Bore hole: SJA20

Depth (cm)	Description
0 - 32	Disturbed sediments. Sc4
32 - 48	Yellow medium and coarse sand. Ga2, Gs2, Ag+ nig. 2, strat. 0, elas. 0, sicc. 2
48 - 57	Coarse organic sand with iron staining. Gs2, Ga1, Ag+, Sh+, Lf+ nig. 2, strat. 0, elas. 0, sicc. 2
57 - 68	Coarse sand and silt with organic material. Occasional fine gravel. Gs2, Ga+, Ag+, Sh+, Gg min+ nig. 2, strat. 0, elas. 0, sicc. 2
68 - 87	Dark mushroom grey organic clayey silt with sand particles. Varying amounts of sand. Ag2, As1, Ga+, Sh+, D1 ²⁺ nig. 3, strat. 0, elas. 0, sicc. 2
87 - 100	Light grey silt and clay with sand particles. Slight iron staining. Ga1, Ag2, As1, Lf+ nig. 1, strat. 0, elas. 0, sicc. 2
100 - 106	Silt with sand. Organic material. Ga1, Ag2, As+, Sh+ nig. 2, strat. 0, elas. 0, sicc. 2
106 - 115	UNSAMPLED
115 - 121	Coarse sand and silt. Very occasional rootlets. Light grey colour. Gs1, Ga1, Ag1, Gg min+, Th ²⁺ nig. 1, strat. 0, elas. 0, sicc. 2
121 - 128	UNSAMPLED
128 - 133	Grey silt and sand with detritus. Ag2, Ga1, As+, D1 ²⁺ nig. 2, strat. 0, elas. 0, sicc. 2
133 - 176	Grey silt clay with large amounts of woody detritus and rootlets. As1, Ag1, Ga+, D1 ²⁺ , T1 ²⁺ nig. 2, strat. 0, elas. 0, sicc. 2

Appendices:

- 176 - 184 Grey sand and silt with organic material.
 Ga1+, Ag1, As1, Sh+
 nig. 2, strat. 0, elas. 0, sicc. 2
- 184 - 191 Grey silt with detritus.
 Ga1, Ag2, As+, D1²⁺
 nig. 2, strat. 0, elas. 0, sicc. 2

Appendices:

Bore hole: SJA21

Depth (cm)	Description
0 - 22	Disturbed sediments Sc4
22 - 29	Heavily iron stained coarse sand. Gs2+, Ga1, Ag+, Lf+ nig. 2, strat. 0, elas. 0, sicc. 2
29 - 37	Yellow coarse sand. Gs2+, Ga1, Ag+ nig. 2, strat. 0, elas. 0, sicc. 2
37 - 52	Brown iron stained coarse sand. Gs2, Ga1, Ag1, Lf+ nig. 2, strat. 0, elas. 0, sicc. 2
52 - 61	Iron stained coarse sand and silt. Decreasing iron staining towards base. Gs1+, Ga1+, Ag1, Lf+ nig. 2, strat. 0, elas. 0, sicc. 2
61 - 75	Dark grey organic silt and sand. Ga2, Ag2, Sh+ nig. 2, strat. 0, elas. 0, sicc. 2
75 - 80	Light grey, yellow and red mottled coarse sand and silt. Some organic material. Ga2+, Ag1, Sh+ nig. 2, strat. 0, elas. 0, sicc. 2
80 - 93	UNSAMPLED
93 - 95	Yellow and red sand and silt. Ga2+, Ag1, Gs+, As+ nig. 2, strat. 0, elas. 0, sicc. 2
95 - 125	White and grey/blue coarse sand and silt. Gs2, Ga1, Ag1 nig. 1, strat. 0, elas. 0, sicc. 2
125 - 145	White grey and blue silt and sand. Gs1, Ga1, Ag2 nig. 1, strat. 0, elas. 0, sicc. 2
145 - 172	White and blue/grey sand and silt. Gs1, Ga2, Ag1 nig. 1, strat. 0, elas. 0, sicc. 2

Appendices:

Bore hole: SJA22

Depth (cm)	Description
0 - 21	Disturbed sediments. Sc4
21 - 55	Iron stained yellow and red coarse sand. Gs2, Ga1, Ag1, Lf+ nig. 2, strat. 0, elas. 0, sicc. 2
55 - 75	Dark buff coloured silty coarse sand with slight organic material. Gs1+, Ga+, Ag1, As+ nig. 2, strat. 0, elas. 0, sicc. 2
75 - 88	Dark mushroom and red organic silt with sand. Ga1+, Ag2, As+, Sh+ nig. 2, strat. 0, elas. 0, sicc. 2
88 - 120	Mottled red, yellow, blue/grey coarse sand. Gs2+, Ga1, Ag1 nig. 2, strat. 0, elas. 0, sicc. 2
120 - 152	White, yellow and blue/grey mottled coarse sand and silt. Gs2, Ga1, Ag1 nig. 1, strat. 0, elas. 0, sicc. 2

Sampling stopped at a depth of 152 cm.

Appendices:

Bore hole: SJA23

Depth (cm)	Description
0 - 32	Disturbed sediment. Sc4
32 - 71	Iron stained coarse sand. Yellowing of sediments towards base. Gs2+, Ga1, Ag+, Lf+ nig. 2, strat. 0, elas. 0, sicc. 2
71 - 78	Coarse and medium sand and silt. A gravel particle found. Gs1+, Ga1+, Ag1 nig. 2, strat. 0, elas. 0, sicc. 2
78 - 89	Dark grey organic silt and sand. Ga1, Ag2, As+, Sh+ nig. 3, strat. 0, elas. 0, sicc. 2
89 - 121	White, yellow and grey mottled coarse sand and silt. Gs2, Ga1, Ag1 nig. 1, strat. 0, elas. 0, sicc. 2
121 - 147	Yellow grey mottled silt and sand. Ga1, Ag2, As1 nig. 1, strat. 0, elas. 0, sicc. 2
147 - 182	Yellow and grey mottled coarse sand, gravel and silt. Iron stained nodules. Organic material - woody particles. Gg maj/min+, Gs2, Ga1, Ag+, D1 ²⁺ , Lf+ nig. 2, strat. 0, elas. 0, sicc. 2

Sampling stopped at a depth of 182 cm.

Appendices:

SJB1

Depth cm.	Description
0 - 88	Sc4
88 - 130	Dark grey silt with detrital woody matter, well humified. Small amount of sand. Ag3, Ga+, D1 ³⁺⁺ nig. 2+, strat.0, elas.0, sicc.2
130 - 167	Dark grey silt with clay and detrital material (woody organic) well humified. Ag2, As1+, D1 ³⁺ nig. 3, strat.0, elas.0, sicc.2
167 - 179	Dark sandy layer with some woody well humidified detrital material. Ga3, Ag1, D1+ nig. 3, strat.0, elas.0, sicc.2
179 - 195	UNSAMPLED

Appendices:

SJB2

Depth cm.	Description
0 - 39	Sc4
39 - 88	Ag3, Ga+, Sh+ nig. 2+, strat. 0, elas. 0, sicc. 2.
88 - 95	UNSAMPLED
95 - 101	Ag3, Ga+, Sh+ nig. 2+, strat. 0, elas. 0, sicc. 2
101 - 110	UNSAMPLED
110 - 118	Ag3, Ga+, Sh+ nig. 2+, strat.0, elas.0, sicc.2
118 - 151	Sand with some silt. Ga3, Ag1 nig. 2+, strat. 0, elas. 0, sicc. 2
151 - 192	Silt with some sand. Ag2++, Ga1, Sh+ nig. 2+, strat.0, elas.0, sicc.2
192 - 210	Silt with greater amount of sand than above. Ag2+, Ga1++ nig. 2+, strat. 0, elas. 0, sicc. 2
210 - 240	Sand with silt. Ga2+, Ag1 nig. 2+, strat. 0, elas. 0, sicc. 2
240 - 264	Silt with sand, some organic material, sand lenses. Ga1, Ag3, Sh+ nig. 2+, strat. 0, elas. 0, sicc. 2
264 - 288	Sand and silt, dark grey. Ga2, Ag2 nig. 2+, strat. 0, elas. 0, sicc. 2
288 - 310	Silt with some sand. Ag3+, Ga+ nig. 2+, strat. 0, elas. 0, sicc. 2
310 - 351	Dark grey silt with small amount very humified detrital branches and twigs. Ag3+, Ga+, D1 ⁴⁺ nig. 2+, strat. 0, elas. 0, sicc. 2

Appendices:

- 351 - 373 Grey sand with detrital material, well
 humified.
 Ga2, Ag1, D11
 nig. 2, strat.0, elas.0, sicc.2
- 373 - 410 Yellow brown silt with little sand.
 Cylindrical manufactured artefact found at
 397 cm.
 Ag3, Ga1
 nig. 2, strat. 0, elas. 0, sicc. 2

Appendices:

Tung O basin, Sham Wan, Lamma Island, Hong Kong
(see figure 3.9)

SW1

Depth cm.	Description
0 - 19	UNSAMPLED
19 - 30	Blue grey medium coarse sand with silt. Ga3, Ag1

Appendices:

SW2

Depth cm.	Description
0 - 29	Disturbed sediment. Sc4
29 - 32	Grey silt with some organic material. Ag2, As1, Ga+, Sh+ nig. 2+, strat. 0, elas. 0, sicc. 2
32 - 36	Light grey sand with well preserved rootlets. Gs2, Ga1+, Th1 ¹ nig. 2, strat. 0, elas. 0, sicc. 2
36 - 56	Dark grey sand with some silt and organic material. Ga2+, Ag1, Sh+ nig. 2, strat. 0, elas. 0, sicc. 2
56 - 70	Light grey sand and silt with some rootlets. Gs+, Ga2+, Ag1, Th ²
70 - 80	Dark grey organic silt/clay with some well preserved rootlets. Ag2+, As1+, Th ² , Sh+ nig. 3, strat. 1, elas. 0, sicc. 2
80 - 121	Very light silt and clay with some organic fragments. Ag3, As1, Sh+ nig. 1, strat. 0, elas. 0, sicc. 2
121 - 124	Very light silt and clay with sand. Ga1+, Ag1, As1, Th ² + nig. 1, strat. 0, elas. 0, sicc. 2
124 - 146	Grey silt and clay with well preserved rootlets and stems of herbaceous plants. Sediments get darker nearer base of sediment layer. Ag2, As1, Th ² +, Sh+ nig. 1, strat. 0, elas. 0, sicc. 2
146 - 170	Dark silt and clay with considerable organic material getting darker near base. Ag1, As2, Th ² 1, Sh+ nig. 3, strat. 0, elas. 0, sicc. 2

Appendices:

- 170 - 183 Very dark silt and sand with well preserved
 rootlets and stems of reed like plants
 (possibly *phragmites*).
 Ga1+, Ag1+, Th¹-, Dh¹-
 nig. 3+, strat. 0, elas. 0, sicc. 2+
- 183 - 195 Very dark organic rich sand and silt.
 Ga2, Ag1, Th¹
 nig. 3+, strat. 0, elas. 0, sicc. 2
- 195 - 238 Brown sand and silt with a little organic
 material.
 Ga3, Ag1, Sh+
 nig. 3, strat. 0, elas. 0, sicc. 1
- 238 - 249 Dark organic rich silt.
 Ag2+, As1, Sh+
 nig. 3, strat. 0, elas. 0, sicc. 2
- 249 - 269 UNSAMPLED
- 269 - 299 Dark organic rich silt.
 Ag2+, As1, Sh+
 nig. 3, strat. 0, elas. 0, sicc. 2
- 299 - 330 UNSAMPLED
- 330 - 430 Highly organic silt with organic matter
 throughout. Large well preserved twig
 fragment found at a depth of 383 cm.
 Ag2, As1, Dl¹
 nig. 3, strat. 0, elas. 0, sicc. 2
- 430 - 470 UNSAMPLED
- 470 - 500 Wet grey sand and silt.
 Gs2, Ga1, Ag1
 nig. 2, strat. 0, elas. 0, sicc. 1-

Sampling stopped at a depth of 500 cm.

Appendices:

SW3

Depth cm.	Description
0 - 41	Sc4
41 - 61	Dark grey sand/silt. Organic matter. Ga3, Ag1 nig. 3, strat. 0, elas. 0, sicc. 3
61 - 76	Grey sand. Ga3, Ag1 nig. 2, strat. 0, elas. 0, sicc. 3
76 - 90	Grey sand/silt. Ga2+, Ag2 nig. 2, strat. 0, elas. 0, sicc. 3
90 - 102	Grey silt with some sand. Ga1, Ag3 nig. 2, strat. 0, elas. 0, sicc. 3
102 - 117	Dark grey brown organic silt. Ag2, As1, Ga1 nig. 2, strat. 0, elas.0 , sicc.0
117 - 146	Very light clay/silt. Getting darker nearer base. As3, Ag1, Sh+ nig. +, strat. 0, elas. 0, sicc. 2
146 - 174	Brown clay/silt with some well preserved herbaceous rootlet. As2, Ag2, Th ¹⁺ /Sh+ nig. 2, strat. 0, elas.0 , sicc. +
174 - 191	Dark organic silt/clay, well preserved rootlets. Ag2, As1, Th ¹ , Sh+ nig. 3, strat. 0, elas. 0, sicc. 2+
191 - 211	Very dark silt with well preserved pieces of wood and rootlets. Th ¹ , Dl ¹⁺ , Sh1, Ag2 nig. 3, strat. 0, elas. 0, sicc. 2+
211 - 220	UNSAMPLED

Appendices:

- 220 - 263 Dark brown silt with sand in matrix. Organic fragments, well preserved.
Ag₂, Ga₁, Dl¹
nig. 3, strat. 1, elas. 0, sicc. 2+
- 263 - 283 Silt, dark brown, humified organic material.
Ag₃, Th²⁺, Dl²⁺
nig. 2+, strat. 2, elas. 0, sicc. 2
- 283 - 311 Silt, organic particles, well preserved but humified. Gravel particle at 290 cms.
Ag₃, Dl²₁, Th²⁺, (Gg)
nig. 2+, strat. 1, elas. 0, sicc. 2+
- 311 - 400 Silt with remains of woody plants and leaves. Small light sand particles within matrix. Large piece of wood at 380 cms.
Ag₃, Dl²₁, Dh²⁺, Ga⁺
nig. 3, strat. 2, elas. 0, sicc. 2
- 400 - 555 UNSAMPLED (Sand). Stopped by rock.

Appendices:

SW4

Depth cm.	Description
0 - 41	Sc4
41 - 62	Blue grey silty sand. Ga3, Ag1, Th1 (modern?) nig. 2+, strat. 0, elas. 0, sicc. +
62 - 82	Grey silty sand. Little iron staining. Ga2+, Ag2, Lf+ nig. 2, strat. 0, elas. 0, sicc. 2
82 - 89	Grey silt with sand. Ag3, Ga1 nig. 2, strat. 0, elas. 0, sicc. 2
89 - 125	Light grey silt. Ag3+, Tl+, Th+ nig. 1, strat. 0, elas. 0, sicc. 2
125 - 132	Light grey silt with well preserved organic material - rootlets. Ag3, Th ¹ -, Dh ² + nig. 1, strat. 0, elas. 0, sicc. 2
132 - 144	Light grey silt and sand. Ga2-, Ag2-, Dh+, Th+ nig. 1+, strat. 0, elas. 0, sicc. 2
144 - 154	Dark grey silt. Ag3, Ga1-, Dh+, Th+ nig. 2, strat. 0, elas. 0, sicc. 2
154 - 157	Ag2, Sh2-, Dh+ nig. 3, strat. 0, elas. 0, sicc. 2+
157 - 164	Organic reed-like plants (phragmites?) in silt matrix. Dh ¹ +, Sh1+, Ag2 nig. 3+, strat. 0, elas. 0, sicc. 2+
164 - 182	Dark brown silt, organic. Th+, Dh+, Ag3, Ga+ nig. 3, strat. 0, elas. 0, sicc. 2+
182 - 200	UNSAMPLED

Appendices:

- 200 - 209 Dark brown organic silt with sand.
Ag2+, Ga1, Dh+
nig. 3, strat. 0, elas. 0, sicc. 2
- 209 - 274 Stratified highly organic silt, well
preserved detrital, woody material, getting
slightly siltier towards base.
Ag2+, As+, D1¹, Sh+
nig. 3, strat. 2, elas. 0, sicc. 2
- 274 - 294 Dark brown organic clay/silt.
As2, Ag1, D11
nig. 2, strat. 0, elas. 0, sicc. 2
- 294 - 340 Organic silt with fine sand.
Ag2, Ga1, Sh1
nig. 2, strat. 0, elas. 0, sicc. 2
- 340 - 390 Coarse sand with silt.
Gg2, Ga1, Ag1
nig. 2, strat. 0, elas. 0, sicc. 2

Appendices:

SW5

Depth cm.	Description
0 - 44	UNSAMPLED
44 - 49	Blue grey sand, small rootlets. Sc4 nig. 2, strat. 0, elas. 0, sicc. 2
77 - 80	Light sand. Ga4 nig. 1+, strat. 0, elas. 0, sicc. 2
80 - 82	Brown sand silt. Ga3, Ag1, Th ¹⁺ nig. 2+, strat. 0, elas. 0, sicc. 2
82 - 91	Light grey/white sand/silt, no organic matter. Ga2, Ag2 nig. 1, strat. 0, elas. 0, sicc. 2
91 - 110	White silt with sand, smallest hint of organic rootlets. Ag3, Ga1, As ⁺⁺ , Tl ⁺ nig. 1, strat. 0, elas. 0, sicc. 2
110 - 112	White sand, silt lens. Ga2, Ag1, As1 nig. 1, strat. 0, elas. 0, sicc. 2
112 - 117	Silt, white/grey. Ag3, Ga1, As ⁺⁺ nig. 1, strat. 0, elas. 0, sicc. 2
117 - 126	UNSAMPLED
126 - 189	UNSAMPLED
189 - 214	Dark brown silt with some organic material. Ag2, As1, Sh1, Ga ⁺ nig. 3, strat. 0, elas. 0, sicc. 2
214 - 258	Dark brown silt with large well-preserved twigs, individual sand particles. Ag2, D1 ²⁺ , Sh1, Ga ⁺ nig. 3, strat. 0, elas. 0, sicc. 2

Appendices:

258 - 275 Stratified dark brown silt with organic
 material, individual sand particles.
 Ag3, Sh1, Ga+
 nig. 3, strat. 2, elas. 0, sicc. 2

275 - 281 UNSAMPLED

281 - 370 Dark brown silt with twigs.
 As1, Ag2, D11, Dh+, Th+
 nig. 3, strat. 2, elas. 0, sicc. 2

370 - 375 Brown organic silt.
 Ag3, Sh1
 nig. 2+, strat. 0, elas. 0, sicc. 2

375 - 386 UNSAMPLED

386 - 434 Ag2, Ga1, D1+, Sh1
 nig. 2+, strat. 0, elas. 0, sicc. 2

434 - 464 Gg1, Ga1, Ag1, As1, Sh+
 nig. 2+, strat. 0, elas. 0, sicc. 2

464 - 475 Ga?
 nig. 2, strat. 0, elas. 0, sicc. 2

Appendices:

SW6

Depth cm.	Description
0 - 45	UNSAMPLED
45 - 81	Modern. Ga3+, Ag1, Th+ nig. 2, strat. 0, elas. 0, sicc. 2
81 - 90	Dark organic silt, with sand. Ga1, Ag3, Sh+ nig. 3, strat. 0, elas. 0, sicc. 2
90 - 103	White/grey silt. Ag3, As1, Sh+ nig. 1, strat. 0, elas. 0, sicc. 2
103 - 115	White/grey sand with silt. Ga3, Ag1 nig. 1, strat. 0, elas. 0, sicc. 2
115 - 124	UNSAMPLED
124 - 151	Ga3+, Ag1 nig. 1, strat. 0, elas. 0, sicc. 2
151 - 175	Light brown clay silt. Ag3, As+, Sh+, Ga+ nig. 2, strat. 0, elas. 0, sicc. 2
175 - 240	Dark brown organic silt with slightly humified organic twigs. Sand particles and occasional lenses. Ag2, D1 ² 1, Sh1, Ga+ nig. 3, strat. 0, elas. 0, sicc. 2
240 - 271	Well stratified silt with well humified twigs. Ag3, D1 ² 1 nig. 3, strat. 2, elas. 0, sicc. 2
271 - 276	Sand/silt, with well humified twigs. Ga2, Ag1, D1 ² 1 nig. 3, strat. 0, elas. 0, sicc. 2
276 - 289	Silt with large twigs, humified. Ag2, D1 ² 2 nig. 3, strat. 0, elas. 0, sicc. 2

Appendices:

289 - 368 Silt with some organic material.
 Ag2+, Sh+
 nig. 2+, strat. 0, elas. 0, sicc. 2

368 - Blue grey sand.
 Ga2, Ag1, Gg1
 nig. 1, strat. 0, elas. 0, sicc. 2

Appendices:

SW7

Depth cm.	Description
0 - 39	Sc4
39 - 89	Grey sand. Ga3+, Ag+ nig. 2, strat. 0, elas. 0, sicc. 2
89 - 122	UNSAMPLED, probably sand, fell from sampler
122 - 151	Grey/buff sand. Ga3+, Ag+ nig. 2, strat. 0, elas. 0, sicc. 2
151 - 170	White grey sand with silt. Ga3, Ag1 nig. 1, strat. 0, elas. 0, sicc. 2
170 - 197	Brown silty sand with some organic material. Ga2+, Ag1+, Sh+ nig. 2+, strat. 0, elas. 0, sicc. 2
197 - 228	UNSAMPLED
228 - 235	Organic rich clay and silt with well preserved rootlets and stems. As1, Ag2+, Th ²⁺ , Dl ²⁺ nig. 3, strat. 0, elas. 0, sicc. 2
235 - 402	Stratified organic silt, with preserved reed stems. The amount of organic material declines nearer the base of the sediment core. Ag3(+), Dh ² 1(-) nig. 3, strat. 2, elas. 0, sicc. 2
402 - 406	Silt with sand particles. Ga2, Ag1, Sh+ nig. 2+, strat. 0, elas. 0, sicc. 2
406 - 412	Dark grey silt with some sand particles. Ag+, Ga+, Sh+ nig. 2+, strat. 0, elas. 0, sicc. 2
412 - 440	Dark grey silt and sand. Gg2, Ga1, Ag1 nig. 2, strat. 0, elas. 0, sicc. 2

Appendices:

SW8

Depth cm.	Description
0 - 34	Sc4
34 - 63	Coarse sand with heavy iron staining at the base. Gg2, Ga2, Lf+ nig. 2, strat. 0, elas. 0, sicc. 2

Borer stopped by very hard sand deposits. This bore hole was located very close to the edge of the main coastal dune complex of Sham Wan. There was no evidence that the lagoon deposits found in the previously recorded bore holes extended further towards the coastline.

Appendices:

SW9

Depth cm.	Description
0 - 45	Sc4
45 - 62	Blue grey silty sand. Ga3, Ag1 nig. 2, strat. 0, elas. 0, sicc. 2
62 - 83	Yellow brown/red sand. Heavy iron staining. Gg1, Ga2, Ag1, Lf+ nig. 2, strat. 0, elas. 0, sicc. 2
83 - 105	Blue/grey silty sand. Ga2+, Ag2- nig. 2, strat. 0, elas. 0, sicc. 2
105 - 113	Dark brown silt with sand particles. Ag3, Ga1, Sh+ nig. 3, strat. 0, elas. 0, sicc. 2
113 - 156	Light grey silt. Ga1, Ag2, As1 nig. 1, strat. 0, elas. 0, sicc. 2
156 - 164	Dark brown organic silty sand. Ag2, Ga1+, Sh+ nig. 2+, strat. 0, elas. 0, sicc. 2
164 - 174	UNSAMPLED
174 - 178	Dark brown organic silty sand. Ag2, Ga1+, Sh+ nig. 2+, strat. 0, elas. 0, sicc. 2
178 - 233	UNSAMPLED
233 - 246	Organic rich silt. Ag3, Ga1, Sh1 nig. 3, strat. 0, elas. 0, sicc. 2
246 - 254	Highly organic rich silt. Well humidified black detritus. Ag2, Dh ³ 1, Ga1 nig. 3, strat. 0, elas. 0, sicc. 2
254 - 277	Stratified silt with organics. Ag3, Sh+, Ga+ nig. 3, strat. 2, elas. 0, sicc. 2

Appendices:

- 277 - 289 Grey sand silt.
Ga²⁺, Ag²⁻
nig. 2, strat. 0, elas. 0, sicc. 2
- 289 - 327 Silt with sand particles and detritus, well
humified twigs.
Ag²⁺, Ga¹⁺, D¹⁺
nig. 2, strat. 0, elas. 0, sicc. 2
- 327 - 358 As above with sand lenses.
Ag³, Ga⁺, D¹⁺
nig. 2, strat. 0, elas. 0, sicc. 2
- 358 - 360 Sand with small amount of silt.
Ga³, Ag¹
nig. 2+, strat. 0, elas. 0, sicc. 2
- 360 - 416 Silt, dark grey with small amount of sand
particles.
Ag³⁺, Ga⁺, Sh⁺
nig. 3, strat. 0, elas. 0, sicc. 2
- 416 - 427 Blue grey sand with some silt and well
humified twigs.
Ga³, Ag⁺, D¹⁺
nig. 2, strat. 0, elas. 0, sicc. 2

Appendices:

TSW/B1

Depth cm.	Description
0 - 25	Unsampled.
25 - 42	Olive brown desiccated silt. Ag2, Ga1, As1, nig. 2, strat. 0, elas. 0, sicc. 2
42 - 55	Dark brown clay and silt As3, Ag1 nig. 3+, strat. 0, elas. 0, sicc. 2
55 - 125	Grey silt with shells getting softer at base. Ag3, Ga++, As1, test. moll.++ nig. 2+, strat. 0, elas. 0, sicc. 2
125 - 130	As above
130 - 134	Grey coarse sand. Gs2, Ga1, Ag1, Gg min+ nig. 2, strat. 0, elas. 0, sicc. 2
134 - 148	Grey silt clay. Ga1, Ag2+, As1 nig. 2, strat. 0, elas. 0, sicc. 2
148 - 172	Grey organic rich silt. Ag2, D1+, Dh+, As1+ nig. 2, strat. 0, elas. 0, sicc. 2
172 - 199	Grey silt, pockets of sand. As1, Ag2+, Ga1 nig. 2, strat. 0, elas. 0, sicc. 2
199 - 218	Brown, mottled. As1, Ag2, Ga+ nig. 2, strat. 0, elas. 0, sicc. 2
218 - 225	Brown, mottled. Ga2, Ag2 nig. 2, strat. 0, elas. 0, sicc. 2
225 - 273	Grey coarse sand. Gs1, Ga2, Ag1 nig. 2, strat. 0, elas. 0, sicc. 2
273 - 282	Grey coarse sand, fine gravel. Gs2, Ga2, Gg min+ nig. 2, strat. 0, elas. 0, sicc. 2

Appendices:

TSW/B2

Depth cm.	Description
0 - 40	Unsampled.
40 - 61	Olive brown desiccated silt. Ag2, Ga1, As1, Lf+ nig. 2, strat. 0, elas. 0, sicc. 2
61 - 80	Black organic clay. As3+, Ag1, Sh1+ nig. 3+, strat. 0, elas. 0, sicc. 2
80 - 92	Brown grey silt. As1, Ag3, Lf+ nig. 2, strat. 0, elas. 0, sicc. 2
92 - 105	Grey shelly silt. Ag2+, Ga+, As1 test moll 1 nig. 2, strat. 0, elas. 0, sicc. 2
105 -145	Grey. Ag3, Ga+, As1 test moll + nig. 2, strat. 0, elas. 0, sicc. 2
145 - 190	As above. Slight D1+ at base
190 - 245	Grey organic silt. Detritus, well humified like a peat. Ag2, D11+, test moll +, Ga+, As+ nig. 2+, strat. 0, elas. 0, sicc. 2
245 - 340	Dark grey silt. As1, D11, Ag2+, Ga+ nig. 2+, strat. 0, elas. 0, sicc. 2
340 - 345	Brown mottled sand with gravel. Ga2-, Gs1, Gg min1, Gg maj+ nig. 2+, strat. 0, elas. 0, sicc. 2

Appendices:

Appendix 2

Bacillariophyta (diatoms) identified in the study and diatom floras used during diatom analysis. The nomenclature follows that of Jin et al (1965, 1982).

Marine (M)	<i>Actinocyclus ehrenbergii</i>
Marine (M)	<i>Actinoptychus trinacriformis</i>
Fresh (F)	<i>Amphora mexicana</i>
Marine (M)	<i>Auliscus incertus</i>
Marine (M)	<i>Caloneis elongata</i>
Marine (M)	<i>Campylodiscus</i> spp.
Marine (M)	<i>Cocconeis pseudomarginata</i>
Marine - brackish (MB)	<i>Cocconeis scutellum</i>
Marine - brackish (MB)	<i>Coscinodiscus blandus</i>
Marine - brackish (MB)	<i>Coscinodiscus eccentricus</i>
Marine (M)	<i>Coscinodiscus kutzingii</i>
Marine (M)	<i>Coscinodiscus marginato lineatus</i>
Marine - brackish (MB)	<i>Coscinodiscus rothii</i>
Marine - brackish (MB)	<i>Coscinodiscus subtilis</i>
Marine (M)	<i>Coscinodiscus wittianus</i>
Brackish (B)	<i>Cyclotella striata</i>
Fresh - brackish (FB)	<i>Cymbella ventricosa</i>
Marine (M)	<i>Diploneis bombus</i>
Marine (M)	<i>Diploneis crabro</i>
Marine - brackish (MB)	<i>Diploneis didyma</i>
Marine (M)	<i>Diploneis fusca</i>
Brackish - marine (BM)	<i>Diploneis incurvata</i>
Brackish - marine (BM)	<i>Diploneis interrupta</i>
Marine - brackish (MB)	<i>Diploneis smithii</i>
Fresh (F)	<i>Epithemia reicgeltii</i>
Fresh (F)	<i>Eunotia arcus</i>
Fresh (F)	<i>Eunotia diodon</i>
Fresh (F)	<i>Eunotia flexuosa</i>
Fresh - brackish (FB)	<i>Eunotia lunaris</i>
Fresh (F)	<i>Eunotia pectinalis</i> v. <i>undulata</i>
Fresh - brackish (FB)	<i>Eunotia polyglyphis</i>
Fresh (F)	<i>Eunotia robusta</i>
Fresh (F)	<i>Eunotia sudetica</i>
Fresh - brackish (FB)	<i>Eunotia tenella</i>
Marine (M)	<i>Eunotogramma marinum</i>
Fresh (F)	<i>Fragilaria bidens</i>
Fresh - brackish (FB)	<i>Fragilaria pinnata</i>
Fresh - brackish (FB)	<i>Gomphonema acuminatum</i> var. <i>coronata</i>
Marine (M)	<i>Grammatophora marina</i>
Marine - brackish (MB)	<i>Grammatophora oceanica</i>
Marine - brackish (MB)	<i>Melosira sulcata</i>
Brackish (B)	<i>Navicula crucicula</i>
Brackish (B)	<i>Navicula elegans</i>
Brackish (B)	<i>Navicula florinae</i>
Marine - brackish (MB)	<i>Navicula marina</i>

Appendices:

Marine (M)	<i>Navicula mollis</i>
Marine (M)	<i>Nitzchia cocconeiformis</i>
Fresh - brackish (FB)	<i>Nitzchia denticula</i>
Brackish (B)	<i>Nitzchia navicularis</i>
Brackish - marine (BM)	<i>Nitzchia punctata</i>
Brackish - fresh (BF)	<i>Nitzchia scalaris</i>
Fresh (F)	<i>Nitzchia subtilis</i>
Marine (M)	<i>Opephora pacifica</i>
Fresh - brackish (FB)	<i>Pinnularia acrosphaeria</i>
Fresh (F)	<i>Pinnularia alpina</i>
Fresh (F)	<i>Pinnularia cardinalis</i>
Fresh - brackish (FB)	<i>Pinnularia cruciformis</i>
Fresh - brackish (FB)	<i>Pinnularia dactylus</i>
Fresh (F)	<i>Pinnularia divergens</i>
Fresh (F)	<i>Pinnularia interrupta</i>
Fresh - brackish (FB)	<i>Pinnularia major</i>
Fresh (F)	<i>Pinnularia mesolepta</i>
Fresh (F)	<i>Pinnularia microstauron</i>
Fresh (F)	<i>Pinnularia nobilis</i>
Fresh (F)	<i>Pinnularia viridis</i>
Marine (M)	<i>Plagiogramma pulchellum</i>
Marine (M)	<i>Plagiogramma staurophorum</i>
Marine - brackish (MB)	<i>Raphoneis ampiceros</i>
Brackish (B)	<i>Rhopalodia gibberula</i>
	<i>Stauroneis actua</i>
Fresh (F)	<i>Stauroneis anceps</i>
Fresh - brackish (FB)	<i>Stauroneis phoencenteron</i>
Fresh - brackish (FB)	<i>Synedra ulna</i>
	<i>Tabellaria flocculosa</i>
Brackish (B)	<i>Terpinsoe americana</i>
Marine (M)	<i>Trachyneis aspera</i>

Diatom flora used to identify diatom frustules:

Cleve-Euler A (1951-1955) *Die Diatomeen von Schweden und Finnland* Kungl Svenska Vetensk, Akademia Handl. Series

Hendey N I (1964) *An introductory account of the smaller algae of British coastal waters. Part V: Bracillariophyceae (diatoms).* London HMSO: 317p.

Jin D X., Cheng S., Lin G., Liu X. (1982) *Benthonic marine diatoms in China*, China Ocean Press, Peking, 323p.

Jin D X., Cheng J. H., Huang H. G. (1965) *Planktonic marine diatoms in China*, Shanghai Scientific Technical Press, Shanghai, 199p.

Appendices:

Smith W (1853-1856) A synopsis of the British diatomaceae; with remarks on their structure, function and distribution; and instructions for collecting and preserving specimens. London, John van Voorst, 2 volumes.

Werff, A. van der and Huls, H (1958-1966) Diatomeenflora van Nederland (8 parts). Published privately by A. van der Werff, Westzijde, 13a De Holf (U), The Netherlands.

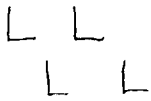
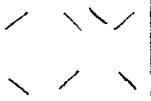
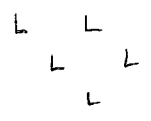
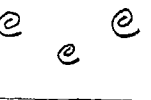
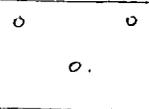
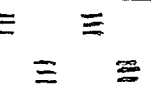
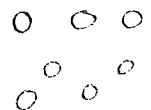
Yim W W S (1988) List of diatoms found around Hong Kong. Privately published list with photographs.

Appendices:

Appendix 3

Key to the stratigraphic symbols

The symbols used in the stratigraphic diagrams follows the system devised by Troels Smith (1955). The complete key to all symbols is illustrated in the paper. The full classification of all sediment layers is shown in appendix 1.

	As		
	Ag		
	Ga		test moll.
	Gs		
	Gg		

Appendices:

Appendix 4

Sources of radiocarbon dated sea-level index points from Hong Kong and the south coast of China.

Chen W., Zhang H. and Li Z. (1986) The velocity of Holocene vertical tectonic motion in the coastal areas of Fujian and Guangdong, *Seismology and Geology*, 8 (2), 33-42 (in Chinese with English abstract)

9

Huang Y. (1984) Holocene sea level changes and recent crustal movements along the northern coasts of the South China Sea, in **Whyte R.O.** ed. *The evolution of the East Asian Environment, II*, (Palaeobotany, Palaeozoology and Palaeoanthropology), Centre of Asian Studies, University of Hong Kong

8

Huang Y. et al (1985) Relations between the faults of the Pearl River Delta and the processes of formation of the delta, *Geological Society of Hong Kong Newsletter*, 3 (5), 1-10

15

Huang Z., Li P., Zhang Z. and Zong Y. (1986) Sea level changes along the coastal area of South China since late Pleistocene, in **Qin, Y. and Zhao S.** eds. *Late Quaternary sea level changes, China Ocean Press, Beijing.*

7

Huang Z. et al eds. (1982) *The evolution of the Pearl River Delta (in Chinese)*

14

Huang Z. et al (1983) *The landform of Shenzhen, Guangdong Scientific Press, 91-99 (in Chinese)*

13

Huang Z. et al (1987) Depositional facies of the Zhujiang Delta from fossil diatom, *Acta Oceanologica Sinica*, 6 (2), 222-228

16

Huang Z. et al (1987) Late quaternary sub fossil wood bed in Zhujiang Delta deposits, *International Geomorphology*, 1986, II, John Wiley & Sons, 801-805

17

Appendices:

Huang Z. et al (1987) Geomorphological evolution of Zhujiang Delta, *International Geomorphology*, 1986, I, John Wiley & Sons, 989-997

18

Li P. (1987) The shoreline evolution and the development model of the Hanjiang river delta during the past 6000 years, *Geographical Research*, 6 (2), 1-13 (in Chinese with English abstract)

3

Li P., Huang Z. and Zong Y. (1988) New views on geomorphological development of the Hanjiang river delta, *Acta Geographica Sinica*, 43 (1), 19-43 (in Chinese with English abstract)

4

Li P., Huang H., Zong Y., Zhang Y. and Zhang Z. (1987) *The Hanjiang Delta*, China Ocean Press, 296pp (in Chinese)

1

Yim W.W.S. (1986) Radiocarbon dates from Hong Kong, *Journal of the Hong Kong Archaeological Society*, 11, 50-63

23

Yim W.W.S. (1987) One hundred radiocarbon dates for Hong Kong, *Geological Society of Hong Kong Newsletter*, 5 (4), 1-8

22

Yim W.W.S. and Nau (1984) Radiocarbon dates of Zhujiang Delta and their implications for Hong Kong

19

Zhang H. (1985) On the relationship between faulting and formation as well as development of Hanjiang Delta, *Acta Oceanological Sinica*, 4 (2), 266-275

5

Zhang H. (1986) On the relationships between Holocene sea level changes as well as seismicity and plate motion, *Sea level changes of China*, China Ocean Press, (in Chinese with English Abstract)

12

Zhang Z. and Liu Z. (1987) The Holocene along the coast of Hainan Island, *Scientia Geographica Sinica*, 7 (2), 129-138

20

Appendices:

Zhao X.T. (1978) Holocene beachrock in Hainan Island, *Scientia Geologica Sinica*, 2, 163-173

21

Zong Y. (1987) Depositional cycles of the Quaternary in the Hanjiang Delta, *Tropical Geography*, 7(2) 117-127 (in Chinese with English abstract)

2

Zong Y. (1989) On depositional cycles and geomorphological development of the Han River delta of South China, *Zeitschrift fur Geomorphologie*, 73, 33-48

5a

Zong Y. and Li P. (1984) Development condition of the Holocene beachrock along the coast of eastern Guangdong, China *Tropical Geography*, 4 (4) (in Chinese with English abstract)

6

Appendices:

Appendix 5:

RADIOCARBON DATED SEA-LEVEL INDEX POINT DATABASE

Altitude: All altitudes are relative to the Yellow Sea Datum, and are the altitudes at which samples were recorded on collection.

Age: Radiocarbon years Before Present using the Libby half-life of 5,568 years.

Laboratory code:

Many dated samples from China do not have laboratory codes. An extensive search of the literature has been undertaken to find as many laboratory codes as possible. Where only the laboratory has been identified, but not the individual sample code, the laboratory initials have been included.

KWG = Guangzhou Institute of Geography Laboratory.

CG = Institute of Geology, State Seismological Bureau, China.

I = Teledyne Isotopes, New Jersey, USA.

GIF = National Centre for Scientific Research, Gif-sur-Yvette, France.

CS = CSIRO Division of Soils, Adelaide, Australia.

SI = South China Sea Institute of Oceanology, Guangzhou, China.

HAR = Atomic Energy Research establishment, Harwell, UK.

ARL = Australian Radiometric Laboratories, Sydney, Australia.

GC = Institute of Geochemistry, Academy of Sciences, China.

Material

- | | |
|----|---|
| 1 | Wood |
| 2 | Rootlet |
| 3 | Organic mud |
| 4 | Shell (marine) |
| 5 | <u>Ostrea</u> shell |
| 6 | Intertidal shell (in sediments with brackish diatoms) |
| 7 | Fresh water shell (in sediments with fresh diatoms) |
| 8 | Coral reef |
| 9 | Beachrock / shell ridge deposit |
| 10 | Beach rock / beach deposit |
| 11 | Marine clay (marine diatoms) |
| 12 | Lagoon clay (brackish diatoms) |
| 13 | Peat |
| 14 | Other |

Sea-level index points extracted from the database by the screening process discussed in chapter 4, section 4.4.2, are labelled either P, B or F.

P = SUPRATIDAL INDICATOR

B = SUBTIDAL INDICATOR

F = FIXED INDICATOR

Appendices:

LOCATION	ALTITUDE (m Y.S.D.)	AGE	LAB. CODE	DATED MATERIAL	INDEX POINT	INDICATOR
HONG KONG:						
Admiralty	-7.3	6520±130	GIF-4387	wood	1	P
Argyle	-11.0	7020±160	GIF-4813	shell/oyster et	4	B
Chung Hom Wan	1.2	5455±105	I-8830	wood	1	P
Deep Bay CLP/E1	-7.7	10060±130	CS-621	organic	14	
San Tin	1.0	520±112	SI86/121	organic mud	3	
High Island (E)	-12.0	5980±180	KWG-286	wood	1	B
High Island (W)	-17.4	7920±110	HAR-871	shell/oyster	4	
High Island (W)	-17.3	7830±140	HAR-869	wood	1	B
High Island (W)	-16.1	7790± 90	HAR-870	shell/oysters	4	
High Island (W)	-16.1	6640±100	HAR-868	wood	1	
Junk Bay JBS11A	-19.7	8080±130	CS-619	shell	4	
Lai Chi Kok	-14.1	8785±125	I-8269	wood	1	
Lai Chi Kok Bay	-17.0	7790±150	GIF-5243	shell	4	
Lok Ma Chau	0.4	5475±155	SI86/123	rootlet	2	F
Lok Ma Chau	0.3	5093±130	SI86/124	rootlet	2	F
Ngon Ping	0.9	1900± 93	SI86/109	wood	1	
Ping Shan	0.2	3110±185	SI86/122	organic mud	3	
Prince Edward	-11.0	6580±130	GIF-4558	shell/oysters	4	B
Sham Wan	-2.0	5520±110	I-10059	shell	4	B
Sham Wan	1.0	3870± 80	HAR-3589	shell	4	B
Sheung Wan	-16.5	8600±270	KWG-407	wood	1	
Sheung Wan	-16.5	8520±270	KWG-407	Organic mud	3	
FUJIAN						
Xiangqian	-30.0	8790±115		lagoon clay	12	
Xiangqian	-14.0	8040±110		lagoon clay	12	
Fuzhou	-16.7	6793±339		lagoon clay	12	
Fuzhou	-5.6	5621±281		lagoon clay	12	
Pingtian	3.0	5260± 96		brackish shell	6	B
Putian	9.0	4820±120		beachrock sr	9	P
Fuqing	5.0	4300± 85		brackish shell	6	B
Putian	6.3	4000±140		beachrock sr	9	P
Longhai	3.2	3800±150	GC-315	brackish shell	6	B
Pingtian	5.5	3500±168		beachrock sr	9	P
Longhai	2.8	3330±150	GC-376	Ostrea	5	B
Longhai	2.3	3150±150	GC-310	Ostrea	5	B
Putian	7.0	3150±180		beachrock sr	9	P
Changpu	1.3	3100±150	GC-321	beachrock sr	9	P
Longhai	5.5	2760±150	GC-307	lagoon saltmarsh	2	P
Changpu	1.3	2600±120	GC-320	beachrock sr	9	P
Lonhai	3.5	2350±120	GC-314	beachrock sr	9	P
Changpu	1.3	1980±100	GC-319	brackish shell	6	B
Longhai	4.5	1870±100	GC-313	beachrock sr	9	P
SHENZHEN						
Chewan	-15.2	7080±160	KWG	marine clay	11	
Chewan	-10.1	6470±180	KWG	marine clay	11	
Shonggang	-6.9	6120±160	KWG	mangrove roots	2	F
Dongtan	-5.9	6030±150	KWG	intertidal clay	3	
Jushixa	-5.2	5530±160	KWG	intertidal clay	3	
Shajing	-13.8	5510±170	KWG	Ostrea in silt	5	
Shajing	-12.2	5220±140	KWG	Ostrea	5	
Fisha	-3.0	5090±160	KWG	Ostrea/dark silt	5	B
Longchi	-7.0	4340±140	KWG	marine clay, sh	11	
Baishizhou	- .5	3980±110	KWG	brackish shell	6	
Chewan	-5.6	3860±110	KWG	marine clay	11	
Dongtan	-4.7	3570±110	KWG	marine clay	11	
Longchi	-4.4	3360±120	KWG	brackish shell	4	
Nantou	-6.5	2890±120	KWG	marine clay	11	

Appendices:

Jushixa	-3.5	2530± 90	KWG	shell (brackish	4	
Jaubeisha	-5.6	2430± 95	KWG	marine clay	11	
Xichong	1.5	2170± 85	KWG-209	beachrock (B)	10	P
Nantou	-5.6	2150± 90	KWG	marine clay	12	
Shajing	-4.1	2040± 95	KWG	Ostrea	5	
Shonggang	-1.1	1460± 80	KWG	intertidal clay	12	
Nantou	2.0	1280± 70	KWG	lagoon clay	12	
Nantou	-4.4	1260± 90	KWG	intertidal clay	12	
Fuyongtan	-3.6	1130± 90	KWG	intertidal clay	12	
Jaubeisha	-3.9	960± 60	KWG	intertidal clay	12	
Fuyongtan	-2.8	640± 70	KWG	intertidal clay	12	
ZHUJIANG DELTA						
Zhuhai	-11.1	11620±380	KWG	Ostrea/clay	5	
Doumen	-54.2	8050±200	KWG	brackish clay	12	
Nanhai	-.2	6985±105		Ostrea	5	
Nanhai	-3.8	6510±150	KWG	intertidal clay	12	
Doumen	-14.9	6350±180	KWG	marine clay	11	
Sinhui	-5.4	6300±330	KWG	intertidal clay	12	
Dongguang	-12.2	6150±160		wood/in'ti'l silt	1	
Boluo	-4.3	5940±300	KWG	wood/tidal sed.	1	
Shunde	-.5	5920±300		Ostrea	5	B
Nanhai	-1.4	5865± 95		brackish shell	6	
Zhongshan	-7.4	5790±170	KWG	Ostr/intid silt	11	B
Panyu	-21.4	5360±160	KWG	marine clay	11	
Zhongshan	0.2	5030±250		Ostrea	5	B
Panyu	-8.9	5020±175	KWG	intertidal clay	12	
Xinhui	-1.4	5020±150	KWG	Ostrea	5	B
Zhongshan	-5.6	4940±250		Ostrea	5	B
Xinhui	-1.4	4790±140	KWG	Brackish shell	6	
Nanhai	3.6	4640±280	KWG	brackish shell	6	
Gaoyao	-.8	3950±100		Charcoal	0	
Panyu	-9.7	3840± 95	KWG-700	intertidal clay	12	
Xinhui	0.1	3670±110	KWG	peat	13	P
Xinhui	-.9	3020± 80		crocodile bone	14	
Zhongshan	-2.0	2700±150		Ostrea	5	B
Shunde	-1.9	2540±120		crocodile bone	14	
Xinhui	-1.5	2510± 90	KWG	Ostrea	5	B
Panyu	-4.4	2430± 90	KWG-690	intertidal clay	12	
Zhongshan	-3.4	2350±110	KWG	Intdl clay/wood	0	
Doumen	-18.2	2350± 90	KWG	intertidal clay	12	
Guangzhou	0.6	2320± 85	KWG	brackish shell	6	
Shanshui	0.3	2270±110	KWG	wood	1	P
Guangzhou	0.0	2120± 90	KWG	intertidal clay	12	
Xinhui	-1.2	2050±100		wood	1	P
Panyu	-3.2	1680± 90	KWG	Ostrea	5	B
Panyu	-4.7	1610± 80	KWG	intertidal clay	11	
Dongguang	-2.1	1520± 90	KWG	intertidal clay	12	
Doumen	-2.2	1390± 70	KWG	intertidal clay	11	
Panyu	-1.4	1310± 65	KWG-693	intertidal clay	12	
Zhongshan	-1.2	1260± 90		Ostrea	5	B
WESTERN GUANGDONG						
Taishan	-12.5	8500±180		intertidal clay	3	
Taishan	-17.3	7340±160		intertidal clay	3	
Pinisula	0.7	7120±165		coral reef	8	P
Yangzhiang	5.4	6000±280		brackish shell	9	
Wuchuan	0.0	4250±190		brackisk shell	6	
Zhanjiang	0.0	3930±150		mangrove wood	2	F
Denbai	4.5	2080±150		beachrock sr	9	P
Guangxi	2.0	1800± 90		lagoon peat	13	P
Pinisula	3.0	1040± 65		coral sand	10	P

Appendices:

HANJIANG DELTA / EASTERN GUANGDONG

Shaxi	-17.4	12390±370	KWG-283	intertidal clay	12	
Lianxia	-16.0	12310±370	KWG-281	intertidal clay	12	
Lugang	-8.8	10190±370	KWG-276	intertidal clay	12	
Dahau	-1.0	7510±140	KWG-486	intertidal clay	12	
Lugang	-3.8	7010±150	KWG-346	intertidal clay	12	
Waisha	-16.6	6230±240	KWG-33	marine clay	11	
Lianxia	-10.8	6190±130	KWG-282	intertidal clay	12	
Guangau	-12.0	6010±130	KWG-484	marine clay	11	
Jili	-7.5	5710±130	KWG-272	intertidal clay	12	
Meilin Lake	-5.5	5440±100	CG-451	brackish shell	6	
Dongli	-7.4	5380±130	KWG-267	intertidal clay	12	
Yuhu	-9.0	5270±130	KWG-266	intertidal clay	12	
Xihu	-5.2	5240±140	KWG-166	intertidal clay	12	
Waisha	-5.4	5220±220	KWG-32	intertidal clay	12	
Chihu	4.0	4820±120	KWG-322	fresh shell	7	P
Haishan	4.1	4790±120	KWG-328	beachrock sr	9	P
Guangau	-8.6	4650± 95	KWG-555	peat	13	
Shaxi	-10.3	4610±120	KWG-265	marine clay	11	
Lianshang	2.0	4330±120	KWG-326	beachrock sr	9	P
Shianzhou	2.5	3940±120	KWG-262	brackish shell	6	
Yanzhou	2.0	3900±110	KWG-297	brackish shell	6	
Shaxi	-5.4	3590±120	KWG-271	intertidal clay	12	
MeilinLake	-3.3	3545± 85	CG-450	Ostrea	5	B
Jingshi	1.5	3490±100	KWG-157	brackish shell	6	
Hepu	5.0	3320±100	KWG-310	beachrock sr	9	P
Zhanglin	1.8	3265± 85	CG-441	beachrock sr	9	P
Lianxia	-6.5	3230±110	KWG-269	brackish shell	6	
Lianshang	3.5	3190± 85	CG-452	beachrock sr	9	P
Zhanglin	2.0	3140±100	KWG-329	beachrock sr	9	P
Haishan	1.2	2820± 85	CG-444	brackish shell	6	
MeilinLake	-2.5	2630± 95	KWG-254	brackish shell	6	
Zhanglin	2.5	2485± 70	CG-440	brackish shell	6	
Haishan	4.6	2420± 75	CG-442	brackish shell	6	
Haishan	4.9	2350± 95	KWG-327	beachrock sr	9	P
Jingzhou	1.5	2205± 85	CG-447	brackish shell	6	
Shaxi	0.6	2120± 90	KWG-349	intertidal clay	12	
Nanao	3.5	1990± 80	KWG-307	beachrock sr	9	P
Waisha	0.0	1840± 85	KWG-302	intertidal clay	12	
Dongwan	-1.2	1580± 65	KWG-463	lagoon clay	12	
Fengzhou	1.5	720± 50	KWG-369	peat	13	
Batou	1.1	150± 0	KWG-464	organic silt	3	

XISHA

Shidao	1.5	5030±200		beachrock b	10	P
Shidao	5.0	4856±200		coral reef	8	P
Dongdao	5.0	4340±250		coral sand	9	P
Ganchuan	2.3	4040±150		beachrock sr	9	P
Ganchuan	2.6	3870±180		beachrock	9	P
Dongdao	4.0	3630±150		beachrock sr	9	P
Ganchuan	3.7	3400±160		coral reef sand	9	P
Dongdao	4.0	3250±120		beachrock sr	9	P
Yongxing	0.0	1754± 95		coral reef	8	P
Shidao	0.5	910±120		beachrock sr	9	P
Shudao	0.0	500± ?		beachrock b	10	P
Shanhoodao	0.0	380± ?		beachrock b	10	P
Dongdao	0.0	237± ?		beachrock b	10	P

HAINAN ISLAND

Wanning	-27.5	10230±320	KWG	Ostrea	5	B
Shanya	-8.9	9480±290	KWG	peat	13	P
Wanning	-19.5	8460±170	KWG	estuarine clay	11	
Shanya	0.0	8420±115	GC	coral reef	8	P

Appendices:

Shanya	0.8	8235±105 GC	coral reef	8	P
Shanya	-6.4	7280±140 KWG	lagoon clay	12	
Dongfang	-11.0	7150±110 KWG	intertidal clay	12	
Qongshan	-14.5	6750±140 KWG	estuarine clay	11	
Shanya	0.8	6345±100 KWG	coral reef	8	P
Ledong	0.0	5995± 95 GC	beachrock b	10	P
Wenhang	0.0	5720±140 KWG	organic sand	3	
Shanya	-.8	5680±140 KWG	intertidal clay	12	
Wanning	0.6	5650±150 KWG	lagoon peat	13	P
Dongfang	0.1	5530±110 KWG	intertidal clay	12	
Shanya	0.6	5450±190 KWG	beachrock b	10	P
Shanya	1.5	5180±190 GC	coral reef	8	P
Shanya	1.2	5025± 85 GC	coral reef	8	P
Shanya	1.8	4930±185 GC	coral reef	8	P
Shanya	2.5	4800±240 GC	coral reef	8	P
Janxian	1.0	4510±110 KWG	coral reef	8	P
Ledong	1.0	4365± 85 GC	beachrock b	10	P
Shanya	2.0	4345±210 GC	beachrock sr	9	P
Shanya	0.6	4170±140 KWG	beachrock b	10	P
Luhuitau	1.2	4020± 85 GC	coral reef	8	P
Shanya	2.0	4010±110 KWG	coral reef	8	P
Luhuitau	-1.0	3880±110 KWG	beach coralsand	10	P
Shanya	2.3	3865± 85 GC	beachrock b	10	P
Shanya	2.0	3810± 85 GC	beachrock b	10	P
Luhuitau	3.0	3750±190 GC	beachrock b	10	P
Luhuitau	4.0	3630±190 GC	beachrock b	10	P
Shanya	0.5	3450± 90 KWG	coral reef	8	P
Janxian	0.0	3260± 90 KWG	coral reef	8	P
Lingao	2.5	3260±110 KWG	beachrock sr	9	P
Changmai	3.5	3140±110 KWG	lagoon clay	8	
Wenhang	2.7	2850±110 KWG	beachrock sr	9	P
Luhuitau	1.3	2710±110 KWG	coral sand	10	P
Shanya	0.5	2360± 90 KWG	beachrock sr	9	P
Wenhang	0.0	2214±156 GC	brackish shell	6	
Lingao	0.0	2160± 90 KWG	beachrock b	10	P
Wenhang	1.0	2054±109 GC	beachrock b	10	P
Wenhang	1.0	2010± 90 KWG	coral sand	10	P
Wenhang	3.0	1890± 90 KWG	beachrock b	10	P
Haikou	0.0	1565±130 KWG	wood/clay	12	
Luhuitau	1.0	1379± 64 GC	lagoon clay	12	
Ledong	1.2	1190± 75 KWG	lagoon peat	13	
Dongfang	0.0	1020± 90	beachrock b	10	P
Ledong	0.0	1020± 90 KWG	beachrock b	10	P
Wenhang	4.0	1020± 80 KWG	beachrock sr	9	P
Wenhang	4.2	625± 65 KWG	coral sand	9	P
Wanning	3.5	260± 60 KWG	lagoon clay?	0	

Appendices:

Appendix 6

Chinese geologists have divided the Quaternary into four major periods. These are used by Huang et al (1982) and Zong (1989) and other authorities when analysing environmental changes along the coasts of southern China during the Quaternary.

The four major divisions, and eight subdivisions, covering the last two million years, are shown in the table below.

Q₁ - Q₃ refer to the Pleistocene. Huang et al (1982) have identified the major stages of the evolution of the Zhujiang delta during this period. Q₄ refers to the Holocene, and has been divided into three parts.

Appendices:

Changes in sea-levels and sedimentation during the Quaternary

	Period	Years B.P.	Zhujiang Delta development (Huang <u>et al</u> 1982)	Sea-level change in Hong Kong (Yim <u>et al</u> 1987)
H O	Q4 ³	0 - 2,500	Marine transgression	Upper marine
L O	Q4 ²⁻²	2,500 - 5,000	Terrestrial deposits	Upper marine
C E	Q4 ²⁻¹	5,000 - 7,500	Marine transgression	Upper marine
N E	Q4 ¹	7,500 - 10,000	Marine transgression / terrestrial deposit	Upper terrestrial
P	Q3 ³	10,000 - 22,000	Terrestrial deposits	Upper terrestrial
L E	Q3 ²⁻²	22,000 - ~35,000	Marine transgression	Upper terrestrial / Middle marine
I S	Q3 ²⁻¹	-35,000 - 40,000	Terrestrial sands and gravels	Middle marine
T O C	Q3 ¹	40,000 - 100,000	Development of main drainage pattern	Middle terrestrial Lower marine (date?) Lower terrestrial
E N	Q2 ¹	100,000 - 700,000	Tectonic movements. Uplift	
E	Q1 ¹	700,000-2,000,000	and subsidence.	

Chapter 5: Possible impacts of future sea-level changes

Quarry Bay the mean settlement rate at the new tide gauge station is 6.1 mm/year. Levelling of three reference points at the tide gauge station has been carried out since 1984.

Statistics on extreme sea-levels measured at various tide gauges in Hong Kong have been analyzed by Chan (1983) and by Yim (1988) and other data provided by the Royal Observatory, Hong Kong, are presented here. Chan provides detailed data on extreme sea-levels between 1906 and October 1982. Many of these extreme sea-levels are due to tropical cyclones. Chan also gives detailed data on the calculated magnitude of storm surges measured at three tide gauge stations: North Point, Tai Po and Chi Ma Wan. All the tidal data from Hong Kong have been corrected for ground settlement, by subtracting the amount of ground settlement that occurred between the time that the tide gauge station was established and the time of the measurement of sea-level using a rate of 5.04 mm/year.

5.7.7.3 Trends in mean sea level

Yim (1988) first drew attention to the use of tide gauge data to examine trends in mean sea-level around Hong Kong over a period of a few years during the recent past. Tidal records collected between 1962 and 1987 from North Point were analyzed. An apparent trend of rising sea-level was found, although Yim emphasised that subsidence at the gauge was likely to have been responsible for most of this apparent rise. When mean annual sea-level at North Point is corrected for ground settlement, sea-level appears to have fallen very slightly over the past 30 years in Hong Kong (Yim 1988). This conflicts with the trend of global sea-levels measured over the past 100 years and reported by Gornitz and Lebedeff (1987). However Yim (1988) suggests that this pattern in Hong Kong may be in part due to land subsidence around the

Bibliography:

Bibliography

Allen P.M. and Stephens E.A. (1971) Report on the Geological Survey of Hong Kong, Hong Kong Government Press.

Arthurton R.S., Lai K.W., Langford R.B., and Shaw R. (1989) Hong Kong Geological Survey Memoir No. 3, Geotechnical Control Office, Hong Kong.

Bard S.M. (1976) Chung Hom Wan, Journal of the Hong Kong Archaeological Society, 6, 9-25.

Barnett T.P. (1984) The estimation of "global" sea level change: a problem of uniqueness, Journal of Geophysical Research, 89, 7980-7988.

Barth M.C. and Titus J.G. (1984) Greenhouse effect and sea level rise. p.325. Van Nostrand Reinhold, New York.

Batterbee R.W. (1986) Diatom analysis. In **Berglund B.** ed. (1986) Handbook of Holocene Palaeoecology and Palaeohydrology, Chichester: John Wiley & Sons. p.527-570.

Beggs C.J. and Tonks D.M. (1985) Engineering geology of the Yuen Long Basin, Hong Kong Engineer, March 1985, 33-40.

Bennett J.D. (1984) Review of Hong Kong stratigraphy, Geotechnical Control Office Publications, 5/84, Geotechnical Control Office Engineering Development Department, Hong Kong.

Berry L. (1959) Changing sea levels and their significance in Hong Kong, Hong Kong University Engineering Journal, 22, 23-34.

Berry L. (1961) Erosion surfaces and emerged beaches in Hong Kong, Geological Society of America Bulletin, 72 (2), 1383-1384.

Binnie and Partners International (1981) Tin Shui Wai Urban Development Land Preparation Technical Report, unpublished report prepared for Mightycity Company Limited.

Bird E.C.F. and Schwartz M.L. (1985) The world's coastline, Van Nostrand Reinhold, New York.

Brimicombe A.J. (1986) 4000 to 6000 years B.P. - a higher relative sea level in Hong Kong?, in **Yim W.W.S.** ed. Sea level changes in Hong Kong during the last 40,000 years, Abstracts, 3, Geological Society of Hong Kong and the Department of Geography and Geology, University of Hong Kong.

British Standards Institution (1967) Methods of testing soils for civil engineering purposes, BS 1377, British standards institution, London.

Brock R.W. and Schofield S.J. (1926) The geological history and metallogenic epochs of Hong Kong, Proceedings of the Third Pan-Pacific Science Congress, Tokyo, 576-581.

Carter R.W.G. (1987) Man's response to sea-level change, in **Devoy R.J.N.** ed. Sea surface studies: a global view, Croom Helm, Beckenham, Kent, 464-498.

Catt P. (1978) Pollen analysis. p.43 - 44 in **Meacham W.** (ed) Sham Wan, Lamma Island: an archaeological site study, Journal monograph III, Hong Kong Archaeological Society, Hong Kong.

Chan K. (1948) Elevated wave cut benches near Canton and the origin of the compound shorelines of Kwangtung, Department of Geology New Series, 1, National Sun Yat Sen University, Canton, 1-11.

Bibliography:

Chan Y.K. (1983) Statistics of extreme sea levels in Hong Kong, Technical Note (Local) 35, Royal Observatory, Hong Kong, 24pp.

Chappell J. (1987) Late Quaternary sea level changes in the Australian region, in **Tooley M.J. and Shennan I.** eds. (1987), Sea-level changes. Oxford, Blackwells. p296-331.

Chappell J., Rhodes E.G., Thom B.G. and Wallensky E. (1982) Hydro-isostasy and the sea level isobase of 5,500 BP in north Queensland, Australia, *Marine Geology*, 49, 81-90.

Chen C. (1988) The direction of the agriculture modernization in the Pearl River Delta. Research of the environment and space development in the Pearl River Delta, Guangzhou, 83-90.

Chen C.H. (1984) China: essays in geography, Hong Kong Joint Publishing Company, Hong Kong. 379pp.

Chen J., Liu C. and Yu Z. (1985) China, in **Bird E.C.F. and Schwartz M.L.** (1985) The world's coastline, Van Nostrand Reinhold, New York.

Chiu T. (1978) Geology, p. 31-32 in Meacham W. (ed) Sham Wan, Lamma Island: an archaeological site study, Journal monograph III, Hong Kong Archaeological Society, Hong Kong.

Chiu T. and Woo N.K. (1966) Late neolithic site in the extreme north west of the New Territories, Hong Kong, *Asian Perspectives*, 11, 93-96.

Clark J.A. and Lingle C.S. (1977) Future sea level changes due to west Antarctic ice sheet fluctuations, *Nature*, 269, 206-209.

Clark J.A. and Primus J.A. (1987) Sea level changes resulting from future retreat of ice sheets: an effect of carbon dioxide warming of the climate, in **Tooley M.J. and Shennan I.** eds. (1987) Sea-level changes, Blackwell, Oxford, 357-370.

Davis S.G. (1952) The geology of Hong Kong, Government Printer, Hong Kong, 210pp.

Deng Y. (1985) Economy of Shenzhen Atlas of natural resources and economic development of Shenzhen, Science Press, Beijing, 165-168.

Deng Y. (1985) Distribution of aquatic, animal and poultry products and orchards of Shenzhen. Atlas of natural resources and economic development of Shenzhen, Science Press, Beijing, 185-192.

Englefield G.J.H., Tooley M.J. and Zong Y. (1990) An assessment of the Clwyd coastal lowlands after the floods of February 1990, Environmental Research Centre Durham, Publication ERC 4.1, 13pp.

ESRI (1988) pcARC/INFO operating manual (six volumes). Environmental Systems Research Institute, Redlands, California.

Fontaine H. and Delibrais G. (1973) Ancient marine levels of the Quaternary in Vietnam. *Journal of the Hong Kong Archaeological Society*, 4, 29-33.

Frost R.J. (1978) Valley study. p39 - 41 in Meacham W. (ed) Sham Wan, Lamma Island: an archaeological site study, Journal monograph III, Hong Kong Archaeological Society, Hong Kong.

Bibliography:

Geotechnical Control Office (1986) Hong Kong Geological Survey, Memoir No. 3, Geotechnical Control Office, Hong Kong.

Gibbs M.J. (1984) Economic analysis of sea level rise: methods and results, in **Barth M.C. and Titus J.G.** eds. Greenhouse effect and sea level rise, Van Nostrand Reinhold, New York, 215-252.

Gornitz V. and Lebedeff S. (1987) Global sea level changes during the past century, in **Nummerdal D., Pilkey O.H. and Howard J.D.** eds. Sea-level fluctuations and coastal evolution, Society of Economic Paleontologists and Mineralogists, Tulsa, Oklahoma, 41, 3-16.

Gornitz V., Lebedeff S. and Hansen J. (1982) Global sea level trends in the past century, *Science*, 215, 1611-1614

Greensmith J.T. and Tucker E.V. (1986) Compaction and consolidation, in **Plassche O. van der,** (ed.) Sea-level research: a manual for the collection and evaluation of data, p.591-603, Free University, Amsterdam.

Griffiths I (1989) From fairy cake to fortune cookie, *Independent*, 2 June 1989, 24.

Grindrod J. and Rhodes E.G. (1984) Holocene sea level history of a tropical estuary: Missionary Bay, north Queensland, in **Thom B.G.** ed. Coastal geomorphology in Australia, Academic Press, Sydney, Australia, 151-178.

Hansen J.E, Lacic A., Rind D., Russell G., Stone P., Fung I., Ruedy R. and Lerner J. (1984) Climatic sensitivity: analysis of feedback mechanisms, in **Hansen J.E. and Takahashi T.** eds. Climatic Processes and Climatic Sensitivity Maurice Ewing Series, 5, American Geophysical Union Washington DC, 138-163.

Hansen J., Gornitz V., Lebedeff S. and Moore E. (1983) Global mean sea level: indicator of climatic change?, *Science*, 219, 996-987.

Hansen J. and Lebedeff S. (1987) Global trends of measured surface air temperatures, *Journal of Geophysical Research*, 92 (D11), 13,345-13,372.

Heanley C.M. and Shellshear J.L. (1932) A contribution to the prehistory of Hong Kong and the New Territories, *Proceedings of the First Congress on Prehistory of the Far East*, Hanoi, 63-76.

Heim A. (1929) Fragmentary observations in the region of Hong Kong compared with Canton, *Geological Survey of Kwangtung and Kwangsi Annual Report*, 2 (1), 1-32.

Henderson-Sellers A. and McGuffie K. (1986) The threat from melting ice caps, *New Scientist*, 1512, 24-25.

Hendey N.I. (1964) An introductory account of the smaller algae of British coastal waters - Part V: bacillariophyceae (diatoms), HMSO, 317pp.

Hoffman J.S. (1984) Estimates of future sea level rise, in **Barth M.C. and Titus J.G.** (1984), 79-104.

Hoffman J.S., Wells J.B. and Titus J.G. (1986) Future global warming and sea-level rise, in **Sigbjarnarson,** ed. Iceland coastal and river symposium 1985, National Energy Authority, Reykjavik.

Hoffman J.S., Keyes D. and Titus J.G. (1983) Projecting future sea level rise: methodology, estimates to the year 2100 and research needs, US Environmental Protection Agency, Washington DC, 121pp.

Bibliography:

- Hopley D.** (1978) Sea level change on the Great Barrier Reef: an introduction, *Philosophical Transactions of the Royal Society, London, Series A*, 291, 159-166.
- Hopley D.** (1986) Beachrock as a sea level indicator, in **Plassche O. van de** ed. *Sea level research: a manual for the collection and evaluation of data*, Geo Books, Norwich, UK, 618pp.
- Holt, J.K.** (1962) The soils of Hong Kong's coastal waters. *Proceedings of the Symposium on Hong Kong Soils, Hong Kong*, 1-32.
- Howat M.D.** (1985a) Late Pleistocene sea levels in Hong Kong and the Pearl River Estuary, *Geological Society of Hong Kong Newsletter*, 3 (3), 7-8.
- Howat M.D.** (1985b) A nearshore colluvial deposit in Western District, Hong Kong Island, *Geological Society of Hong Kong Newsletter*, 3 (6), 6-12.
- Howat M.D.** (1986a) Discussion of "Results of a palaeontological investigation of Chep Lak Kok borehole (B13/B13A) North Lantau" by **Shaw, Zhou, Gervais and Allen**, *Geological Society of Hong Kong Newsletter*, 4 (3), 24-25.
- Howat M.D.** (1986b) Sea level changes deduced from excavation and tunnelling in western district, Hong Kong Island, in **Yim W.W.S.** ed. *Sea level changes in Hong Kong during the last 40,000 years, Abstracts*, 3, Geological Society of Hong Kong and Department of Geography and Geology, University of Hong Kong, 15-22.
- Huang Y. and Chen J.** (1988, personal communication) Sea level changes along the coasts of the South China Sea since the late Pleistocene.
- Huang Z., Li P., Zhang Z. and Li K.** (1987a) The geomorphological evolution of the Zhujiang Delta in **Gardiner V.** ed. *International Geomorphology 1986 Part I*, John Wiley & Sons, 989-997.
- Huang Z., Li P., Zhang Z. and Li K.** (1987b) Late Quaternary sub-fossil wood beds in the Zhujiang Delta deposits, in **Gardiner V.** ed. *International Geomorphology 1986 Part II*, John Wiley & Sons.
- Huang Z., Li P., Zhang Z. and Li K.** (personal communication) A new approach to the geomorphological evolution of the Zhujiang Delta.
- Huang Z., Li P., Zhang Z., Li K., Qau P. and Zong Y.** (1983) *The landform of Shenzhen*, Guangdong Scientific Press, Guangzhou, China.
- Huang Z., Li P., Zhang Z. and Qiao P.** (1982) *Zhujiang Delta: formation, development and evolution*. Guangzhou Institute of Geography Research Results, Universal Publishing House, Guangzhou, 274pp (in Chinese).
- Huang Z., Li P., Zhang Z. and Zong Y.** (1986) Sea level changes along the coastal area of south China since late Pleistocene, *Guangzhou Institute of Geography*, 14pp.
- Hubbard G.D.** (1929) The Pearl River delta, *Lingnan Scientific Journal*, 7, 35-67.
- Hustedt F.** (1953) Die systematik der diatomeen in ihren Beziehungen zur geologie und okologie nebst einer revision des halobien-systems. *Svensk. Bot. Tidskr.* 47, 509-519.
- Ireland S.** (1987) The Holocene sedimentary history of the coastal lagoons of Rio de Janeiro State, Brazil. In **Tooley M.J. and Shennan I.** (eds) *Sea-level changes*. Oxford: Blackwells, p.25-66.

Bibliography:

- Ireland S** (1988) Holocene coastal changes in Rio de Janeiro State, Brazil. Unpublished PhD thesis, University of Durham.
- Irving R. and Morton B.** (1988) A geography of the Mai Po marshes, World Wide Fund for Nature, Hong Kong, 58p.
- Jelgersma S.** (1961) Holocene sea-level changes in The Netherlands. *Mededelingen van de Geologische Stichting. Serie C, VI, 7, 1-100.*
- Jin D X., Cheng J. H., Huang H. G.** (1965) Planktonic marine diatoms in China, Shanghai Scientific Technical Press, Shanghai, 199p.
- Jin D X., Cheng S., Lin G., Liu X.** (1982) Benthonic marine diatoms in China, China Ocean Press, Peking, 323p.
- Kates R.W.** (1978) Risk assessment of environmental hazard. Scientific Committee on Problems of the Environment, 8, John Wiley and Sons, 112pp.
- Kendall F.H.** (1975) High Island - a study of undersea deposits, *Journal of Hong Kong Archaeological Society*, 6, 26-32.
- Kidson C.** (1982) Sea-level changes in the Holocene. *Quaternary Science Review*. 1, 121-151.
- Kingsmill T.W.** (1862) Notes of the geology of the east coast of China, *Proceedings of the Geological Society of Dublin*, 10, 1-6.
- Laborel J.** (1979) Fixed marine organisms as biological indicators for the study of recent sea level and climatic variations along the Brazilian tropical coast. In Suguio K., Fairchild T.R., Martin L and Flexor J.M. (eds) 1979 *Proceedings of the "1978 International symposium on coastal evolution in the Quaternary" Sao Paulo, Brazil.* p.193-211.
- Landon J R** (ed) 1984 *Booker Tropical Soil manual*, Booker Agricultural International Ltd., London.
- Li P.** (1988) The sea level change of Pearl River Delta since 7,000 years ago and the possible effects on environment resulting from the future sea level rise, *Research of Environment and Space Development in the Pearl River Delta*, Academia Sinica Guangzhou, 15-26.
- Li P., Huang Z., Zhang Z. and Zong Y.** (undated) Holocene strata along the coastal area of eastern Guangdong, Institute of Geography, Guangzhou, China, 11p.
- Liu Y.** (personal communication) Quaternary geology along the coast from Pearl River mouth to Honghai Bay, South China Sea Institute of Oceanology Academia Sinica.
- Lumb P.** (1987) The marine soils of Hong Kong and Macau, *Proceedings of the International Symposium on Soft Clay, Bangkok, Thailand*, 45-58.
- McLean R.F., Stoddart D.R., Hopley D. and Polach H.** (1978) Sea level change in the Holocene on the northern Great Barrier Reef, *Philosophical Transactions of the Royal Society, London, Series A*, 291, 167-186.
- Maguire D.J., Goodchild M.F. and Rhind D.W.** (1991) *Geographical Information Systems: principles and applications*, Longman, Harlow. 2 volumes.
- Meacham W.** (1975) Lai Chi Kok, *Journal of the Hong Kong Archaeological Society*, 6, 33-36.

Bibliography:

- Meacham W.** (1978) (ed) Sham Wan, Lamma Island: an archaeological site study, Journal monograph III, Hong Kong Archaeological Society, Hong Kong.
- Meacham W.** (1979) C-14, Thermo-luminescence dates from geological and prehistorical sites in Hong Kong, Journal of Hong Kong Archaeological Society, 7, 91-92.
- Meacham W.** (1980) New C-14 dates from Hong Kong, Journal of the Hong Kong Archaeological Society, 8, 126-128.
- Meacham W.** (1986) Archaeological evidence on higher sea levels in Hong Kong in **Yim W.W.S.** ed. (1986), 31-33.
- Meacham W. and Yim W.W.S.** (1983) Coastal bar deposits at Pui O, Journal of Hong Kong Archaeological Society, 10, 70-71.
- Meier M.** (1984) Contribution of small glaciers to global sea-level. Science, 226, p.1418-21.
- Milliman J.D., Broadus J.M. and Gable F.** (1989) Environmental and economic implications of rising sea level and subsiding deltas: the Nile and Bengal examples, Ambio, 18 (6), 340-345.
- Milliman J.D. and Emery K.O.** (1968) Sea levels during the last 35,000 years, Science, 162, 1121-1122.
- Ministry of Agriculture Fisheries and Food** (1981) The analysis of agricultural materials. Technical Bulletin, RB427.
- Mook W.G. and Plassche O. van de** (1986) Radiocarbon dating, in **Plassche O. van de** ed. Sea level research: a manual for the collection and evaluation of data, Geo Books, Norwich, UK, 618pp.
- Morton B.** (1978) Molluscan evidence of environmental changes at Sham Wan, Journal of the Hong Kong Archaeological Society Monograph No. III, 45-56.
- Neftel A., Moor E., Oeschger H. and Stauffer B.** (1985) Evidence from polar ice cores for the increase in atmospheric carbon dioxide in the past two centuries, Nature, 315, 45-47.
- National Research Council** (1987) Responding to changes in sea level: engineering implications, National Academy Press Washington DC, 148pp.
- Olsson I.U.** (1986) Radiocarbon dating. In **Berglund B.** ed. (1986) Handbook of Holocene Palaeoecology and Palaeohydrology, John Wiley & Sons, 273-312.
- Orford J.** (1987) Coastal processes: the coastal response to sea level variation, in **Devoy R.J.N.** ed. Sea surface studies: a global view, Croom Helm Beckenham, Kent, 415-463.
- Qin Y.S., Zhao S.L. and Chng S.X.** (personal communication) Recent sea level changes in eastern coastal region of China and the possible impacts in the future, Institute of Oceanology Academia Sinica, Qingdao, China.
- Palmer A.J.M. and Abbott W.H.** (1986) Diatoms as indicators of sea level change in **Plassche O. van de** ed. Sea level research: a manual for the collection and evaluation of data, Geo Books, Norwich, UK, 618pp.
- Pascall D.** (undated) Alluvial sediments in the Hu Men/Boca Tigris channel Guangdong Province, China.
- Pirazzoli P.A.** (1991) World atlas of Holocene sea-level changes, Elsevier Oceanography Series, 58, Amsterdam.

Bibliography:

Plassche O. van de (1981) Sea level, groundwater and basal peat growth - a reassessment of data from the Netherlands, *Geologie en Mijnbouw*, 60, 401-408.

Plassche O. van de (1986) ed. Sea level research: a manual for the collection and evaluation of data, Geo Books, Norwich, UK, 618pp.

Polach H.A., McLean R.F., Caldwell J.R. and Thom B.G. (1978) Radiocarbon ages from the Great Barrier Reef, *Philosophical Transactions of the Royal Society, London, Series A*, 291, 139-158.

Population Census Office (1987) Atlas of the Peoples' Republic of China, Academia Sinica, Beijing, China.

Rhodes E.G., Polach H.A., Thom B.G. and Wilson S.R. (1980) Age structure of Holocene coastal sediments: Gulf of Carpentaria, Australia, *Radiocarbon*, 22 (3), 718-727.

RMP Econ. (1982) Replacement Airport at Chep Lap Kok - Civil Engineering Design Studies Study Report No. 1 - Site Investigations, Vol I & II, Civil Engineering Office, Hong Kong.

Robin G. de Q. (1986) Changing sea level. In **Bolin B.** ed. Greenhouse effect, climatic change and ecosystems. 323p John Wiley and Sons, New York.

Rossiter J. (1962) Long term variations in sea-level. In **Mill N.M.** (ed) *The Sea*. 1, London: Interscience Publishers, 590-610.

Roveda V.L., Waton P.V., Zhou K.S. and Zhang Q.R. (1986) Junk Bay cores JBS1/1A: paleontological and stratigraphical final report: Project No. 135C: Paleoservices China Limited, Shenzhen, 21pp.

Schofield W. (1942) Recent changes of sea level on the coasts of Eastern Asia, *Liverpool Geological Society Journal*, 18, 101-112.

Shaw R. (1986) Reply to the discussion by M.D. Howat, *Geological Society of Hong Kong Newsletter*, 4 (3), 26-27.

Shaw R. and Arthurton R.S. (1988) Palaeoenvironmental interpretation of offshore Quaternary sediments in Hong Kong, in *Proceedings of the Second International Conference on the Palaeoenvironment of East Asia from the mid-Tertiary*, Centre of Asian Studies, University of Hong Kong, 1, 138-150.

Shaw R., Zhou K., Gervais E. and Allen L.O. (1986) Results of a palaeontological investigation of Chep Lap Kok borehole B13/B13A, North Lantau, *Geological Society of Hong Kong Newsletter*, 4 (2), 1-12.

Shennan I. (1982) Interpretation of Flandrian sea-level data from the Fenland, England. *Proceedings of the Geologists Association*, 93(1), 53-63.

Shennan I. (1986) Flandrian sea-level changes in the Fenland. II: tendencies of sea-level movement, altitudinal changes, and local and regional factors. *Journal of Quaternary Science*, 1, 155-179.

Shennan I. (1987) Impacts on the Wash of sea-level change, in **Doody P. and Barnett B.** eds. *The Wash and its environment, research and survey in nature conservation*, 7, 77-90, Nature Conservancy Council Peterborough, UK.

Shennan I. (1989) Holocene crustal movements and sea-level changes in Great Britain, *Journal of Quaternary Studies*, 4, 77-89.

Shennan I. and Tooley M.J. (1987) Conspectus of fundamental and strategic research on sea-level changes, in **Tooley M.J. and Shennan I.** eds. *Sea-level changes*, 371-390, Basil Blackwell, Oxford.

Bibliography:

Shennan I., Tooley M.J., Davis M.J. and Haggart B.A. (1983) Analysis and interpretation of Holocene sea level data. *Nature*, 302, 404-406.

Shennan I and Sproxton I. (1991) Impacts of future sea level rise on the Tees estuary. An approach using a geographical information system (GIS). p81-92 in **Frassetto R.** ed. Impact of sea level rise on cities and regions, Proceedings of the First International Meeting "Cities on water", Venice, December 11-13, 1989. Marsilio Editori, Venice.

So C.L. (1969) Landforms and archaeology, *Journal of the Hong Kong Archaeological Society*, 1, 24-28.

Strange P.J. (1986) High level beach rock on Hong Kong Island, *Geological Society of Hong Kong Newsletter*, 4 (2), 13-16.

Stuiver M. and Polach H.A. (1977) Discussion - reporting of C-14 data, *Radiocarbon*, 19 (3), 355-363.

Tegart W.J. McG., Sheldon G.W. and Griffiths D.C. (eds.) (1990) Climate change: the IPCC Impacts Assessment. Final report prepared for IPCC by Working Group II, Intergovernmental Panel on Climate Change, Australia.

Thom B.G. and Chappell J. (1978) Holocene sea level change: an interpretation, *Philosophical Transactions of the Royal Society, London, Series A*, 291, 187-194.

Titus J.G. (1986) Greenhouse effect, sea level rise and coastal zone management, *Coastal Zone Management Journal*, 14 (3), 147-171.

Titus J.G. (1987) The greenhouse effect, rising sea level and society's response, in **Devoy R.J.N.** ed. *Sea surface studies: a global view*, Croom Helm Beckenham, Kent, 499-528.

Tooley M.J. (1971) Changes in sea level and the implications for coastal development. *Association of River Authorities Year Book 1971*. 220-225.

Tooley M.J. (1978) *Sea-level changes in North-west England during the Flandrian stage*. Oxford: Clarendon Press.

Tooley M.J. (1981) Methods of reconstruction. In **Simmons I.G. and Tooley M.J.** (eds), *The environment in British prehistory*, London: Gerald Duckworth and Co., 1-48.

Tooley M.J. (1987a) Sea level change, *Progress in Physical Geography*, 11(1).

Tooley M.J. (1987b) Sea-level studies. In **Tooley M.J. and Shennan I.** eds. (1987) *Sea level changes*, Blackwell, Oxford, p.1-24.

Tooley M.J. and Shennan I. eds. (1987) *Sea level changes*, Blackwell, Oxford.

Troels-Smith J. (1955) Characterisation of unconsolidated sediments, *Geological Survey of Denmark, Series IV*, vol. 3 No. 10. 73p and 13 tables.

Wang P. and Yim W.W.S. (1985) Preliminary investigations on the occurrence of marine microfossils in an offshore drill-hole from Lei Yue Mun Bay, *Geological Society of Hong Kong Newsletter*, 3(1), 1-5.

Wen C., Xu J., Lin H., Xia Y., Wang W., Xiao Z., Yan Z. and Zeng W. (1985) Land utilization of Shenzhen, *Atlas of natural resources and economic development of Shenzhen*, Science Press, Beijing, 125-132.

Whiteside P.G.D. (1984) Pattern of Quaternary sediments revealed during piling works at Sha Tin, Hong Kong, in **Yim W.W.S.** ed. (1984b).

Bibliography:

- Whiteside P.G.D. and Arthurton R.S. eds. (1985) Proceedings of the Seminar on Marine Geology of Hong Kong and the Pearl River mouth, Geological Society of Hong Kong, 97pp.
- Willis A.J. and Shirlaw J.N. (1984) Deep alluvial deposits beneath Victoria Park, Causeway Bay, in Yim W.W.S. ed. (1984b) 143-152.
- Wu X. (1987) Sea level changes and stratigraphy during late Quaternary in the basin and plains along the coast of Fujian Province, south eastern China, in Qui Y. and Zhao S. Late Quaternary sea level changes, China Ocean Press, Beijing, 223-238.
- Yong (1989) Untitled article. The ASEAN-US Cooperative Program on Marine Sciences Newsletter. April 1989. Manilla: Philippines.
- Yim W.W.S. (1983) Pumice-like material at Pui O - pumice or slag?, Journal of the Hong Kong Archaeological Society, 10, 72-73.
- Yim W.W.S. (1984a) Evidence for Quaternary environmental changes from sea floor sediments in Hong Kong, in Whyte R.O. ed. The evolution of the East Asia environment, Geology and Palaeoclimatology, 1, Centre of Asian Studies, University of Hong Kong.
- Yim W.W.S. ed. (1984b) Geology of surficial deposits of Hong Kong, Bulletin No. 1, Geological Society of Hong Kong, University of Hong Kong.
- Yim W.W.S. (1984c) A sedimentological study of sea floor sediments exposed during excavation of the East Dam site, High Island, Sai Kung, in Yim W.W.S. ed. (1984b) Geology of surficial deposits of Hong Kong, Bulletin No. 1, Geological Society of Hong Kong, University of Hong Kong, 131-142.
- Yim W.W.S. (1986a) Sea level changes in Hong Kong during the last 40,000 years, Abstracts, 3, Geological Society of Hong Kong and the Department of Geography and Geology, University of Hong Kong, 51pp.
- Yim W.W.S. (1986b) Radiocarbon dates from Hong Kong and their geological implications, Journal of the Hong Kong Archaeological Society, 11, 50-63.
- Yim W.W.S. (1988a) An analysis of tide gauge and storm surge data in Hong Kong, in Yim W.W.S. ed. Future sea-level rise and coastal development, Abstracts, 5, Geological Society of Hong Kong, Hong Kong.
- Yim W.W.S. ed. (1988b) Future sea level rise and coastal development, Abstracts, 5, 59pp.
- Yim W.W.S. (1988c) Report on coastal and sea level changes in China, in Proceedings of the Second International Conference on the Palaeoenvironment of East Asia from the mid-Tertiary, Centre of Asian Studies, University of Hong Kong, 1, 249-254.
- Yim W.W.S. (1989) The impact on sea water level, Proceedings of the International Conference on Atmosphere, Climate and Man, Torino, Italy, 13pp.
- Yim W.W.S., Fan S.Q., Wu Z.J., Yu K.F., He X.X., and Jim C.Y. (1988) Late Quaternary palaeoenvironment and sedimentation in Hong Kong, Proceedings of the Second Conference on the Palaeoenvironment of East Asia from the mid-Tertiary, 1, Centre of Asian Studies, University of Hong Kong, 117-137.
- Yim W.W.S., Ivanovich M. and Yu K.F. (personal communication) Age of pre Holocene marine deposits in Hong Kong.

Bibliography:

Yim W.W.S. and Nau P.S. (1984a) Zhujiang Delta - extracts from a research publication by the Guangzhou Institute of Geography, Geological Society of Hong Kong Newsletter, 2 (4), 1-5.

Yim W.W.S. and Nau P.S. (1984b) Radiocarbon dates of the Zhujiang Delta and their implications for Hong Kong, Geological Society of Hong Kong Newsletter, 2(5), 10-14.

Yim W.W.S. and Yu K.F. (in press) Evidence for multiple Quaternary marine transgressions in a borehole from the West Lamma Channel, Hong Kong. In Proceedings of the 3rd Palaeo

Yu X., Lin J., Li X., Shen J., Yan Z., Chen C. and Pan Z. (1985) Land resources of Shenzhen. Atlas of natural resources and economic development of Shenzhen. Science Press, Beijing. p.121-124.

Zhang H 1982 On activity of the north-west trending fractures along the Fujian-Guangdong region, Seismology and Geology, 4(3), p17-25, Academia sinica (in Chinese).

Zhang H. (personal communication, undated) On the relationships between Holocene sea level changes as well as seismicity and plate motion, Guangdong Seismological Bureau, Guangzhou, China.

Zhang Z. and Liu R. (1987) The Holocene along the coast of Hainan Island. Scientia Geographica Sinica. 7(2) 129-138. (In Chinese, English abstract).

Zhao X. and Zhang J. (1982) Basic characteristics of the Holocene sea level changes along the coastal areas in China, in Liu T. ed. Quaternary geology and environment of China, China Ocean Press, Beijing, 155-160.

Zhong Y. (1985) Communications and transportation. In Atlas of natural resources and economic development of Shenzhen, Science Press, Beijing, 157-164.

Zhou D. (Ed.) (1985) Atlas of natural resources and economic development of Shenzhen. Science Press, Beijing, China.

Zong Y. (1989) On depositional cycles and geomorphological development of the Han River Delta of south China, Zeitschrift fur Geomorphologie, 73, 33-48.

Zong Y. (1992) Postglacial stratigraphy and sea-level changes in the Han river delta, China. Journal of Coastal Research, 8(1), p1-28.

Zong Y. and Li P. (1985) Development conditions of the Holocene beachrock along the coasts of eastern Guangdong, China, Institute of Geography Guangzhou, 10pp.

